

(NASA-CR-183585) SPACE STATION PROTECTIVE
COATING DEVELOPMENT Final Report (Boeing
Aerospace Co.) 304 p CSCL 22B

N89-21821

Unclas
G3/18 0197290

SPACE STATION PROTECTIVE COATING DEVELOPMENT

Final Report

H. G. Pippin and S. G. Hill

**Boeing Aerospace
Seattle, Washington 98124-2499**

**Contract NAS8-36586
January 1989**



**National Aeronautics and
Space Administration**

**George C. Marshall Space Flight Center
Marshall Space Flight Center, Alabama 35812**

FOREWORD

This report describes the work accomplished by Boeing Aerospace under Contract NAS8-36586, "Space Station Protective Coatings Development." The contract was sponsored by the National Aeronautics and Space Administration, George C. Marshall Space Flight Center.

Mrs. Ann Whitaker and Mr. Roger Linton were the NASA Technical Monitors. The Materials and Processes Technology organization of Boeing Aerospace was responsible for the work performed under this contract. Boeing Aerospace Failure Analysis Laboratory and the Boeing Physical Sciences Research Center supported the efforts in Task 4. Mr. Sylvester Hill was program manager; Mr. Bruce Zornes, Mr. Roger Bourassa, and Dr. Gary Pippin served as technical leaders. The following personnel provided essential support to various task activities.

Joseph P. Brown	M&P, construction, maintenance, operation of AO test chamber
Walter L. Plagemann	Coordination of analyses to determine coating optical properties.
Lawrence B. Fogdall	Supervision of CRETC II tests
Dennis A. Russell	Supervision of combined Vacuum Thermal Cycling/Ultraviolet Radiation exposure tests

Use of commercial products or names of manufacturers in this report does not constitute official endorsement of such products or manufacturers, either expressed or implied, by the National Aeronautics and Space Administration or The Boeing Company.

TABLE OF CONTENTS

<u>SECTION</u>	<u>PAGE</u>
Foreword	i
List of Figures	iv
List of Tables	xiv
CHAPTER 1 - INTRODUCTION	
Task Element I	1
Task Element II	1
Task Element III	1
Task Element IV	2
Task Element V	3
Task Element VI	3
Task Element VII	3
CHAPTER 2 - Candidate Exterior Space Station Surfaces And Their Environmental Exposures	5
CHAPTER 3 - Requirements of Space Station External Surfaces	11
Outgassing	11
Optical Properties	12
CHAPTER 4 - Critical technology Deficient Areas	19
Risks	22
CHAPTER 5 - Materials Testing	23
Atomic Oxygen Test Apparati	78
Combined Radiation Effects on Optical Properties	121
Thermal Vacuum Cycling and UV Exposure Tests	136
Lyman-Alpha Far UV Lamps	140
Dosimetry For Other kinds of Radiation	151
Test Sequence	151

TABLE OF CONTENTS (Continued)

<u>SECTION</u>	<u>PAGE</u>
CHAPTER 5 - Materials Testing (Continued)	
Uniformity of Radiation Exposure	152
Notes Specific To Certain Samples or Materials	154
Peel Tests	164
Bend Radius Testing	170
Outgassing Tests	170
Flatwise Tension Tests	170
Stress Effects on Atomic Oxygen Degradation	178
Results of SEM Measurements	178
CHAPTER 6 - Large Scale Technology Demonstration	387
Tracking	387
Powder Formation	387
Coating Stress	390
Material Flaking	390
CHAPTER 7 - Discussion	397
Atomic Oxygen Flux	397
Data Base	399
Candidate Materials	405
Materials Lifetime Estimates	416

LIST OF FIGURES

	<u>PAGE</u>
Figure 1: Original Configuration of Atomic Oxygen Test Apparatus	79
Figure 2: Current Configuration of AO Test Apparatus	81
Figure 3: Mass Loss of Kapton, Held at 85°C, vs. Fluence of Atomic Oxygen	95
Figure 4: Mass Loss of Kapton, Held at 85°C, per Flux of Atomic Oxygen vs. Fluence of Atomic Oxygen	97
Figure 5: Mass Loss of Kapton, Held at 100°C, vs Fluence of Atomic Oxygen	99
Figure 6: Mass Loss of Kapton, Held at 100°C, Per Flux of Atomic Oxygen vs. Fluence of Atomic Oxygen	101
Figure 7: Mass Loss of Kapton, Held at 195°C, Per Flux of Atomic Oxygen Per Flux of Atomic Oxygen	103
Figure 8: Mass Loss of Kapton, Held at 195°C, vs. Fluence of Atomic Oxygen	105
Figure 9: Thermal Vacuum Cycling and UV Exposure Test Chamber	115
Figure 10: Vacuum Test Chamber With IR Lamp Array Used For Thermal Cycling Test	117
Figure 11: Schematic of Boeing Combined Radiation Effects Test Chamber (CRETC) II	123
Figure 12: Photo of Boeing Combined Radiation Effects Test Chamber II	125
Figure 13: Sample Arrangement During The Latest Combined Effects Test, Showing The Areas Exposed To The Proton And UV Flux _____, And The Areas Exposed To The Vacuum UV Flux -----.	137
Figure 14: Identity of Each Material at Each Location in the Test Chamber	139
Figure 15: Proton And Electron Fluence As A Function of UV Radiation Dose	153
Figure 16: Changes In Absorptance Of White Pigmented Coatings As A Function Of Combined Proton, Electron, UV and VUV Exposure. Sample Locations Are in Parentheses. Sample at Location 31 Was Exposed to Slightly Reduced Levels of All Radiation Types.	157
Figure 17: Bend Radius Test Sample Configuration	171

	<u>PAGE</u>
Figure 18: Flatwise Tension Test Sample Configuration	176
Figure 19: Results of Scanning Electron Microscopy of Kapton After Exposure to Combined Radiation Effects Test Environment	179
Figure 20: Results of Scanning Electron Microscopy of HMDS Coating After Exposure to Combined Radiation Effects Test Environment	181
Figure 21: Results of Scanning Electron Microscopy on S13-G/L0-1 Coating After Exposure to Combined Radiation Effects Test Environment	183
Figure 22: Results of Scanning Electron Microscopy of HMDS/TFE and Fluorophosphazene Coatings After Exposure to Combined Radiation Effects Test Environment	185
Figure 23: Results of Scanning Electron Microscopy of Silicone (CV-1144) Coating After Exposure to Combined Radiation Effects Test Environment	187
Figure 24: Results of Scanning Electron Microscopy of Fluorosilicone (CV-3530) Coating After Exposure to Combined Radiation Effects Test Environment	189
Figure 25: Results of Scanning Electron Microscopy on HMDS Coating. The Sample was Previously Exposed to Atomic Oxygen for 25 Hours.	191
Figure 26: Results of Scanning Electron Microscopy on HMDS Coating. The Sample was Previously Exposed to Atomic Oxygen for 48 Hours.	193
Figure 27: Results of Scanning Electron Microscopy on Polyimide-Siloxane Coating. The Sample was Previously Exposed to Atomic Oxygen for 93 Hours.	195
Figure 28: Results of Scanning Electron Microscopy on HMDS/TFE Coating. The Sample was Previously Exposed to Atomic Oxygen for 96 Hours.	197
Figure 29: X-Ray Photoelectron Spectrum of Fluorophosphazene Coating on Kapton. The Sample was Previously Exposed to Atomic Oxygen for 49 Hours.	199
Figure 30: X-Ray Photoelectron Spectrum of Siloxane-Polyimide Co-Polymer Coating on Kapton. The Sample Was Previously Exposed to Atomic Oxygen for 6 Hours.	201

	<u>PAGE</u>
Figure 31: X-Ray Photoelectron Spectrum of Siloxane-Polyimide Co-Polymer Coating on Kapton. The Sample was Previously Exposed to Atomic Oxygen for 51 Hours.	203
Figure 32: X-Ray Photoelectron Spectrum of Silicone (CV-1144) Coating on Kapton. The Sample was Previously Exposed to Atomic oxygen for 48 Hours.	205
Figure 33: Scanning Electron Micrograph of Plasma Polymerized Hexamethyldisiloxane	209
Figure 34: Scanning Electron Micrograph (SEM) of Plasma Polymerized HMDS After Exposure to a Combined Radiation Effects Environment (Electrons, Protons, Simulated Solar UV) and Subsequent Exposure to Atomic Oxygen for 48 Hours.	211
Figure 35: SEM of Plasma Polymerized HMDS After Exposure to a Combined Radiation Effects Environment and Subsequent Exposure to Atomic Oxygen for 48 Hours.	213
Figure 36: SEM of Kapton After Exposure to a Combined Radiation Effects Environment and Subsequent Exposure to Atomic Oxygen for 48 Hours.	217
Figure 37: SEM of Fluorophosphazene After Exposure to a Combined Radiation Effects Environment and Subsequent Exposure to Atomic Oxygen for 48 Hours.	219
Figure 38: SEM of Fluorophosphazene After Exposure to a Combined Radiation Effects Environment and Subsequent to Atomic Oxygen for 48 Hours.	221
Figure 39: SEM of S13-G/LO After Exposure to a Combined Radiation Effects Environment and Subsequent Exposure to Atomic Oxygen for 48 Hours.	223
Figure 40: SEM of a Silicone (CV-1144) After Exposure to a Combined Radiation Effects Environment and Subsequent Exposure to Atomic Oxygen for 48 Hours.	225
Figure 41: SEM of a Fluorosilicone (CV-3530) After Exposure to a Combined Radiation Effects Environment and Subsequent Exposure to Atomic Oxygen for 48 Hours.	227
Figure 42: SEM of Plasma Polymerized Hexamethyldisiloxane /Tetrafluoroethylene (8:1), After Exposure to a Combined Radiation Effects Environment and Subsequent Exposure to Atomic Oxygen for 48 Hours.	229
Figure 43: SEM of Plasma Polymerized HMDS/TFE After Exposure to a Combined Radiation Effects Environment and Subsequent Exposure to Atomic Oxygen for 48 Hours.	231

	PAGE
Figure 44: Plasma Polymerized HMDS (#46) on 1-Mil Kapton	233
Figure 45: HMDS Coating (#46) on Kapton. Sample Exposed to Atomic Oxygen for 4 Hours.	233
Figure 46: Detail of Damage at Boundary of Exposed and Covered Regions of HMDS Coating After 4 Hours Exposure to Atomic Oxygen.	235
Figure 47: Detail of Area Near Edge of Exposed Region Showing Attack of Kapton Substrate by Atomic Oxygen Upon Coating Loss.	235
Figure 48: Uncoated 2-Mil Kapton Film	237
Figure 49: Uncoated 2-Mil Kapton Film After 4 Hours of Exposure to Atomic Oxygen	237
Figure 50: EDAX Spectrum of Kapton Exposed to Atomic Oxygen For 4 Hours	239
Figure 51: EDAX Spectrum of Unexposed Edge Area of Kapton. Region of Sample Under Lip of Specimen Holder.	241
Figure 52: EDAX Spectrum of Large Debris Particle on Surface of Kapton Exposed to Atomic Oxygen for 4 Hours.	243
Figure 53: Texture of Uncoated Kapton Film After 4 Hours Atomic Oxygen Exposure	247
Figure 54: Ethyl Eypel (R)-Type (X-129) Coating on Kapton. Sample was Exposed to Atomic Oxygen for 2 Hours.	247
Figure 55: Eypel (R)-Type Coating (X-128) on Kapton. Sample Exposed to Atomic Oxygen Plasma for 2 Hours.	249
Figure 56: Interface Between X-128 Coating Exposed to Atomic Oxygen (Left) and Unexposed (Right).	249
Figure 57: Ethyl X-128 (#58) Coating on 2-Mil Kapton Film	251
Figure 58: EDAX Spectrum of Unexposed Ethyl Eypel X-128 Fluorophosphazene	253
Figure 59: IITRI Silicone Glass Coating on 1-Mil Kapton Film	251
Figure 60: EDAX Spectrum of Unexposed IITRI Silicone Glass Coating	255
Figure 61: IITRI S13G/L0-1 on Glass Fiber/Epoxy Substrate	257

	<u>PAGE</u>
Figure 63: HMDS (#3) on 1-Mil Kapton Film	257
Figure 64: EDAX Spectrum of HMDS Coating on Kapton	261
Figure 65: EDAX Spectrum of Debris Particles on HMDS Coating	263
Figure 66: HMDS Coating on Kapton. Sample Exposed to Atomic Oxygen for 2 Hours.	265
Figure 67: Surface Feature of HMDS on Kapton. Sample Previously Exposed to Atomic Oxygen.	265
Figure 68: Plasma Polymerized HMDS/TFE (#52) Coating on Kapton.	267
Figure 69: EDAX Spectrum of Plasma Polymerized HMDS/TFE Coating on Kapton	269
Figure 70: IITRI Glassy Silicone Coating (#59) on Kapton. Sample Exposed to Atomic Oxygen for 2 Hours.	267
Figure 71: Area of Coating (#59) Loss and Kapton Exposure to Atomic Oxygen Attack	271
Figure 72: Localized Charging Along Cracks in Coating Material (#59) Subsequent to Atomic Oxygen Exposure	271
Figure 73: EDAX Spectrum of IITRI Glass Resin on Kapton Subsequent to Atomic Oxygen Exposure	273
Figure 74: HMDS/TFE (#54) Coating on Kapton	275
Figure 75: Clouded Region of HMDS/TFE Coating (#54) on Kapton	275
Figure 76: EDAX Spectrum of Debris on Surface of HMDS/TFE Coating	277
Figure 77: EDAX Spectrum of Plasma Polymerized HMDS/TFE Coating	279
Figure 78: IR Spectrum of Battelle Plasma-Polymerized HMDS/TFE (Ratio 4/1) Coating Material (Unexposed) Scraped Off Coating Material (Unexposed) Scraped Off Kapton Film Substrate	281
Figure 79: Plasma Polymerized HMDS/TFE Coating (#55) on 1-Mil Kapton. Sample Exposed to Atomic Oxygen Plasma for 2 Hours	283
Figure 80: Kapton Film Heavily Degraded by Atomic Oxygen Exposure	283
Figure 81: Kapton Film After Atomic Oxygen Exposure for 4 Hours	285
Figure 82: IITRI Glassy Silicone Bent Over a 15-Mil Radius	285
Figure 83: NASA LeRC 8% PTFE-SiO ₂ Coating on 1-Mil Kapton Bent Over a 40-Mil Radius	289

	<u>PAGE</u>
Figure 84: NASA LeRC 8% PTFE-SiO ₂ Coating on 1-Mil Kapton Bent Over a 15-Mil Radius	289
Figure 85: HMDS Coating (#56) on Kapton Bent Over 40-Mil Radius	291
Figure 86: HMDS Coating (#56) on Kapton Bent Over 15-Mil Radius	291
Figure 87: CVI-1144-0 Siloxane Coating (#65) on Kapton Bent Over a 40-Mil Radius	293
Figure 88: CVI-1144-0 Siloxane Coating (#65) on Kapton Bent Over a 15-Mil Radius	293
Figure 89: CVI-3530 Fluorosilicone Coating (#66) on Kapton Bent Over a 40-Mil Radius	295
Figure 90: CVI-3530 Fluorosilicone Coating (#66) on Kapton Bent Over a 15-Mil Radius	295
Figure 91: HMDS/TFE Coating (#49) on Kapton Bent Over a Radius of 40-Mil	297
Figure 92: HMDS/TFE Coating (#49) on Kapton Bent Over a Radius of 15-Mil	297
Figure 93: Plasma Polymerized HMDS/TFE Coating (#51) on Kapton Bent Over a 40-Mil Radius	299
Figure 94: Ethyl X-128 (#58) Coating on 1-Mil Kapton Bent Over a Radius of 15-Mil	299
Figure 95: CVI-3530 Fluorosilicone Coating (#70) on Kapton Bent Over 40-Mil Radius	301
Figure 96: CVI-3530 Fluorosilicone Coating (#70) on Kapton Bent Over 15-Mil Radius	301
Figure 97: Largest Cracks Observed in CVI-3530 Fluorosilicone Coating (#70) When Bent Over 15-Mil Radius When Bent Over 15-Mil Radius	303
Figure 98: CVI-1144-0 Silicone Coating (#71) on Kapton Bent Over a 15-Mil Radius	303
Figure 99: LeRC Siloxane Coating on Kapton Bent Over 40-Mil Radius	305
Figure 100: LeRC Siloxane Coating on Kapton Bent Over 15-Mil Radius	305
Figure 101: X-128 Coating (#58) on Kapton Bent Over 15-Mil Radius. Sample Previously Exposed to Combined Vacuum Thermal Cycling/UV Radiation	307

	<u>PAGE</u>
Figure 102: X-128 Coating (#58) on Kapton Bent Over 15-Mil Radius. Sample Previously Exposed to Combined Vacuum Thermal Cycling/UV Radiation	307
Figure 103: EDAX Spectrum of X-128 Coating. Sample Was Previously Exposed to Combined Vacuum Thermal Cycling/UV Radiation	309
Figure 104: CV1-1144-0 Silicone Coating (#65) on Kapton Bent Over 15-Mil Radius. Sample Previously Exposed to Combined Vacuum Thermal Cycling/UV Radiation.	311
Figure 105: CV1-1144-0 Silicone Coating (#65) on Kapton Bent Over 15-Mil Radius. Sample Previously Exposed to Combined Vacuum Thermal Cycling/UV Radiation.	311
Figure 106: CV1-1144-0 Siloxane Coating (#65) on Kapton Bent Over a 15-Mil Radius	313
Figure 107: CV1-1144-0 Siloxane Coating (#65) on Kapton Bent Over a 40-Mil Radius	313
Figure 108: EDAX Spectrum of CV1-1144-0 Siloxane Coating on Kapton	315
Figure 109: EDAX Spectrum of CV1-1144-0 Siloxane Coating on Kapton Sample Previously Exposed to Combined Vacuum Thermal Cycling/UV Radiation	317
Figure 110: Region of HMDS Coating (#50) on Kapton Showing a Crack When Bent Over a 15-Mil Radius. Sample Previously Exposed to Combined Vacuum Thermal Cycling/UV Radiation	319
Figure 111: HMDS Coating (#50) on Kapton. Sample Previously Exposed to Combined Vacuum Thermal Cycling/UV Radiation.	319
Figure 112: EDAX Spectrum of HMDS Coating (#50) on Kapton	321
Figure 113: EDAX Spectrum of HMDS Coating on Kapton. Specimen Previously Exposed to Combined Vacuum Thermal Cycling/UV Radiation	323
Figure 114: HMDS Coating (#50) on Kapton Bent Over 40-Mil Radius. Sample Exposed to Combined Vacuum Thermal Cycling/UV Radiation.	325
Figure 115: HMDS Coating (#50) on Kapton Bent Over 15-Mil Radius	325
Figure 116: HMDS Coating (#50) on Kapton Bent Over a 40-Mil Radius	327

	<u>PAGE</u>
Figure 117: Plasma Polymerized HMDS/TFE Coating on Kapton Bent Over a 15-Mil Radius. Sample Previously Exposed to Combined Vacuum Thermal Cycling/UV Radiation.	327
Figure 118: EDAX Spectrum of HMDS/TFE Coating on Kapton	329
Figure 119: EDAX Spectrum of HMDS/TFE Coating on Kapton. Sample Previously Exposed to Combined Vacuum Thermal Cycling/UV Radiation	331
Figure 120: HMDS/TFE on Kapton Bent Over 40-Mil Radius. Sample Previously Exposed to Combined Vacuum Thermal Cycling/UV Radiation.	333
Figure 121: HMDS/TFE Coating on Kapton Bent Over 15-Mil Radius	333
Figure 122: HMDS/TFE Coating on Kapton Bent Over 40-Mil Radius	337
Figure 123: CV1-3530 Fluorosilicone Coating (#66) on Kapton Bent Over 15-Mil Radius. Sample Previously Exposed to Combined Vacuum Thermal Cycling/UV Radiation.	337
Figure 124: EDAX Spectrum of CV1-3530 Fluorosilicone Coating (#66) on Kapton	339
Figure 125: EDAX Spectrum of CV1-3530 Coating on Kapton. Sample Previously Exposed to Combined Vacuum Thermal Cycling/UV Radiation	341
Figure 126: CV1-3530 Fluorosilicone Coating on Kapton Bent Over a 40-Mil Radius. Sample Previously Exposed to Combined Vacuum Thermal Cycling/UV Radiation.	343
Figure 127: CV1-3530 Fluorosilicone Coating on Kapton Bent Over 40-Mil Radius	343
Figure 128: SEM Beam Damage to Previously Identified Region of CV1-3530 Fluorosilicone Coating (#66) on Kapton Bent Over 15-Mil Radius	345
Figure 129: SEM Beam Damage to Previously Identified Region of CV1-3530 Fluorosilicone Coating (#66) on Kapton Bent Over 15-Mil Radius. Sample Previously Exposed to 15-Mil Radius. Sample Previously Exposed to Combined Vacuum Thermal Cycling/UV Radiation	345
Figure 130: CV1-3530 Fluorosilicone Coating on Kapton Bent Over 15-Mil Radius	347
Figure 131: X-Ray Photoelectron Spectrum of CV1-1144-0 (Silicone) Coating on Kapton. The Sample Was Not Previously Exposed to Atomic Oxygen.	355

	<u>PAGE</u>
Figure 132: X-Ray Photoelectron Spectrum of CV1-1144-0 (Silicone) Coating on Kapton. The Sample Was Previously Exposed to Atomic Oxygen for 48 Hours.	357
Figure 133: X-Ray Photoelectron Spectrum of CV-3530 (Fluorosilicone) Coating on Kapton. The Sample Was Not Previously Exposed to Atomic Oxygen.	359
Figure 134: X-Ray Photoelectron Spectrum of CV-3530 (Fluorosilicone) Coating on Kapton. The Sample Was Previously Exposed to Atomic Oxygen for 24 Hours.	361
Figure 135: X-Ray Photoelectron Spectrum of X-128 (Phosphazene) Coating on Kapton. The Sample Was Not Previously Exposed to Atomic Oxygen.	363
Figure 136: X-Ray Photoelectron Spectrum of X-128 (Phosphazene) Coating on Kapton. The Sample Was Previously Exposed to Atomic Oxygen for 49 Hours.	365
Figure 137: X-Ray Photoelectron Spectrum of Plasma Polymerized Hexamethyldisiloxane Coating on Kapton. The Sample was not Previously Exposed to Atomic Oxygen.	367
Figure 138: X-Ray Photoelectron Spectrum of Plasma Polymerized Hexamethyldisiloxane Coating on Kapton. The Sample was Previously Exposed to Atomic Oxygen for 48 Hours.	369
Figure 139: X-Ray Photoelectron Spectrum of Plasma Polymerized Hexamethyldisiloxane Coating on Kapton. The Sample was Previously Exposed to Atomic Oxygen for 25 Hours.	371
Figure 140: X-Ray Photoelectron Spectrum of Plasma Polymerized Hexamethyldisiloxane/Tetrafluoroethylene Coating on Kapton. The Sample Was Not Previously Exposed to Atomic Oxygen.	373
Figure 141: X-Ray Photoelectron Spectrum of Plasma Polymerized Hexamethyl-disiloxane/Tetrafluoroethylene Coating on Kapton. The Sample Was Previously Exposed to Atomic Oxygen for 95.75 Hours.	375
Figure 142: X-Ray Photoelectron Spectrum of Plasma Polymerized Hexamethyl-disiloxane/Tetrafluorethylene Coating on Kapton. The Sample Was Previously Exposed to Atomic Oxygen for 95.75 Hours.	377
Figure 143: X-Ray Photoelectron Spectrum of Plasma Polymerized Hexamethyl-disiloxane/Tetradfluoroethylene Coating on Kapton. This Spectrum is an Expansion of the Region Around the Nitrogen Peak in the Spectrum From Figure 142.	379

	<u>PAGE</u>
Figure 144: Atomic Oxygen Facility Data Base	400
Figure 145: Combined UV/Thermal Cycling Test Results & Blocking and Peel Test Results	401
Figure 146: Combined Effects Data Base	401
Figure 147: X-Ray Photoelectron Spectroscopy Data	403
Figure 148: Atomic Oxygen Data Base - Results	404
Figure 149: Mass Loss of Kapton Exposed to an Atomic Oxygen Plasma. Specimens Were 1.5" in Diameter.	406
Figure 150: Mass Loss of TFE Exposed to an Atomic Oxygen Plasma. Specimens Were 1.5" in Diameter.	407
Figure 151: Mass Loss of FEP Exposed to an Atomic Oxygen Plasma. Specimens Were 1.5" in Diameter.	408

LIST OF TABLES

	<u>PAGE</u>
Table 1: Space Station External Surfaces and Candidate Materials Types	7-8
Table 2: Atomic Oxygen Flux and Fluence on Space Station	14
Table 3: Data From Plasmod Measurements	25-35
Table 4: Material Identification Code For Test Specimens Examined Under This Contract	37-65
Table 5: Mass Loss Data Obtained From Original Chamber	67-77
Table 6: Mass Loss of Kapton as a Function of Atomic Oxygen Exposure. Sample Temperature was 149°C.	83
Table 7: Mass Loss of Kapton as a Function of Atomic Oxygen Exposure. Sample Temperature was 185°C.	83
Table 8: Mass Loss of Kapton as a Function of Atomic Oxygen Exposure. Sample Temperature was 195°C.	85
Table 9: Mass Loss of Kapton as a Function of Atomic Oxygen Exposure. Sample Temperature was 100°C.	87
Table 10: Mass Loss of Kapton as a Function of Atomic Oxygen Exposure. Sample Temperature was 85°C.	89-93
Table 11: Test Parameters for the Combined Vacuum Thermal Cycling/Ultraviolet Radiation Exposure, Fall 1986.	107
Table 12: Test Parameters for the Combined Vacuum Thermal Cycling/Ultraviolet Radiation Exposure, Spring 1988.	109
Table 13: Parameters For Combined Effects Test Exposure, Spring 1987	111
Table 14: Irradiation Parameters and Test Sequence for Combined Effects Exposure: Mid-1988	113
Table 15: Optical Properties of Selected Samples Before and After Sample Exposure to Vacuum Thermal Cycling Conditions. Data From Test Conducted in Late 1986.	118
Table 16: Average Weight Loss of Materials Exposed to UV/Thermal Vacuum Cycling Conditions. Data From Test Conducted in Late 1986.	118

	<u>PAGE</u>
Table 17: Results of Optical Properties Measurements on Selected Materials. Coatings are Applied to Kapton. Specimens are Control Samples for Comparison With Samples From Combined Vacuum Thermal Cycling/UV Exposure Test of Early 1988.	127
Table 18: Results of Measurements of Optical Properties of Specimens Exposed to the Combined Vacuum Thermal Cycling/UV Environment.	129
Table 19: Average Change in Optical Properties of Selected Materials Due to Exposure to the Combined Thermal Vacuum Cycling/Ultraviolet Radiation Environment.	131
Table 20: Optical Properties of Materials Exposed to the Combined Radiation Effects Test Chamber Environment at the Boeing Radiation Effects Laboratory. Results From Tests Conducted in Early 1987.	134
Table 21: Solar Absorptance Values for Selected Materials as a Function of Combined Radiation Effects Dose Level. Values are for In Situ Measurements From Test of Early 1987.	135
Table 22: In Situ Absorptance Measurements on Materials Under Simultaneous Exposure to Protons, Electrons, and Simulated Solar UV Radiation.	141- 147
Table 23: Emissivity of Specimens Subsequent to Exposure in the Boeing Combined Effects Test Chamber.	149
Table 24: Results of XPS Analysis of Specimens Previously Exposed to the Combined Vacuum Thermal Cycling, Simulated Solar UV Environments During Test of Early 1988.	159
Table 25a: Mass Loss of Selected Materials After Exposure to Atomic Oxygen for 24 Hours. Samples Designated (BREL) Were Previously Exposed to a Combined Vacuum Thermal Cycling Ultraviolet Radiation Environment During Test of Early 1988. Samples Were Held at 85°C During Exposure to Atomic Oxygen.	161
Table 25b: Mass Loss of Selected Materials, Held at 85°C, After Varying Periods of Exposure to Atomic Oxygen.	163
Table 26: Summary of Results of Peel Tests. Sample Contact Areas Were 1 Inch Square. Ten Samples Were Held Under a Total Weight of 10.18 lbs. for 8 Days.	165
Table 27: Results of 90° Peel Test on Selected Specimens.	166
Table 28: Results of 90° Peel Test on Selected Specimens.	167

	<u>PAGE</u>
Table 29: Results of Peel Tests for Specimens Previously Exposed to Atomic Oxygen in the Materials Screening Chamber.	168
Table 30: Results of Bend Radius Tests on Selected Materials	169
Table 31: Results of Outgassing Tests on Selected Materials	173
Table 32: Results of Flatwise Tension Tests on Selected Materials	175
Table 33: Results of X-Ray Photoelectron Spectroscopy Surface Analysis on Selected Coating Specimens.	207
Table 34: Results of XPS Analysis of Specimens Previously Exposed to the Combined Vacuum Thermal Cycling, Simulated Solar UV Environments.	215
Table 35: Results of X-Ray Photoelectron Spectroscopy Surface Analysis on Coating Specimens. Coating Thickness Greater Than 0.1 Mil.	351
Table 36: Results of X-Ray Photoelectron Spectroscopy Surface Analysis on Ultrathin (20000 A) Coatings From Battelle.	353
Table 37: Results of X-Ray Photoelectron Spectroscopy Surface Analysis on Selected Coating Specimens.	381
Table 38: Results of X-Ray Photoelectron Spectroscopy Surface Analysis on Ultrathin (20000 A) Coatings From Battelle.	383
Table 39: Results of X-Ray Photoelectron Spectroscopy Surface Analysis Ultrathin (20000 A) Coatings From Battelle.	385
Table 40: Parameters For Battelle's Large Scale Demonstration	389
Table 41: Plasma Polymerized Coatings Deposited Onto One Side Of 18-Inch Wide Kapton	391
Table 42: Plasma Polymerized Coatings Deposited Onto Both Sides Of 6-Inch-Wide Kapton	393
Table 43: Coatings on 18 x 18-inch Samples	395
Table 44: Mass Loss of Selected Materials Relative to Kapton Mass Loss, Under Exposure to Atomic Oxygen. For Long Term Exposure RF Power was 200 Watts During First Six Hours of Exposure and 350 Watts for Remainder of Exposure. For Short Term of Six Hour Exposure, RF Power was 250 Watts. Samples Were Maintained at 195°C.	411
Table 45: Mass Loss of Selected Materials Relative to Kapton Mass Loss Under Exposure to Atomic Oxygen. Samples Maintained at 85°C.	412

	<u>PAGE</u>
Table 46: Mass Loss Ratio of Selected Coatings vs. Uncoated Kapton Upon Exposure to Atomic Oxygen. Sample Temperature Maintained at 85°C.	413
Table 47: Mass Loss of Battelle HMDS/TFE Mixtures Relative to Kapton Mass Loss, Under Exposure to Atomic Oxygen. Samples Were Maintained at 85°C. Atomic Oxygen Flux was $4 \times 10^{16}/\text{cm}^2\text{-Sec.}$	414
Table 48: Mass Loss Ratio fo CV-3530 (#66) and HMDS/TFE, 9:1 Ratio (#112) Coatings Relative to Kapton vs. Exposure to Atomic Oxygen. Samples Were Maintained at 85°C.	415
Table 49: Mass Loss of Kapton and Apical Under Exposure to Atomic Oxygen of Simultaneous Exposure to Atomic Oxygen and UV Radiation.	417
Table 50: Material Lifetime Estimates for Selected Candidate Materials	418

CHAPTER 1

Introduction

This report is organized by contract task element. This introduction includes a summary statement of efforts carried out under each task element. Each task element is the subject of a separate chapter. Conclusions based on this contract are presented in the final section; the relative ranking of the candidate materials, together with the limitations of each; and a prediction of on-orbit lifetimes for the better materials.

Task Element 1

The first section is a generic list of Space Station surfaces and candidate material types. Each specific material considered must meet NASA specification SSP 30233 for materials, as a minimum to be qualified for space use.

Task Element II

This section is a list of environmental exposures and performance requirements for the different Space Station surfaces. These requirements are generic. Detailed requirements will be written into the program specifications.

Task Element III

There are two technological issues to be solved regarding development of Space Station external coatings. The first is development of the coating materials and the processing required to produce a viable system. The second is the development of appropriate environmental simulation test facilities. Neither of these issues has reached a satisfactory stage of development for

coatings which are also required to be flexible. The lifetime of the relatively best systems are still short relative to the Space Station life. Efforts under this contract were to look primarily at flexible coatings on Kapton. There is very little long term space qualification data available for materials. The best indications are from actual on orbit performance of materials. However, material performance is very orbit dependent and direct observation is limited to the few shuttle flights and the hardware recovered from the Solar Maximum Recovery Mission. While the development of test chambers has continued long term, the efforts have been to develop sources and conduct short term simulations. This has been in response to direct needs and is appropriate. However, with the unique combination of factors at Low Earth Orbit and the long term requirements of Space Station and other spacecraft being considered, the needs have shifted. The materials test capability and means to verify hardware performance are not in place.

Task Element IV

This section contains the results of the majority of the technical effort on this contract. There are three major parts to this discussion. One, the mass loss data from the original version of the atomic oxygen test chamber and from the improved test facility of the type built for NASA-MSFC under this contract. Two, the additional environmental exposures carried out on candidate materials. This includes the combined vacuum thermal cycling/simulated solar ultraviolet exposure and the combined radiation effects tests which included exposures to some or all of available proton, electron, simulated solar UV, and Lyman (121.6 nm) vacuum ultraviolet radiation fluxes. Three, materials properties measurements on candidate coatings to determine the effects of the exposures. Measurements include solar absorptance, infrared

emittance, surface analysis by scanning electron microscopy and X-ray photo-electron spectroscopy, blocking and peel tests, bend radius tests for flexibility, outgassing, and flatwise tension measurements.

Task Element V

This section describes the methodologies of production, and coating materials, used to produce the large scale demonstration articles. These are relatively large area specimens built to establish the feasibility of producing quality coatings on Kapton with currently available processes.

Task Element VI

This section describes the electronic data base developed for this contract. This data base was built using the SMART software package on a Zenith 150 PC. The subjects included are, data from mass loss of materials exposed to atomic oxygen in the lab, on-orbit data, data from the four combined effects test exposures, data from optical and surface properties of lab test samples, a summary of atomic oxygen test facilities under development, and a literature survey on effects of atomic oxygen on materials.

Task Element VII

A test chamber to be used for exposure of materials to atomic oxygen has been built. This section describes the capabilities and limitations of the test chamber, the methodology for measuring the oxygen atom flux, and experimental and maintenance procedures for this apparatus.

(THIS PAGE INTENTIONALLY LEFT BLANK)

ORIGINAL PAGE IS
OF POOR QUALITY

CHAPTER 2

Candidate Exterior Space Station Surfaces and Their Environmental Exposures

While the detailed definition of the Space Station external surfaces waits on the final design, there are several points which will be only slightly affected by the final configuration. A very large fraction of the external surface area will be meteoroid shielding covered by a thermal control system. The surface which will be in the most severe environment is the sun facing side of the solar array panels. All surfaces must withstand the general types of environmental exposures discussed in the section on task element II.

External surfaces for the Space Station can be grouped into twelve broad categories. The categories are listed in table 1, together with candidate materials for each surface.

PRECEDING PAGE BLANK NOT FILMED

(THIS PAGE INTENTIONALLY LEFT BLANK)

Flexible Elements of Solar Array Panel Assembly	Kapton H Film Silver
Circuit Interconnects	Molybdenum
Composite Structural Elements	Epoxy/Fiberglass Epoxy/Graphite
Metal Structural Elements	Aluminum Inconel Chrome Plate Steel Alloys
View Ports	Fused Silica Vycon Aluminosilicate Glass Chemically Tempered Glass Soda Lime Glass Acrylic (Inner Pane) Polycarbonate (Inner Pane)
Multilayer Insulation (MLI)	Beta Cloth Aluminized Kapton Dacron Net Teflon Fasteners Adhesives for Standoff-Module Bonds Thermal Isolation Plates "Velcro" Fasteners Aluminized Mylar

Table 1: Space Station External Surfaces and Candidate Materials Types

(THIS PAGE INTENTIONALLY LEFT BLANK)

Thermal Radiation Surfaces	Silver-Teflon Thermal Control Coating Silicone Coating
Micrometeoroid/Debris Shield For MLI	Silver-Teflon Thermal Control Coating White Pigmented Coating on Aluminum Aluminum Pigmented Silicone Thermal Control Coating Ceramic Standoff For Debris Shield
Hatch and Shaft Seals	Silicones Fluorosilicones Fluorophosphazenes Butyl Rubber
Power Harness	Modified Silicone Polyimide
Metallic Electrical Connectors and Accessories	Aluminum Alloys Beryllium Copper Stainless Steel Alloys Steel Alloys Nickel Gold Plating Tin Silver

Table 1 (Continued): Space Station External Surfaces And
Candidate Material Types

(THIS PAGE INTENTIONALLY LEFT BLANK)

CHAPTER 3

Requirements of Space Station External Surfaces

The critical requirements of spacecraft external surface materials relate to the nature of the orbital environment and functions of the surface. Critical requirements include; vacuum stability, low solar absorptance; high infrared emittance; resistance to electron, proton and ultraviolet radiation; resistance to atomic oxygen; and durability under meteoroid impact. Consideration must also be given to the prelaunch environment and ground handling operations. However, the problems presented by qualification to prelaunch conditions are not unique to spacecraft and can generally be handled by familiar methodology. Resistance to handling, solvents, salt water mist exposure, fungus, and to temperature extremes are some considerations.

Outgassing

The specification covering vacuum stability is NASA SP-R-0022A, General Specification, Vacuum Stability Requirements of Polymeric Materials for Spacecraft. The Specification applies to polymeric materials used around sensitive optical or thermal control surfaces in vacuum and is applicable to external thermal control and solar array materials. The general requirement for outgassing defined by the specification is that polymeric materials shall not contaminate sensitive surfaces within an assembly and shall not affect adjacent equipment. Specific requirements are also defined for total mass loss (TML) and for volatile condensable material (VCM). The limits specified are 1% for TML and 0.1% for VCM when measurements are taken according to specified procedures. Materials failing the specific TML and VCM requirements can be used if the design organization can show that the general requirements of the

specification are satisfied. However, vacuum stability is a very severe requirement that can not be passed by most polymeric materials that are compounded for commercial applications.

Optical Properties

Overall specifications for surface optical properties are not available. Specifications for a number of thermal control paint and foil materials are available and these can be considered space qualified. In general, thermal management requirements necessitate that the ratio of solar absorptance to infrared emittance be less than 0.3 at the end of service. Coating optical properties degrade during service life. This means that the beginning of life absorptance to emittance ratio be very much less than the limit used for design of the thermal management system. A beginning life ratio of 0.10 would be typical for a transparent thermal control foil with a reflective, opaque coating on the second surface.

Optical properties of surfaces are affected by interaction of the various factors that define the orbital environment; vacuum, thermal cycling, atomic oxygen, meteoroids and debris, proton flux, electron flux, and solar ultraviolet radiation. Testing and qualification of external surface materials is complex. One complication is introduced by the tendency of a coating material to recover a part of its lost transparency upon being returned to atmospheric pressure after exposure to any of the above environments. Reliance cannot generally be placed on optical property changes determined from measurements taken ex situ before and after exposure to simulated conditions of service. However, the dictates of economy require that materials research and development efforts be guided by sample measurements taken at atmospheric pressure. Truly reliable measurements should be made in situ under simulated conditions of exposure.

Final qualification of materials requires testing in elaborate facilities. The accuracy of testing for a material intended to survive 15 years in space is marginal.

Resistance to atomic oxygen is required for external surface materials used on vehicles operating in low earth orbit. Three factors are thought to contribute to the reaction of oxygen with polymeric materials in orbit. These factors are the translational energy of atomic oxygen colliding with the spacecraft surface, the thermodynamic stability of potential oxidation products, and the release of energy caused by recombination of atomic oxygen to form molecular oxygen. Each of these processes provides 4 to 5 electron volts of energy, sufficient to disrupt all but the strongest bonds in a polymeric material. Materials screening tests are currently being conducted by Boeing in an atomic oxygen test apparatus using oxygen atoms at thermal energies. It should also be appreciated that facilities simulating translational velocity and/or the large mean free path between collisions may be needed to verify and to extend the theoretical work done thus far.

The qualification of external surface materials for prelaunch conditions, although demanding, follows methods already developed for non-space systems. A laboratory test was carried out which simulates the exposure a material experiences during the solar array manufacturing process. Several candidate coatings were tested.

Lockheed is using a design temperature range of +25°C to -80°C for the Space Station solar arrays, -80°C to 80°C for silver interconnects and a test temperature range of +40°C to -100°C. A design lifetime of 15 years is used for the arrays, except 3 to 10 years is used for electrical sizing for degradation.

Table 2 is a summary generated in 1986 by the System Dynamics Laboratory

at MSFC showing flux and fluence of atomic oxygen on Space Station solar arrays under worst case conditions of constant atomic oxygen density. Data in Table 2 is based on the Space Station operating with a drag acceleration $0.3 \times 10^{-6} \text{ g's}$.

Ballistic Coefficient, BC	=	60.0 (Kg/m ²)
Relative Velocity, VR	=	7223 (m/s)
Atomic Oxygen Density Number	=	$0.218 \times 10^{+09}$ (Counts/cm ³)
Flux	=	$1.575 \times 10^+ 14$ (Counts/cm ² -Sec)
Fluence:		
RAM Direction	=	$4.983 \times 10^+ 22$ (Counts/cm ² -10 yrs)
Solar Arrays, Track Sun		
Sun Side	=	$1.006 \times 10^+ 22$ (Counts/cm ² -10 yrs)
Black Side	=	$1.869 \times 10^+ 22$ (Counts/cm ² -10 yrs)
Thermal Radiators each side	=	$1.053 \times 10^+ 22$ (Counts/cm ² -10 yrs)

Table 2: Atomic Oxygen Flux and Fluence on Space Station

All external surface materials are required to be atomic oxygen resistant. This requires that a protective coating be applied to the surface of the Kapton H, because Kapton H is not itself resistant to atomic oxygen. The coating must have low outgassing characteristics and must be an electrical insulator for the application.

Circuit interconnects also require protection from atomic oxygen. However, closure of cut-outs made in the panel assemblies in order to weld or connect electrical conductors is needed to protect exposed Kapton surfaces. Silver is readily attacked by atomic oxygen and will require an atomic oxygen resistant coating.

Epoxy/fiberglass is being considered for the mast assembly and Epoxy/graphite for the blanket container box. Protection of these surfaces could be provided by a number of different schemes, however an opaque white paint with an atomic oxygen resistant binder or an aluminum foil wrap are probably the most effective approaches.

Most metals are resistant to atomic oxygen attack. They require coatings to control surface optical properties. The coating should provide for low solar absorptance and high infrared emittance. Metal structural elements, thermal radiation surfaces and micrometeoroid/debris shields have similar requirements for coatings. Either a white paint can be applied to these surfaces or a second surface thermal control coating can be bonded over the metal. A silverized Teflon film could have an absorptance to emittance ratio of 0.15 or less for a 1-mil Teflon film. However, problems may be encountered in the atomic oxygen resistance of Teflon. Teflon (TFE) is much more resistant to atomic oxygen attack than are organic and polyfluorinated organics, however results of laboratory screening tests show that TFE can be rapidly eroded in certain conditions. View ports for the module will need to be made of atomic oxygen resistant transparencies. Glass and fused silica are both resistant to atomic oxygen.

Multilayer insulation is a special category. If the shielding provided prevents exposure of the insulation to atomic oxygen then, atomic oxygen resistance is not a requirement and existing materials can be used. However, some theoretical work shows that atomic oxygen may migrate through shield surface openings and that the rate of attack on imperfectly shielded materials could be substantial.

Should an atomic oxygen resistant multilayer insulation be needed, then ion implanted metalized coatings would be a good choice for research.

Ordinary vacuum deposited coatings without treatment do not protect organic substrates sufficiently.

Double metalized radiation barriers used in multilayer insulation cannot be overcoated without increasing infrared emittance. This situation precludes the use of protective coatings such as silicones for atomic oxygen protection of MLI barrier plies.

Hatch and shaft seals can be fabricated from molded silicone, fluorosilicone and fluorophosphazene rubber materials. These materials are atomic oxygen resistant, have low outgassing characteristics, and can be molded in various shapes. Because of the small areas exposed, optical properties should not be of concern.

The power harness application can be met in various ways. For example, a white paint could be applied over an adhesively held wire sheath.

Solar Power Panels

There are three classes of surface to be considered, the structure between the cells on the sun facing side of the panel, the structure of the opposite side of the panel, and the transparent covers over the cells on the sun facing side of the panels. The structure exposed to solar radiation should have a high thermal emittance and low solar absorptance. A white paint would best meet the requirements. Typical properties are as follows: $\epsilon = 0.26/0.83 = 0.31$ (end life maximum). The allowable change in the ϵ/α ratio is a 10% increase over a ten year life.

The structure opposite the sun facing side of the solar power panel also requires high thermal emittance and low solar absorptance. However, the emphasis is on high thermal emittance because the only solar radiation normally received by the panel is planetary reflected at relatively low intensities. The optical properties requirements of the panels are not

effected by earth thermal radiation because the panel temperature and earth average temperature are of the same order of magnitude. The paint used on this portion of the structure should be white rather than black, because white paint has thermal emittance almost as high as black paint and has much lower solar absorptance. In addition, white paint handles earth reflected radiation and incidental exposure to direct solar radiation better than black paint. Typical requirements on the ratio would be the same as for the sun facing side.

The transparent covers for the solar cells are an integral part of the cell design and the responsibility of the solar cell designer. Ideally, the cover would be transparent for wavelengths shorter than 0.3 micrometers and black for wavelengths in the infrared region.

The requirement cited above are quite severe. It is not clear that any white thermal control paint exists which will survive long term in a space environment without much thicker applications than now appear reasonable.

(THIS PAGE INTENTIONALLY LEFT BLANK)

CHAPTER 4

Critical Technology Deficient Areas

Critical technology deficient areas include the following requirements for solar array design; flexible atomic oxygen resistant protective coatings for Kapton H film, and atomic oxygen resistant protective coatings for epoxy/fiberglass structural elements, and for silver interconnects.

To the above list of critical technology deficient areas, it may be necessary to add an atomic oxygen resistant multilayer insulation material, if it is shown that multilayer insulation used on the Space Station modules is subject to attack by atomic oxygen leaking through openings in module shields.

Data deficiencies for candidate materials include:

1. Fabrication and processing details for plasma deposited siloxane films and sputter deposited oxide films.
2. Processing and compounding requirements to produce tack free silicone and fluorosilicone coatings.
3. Refined processing and compounding requirements for fabrication of coatings from fluorophosphazene.
4. Atomic oxygen resistance data on candidate materials.
5. Thermal-vacuum cycling and UV resistance data on materials.
6. Combined radiation effects on optical properties.
7. Processing integrity data and design data for the various applications.

The flexibility requirement for the coating on the solar array panel is an extremely tough requirement. To date, no coating which passes the initial flexibility standard has also been free of the tack/blocking problem.

Test coatings were not optimized with respect to processing quality. This

leads to consideration of certain commercial techniques for the large scale demonstration of candidate coating(s). A general consideration for all types of coatings is how to achieve as high quality coatings as possible in terms of uniformity of thickness, minimization of pinholes, scratches or other processing damage, and adhesion to substrate. Coatings must be non-porous, low outgassing, non-tacky, must not "block" when rolled, and any filler material must be blended uniformly into the coatings. Achievement of coatings of sufficient quality may require extraordinary processing steps, close control of application conditions, and possibly multiple applications of very thin coatings and/or production of extra units to achieve enough pieces of satisfactory quality. Extra steps will cause increased costs, but this may be necessary to produce a quality coating which will meet all the requirements for long term (10-30 years) survivability in the low Earth orbit environment.

Silicones, fluorosilicone, and fluorophosphazene materials which we have been testing have a general problem with tackiness. Attempts to overcome this problem by adding fillers to certain of these materials have created brittle coatings which crack upon bending.

To date no sufficiently oxidation resistant, transparent, flexible coating material exists which will withstand the LEO environment for the lifetimes required by the Space Station.

No currently existing test chamber allows simultaneous exposure to all the relevant environmental factors. In particular, resistance to simultaneous exposure to atomic oxygen and solar ultraviolet radiation will be an essential property of selected materials. No facility with this testing capability exists, particularly with a source of vacuum ultraviolet emission.

While many of the elements required for a meaningful simulation exist in one or more facilities, all necessary features have yet to be combined in one

apparatus. Attempts are being made to use light titration techniques in plasma chambers to overcome lack of knowledge of flux levels in test chambers.

Beam facilities offer mean free paths which are large compared with sample size. The particle dynamics are thus similar to the on-orbit situation.

The atomic oxygen facility used for this study allows measurement of the temperature dependence of coating oxidation and isolates the effect of neutral atomic oxygen from other factors. However, it suffers from the drawback of operating at relatively high pressure (0.1 torr) with short mean free paths and the potential for product species to be scattered back onto the specimen. Furthermore, the gas stream to the sample is a mixture of oxygen atoms and molecules. The presence of the molecular species can slow the oxidation rate by blocking the atoms from reaching reactive sites on the surface. This effect may be very important because plasma sources of moderate energies (50-500 watts) typically produce only a few percent (20%) oxygen atoms.

Risks

Current attempts to solve the problems of long term survivability of materials in space offer rather temporary fixes with high maintenance and refurbishment costs. One option is to accept short lifetimes and replace components as they fail. A second option for extending lifetimes is to make thicker coatings and/or substrate materials, pay the weight penalty and accept the high degradation rates. These "solutions" have serious problems.

An attempt at a true solution is to make intrinsically stable materials. This involves a risk; not all potential candidates can be developed, a selection process must be used to select the most promising molecular structures. One cannot know in advance if a new material will perform as expected. If more intrinsically resistant materials are developed it should still be recognized that the chemical stability of any material is finite; even the strongest bonds are at most about 10 ev, and given the opportunity (presence of oxygen atoms and energy), eventually the most thermodynamically stable forms will dominate.

CHAPTER 5

Materials Testing

The epoxy/S-glass will degrade due to attack of AO on epoxy matrix. This may result in reduced strength of members made of epoxy/S-glass. The S-glass fibers are silicate based (fully oxidized) and are not expected to degrade. The members which are used in deployment are subject to high strain and abrasion.

In the Boeing Materials screening chamber, preferential attack by atomic oxygen occurs near the edge of the exposed area of individual test specimens. The samples are held under compression between two plates of aluminum. The region of the sample near the lip of the front plate of aluminum is stretched. Subsequent to exposure to atomic oxygen a ring pattern of visibly thinner material, when compared with the thickness at the center of the exposed area, is observed.

During certain runs samples were etched completely through the material. Samples of Kapton put on a ceramic mount and placed under tension severed where the Kapton was pulled over a curved surface. The effect of a material being under tension or compression during exposure to atomic oxygen has not been quantitatively determined. The expectation is that materials in this situation will be subject to greater deterioration than identical materials at equilibrium.

Sealant tapes, wire insulation and urethane paints have been exposed simultaneously to oxygen atoms, excited state molecules, ions, UV and RF energy in a Plasmod. The wire insulation was significantly affected and the sealant tapes exhibited an eroded surface layer. Most of the urethane paints were

severely degraded; complete mass loss occurred in some cases and a chalky surface remained in others.

During extended exposure (72 hours) tests, sheet teflon exhibited little weight loss, but did show a definite loss in hardness as shown by decreased durometer measurements. Further extended exposure tests on sheet teflon continued to show a small effect due to atomic oxygen. LTV-FOSR (flexible optical solar reflector) exhibited little weight loss during a 2 hour exposure. Dow Corning sealants RTV 730 and 1-2577 showed low weight losses and were slightly discolored. GE-RTV 566 also showed resistance to the effects of atomic oxygen during preliminary (2 hour) screening tests. Results of these measurements are shown in table 3.

Teflon-coated Kapton from Dupont was tested in the Plasmod and showed little improvement over uncoated Kapton. The Dupont elastomer Kalrez 4079 exhibited little weight loss during preliminary screening tests, however a fine ash layer was observed on the samples at the conclusion of each test. Aclar (a polyimide) film made by Allied Chemical was similar to Kapton in performance.

Atomic oxygen screening tests have been conducted on a wide variety of materials. Materials with low atomic oxygen resistance include the following classes; polyimides, untreated metallized coatings, fluorocarbon blends, fluoroelastomers, and hydrocarbons in general. Table 4 provides a summary of materials considered for testing under this contract.

Additional testing is needed to evaluate teflon films. It may work out that a substitute for the silverized-teflon thermal control coating being considered for the module radiators will be needed.

<u>Material</u>	<u>Exposure (Mins)</u>	<u>Ave. Mass Loss %</u>	<u>Comments</u>
FC-721, 3M "Fluorad'	120	100.000	No Visible Remains
PBI, Celanese Polybenzimidazole	120	98.710	Only Brownish Caste Left on Slide
0.2 Mil Kapton in O2	60	87.240	
FC-725, 3M "Fluorad'	120	58.280	Brownish Caste on Samples
G405120, Sheldahl 2 Mil Kapton x AL	120	51.400	Samples Were Wrinkled And Then Exploded When The Vacuum Was Released
PPS, Polyphenylsulfide	120	47.780	
Teflon Tape	180	39.710	Tape Was Like Tissue Paper
G411520, Sheldahl AL/2.MIL/Kapton	120	38.320	Samples Had Crinkled Edges
Teflon Tape	120	34.760	
Teflon Tape	90	22.650	
0.2 Mil Kapton in Air (Compressed)	60	21.400	
Teflon Tape	60	17.960	
G411474, Al/0.3 Mil/Kapton Sheldahl Perforated	120	16.380	
G404950, Sheldahl Gold On 5. Mil Kapton	120	14.630	Sample Surface Was Etched
Polycarbonate	120	11.160	Samples Went From Clear To Milky White, Heat Distortion
Teflon Tape	30	8.020	
FX-9070, 3M Fluoroelastomer	120	6.160	Samples Turned Purple-Brown

Table 3: Data From Plasmod Measurements

(THIS PAGE INTENTIONALLY LEFT BLANK)

<u>Material</u>	<u>Exposure (Mins)</u>	<u>Ave. Mass Loss %</u>	<u>Comments</u>
G410630, Sheldahl TCC/AL/3, Mil Kapton	120	4.370	Samples Were Severely Etched
0.2 Mil Kapton in N2	60	4.050	
SRT-300, XYDAR Thermoplastic, 507-102V	120	3.940	
0.2 Mil Kapton in Vacuum	60	1.140	
Sheet Teflon	180	0.630	Teflon Appears Undis- turbed, Brownish Film On Slides
PNF-245-003	5760	0.450	Oil Stain Appearance on Top of Specimens
PNF-245-003	4320	0.420	
PNF-245-003	2880	0.399	
Aluminum Foil	30	0.330	
FRV-1106, GE	120	0.115	
1-2577, Dow Corning	5760	0.086	Brown Yellow
730-RTV, Dow Corning	5760	0.060	Slightly Brown Areas
1-2577, Dow Corning	4320	0.050	Brown Yellow
730-RTV, Dow Corning	4320	0.047	
730-RTV, Dow Corning	2880	0.046	
1-2577, Dow Corning	2880	0.044	Brown Yellow
Aluminum Foil	30	0.330	
Teflon Tape	30	8.020	
0.2 Mil Kapton in Vacuum	60	1.140	
0.2 Mil Kapton in N2	60	4.050	
0.2 Mil Kapton in Air (Compressed)	60	21.040	

Table 3 (Continued): Data From Plasmod Measurements

(THIS PAGE INTENTIONALLY LEFT BLANK)

<u>Material</u>	<u>Exposure (Mins)</u>	<u>Ave. Mass Loss %</u>	<u>Comments</u>
Teflon Tape	60	17.960	
0.2 Mil Kapton in 02	60	87.240	
Teflon Tape	90	22.650	
Teflon Tape	120	34.760	
PPS, Polyphenylsulfide	120	47.780	
FX-9070, 3M Fluoroelastomer	120	6.160	Samples Turned Purple-Brown
Polycarbonate	120	11.160	Samples Went From Clear to Milky White, Heat Distortion
PBI, Celanese Polybenzimidazole	120	98.710	Only Brownish Caste Left on Slide
G410630, Sheldahl TCC/AL/3.Mil Kapton	120	4.370	Samples Were Severely Etched
FC-725, 3M 'Fluorad'	120	58.280	Brownish Caste on Samples
FC-721, 3M 'Fluorad'	120	100.000	No Visible Remains
SRT-300, XYDAR Thermoplastic, 507-102V	120	3.940	
FRV-1106, GE	120	0.115	
G405120, Sheldahl 2. Mil Kapton x AL	120	51.400	Samples Were Wrinkled And Then Exploded When The Vacuum Was Released
G411520, Sheldahl AL/2.MIL/Kapton	120	38.320	Samples Had Crinkled Edges
G411474, Sheldahl AL/.3 Mil/Kapton Perforated	120	16.380	
G404950, Sheldahl Gold on 5. Mil Kapton	120	14.630	Sample Surface Was Etched
Teflon Tape	180	39.710	Tape was Like Tissue Paper

Table 3 (Continued): Data From Plasmod Measurements

(THIS PAGE INTENTIONALLY LEFT BLANK)

<u>Material</u>	<u>Exposure (Mins)</u>	<u>Ave. Mass Loss %</u>	<u>Comments</u>
Sheet Teflon	180	0.630	Teflon Appears Undisturbed, Brownish Film on Slides
PNF-245-003	2880	0.399	
730-RTV, Dow Corning	2880	0.046	
1-2577, Dow Corning	2880	0.044	Brown Yellow
PNF-245-003	4320	0.420	
730-RTV, Dow Corning	4320	0.047	
1-2577, Dow Corning	4320	0.050	Brown Yellow
PNF-245-003	5760	0.450	Oil Stain Appearance on Top of Specimens
730-RTV, Dow Corning	5760	0.060	Slightly Brown Areas
1-2577, Dow Corning	5760	0.086	Brown Yellow
PNF-245-003	2880	0.399	
PNF-245-003	4320	0.420	
PNF-245-003	5760	0.450	Oil Stain Appearance on Top of Specimens
730-RTV, Dow Corning	2880	0.046	
730-RTV, Dow Corning	4320	0.047	
730-RTV, Dow Corning	5760	0.060	Slightly Brown Areas
1-2577, Dow Corning	2880	0.044	Brown Yellow
1-2577, Dow Corning	4320	0.050	Brown Yellow
1-2577, Dow Corning	5760	0.086	Brown Yellow
PPS, Polyphenylsulfide	120	47.780	
0.2 Mil Kapton in O2	60	87.240	
0.2 Mil Kapton in N2	60	4.050	
0.2 Mil Kapton in AIR (Compressed)	60	21.400	

Table 3 (Continued): Data From Plasmod Measurements

(THIS PAGE INTENTIONALLY LEFT BLANK)

<u>Material</u>	<u>Exposure (Mins)</u>	<u>Ave. Mass Loss %</u>	<u>Comments</u>
0.2 Mil Kapton in Vacuum	60	1.140	
Teflon Tape	30	8.020	
Teflon Tape	60	17.960	
Teflon Tape	90	22.650	
Teflon Tape	120	34.760	
Teflon Tape	180	39.710	Tape was Like Tissue Paper
Polycarbonate	120	11.160	Samples Went From Clear to Milky White, Heat Distortion
Aluminum Foil	30	0.330	
Sheet Teflon	180	0.630	Telfon Appears Undisturbed, Brownish Film on Slides
FC-725, 3M 'Fluorad'	120	58.280	Brownish Caste on Samples
FC-721, 3M 'Fluorad'	120	100.000	No Visible Remains
PBI, Celanese Polybenzimidazole	120	98.710	Only Brownish Caste Left on Slide
FRV-1106, GE	120	0.115	
FX-9070, 3M Fluoroelastomer	120	6.160	Samples Turned Purple-Brown
GA11520, Sheldahl AL/2.Mil/Kapton	120	38.320	Samples Had Crinkled Edges
G411474, Sheldahl Perforated	120	16.380	
G410630, Sheldahl TCC/AL/3.MIL Kapton	120	4.370	Samples Were Severely Etched

Table 3 (Continued): Data From Plasmod Measurements

(THIS PAGE INTENTIONALLY LEFT BLANK)

<u>Material</u>	<u>Exposure (Mins)</u>	<u>Ave. Mass Loss %</u>	<u>Comments</u>
G405120, Sheldahl 2 Mil Kapton x AL	120	51.400	Samples Were Wrinkled And Then Exploded When The Vacuum Was Released
G404950, Sheldahl Gold on 5.Mil Kapton	120	14.630	Sample Surface Was Etched
SRT-300, XYDAR Thermoplastic, 507-102V	120	3.940	

Table 3 (Continued): Data From Plasmod Measurements

PRECEDING PAGE BLANK NOT FILMED

The choice of silverized-teflon for the radiator surfaces implies a need for a very low solar absorptance to infrared emittance for this application. Possible substitutes would be silverized-Mylar or Kapton N film with an atomic oxygen protective coating. The methodology for developing a substitute thermal control coating will be demonstrated by the work being conducted under this contract.

Sol-gels have been dropped as candidate coatings for Kapton H. The materials that were being considered were alkoxide derived silicate and aluminate sols. These materials form thin films easily and air set to form a flexible coating with primary carbon-carbon bonding predominating in the structure. Further heat treatment would drive off the organic groups resulting in a brittle oxide coating. The concept evaluated was to use the coating in the alkoxide form to preserve flexibility. However, atomic oxygen testing of the alkoxide silicate and aluminate showed that they are not resistant to atomic oxygen; the coatings disintegrate leaving a fine oxide powder.

To develop an understanding of the effects of the space environment on external coating materials a number of simulated exposures and supporting analytical tests were conducted on candidate coating materials. The majority of the test effort was to expose materials to an atomic oxygen flux and examine the effects on each sample.

Material Number: 1
 Source: Dupont
 Vendor's Designation: Kapton H
 Vendor's Description: 2-mil polyimide film. Used as standard for Atomic Oxygen resistance evaluation

Material Number: 2
 Source: Battelle-Columbus Ohio Laboratories
 Vendor's Designation: 41641-2-2 HMDS
 Vendor's Description: Plasma polymerized silica coating on 1-mil Kapton H/Sputter etch, Plasma Power: 50 watts, Film Thickness: 5000 angstrom

Material Number: 3
 Source: Battelle-Columbus Ohio Laboratories
 Vendor's Designation: 41641-3-3A HMDS
 Vendor's Description: Plasma polymerized silica coating on 1-mil Kapton H/Sputter etch, Plasma Power: 50 watts, Film Thickness: 10,000 angstrom

Material Number: 4
 Source: Battelle-Columbus Ohio Laboratory
 Vendor's Designation: 41641-7-6 HMDS
 Vendor's Description: Plasma polymerized silica coating on 1-mil Kapton H/Sputter etch, Plasma Power: 20 watts, Film Thickness: 5,000 angstrom

Material Number: 5
 Source: Battelle-Columbus Ohio Laboratory
 Vendor's Designation: 41641-8-7 HMDS
 Vendor's Description: Plasma polymerized silica coating on 1-mil Kapton H/Sputter etch, Plasma Power: 20 watts, Film Thickness: 10,000 angstrom

Material Number: 6
 Source: Battelle-Columbus Ohio Laboratory
 Vendor's Designation: 41641-9-8 TFE
 Vendor's Description: Plasma polymerized Teflon coating on 1-mil Kapton H/Sputter etch, Plasma Power: 50 watts, Film Thickness: 5,6000 angstrom

Material Number: 7
 Source: Battelle-Columbus Ohio Laboratory
 Vendor's Designation: 41641-11-10 TFE
 Vendor's Description: Plasma polymerized Teflon coating on 1-mil Kapton H/Sputter etch, Plasma Power: 50 watts, Film Thickness: 4,200 anstrom

Table 4: Material Identification Code For Test Specimens
 Examined Under This Contract

(THIS PAGE INTENTIONALLY LEFT BLANK)

Material Number: 8
Source: Battelle-Columbus Ohio Laboratory
Vendor's Designation: 41641-12-11 TFE
Vendor's Description: Plasma polymerized Teflon coating on 1-mil Kapton
H/Sputter etch, Plasma power: 50 watts,
Film Thickness: 4,200 angstrom

Material Number: 9
Source: Battelle-Columbus Ohio Laboratory
Vendor's Designation: 41641-13-12 TFE
Vendor's Description: Plasma polymerized Teflon coating on 1-mil Kapton
H/Sputter etch, Plasma Power: 50 watts,
Film Thickness: 8,000 angstrom

Material Number: 10
Source: Battelle-Columbus Ohio Laboratory
Vendor's Designation: 41641-15-13 HMDS/TFE (ratio 8/5)
Vendor's Description: Plasma co-polymerized silica/Teflon coating on
1-mil Kapton H, Sputter etch, Plasma Power: 50
watts,

Material Number: 11
Source: Battelle-Columbus Ohio Laboratory
Vendor's Designation: 41641-18-16 HMDS/TFE (ratio 9/5)
Vendor's Description: Plasma co-polymerized silica/Teflon coating on
1-mil Kapton H, Sputter etch, Plasma Power: 50
watts, Film Thickness: 9,800 angstrom

Material Number: 12
Source: Battelle-Columbus Ohio Laboratory
Vendor's Designation: 41641-20-18 HMDS/TFE (ratio 9/5)
Vendor's Description: Plasma co-polymerized silica/Teflon coating on
1-mil Kapton H, Sputter etch, Plasma Power:
20 watts, Film Thickness: 9,400 angstrom

Material Number: 13
Source: Battelle-Columbus Ohio Laboratory
Vendor's Designation: 41641-22-20 HMDS/TFE (ratio 4/1)
Vendor's Description: Plasma co-polymerized silica/Teflon coating on
1-mil Kapton H, Sputter etch, Plasma Power:
50 watts, Film Thickness: 10,400 anstrom

Material Number: 14
Source: Battelle-Columbus Ohio Laboratory
Vendor's Designation: 41641-23-21 HMDS/TFE (ratio 4/1)
Vendor's Description: Plasma co-polymerized silica/Teflon coating on
1 mil Kapton H, Sputter etch, Plasma Power:
20 watts, Film Thickness: 8,000 anstrom

Table 4 (Continued): Material Identification Code For Test Specimens
Examined Under This Contract

(THIS PAGE INTENTIONALLY LEFT BLANK)

Material Number: 15
Source: Sheldahl Company
Vendor's Designation: CV1144
Vendor's Description: 0.5 mil CV1144 Silicone coating on 2-mil Kapton/
Reverse side silver inconnel.

Material Number: 16
Source: Sheldahl Company
Vendor's Designation: CV3530
Vendor's Description: .5-mil CV3530 Silicone coating on 2-mil Kapton/
Reverse side silver inconnel.

Material Number: 17
Source: Lockheed Missiles & Space Company, Inc.
Vendor's Designation: LeRC# 52286 A&B
Vendor's Description: 1040 Angstrom 92%SiO₂/8%PTFE on both sides of
1-mil Kapton. Reactive coated both sides by
NASWA-LeRC.

Material Number: 18
Source: Lockheed Missiles & Space Company, Inc.
Vendor's Designation: LeRC# 51386
Vendor's Description: 815 Angstrom SiO₂ coating on both sides of 1-mil
Kapton. Reactive coated both sides by NASA-LeRC.

Material Number: 19
Source: General Electric-Silicone Products Division
Vendor's Designation: RTV 655
Vendor's Description: Phenyl substituted silicone polymer material.
Thickness: 0.11 in.

Material Number: 21
Source: General Electric-Silicone Products Division
Vendor's Designation: RTV 615
Vendor's Description: Dimethyl Silicone Polymer. Thickness: 0.11 in.

Material Number: 22
Source: General Electric-Silicone Products Division
Vendor's Designation: Siltem
Vendor's Description: Polyimide Copolymer. Thickness: 0.12 in.

Material Number: 23
Source: Battelle-Columbus Ohio Division
Vendor's Designation: Copolymerized HMDS/TFE. Coating designation 'A'
Vendor's Description: Polymer Pressure: HMDS 40 micrometers of Hg,
TFE 2 micrometers of Hg; Web Speed: 3.7 in/min;
Max Thickness: 5000 angstroms; Tape Test: pass.
Coated onto 1-mil Kapton.

Table 4 (Continued): Material Identification Code For Test Specimens
Examined Under This Contract

(THIS PAGE INTENTIONALLY LEFT BLANK)

Material Number: 24

Source: Battelle-Columbus Ohio Division

Vendor's Designation: Copolymerized HMDS/TFE. Coating designation 'B'

Vendor's Description: Polymer Pressure: HMDS 40 micrometers of Hg, TFE
5 micrometers of Hg; Web Speed: 3.7 in/min.
Maximum Thickness: 5000 angstroms; Tape Test:
pass. Coated onto 1-mil Kapton.

Material Number: 25

Source: Battelle-Columbus Ohio Division

Vendor's Designation: Copolymerized HMDS/TFE. Coating designation 'G'

Vendor's Description: Polymer Pressure: HMDS 40 micrometers of Hg, TFE
10 micrometers of Hg; Web Speed: 3.7 in/min;
Maximum Thickness: 5000 angstroms; Tape Test:
pass. Coated onto 1-mil Kapton.

Material Number: 26

Source: Battelle-Columbus Ohio Division

Vendor's Designation: Copolymerized HMDS/TFE. Coating Designation 'F'

Vendor's Description: Polymer Pressure: HMDS 40 micrometers of Hg,
TFE 40 micrometers of Hg; Web Speed: 3.7 in/min;
Maximum Thickness: 5000 angstroms; Tape Test:
pass. Coated onto 1-mil Kapton.

Material Number: 27

Source: Battelle-Columbus Ohio Division

Vendor's Designation: Copolymerized HMDS/TFE. Coating Designation 'G'

Vendor's Description: Polymer Pressure: HMDS 40 micrometers of Hg,
TFE 10 micrometers of Hg; Web Speed: 3.7 in/min;
Maximum Thickness: 5000 angstroms; Tape Test:
pass. Coated onto 1-mil Kapton.

Material Number: 28

Source: Battelle-Columbus Ohio Division

Vendor's Designation: Copolymerized HMDS/TFE. Coating Designation 'H'

Vendor's Description: Polymer Pressure: HMDS 40 micrometers of Hg, TFE
15 micrometers of Hg; Web Speed: 3.7 in/min;
Maximum Thickness: 5000 angstroms; Tape Test:
pass. Coated onto 1-mil Kapton.

Material Number: 29

Source: Dupont-Polymer Products Department, Chestnut Run
Laboratory

Vendor's Designation: Kapton F

Vendor's Description: 1-mil Kapton coated both sides with 0.1-mil
Teflon.

Table 4 (Continued): Material Identification Code For Test Specimens
Examined Under This Contract

(THIS PAGE INTENTIONALLY LEFT BLANK)

Material Number: 30
 Source: Dupont-Polymer Products Department, Chestnut Run Laboratory
 Vendor's Designation: Kapton F
 Vendor's Description: 1-mil Kapton coated both sides with 0.5-mil Teflon.

Material Number: 31
 Source: Dupont-Polymer Products Department, Chestnut Run Laboratory
 Vendor's Designation: Kapton F
 Vendor's Description: 2-mil Kapton coated one side with 0.5-mil Teflon.

Material Number: 32
 Source: Lockheed-Missiles & Space Company, Inc.
 Vendor's Designation: Longeron
 Vendor's Description: Epoxy S-glass. Round bar stock.

Material Number: 33
 Source: Lockheed-Missiles & Space Company, Inc.
 Vendor's Designation: Longeron
 Vendor's Description: Epoxy S-glass. Rectangular bar stock.

Material Number: 34
 Source: Spire Corporation-Patriots Park, Massachusetts
 Vendor's Designation: Ion Implanted Al
 Vendor's Description: 2-mil Kapton sputter coated with 1200 Angstroms of Aluminum. Oxygen ion implanted.

Material Number: 35
 Source: Spire Corporation-Patriots Park, Massachusetts
 Vendor's Designation: Ion Implanted Al
 Vendor's Description: 2-mil Kapton sputter coated with 2000 Angstroms of Aluminum. Oxygen ion implanted into the Aluminum.

Material Number: 36
 Source: Spire Corporation-Patriots Park, Massachusetts
 Vendor's Designation: Ion Implanted Al
 Vendor's Description: 2-mil Kapton sputter coated with 4000 Angstroms of Aluminum. Oxygen ion implanted into the Aluminum.

Material Number: 37
 Source: Spire Corporation-Patriots Park, Massachusetts
 Vendor's Designation: Ion Implanted Al
 Vendor's Description: 2-mil Kapton sputter coated with 1000 Angstroms of Aluminum. Nitrogen ion implanted into the Aluminum.

Table 4 (Continued): Material Identification Code For Test Specimens
 Examined Under This Contractx

(THIS PAGE INTENTIONALLY LEFT BLANK)

Material Number: 38
 Source: Spire Corporation-Patriots Park, Massachusetts
 Vendor's Designation: Ion Implanted Al
 Vendor's Description: 2-mil Kapton sputter coated with 2000 Angstroms of Aluminum. Nitrogen ion implanted into the Aluminum.

Material Number 39
 Source: Spire Corporation-Patriots Park, Massachusetts
 Vendor's Designation: Ion Implanted Al
 Vendor's Description: 2-mil Kapton sputter coated with 4000 Angstroms of Aluminum. Nitrogen ion implanted into the Aluminum.

Material Number: 40
 Source: Boeing-BA Thin Films Lab
 Vendor's Designation: Al Sputter Coating
 Vendor's Description: 2-mil Kapton sputter coated with 1200 Angstrom Al.

Material Number: 41
 Source: Boeing-BA Thin Films Lab
 Vendor's Designation: Al Sputter Coating
 Vendor's Description: 2-mil Kapton sputter coated with 2000 Angstrom Al.

Material Number: 42
 Source: Boeing Thin Films Lab
 Vendor's Designation: Al Sputter Coating
 Vendor's Description: 2-mil Kapton sputter coated with 4000 Angstrom Al.

Material Number: 43
 Source: Battelle-Columbus Ohio Laboratories
 Vendor's Designation: HMDS/TFE
 Vendor's Description: Plasma polymerized coating-roll coated. HMDS/TFE ratio 8/5 on 1-mil Kapton.

Material Number: 44
 Source: Battelle-Columbus Ohio Laboratories
 Vendor's Designation: 41641-29-26 HMDS/TFE
 Vendor's Description: Plasma polymerized coating-roll coated. HMDS/TFE ratio 1/0 on 1-mil Kapton.

Material Number: 45
 Source: Battelle-Columbus Ohio Laboratories
 Vendor's Designation: 42641-30-27 HMDS/TFE
 Vendor's Description: Plasma polymerized coating-roll coated. HMDS/TFE ratio 20/1 on 1-mil Kapton.

Table 4 (Continued): Material Identification Code For Test Specimens
 Examined Under This Contract

(THIS PAGE INTENTIONALLY LEFT BLANK)

Material Number: 46
 Source: Battelle-Columbus Ohio Laboratories
 Vendor's Designation: HMDS/TFE
 Vendor's Description: Plasma polymerized coating-roll coated. HMDS/TFE ratio 1/0 on 1-mil Kapton.

Material Number: 47
 Source: Battelle-Columbus Ohio Laboratories
 Vendor's Designation: HMDS/TFE
 Vendor's Description: Plasma polymerized coating-roll coated. HMDS/TFE ratio 2-1 on 1-mil Kapton.

Material Number: 48
 Source: Battelle-Columbus Ohio Laboratories
 Vendor's Designation: HMDS/TFE
 Vendor's Description: Plasma polymerized coating-roll coated. HMDS/TFE ratio 8/1 on 1-mil Kapton.

Material Number: 49
 Source: Battelle-Columbus Ohio Laboratories
 Vendor's Designation: HMDS/TFE
 Vendor's Description: Plasma polymerized coating-roll coated. HMDS/TFE ratio 4/1 on 1-mil Kapton.

Material Number: 50
 Source: Battelle-Columbus Ohio Laboratories
 Vendor's Designation: 41641-33-30 HMDS/TFE
 Vendor's Description: Plasma polymerized coating-stationary. HMDS/TFE ratio 1/0 on 1-mil Kapton.

Material Number: 51
 Source: Battelle-Columbus Ohio Laboratories
 Vendor's Designation: 41641-33-30 HMDS/TFE
 Vendor's Description: Plasma polymerized coating-stationary. HMDS/TFE ratio 20/1 on 1-mil Kapton.

Material Number: 52
 Source: Battelle-Columbus Ohio Laboratories
 Vendor's Designation: 41641-35-32 HMDS/TFE
 Vendor's Description: Plasma polymerized coating-stationary. HMDS/TFE ratio 8/1 on 1-mil Kapton.

Material Number: 53
 Date Received: 09-15-86
 Source: Sheldahl Company, Northfield Minnesota
 Vendor's Designation: TCC
 Material Description: TCC coated onto 1-mil Kapton (no metal-
 lization)

Table 4 (Continued): Material Identification Code For Test Specimens
 Examined Under This Contract

(THIS PAGE INTENTIONALLY LEFT BLANK)

Material Number: 54
 Date Received: 10-16-86
 Source: Battelle-Columbus Ohio Laboratories
 Vendor's Designation: Run D - HMDS 40/TFE 5
 Material Description: HMDS to TFE ratio 8/1

Material Number: 55
 Date Received: 10-16-86
 Source: Battelle-Columbus Ohio Laboratories
 Vendor's Designation: Run E - HMDS 40/TFE 2
 Material Description: HMDS to TFE ratio 20/1

Material Number: 56
 Date Received: 10-16-86
 Source: Battelle-Columbus Ohio Laboratories
 Vendor's Designation: Run F - HMDS 40
 Material Description: HMDS to TFE ratio 1/0

Material Number: 57
 Date Received: 10-23-86
 Source: Ethyl Corporation-Baton Rouge, Louisiana
 Vendor's Designation: Expel-F Polyphosphazene
 Material Description: Compound No. X129: 10/16/86 Lot No. 6037-51B

Material Number: 58
 Date Received: 10-23-86
 Source: Ethyl Corporation-Baton Rouge, Louisiana
 Vendor's Designation: Eypel-F Polyphosphazene
 Material Description: Compound No. X128 Date: 10/16/86 Lot No. 6037-51A

Material Number: 59
 Date Received: 10-23-86
 Source: IIT Research Insitite (IITRI)
 Vendor's Designation: Glass Resin on Kapton
 Material Description: Glass Resin on Kapton

Material Number: 60
 Date Received: 10-23-86
 Source: IIT Research Institute (IITRI)
 Vendor's Designation: Glass Resin on Aluminum
 Material Description: Glass Resin on Aluminum

Material Number: 61
 Date Received: 10-23-86
 Source: IIT Research Institute (IITRI)
 Vendor's Designation: S13G/LO-1 on Aluminum
 Material Description: S13G/LO-1 (Lot No. L-048) on Aluminum

Table 4 (Continued): Material Identification Code For Test Specimens
 Examined Under This Contract

(THIS PAGE INTENTIONALLY LEFT BLANK)

Material Number: 62

Date Received: 10-24-86

Source: IIT Research Institute (IITRI)

Vendor's Designation: S13G/L0-1 on FG-Epoxy

Material Description: S13G/L0-1 on FG-Epoxy

Material Number: 63

Date Received: 10-29-86

Source: Ethyl Corporation, Baton Rouge, Louisiana

Vendor's Designation: Eypel-F Polyphosphazene

Material Description: Compound No. X130, Date 10/21/86, Lot No. 6037-51C, Weight: 2gm, Thickness: 1 mil

Material Number: 64

Date Received: 10-29-86

Source: Ethyl Corporation, Baton Rouge, Louisiana

Vendor's Designation: Eypel-F Polyphosphazene

Material Description: Compound No. X130, Date 10/21/86, Lot No. 6037-51C, Weight: 2 gm, Thickness: .5 mil

Material Number: 65

Date Received: 10-30-86

Source: Sheldahl-Northfield, Minnesota

Vendor's Designation: CV1-1144-0

Material Description: Apply 0.5-mil thick Mcghan Nusil CV1-1144-0 coating on one side of 1.0-mil type H Kapton T/H using primer SP-120 Item 1.

Material Number: 66

Date Received: 10-30-86

Source: Sheldahl-Northfield, Minnesota

Vendor's Designation: CV1-3530

Material Description: 0.5-mil Mcghan Nusil CV1-3530 coating on one side of 1.0-mil, type H Kapton. Using primer CF 1-135, lab not book #664-16. 8-each sheet size 4 in by 8 in.

Material Number: 67

Date Received: 10-16-86

Source: Battelle-Columbus Ohio Laboratories

Vendor's Designation: Run 44641-42-39, 40 HMDS

Material Description: Run 'A', HMDS to TFE ratio 1/0, adhesive backing. Coating thickness: 29000 Angstrom; deposition time: 15 min.

Table 4 (Continued): Material Identification Code For Test Specimens
Examined Under This Contract

(THIS PAGE INTENTIONALLY LEFT BLANK)

Material Number: 68

Date Received: 10-16-86

Source: Battelle-Columbus Ohio Laboratories

Vendor's Designation: Run 44641-43-40, 40 HMDS/2 TFE

Material Description: Run 'B', HMDS to TFE ratio 20/1, adhesive backing. Coating thickness: 29000 Angstrom; deposition time: 15 min.

Material Number: 69

Date Received: 10-16-86

Source: Battelle-Columbus Ohio Laboratories

Vendor's Designation: Run 44641-44-41, 40 HMDS/5 TFE

Material Description: Run 'C', HMDS to TFE ratio 8/1, adhesive backing. Coating thickness: 17000 Angstrom; deposition time: 15 min.

Material Number: 70

Date Received: 10-23-86

Source: Battelle-Columbus Ohio Laboratories

Vendor's Designation: Run 44641-44-41, 40 HMDS/5 TFE

Material Description: Run 'C', HMDS to TFE ratio 8/1, adhesive backing. Coating thickness: 17000 Angstrom; deposition time: 15 min.

Material Number: 70

Date Received: 10-23-86

Source: Sheldahl-Northfield, Minnesota

Vendor's Designation: CV1-3530, Adhesive backed.

Material Description: 0.5-mil thickness of Mcghan Nusil CV1-3530 coating x 1.0-mil Kapton, T/H x aluminizing x 966 Acrylic pressure sensitive adhesive.

Material Number: 71

Date Received: 10-23-86

Source: Sheldahl-Northfield, Minnesota

Vendor's Designation: CV1-1144-0, Adhesive backed.

Material Description: 0.5-mil thickness of Mcghan Nusil CV1-3530 coating x 1.0-mil Kapton, T/H x aluminizing x 966 Acrylic pressure sensitive adhesive.

Material Number: 71

Date Received: 10-23-86

Source: Sheldahl-Northfield, Minnesota

Vendor's Designation: CV1-1144-0, Adhesive backed

Material Description: 0.5-mil thickness of Mcghan Nusil CV1-1144-0 coating x 1.0-mil Kapton, T/H x aluminizing x 966 Acrylic pressure sensitive adhesive using primer SP-120.

Table 4 (Continued): Material Identification Code For Test Specimens
Examined Under This Contract

(THIS PAGE INTENTIONALLY LEFT BLANK)

Material Number: 72
 Date Received: 02-07-86
 Source: Sheldahl-Northfield, Minnesota
 Vendor's Designation: TF515
 Material Description: 2-mil Teflon x Silver x Inconel x 966
 Acrylic pressure sensitive adhesive.

Material Number: 73
 Date Received: 02-07-86
 Source: Sheldahl-Northfield, Minnesota
 Vendor's Designation: Kapton x Silver x Inconel
 Material Description: 2-mil Teflon x Silver x Inconel x 966
 Acrylic pressure sensitive adhesive.

Material Number: 74
 Date Received: 02-07-86
 Source: Sheldahl-Northfield, Minnesota
 Vendor's Designation: TF510
 Material Description: 2-mil Mylar x Silver x Inconel x 966 Acrylic
 pressure sensitive adhesive.

Material Number: 75
 Date Received: 10-10-86
 Source: Battelle-Columbus Ohio Laboratories
 Vendor's Designation: Run 41825-6-6, sputtered SiO₂/Teflon
 Material Description: Sputtered SiO₂/Teflon, nominal material
 ratio 8/1, nominal coating thickness 9000
 Angstrom.

Material Number: 76
 Date Received: 10-10-86
 Source: Battelle-Columbus Ohio Laboratories
 Vendor's Designation: 'A'
 Material Description: Plasma polymerized HMDS/TFE, nominal material
 ratio 1/0, nominal coating thickness: 15000
 Angstrom. Deposited onto both sides of Kapton
 simultaneously. Siloxane

Material Number: 77
 Date Received: 10-10-86
 Source: Battelle-Columbus Ohio Laboratories
 Vendor's Designation: Run 41641-36-33, 1 HMDS/0-TFE
 Material Description: Plasma polymerized HMDS (40 micrometers),
 nominal material ratio 1/0, nominal coating
 thickness 2000 Angstrom. Adhesive backed.

Table 4 (Continued): Material Identification Code For Test Specimens
 Examined Under This Contract

(THIS PAGE INTENTIONALLY LEFT BLANK)

Material Number: 78

Date Received: 10-10-86

Source: Battelle-Columbus Ohio Laboratories

Vendor's Designation: Run 41641-37-34, 1-HMDS/0-TFE

Material Description: Plasma polymerized HMDS (40 micrometers), nominal material ratio 1/0, nominal coating thickness 3300 Angstrom. Adhesive backed.

Material Number: 79

Date Received: 10-10-86

Source: Battelle-Columbus Ohio Laboratories

Vendor's Designation: Run 41641-38-35, 20 HMDS/1-TFE

Material Description: Plasma polymerized HMDS (40 micrometers)/TFE (2 micrometers), nominal material ratio 20/1, nominal coating thickness 2400 Angstrom. Adhesive backed.

Material Number: 80

Date Received: 10-10-86

Source: Battelle-Columbus Ohio Laboratories

Vendor's Designation: Run 41641-38-35, 8 HMDS/1-TFE

Material Description: Plasma polymerized HMDS (40 micrometers)/TFE (5 micrometers), nominal material ratio 8/1, nominal coating thickness 2000 Angstrom. Adhesive backed.

Material Number: 91

Date Received: 3-24-87

Source: GE Silicone Products Division

Vendor's Designation: GC604

Material Description: Silicone solvent dispersed resin pigmented with TiO_2 . Coating air dried then cured 0.5 hour at 200°C.

Material Number: 92

Date Received: 3-24-87

Source: GE Silicone Products Division

Vendor's Designation: GC605

Material Description: Silicone solvent dispersed resin pigmented with TiO_2 . Coating air dried then cured 0.5 hour at 200°C.

Material Number: 93

Date Received: 3-24-87

Source: GE

Vendor's Designation: 1081-105-18

Material Description: #93 Through 99 are silicone polyimide copolymers with various silicone to organic ratios and different structural arrangements.

Table 4 (Continued): Material Identification Code For Test Specimens
Examined Under This Contract

(THIS PAGE INTENTIONALLY LEFT BLANK)

Material Number: 94
Date Received: 3-24-87
Source: GE
Vendor's Designation: 1081-105-2S
Material Description:

Material Number: 95
Date Received: 3-24-87
Source: GE
Vendor's Designation: 1081-105-38
Material Description:

Material Number: 96
Date Received: 3-24-87
Source: GE
Vendor's Designation: 1081-105-48
Material Description:

Material Number: 97
Date Received: 3-24-87
Source: GE
Vendor's Designation: 2676-068
Material Description:

Material Number: 98
Date Received: 3-24-87
Source: GE
Vendor's Designation: 2676-075
Material Description:

Material Number: 99
Date Received: 3-24-87
Source: GE
Vendor's Designation: 2676-078
Material Description:

Material Number: 100
Date Received: 3-24-87
Source: GE
Vendor's Designation: WRL-1a
Material Description: Diphenyl Dimethyl Silicone, RTV

Material Number: 101
Date Received: 3-24-87
Source: GE
Vendor's Designation: WRL-2a
Material Description: Fluorosilicone, RTV

Table 4 (Continued): Material Identification Code For Test Specimens
Examined Under This Contract

(THIS PAGE INTENTIONALLY LEFT BLANK)

Material Number: 102
Date Received: 3-24-87
Source: GE
Vendor's Designation: WR-3a
Material Description: Dimethyl Silicone, RTV

Material Number: 103
Date Received: 3-24-87
Source: GE
Vendor's Designation: WRL-4a
Material Description: Dimethyl Silicone, RTV

Material Number: 104
Date Received: 3-24-87
Source: GE
Vendor's Designation: 87-386-002
Material Description: Silicone Pressure Sensitive Adhesive Cured
@ 500°F

Material Number: 105
Date Received: 3-24-87
Source: GE
Vendor's Designation: 87-386-003
Material Description: Silicone Pressure Sensitive Adhesive Cured
@ 500°F

Material Number: 106
Date Received: 3-24-87
Source: Applied Signal
Vendor's Designation: Apical
Material Description: 2 Mil Polyimide Sheet

Material Number: 108
Date Received: 8-12-87
Source: Battelle-Columbus Ohio Laboratories
Vendor's Designation: 41541-55-50
Material Description: Plasma Polymerized HMDS, Side-1 5100 Angstroms,
Side 2, 8100 Angstroms

Material Number: 109
Date Received: 8-12-87
Source: Battelle-Columbus Ohio Laboratories
Vendor's Designation: 41641-56-51
Material Description: Plasma Polymerized HMDS, Side 1 16000 Angstroms,
Side 2 14900 Angstroms

Table 4 (Continued): Material Identification Code For Test Specimens
Examined Under This Contract

(THIS PAGE INTENTIONALLY LEFT BLANK)

Material Number: 110

Date Received: 8-12-87

Source: Battelle-Columbus Ohio Laboratories

Vendor's Designation: 41641-57-52

Material Description: Plasma Polymerized HMDS, Side 1 22700 Angstroms,
Side 2 15600 Angstroms

Material Number: 111

Date Received: 8-12-87

Source: Battelle-Columbus Ohio Laboratories

Vendor's Designation: 41641-58-53

Material Description: Copolymerized HMDS/TFE (9/1 Ratio) Side 1
12500 Angstroms, Side 2 12500 Angstroms

Material Number: 112

Date Received: 8-12-87

Source: Battelle-Columbus Ohio Laboratories

Vendor's Designation: 41641-60-55

Material Description: Copolymerized HMDS/TFE Side 1, 11400 Angstroms,
Partial Pressures 18/2 Micrometers of Hg,
Side 2, 17900 Angstroms, Partial Pressures 36/4
Micrometers of Hg

Table 4 (Continued): Material Identification Code For Test Specimens
Examined Under This Contract

PRECEDING PAGE BLANK NOT FILMED

(THIS PAGE INTENTIONALLY LEFT BLANK)

Date	Exposure Time (Hrs)	Material	Mass Loss (mg)
3/22/86	4.0	Kapton	4.42
			0.58
		Kapton	3.64
			0.24
			0.38
			1.03
3/23/86	5.0	Kapton	29.33
		FEP	16.05
		TFE	8.39
		FEP/K	22.90
		FEP/K	9.09
		FEP/K	23.37
3/24/86		Kapton	10.53
			1.07
			0.98
		TFE	3.44
		FEP	5.53
		FEP/K	8.01
3/25/86	4.0	Kapton	31.99
		DC93-500	1.92
			1.70
		PNF GUM	0.44
		PNF/ZnO	2.67
		PNF	3.83
3/26/86	6.0	Kapton	30.30
		FEP	14.72
		PNF GUM	0.82
		Kapton	26.93
		PNF/ZnO	12.60
		TFE	10.53
3/27/86	6.0	Kapto	25.29
		FEP/K	16.96
		FEP/K	15.18
		Kapton	15.42
		Sheldahl G405120	13.50
		Sheldahl G411120	1.70

Table 5. Mass Loss Data Obtained From Original Chamber

(THIS PAGE INTENTIONALLY LEFT BLANK)

Date	Exposure Time (Hrs)	Material	Mass Loss (mg)
3/28/86	6	Kapton	35.28
		PNF/ZnO	1.76
		PNF	2.22
		Kapton	33.95
		K93-500	6.28
		CCF2-1144-1/ZOT	2.01
4/18/86	6	Kapton	26.06
		Sheldahl INAGKEP	29.55
		Sheldahl INAGFEP	15.32
		Kapton	21.41
		Sheldahl SWS 7220	2.51
		Sheldahl INAGMYL	33.01
6/24/86	3	Kapton	2.75
			2.50
			2.29
			2.20
			2.14
			2.63
6/24/86	3	Kapton	0.19
			0.61
			0.28
			0.29
			0.34
			0.81
6/24/86	1.55	Kapton	6.97
		HMDS/TFE (9/5) #12	0.57
		HMDS/TFE(4/1)	0.54
		Kapton	6.93
		#15CV1144	Gain (0.22) (3 of 4)
		#16CV3530	1.03 (1 gain)
6/24/86	1.55	Kapton	4.84
		(#2) HMDS 5KA thick	0.43
		(#3) HMDS 10KA thick	+0.14 (Gain)
		Kapton	4.68
		#8 TFE	4.59
		#9 TFE	5.14
7/3/86	3	Kapton	25.94
			25.57
			26.07
			26.50
			26.90
			26.41

Table 5 (Continued): Mass Loss Data Obtained From Original Chamber

(THIS PAGE INTENTIONALLY LEFT BLANK)

Date	Exposure Time (Hrs)	Material	Mass Loss (mg)
7/16/86	2	Kapton	3.68
			4.18
			4.31
			4.46
			3.82
			3.99
7/17/86	4	Kapton	11.55
			13.11
			12.39
			13.81
			11.72
			11.92
7/18/86	4	Kapton	13.24
		#4 HMDS	7.33
		#4 HMDS	8.71
		Kapton	17.56
		#6 TFE	14.81
		#6 TFE	14.89
7/21/86	4	Kapton	12.01
		#7 TFE	15.05
		#7 TFE	15.18
		Kapton	14.16
		#10 HMDS/TFE (8/5)	1.48
		#10	1.68
7/24/86	4	Kapton	18.14
		#11 (HMDS/TFE 4/5)	3.00
		#11	2.80
		Kapton	26.07
		#13 HMDS/TFE (4/1)	2.68
		#13	3.17
7/25/86	4	Kapton	11.33
		#18 LeRC #51386	0.29
		#18	0.20
		Kapton	14.00
		#17 LeRC #52286A&B	7.33
		#17	11.64
7/28/86	4	Kapton	9.88
		#19	14.26
		#19	14.51
		Kapton	11.09
		#19	12.99
		#19	12.50

Table 5 (Continued): Mass Loss Data Obtained From Original Chamber

(THIS PAGE INTENTIONALLY LEFT BLANK)

Date	Exposure Time (Hrs)	Material	Mass Loss (mg)
8/4/86	4	Kapton	3.41
		#30 Kapton F	5.01
		Kapton F	3.47
		Kapton	4.21
		#30 Kapton F	5.33
		Kapton F	3.12
8/7/86	4	Kapton	11.03
		#23 HMDS/TFE(20/1)	3.58
		#24 HMDS/TFE(8/1)	4.51
		Kapton	14.85
		#23	3.53
		#24	5.63
8/8/86	4	Kapton	12.68
		#24 HMDS/TFE(8/5)	3.32
		#26 HMDS/TFE(1/1)	8.70
		Kapton	15.08
		#25	4.40
		#26	9.41
8/11/86	4	Kapton	9.41
		#27 HMDS/TFE(4/1)	2.58
		#28 HMDS/TFE(8/3)	2.93
		Kapton	11.38
		#27	2.53
		#28	3.44
9/26/88	4	Kapton	10.88
			11.04
			12.46
			14.18
			18.64
			12.78
9/30/86	4	Kapton	13.29
		#46 HMDS	3.76
		#47 HMDS/TFE	10.20 (1 sample) had wt gain)
		Kapton	17.24
		#46 HMDS	1.43
		#47 HMDS/TFE	12.27
10/1/86	4	Kapton	12.71
		#48	2.00
		#49	2.08
		Kapton	16.75
		#48 HMDS/TFE (8/1)	2.08
		#49 HMDS/TFE (4/1)	2.98

Table 5 (Continued): Mass Loss Data Obtained From Original Chamber

(THIS PAGE INTENTIONALLY LEFT BLANK)

<u>Date</u>	<u>Exposure Time (Hrs)</u>	<u>Material</u>	<u>Mass Loss (mg)</u>
10/2/86	4	Kapton	11.16
		#50 HMDS	4.26
		#51 HMDS/TFE (20/1)	5.65
		Kapton	13.94
		#50	3.55
		#51	4.62
10/8/86	4	Kapton	13.00
		#53 TCC Sheldahl	4.58
		Kapton	19.44
		Kapton	17.73
		#53	4.61
		Kapton	13.78
10/9/86	4	Kapton	12.80
		#40 Al 1200A	0.54, 14.43 (Inner, Outer)
		#41 Al 2000A	0.58, 15.50
		Kapton	20.56
		#42 Al 4000A	0.40, 16.74
		Kapton	13.84
10/20/86	2	Kapton	3.42
		#55	0.27
		#56	0.28
		Kapton	3.66
		#56 HMDS	0.29
		#55 HMDS/TFE (20/1)	0.33
10/28/86	2	Kapton	4.99
		#58 X-128	0.51
		#57 X-127	0.85
		Kapton	5.60
		#57	0.81
		#58	0.56
10/29/86	2	Kapton	4.02
		#50 HMDS	0.61
		#51 HMDS/TFE	0.52
		Kapton	4.37
		#52 HMDS/TFE (8/1)	0.32
		#54 HMDS/TFE (8/1)	0.29

Table 5 (Continued): Mass Loss Data Obtained From Original Chamber

(THIS PAGE INTENTIONALLY LEFT BLANK)

<u>Date</u>	<u>Exposure Time (Hrs)</u>	<u>Material</u>	<u>Mass Loss (mg)</u>
10/30/86	2	Kapton	7.48
		#62 S13G/L0 FG-Epoxy	3.21 (2 wt gains 1.96)
		#63 X-130	1.75
		Kapton	8.45
		#64 X-130	2.84
		#59 glass resin on Kapton	3.26
11/11/86	2	Kapton	4.31
		#65CV 1-1144-0	0.39
		#66CV 1-3530	0.66
		Kapton	5.04
		#60 glass resin on Al	0.09
		Kapton	4.36
11/19/86	2	Kapton	2.60
		#61 S13G/L0 on Al	0.18
		Kapton	2.68
		#61	0.20
11/21/86	2	Kapton	2.71
		#54 HMDS/TFE (8/1)	1.53
		Kapton	2.99
		#63 X-130	1.11
		#81 Al on Kapton	0.20

Table 5 (Continued): Mass Loss Data Obtained From Original Chamber

REMOVED FROM BLACK BOX FILMED

Atomic Oxygen Test Apparatus

The initial test facility was the vacuum chamber shown in figure 1. The oxygen was produced in a radio frequency discharge induced plasma. Due to the nature of the circuit, the RF was present throughout the chamber and thus the plasma glow was sustained virtually throughout the vacuum chamber to the valve opening to the vacuum pump. In this configuration, the samples were exposed to the RF field, the ions associated with the plasma, emission of UV, and excited state neutral oxygen atoms and molecules, as well as the ground state oxygen atoms of interest. This chamber was a very harsh test environment and suffered from the fact that the different environmental factors were not well separated or well characterized. Materials tested in this environment were also subjected to severe heating due to the susceptibility of the aluminum sample holder. Table 5 is a summary of all the mass loss data and exposure conditions for tests with this apparatus. The pressure for these early experiments range between about 360 and 460 millitorr. The sample temperature was difficult to ascertain. A standard type K thermocouple placed within the chamber provided a reading of about 450°C for the temperature of the sample holder. Measurements taken as soon as possible after shut off of the RF and venting the chamber to atmosphere provide a reading of just over 200°C. Given the facts that the sample holder is cooling during the vent and that the thermocouple is heated by the RF field, the sample holder was estimated to be about 350-400°C during the exposure.

During October of 1986, fabrication of a new balanced impedance matching circuit was completed under Boeing funding. This circuit alters the radio frequency potential relationships between the electrodes in the flow discharge section of the atomic oxygen test apparatus. The circuit replaced the unbalanced impedance matching circuit. The following results were noted with the

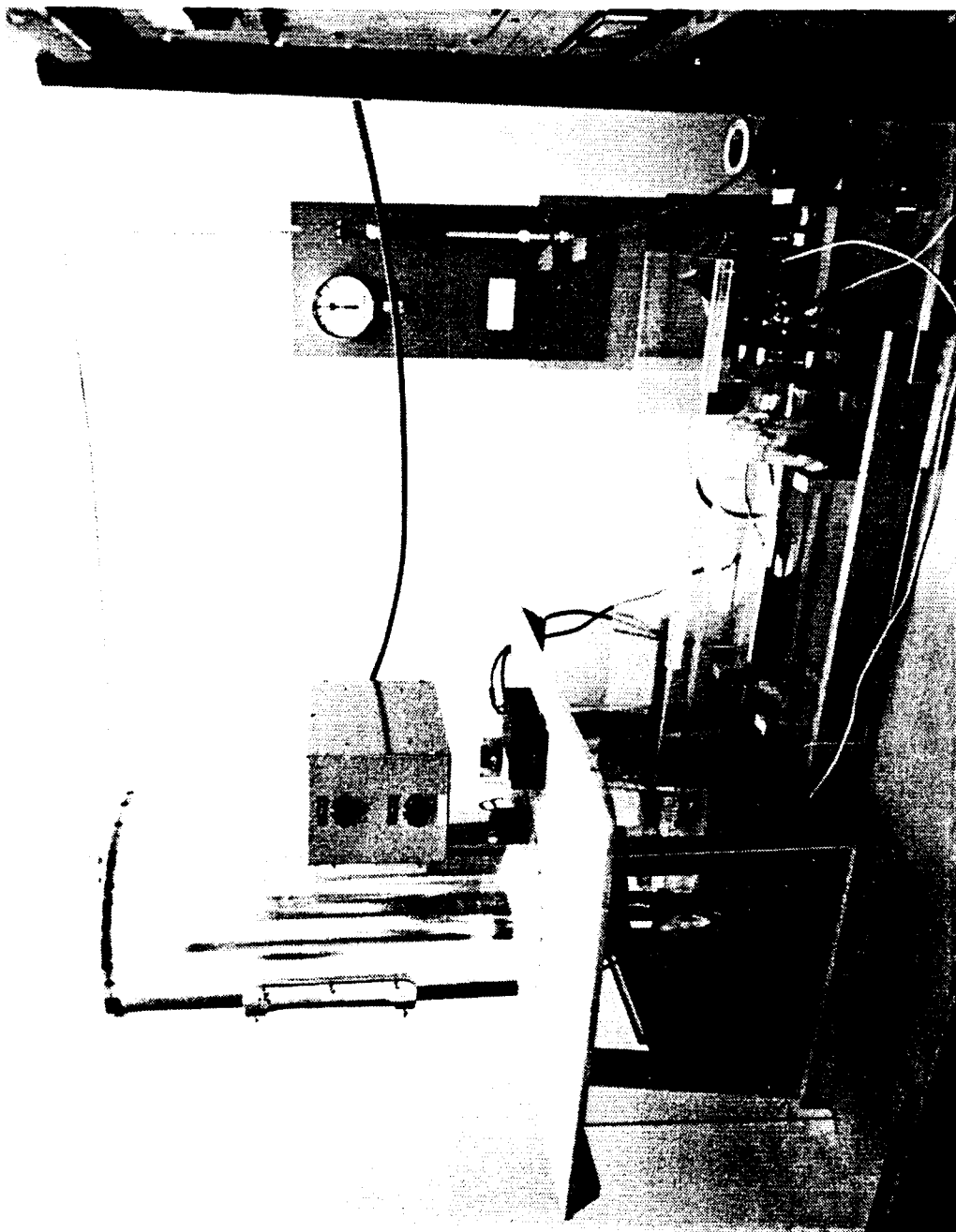


Figure 1: Original Configuration of Atomic Oxygen Test Apparatus

ORIGINAL PAGE IS
OF POOR QUALITY

new circuit.

- (1) RF current in the test section was either greatly reduced or eliminated.
- (2) Microwave heating of the aluminum specimen holder was eliminated.
- (3) Stray RF radiation generation by the test unit was reduced below detectable limits even at the highest power settings.
- (4) The new circuit produced a much brighter glow discharge at every much lower power settings than the previous unbalanced matching circuit.
- (5) The glow discharge was confined to the 3" side tube. No traces of glow discharge were visible in the test section.
- (6) The erosion rate of Kapton H film used as a standard in the check-out run was reduced by about a factor of 100 relative to operation with the unbalanced circuit.

The very large reduction in sample erosion rate is probably related to the elimination of atomic oxygen generation directly in the test section, but may be caused by reduction of sample temperature or a combination of effects.

Figure 2 is a picture of the current test apparatus.

X-Ray photoelectron spectroscopy was used to determine the elemental compositions of coating surfaces before and after exposure to various environments. The mol fraction of each element on the surface is obtained from these measurements. The technique is sensitive to a depth of about 50 angstroms.

Data on surface elemental compositions was also obtained using the Energy Dispersive Analysis of X-rays (EDAX) measurement capability of the Scanning Electron Microscope.



Figure 2. Current Configuration of A0 Test Apparatus

Many measurements of mass loss under exposure to atomic oxygen have been made under this contract. Measurements were made at several different temperatures. Tables 6 through 10 show the results of these measurements. Figures 3 through 8 are graphical summaries of mass loss data for Kapton. There are many measurements on Kapton because this material was used as the reference standard. Mass loss measurements for coatings on Kapton are a measure of the effectiveness of these systems but are not necessarily true measures of the intrinsic resistance of the coating material because of the possibility that cracks in the coating allow the Kapton to be exposed and oxidized.

The solar absorbance and emissivity of these thin films are determined by measuring the UV transmission and reflectivity of the material or the IR reflectivity and transmission of the material and then using the appropriate equation;

$$\alpha = 1 - T_{UV} - R_{UV} \quad \text{or}$$

$$\epsilon = 1 - T_{IR} - R_{IR}.$$

The wavelength range of each measurement is selected to correspond to the range of wavelengths of the solar spectrum. In each case values of transmittance or reflectance are determined at specific wavelengths and then averaged to give a single number.

The solar absorptance was measured in situ for samples exposed to the combined H^+ , e^- , UV environment. For all the other specimens, the optical measurements were made at ambient atmospheric conditions. This is a concern because previous studies have shown a difference between optical properties measured in situ and ex situ, following combined effects exposure. When samples

Fluence (10^{20} atoms/cm ²)	Mass Loss (mg)	Mass Loss/Flux Rate (mg/ 10^{16} atoms/cm ² sec)
9.60	9.72	2.00
13.97	12.83	2.64
40.16	28.29	5.83
10.86	19.98	8.15

Table 6: Mass Loss of Kapton as a function of atomic oxygen exposure.
Sample temperature was 149°C.

Fluence (10^{20} atoms/cm ²)	Mass Loss (mg)	Mass Loss/Flux Rate (mg/ 10^{16} atoms/cm ² sec)
2.25	9.50	3.80
2.70	14.67	5.43
3.60	17.50	7.00

Table 7: Mass loss of Kapton as a function of atomic oxygen exposure.
Sample temperature was 185°C.

(THIS PAGE INTENTIONALLY LEFT BLANK)

Fluence (10^{20} atoms/cm ²)	Mass Loss (mg)	Mass Loss/Flux Rate (mg/ 10^{16} atoms/cm ² sec)
1.04	8.00	5.52
1.04	18.50	12.76
1.46	9.00	3.33
1.57	19.50	13.45
1.94	19.00	7.04
1.94	6.00	2.22
1.94	11.00	4.07
2.09	29.50	20.34
2.09	16.50	11.38
2.35	18.50	12.76
2.43	12.60	5.60
2.43	16.00	5.93
2.43	6.50	2.89
2.61	24.00	16.55
2.92	14.00	5.19
2.92	14.00	5.19
2.92	5.00	1.85
2.92	17.00	6.30
2.92	6.00	2.22
2.92	12.00	4.44
2.92	16.00	5.93
3.13	37.00	25.52
3.40	14.00	5.19
3.40	21.00	7.78
3.89	26.00	9.63
4.64	15.00	6.98
4.64	16.00	7.44
4.86	19.00	7.04
4.86	17.00	6.30
4.86	30.00	11.11
4.86	38.00	14.07
5.83	13.00	4.81
5.83	14.00	5.19
5.94	72.00	26.18
5.94	65.00	23.64
8.10	27.00	12.00
8.10	27.00	12.00
9.90	34.00	12.36
9.72	35.00	12.96
11.34	34.95	15.53
11.34	23.45	10.42
13.61	74.00	27.41
13.86	68.00	24.73

Table 8: Mass loss of Kapton as a function of atomic oxygen exposure. Sample temperature was 195°C.

PRECEDING PAGE BLANK NOT FILMED

(THIS PAGE INTENTIONALLY LEFT BLANK)

ORIGINAL PAGE IS
OF POOR QUALITY

Fluence (10^{20} atoms/cm ²)	Mass Loss (mg)	Mass Loss/Flux Rate (mg/ 10^{16} atoms/cm ² sec)
5.24	0.65	0.13
5.89	1.60	0.29
15.71	1.35	0.28
17.66	2.60	0.48
27.94	2.50	0.52
27.94	3.30	0.68
27.94	3.40	0.70
27.94	3.60	0.74
31.39	3.70	0.68
31.39	4.50	0.83
31.39	5.50	1.01
31.39	3.70	0.68
34.85	2.94	0.49
34.85	1.90	0.31
97.20	7.76	3.45
97.20	14.95	6.64
97.78	20.40	4.21
109.87	20.40	3.74
121.97	16.40	2.71
121.97	20.50	3.39
121.97	15.80	2.61
121.97	21.90	3.62

Table 9: Mass loss of Kapton as a function of atomic oxygen exposure. Sample temperature was 100°C.

PRECEDING PAGE BLANK NOT FILMED

(THIS PAGE INTENTIONALLY LEFT BLANK)

Fluence (10^{20} atoms/cm ²)	Mass Loss (mg)	Mass Loss/Flux Rate (mg/ 10^{16} atoms/cm ² sec)
3.13	0.55	0.38
3.49	0.00	0.00
3.92	0.30	0.06
3.96	0.30	0.11
3.96	0.30	0.11
4.03	0.00	0.00
4.75	0.60	0.18
4.75	0.20	0.06
4.75	0.60	0.18
4.75	0.20	0.06
4.75	0.40	0.12
4.75	0.50	0.15
4.95	0.70	0.26
5.94	0.90	0.33
5.94	0.50	0.12
5.94	0.70	0.26
6.44	0.50	0.18
6.44	1.00	0.36
7.85	0.35	0.06
7.92	0.55	0.20
7.92	0.45	0.16
8.06	0.90	0.16
8.06	0.25	0.05
8.06	0.60	0.11
8.06	0.20	0.04
8.06	0.50	0.09
8.06	0.45	0.08
9.81	1.45	0.27
9.90	1.00	0.36
9.90	1.10	0.40
10.08	0.35	0.09
10.08	0.90	0.23
10.08	0.50	0.09
10.40	1.70	0.62
10.40	0.90	0.33
10.48	0.65	0.13
10.69	0.90	0.18
11.77	0.45	0.08
11.77	0.70	0.13
12.10	0.55	0.10
13.86	1.00	0.36
13.86	0.90	0.33
14.11	0.11	0.19
14.85	0.90	0.33
14.85	0.85	0.31
15.35	1.80	0.66
15.35	1.20	0.44

Table 10: Mass Loss of Kapton as a Function of Atomic Oxygen Exposure. Sample Temperature was 85°C.

(THIS PAGE INTENTIONALLY LEFT BLANK)

Fluence (10^{20} atoms/cm ²)	Mass Loss (mg)	Mass Loss/Flux Rate (mg/ 10^{16} atoms/cm ² sec)
17.28	0.65	0.16
17.28	0.75	0.19
17.46	1.25	0.26
18.14	0.70	0.13
19.01	0.75	0.23
19.80	1.30	0.47
19.80	1.20	0.44
20.16	1.30	0.23
20.60	1.40	0.26
21.78	1.10	0.40
21.78	1.00	0.36
25.92	0.73	0.18
25.92	0.28	0.07
25.92	1.65	0.41
25.92	0.93	0.23
25.92	0.65	0.16
25.92	2.30	0.58
28.51	1.25	0.38
28.51	1.55	0.47
28.51	1.35	0.41
29.70	1.85	0.56
32.26	1.10	0.20
34.46	1.40	0.35
34.56	1.20	0.30
34.56	1.10	0.28
34.56	0.65	0.16
34.56	0.90	0.23
40.16	2.40	0.50
40.16	2.20	0.45
41.90	1.80	0.37
41.90	1.30	0.27
41.90	1.35	0.28
47.52	2.25	0.68
48.38	1.70	0.30
48.38	2.55	0.46
48.38	2.15	0.38
49.41	3.19	1.05
49.41	2.22	0.73
50.40	2.40	0.43
56.95	1.65	0.29
57.02	3.30	1.00
57.02	2.85	0.86
57.02	2.80	0.85
57.02	1.80	0.55
58.21	3.50	1.06
67.68	3.30	0.83

Table 10 (Continued): Mass Loss of Kapton as a Function of Atomic Oxygen Exposure. Sample Temperature was 85°C.

(THIS PAGE INTENTIONALLY LEFT BLANK)

Fluence (10^{20} atoms/cm ²)	Mass Loss (mg)	Mass Loss/Flux Rate (mg/ 10^{16} atoms/cm ² sec)
67.68	4.10	1.03
69.12	4.40	1.10
69.12	2.60	0.65
69.12	4.00	1.00
69.12	1.55	0.39
74.88	4.35	0.84
76.03	3.70	1.12
80.64	3.45	0.62
82.06	3.70	0.76
82.06	3.00	0.62
85.54	2.95	0.89
96.77	3.20	0.57
96.77	4.25	0.76
96.77	3.30	0.59
96.77	5.00	0.89
98.78	4.85	0.87
102.11	8.66	2.51
102.11	5.43	1.79
123.14	6.66	2.18
123.14	9.05	2.97
129.02	4.65	0.83
145.15	4.85	0.87

Table 10 (Continued): Mass Loss of Kapton as a Function of Atomic Oxygen Exposure. Sample Temperature was 85°C.

* PRECEDING PAGE BLANK NOT FILMED

(THIS PAGE INTENTIONALLY LEFT BLANK)

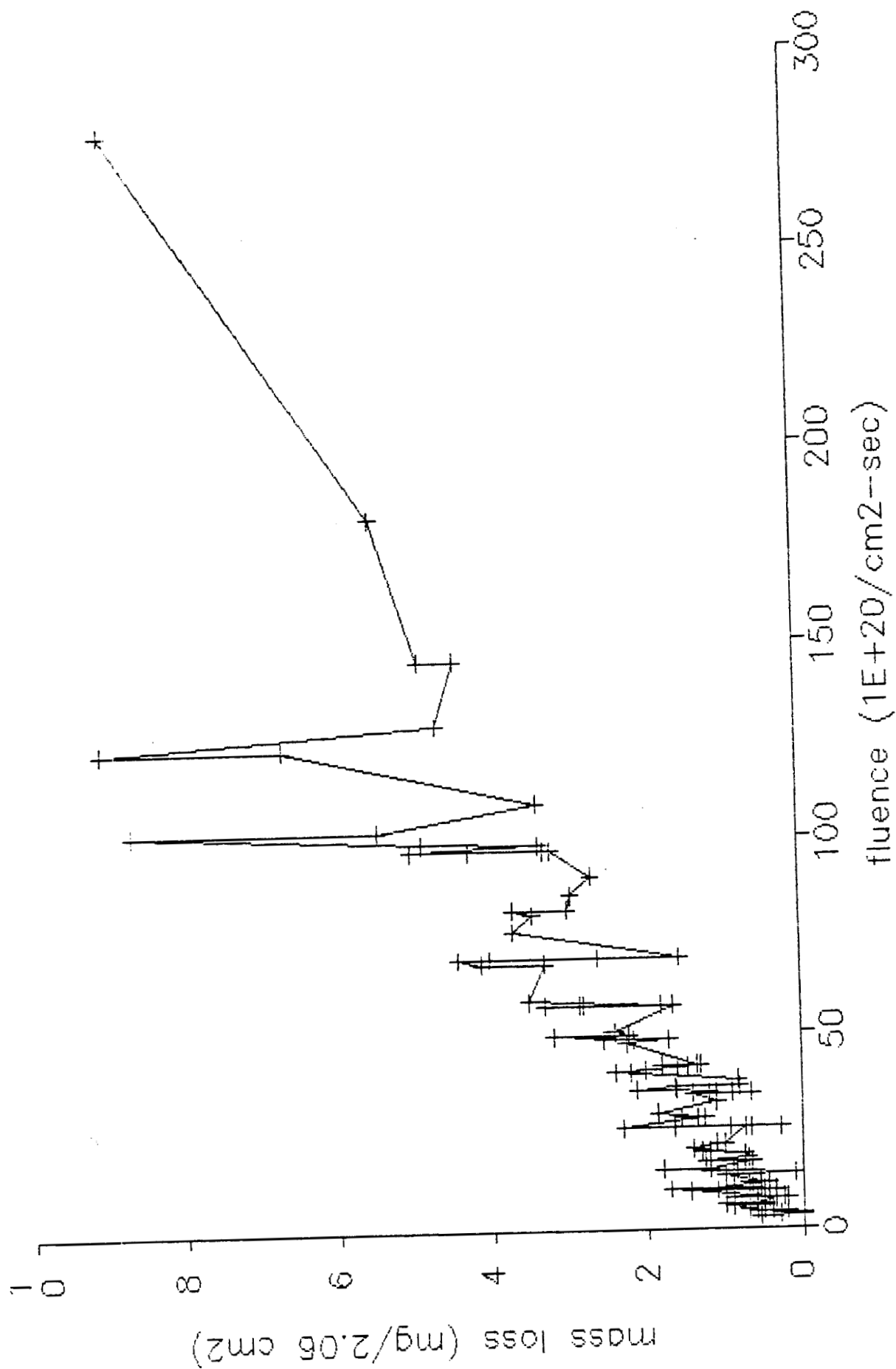


Figure 3: Mass Loss of Kapton, Held at 850°C, vs. Fluence of Atomic Oxygen

(THIS PAGE INTENTIONALLY LEFT BLANK)

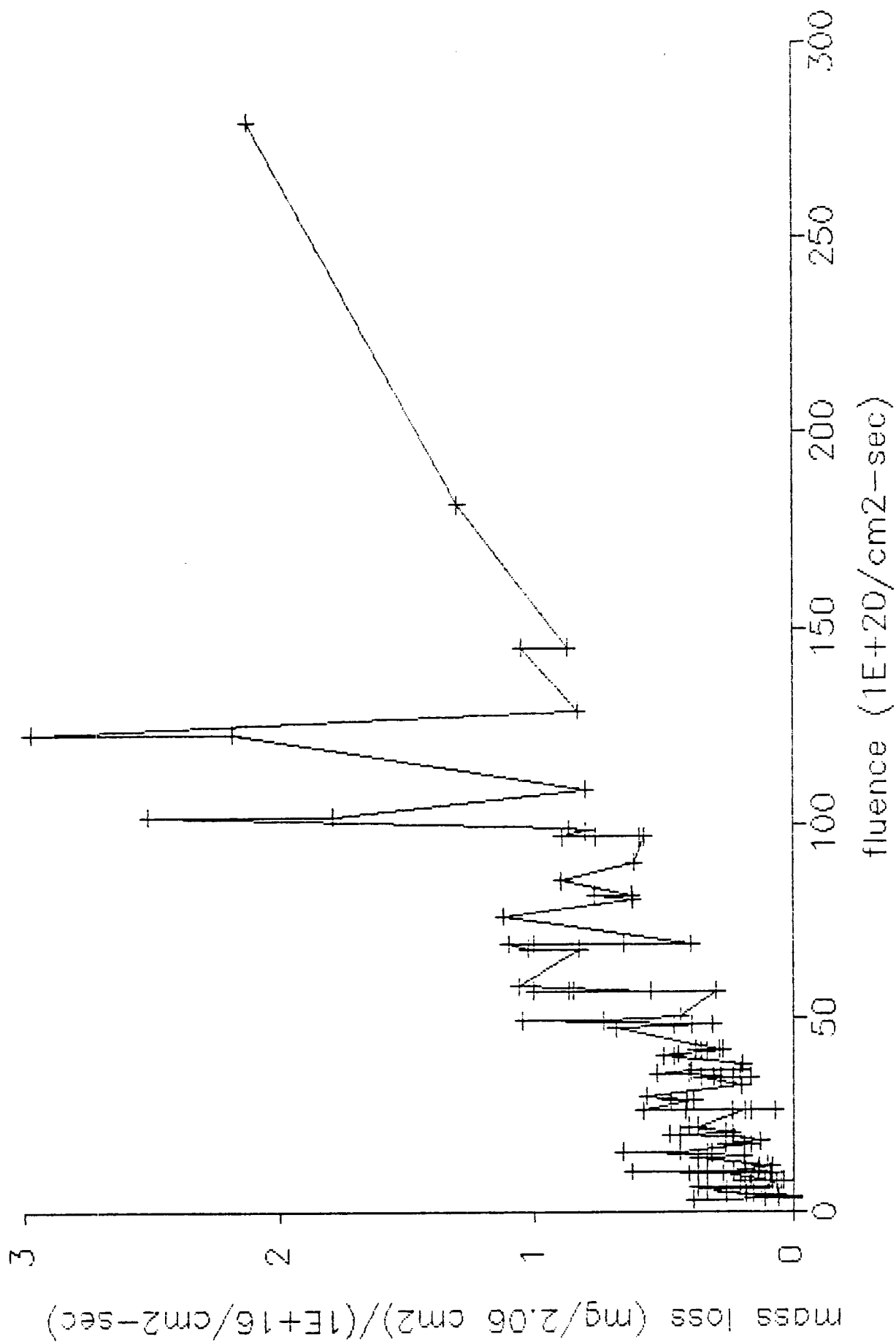


Figure 4: Mass Loss of Kapton, Held at 850C, per Flux of Atomic Oxygen vs. Fluence of Atomic Oxygen

(THIS PAGE INTENTIONALLY LEFT BLANK)

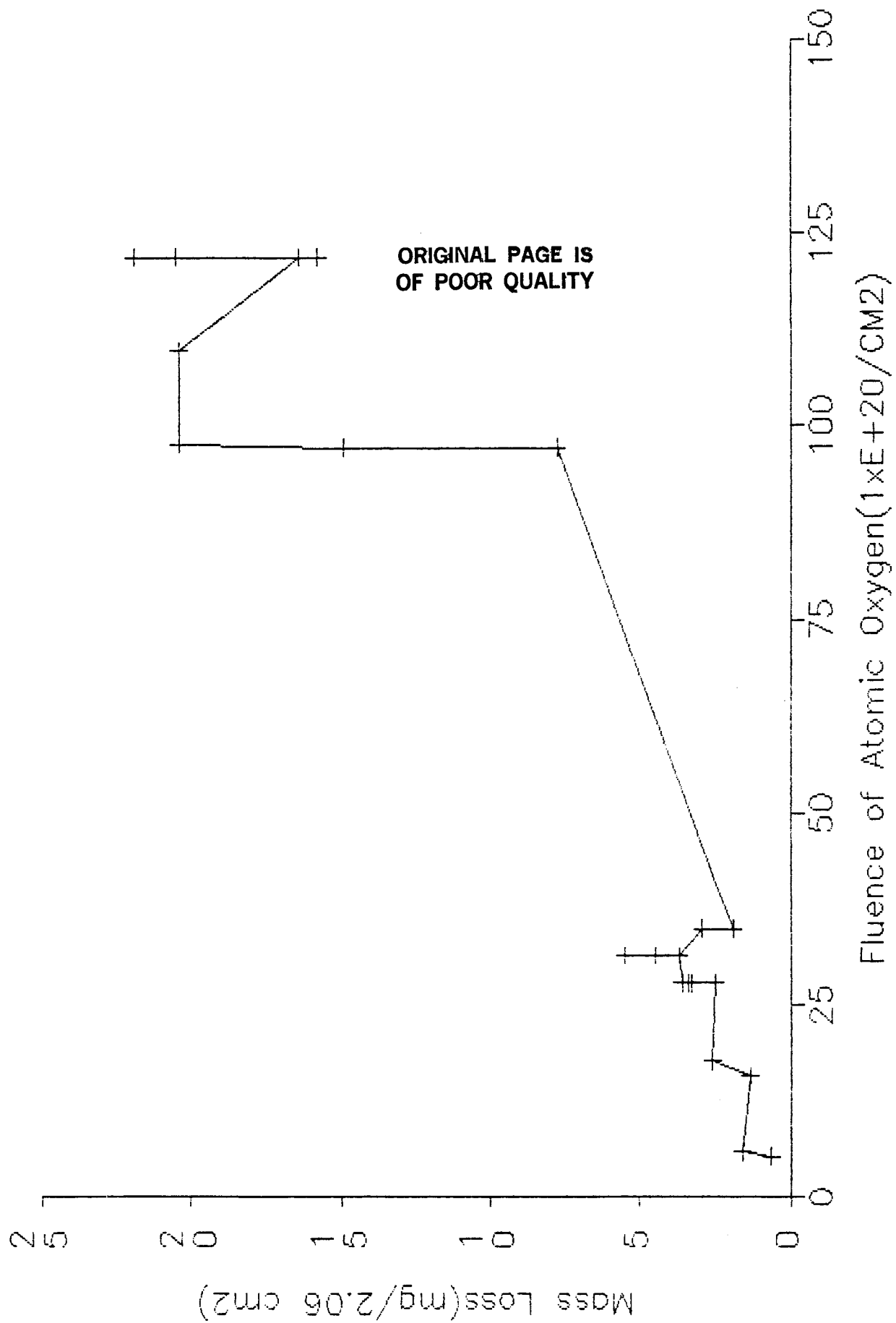


Figure 5: Mass Loss of Kapton, Held at 1000°C, vs Fluence of Atomic Oxygen

(THIS PAGE INTENTIONALLY LEFT BLANK)

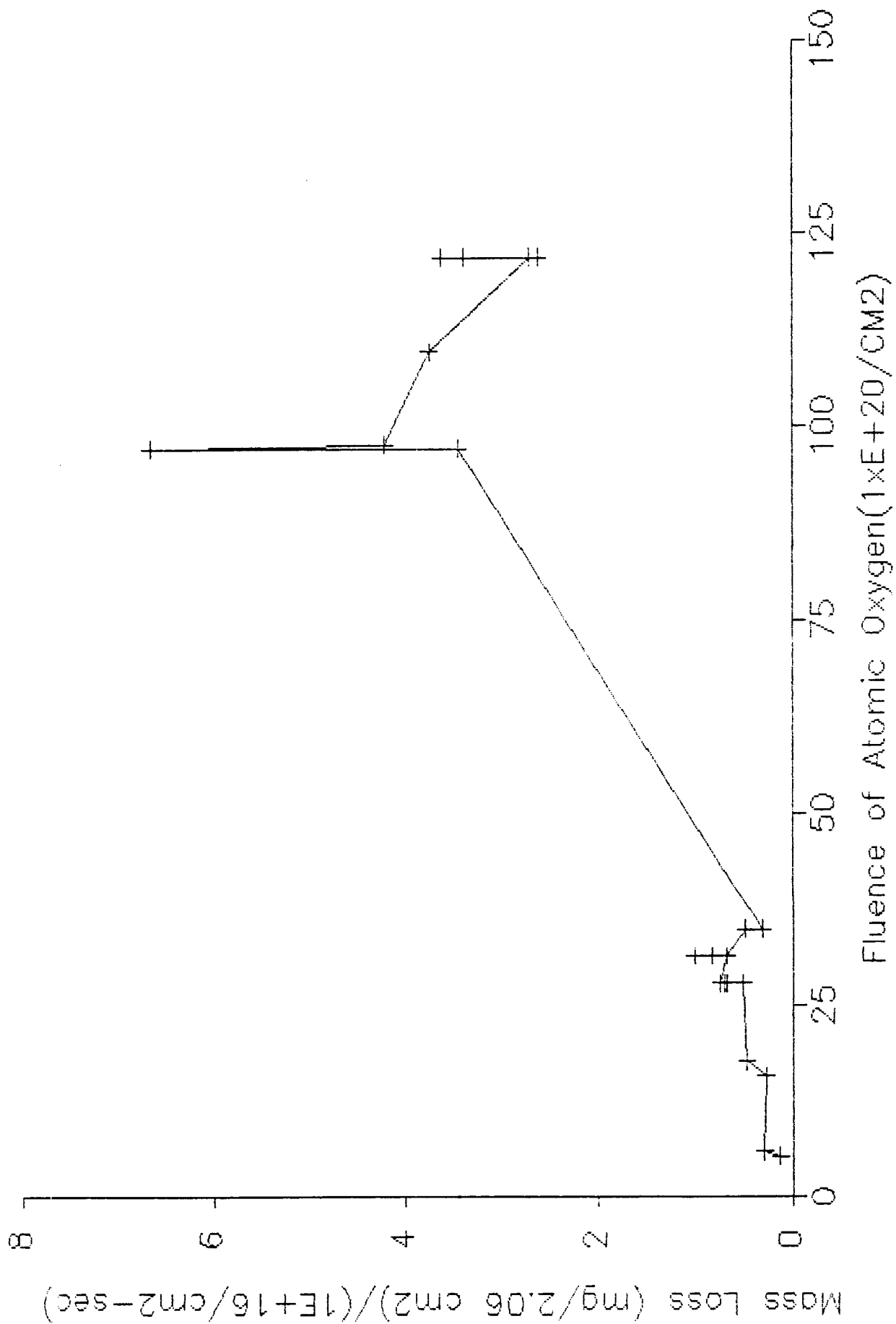


Figure 6: Mass Loss of Kapton, Held at 100°C, Per Flux of Atomic Oxygen vs. Fluence of Atomic Oxygen

(THIS PAGE INTENTIONALLY LEFT BLANK)

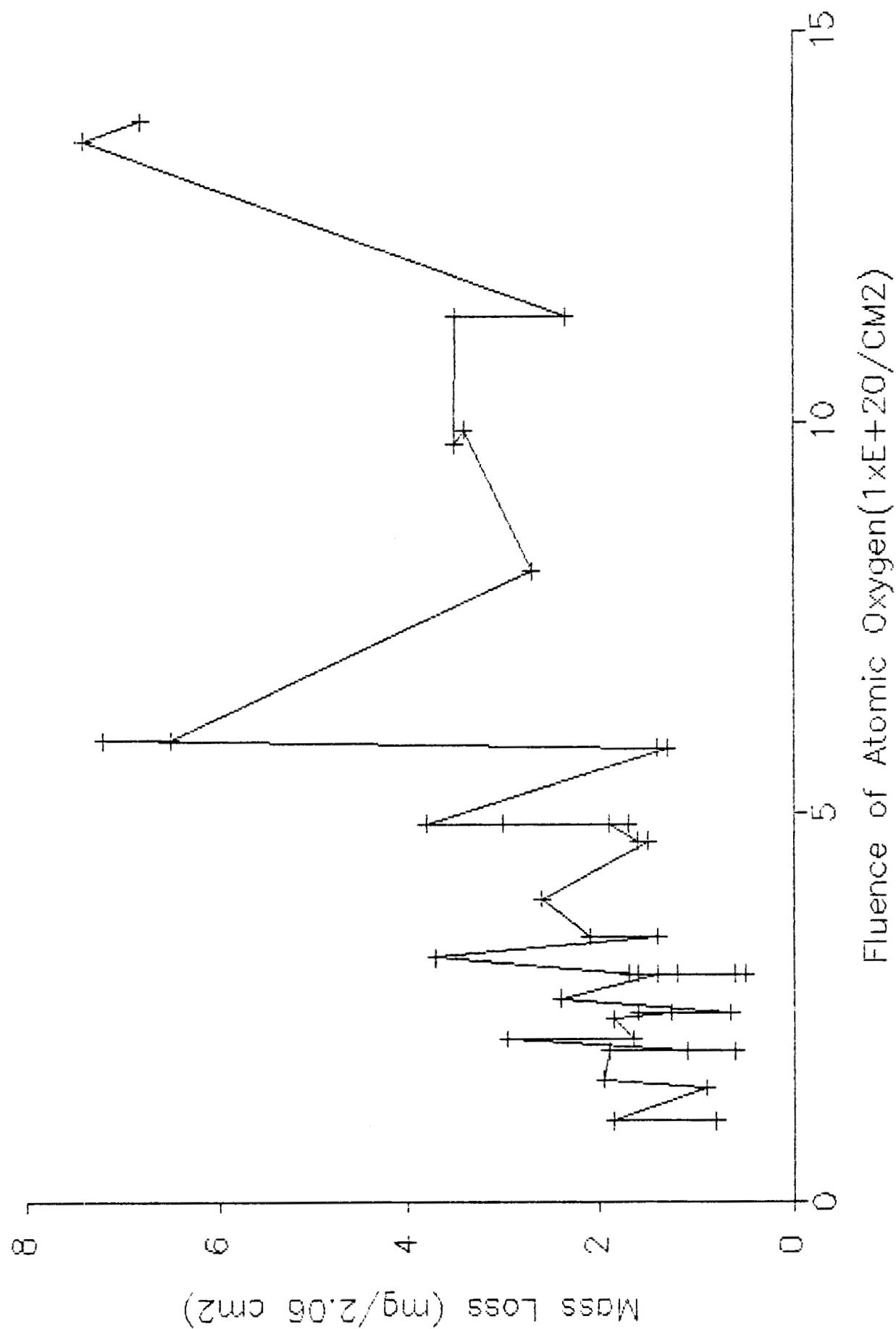


Figure 7: Mass Loss of Kapton, Held at 195°C, Per Flux of Atomic Oxygen
Per Flux of Atomic Oxygen

(THIS PAGE INTENTIONALLY LEFT BLANK)

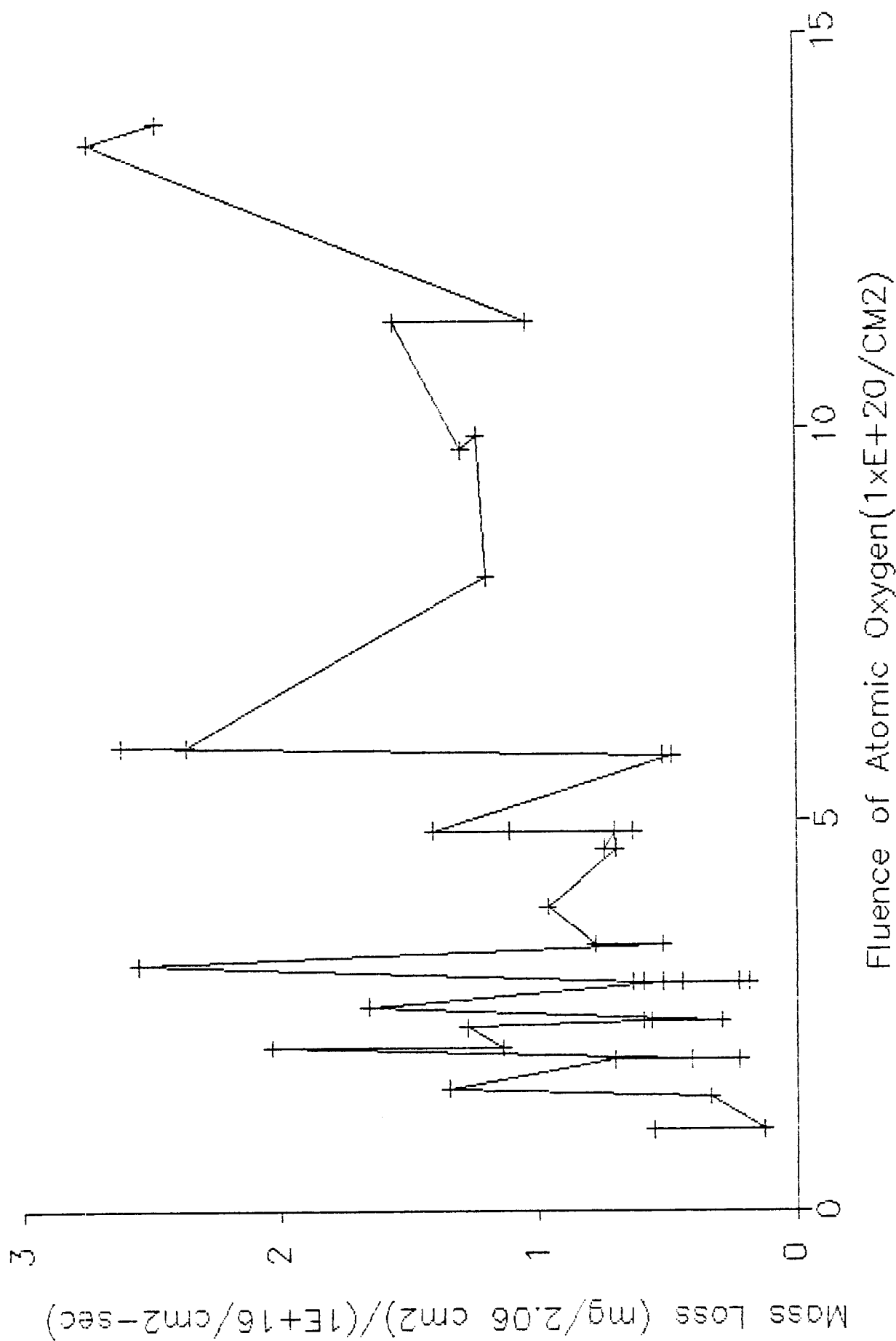


Figure 8: Mass Loss of Kapton, Held at 195°C, vs. Fluence of Atomic Oxygen

are exposed to air they exhibit a partial recovery toward their original optical properties.

There have been four tests conducted at the Boeing Physical Sciences Research Center exposing coating specimens to combinations of simulated space environmental effects. Two tests were exposures of samples to simulated solar UV alternated with periods of thermal cycling. Conditions for these tests are listed in tables 11 and 12. Two tests were exposures of samples to simultaneous simulated solar UV, protons, and electrons. Conditions for these tests are listed in tables 13 and 14.

The combined vacuum thermal cycling/UV exposure testing was performed in a turbo-molecular pumped vacuum chamber shown in figures 9 and 10. The sample holder frame was connected to a motor driven shaft which moves the samples between the cooling chamber and the window area.

Test samples were attached by snap-ring retainers to a black anodized aluminum test fixture of low thermal mass. This test fixture was then mounted in the space simulation test chamber. The fixture was suspended from an aluminum mounting frame by thermally insulating connectors. Three thermocouples were attached with high thermal conductivity epoxy to the surface of the fixture opposite the test samples. One of these thermocouples was monitored continuously and its output recorded on chart paper for later reference. A second thermocouple provided control input information to the microprocessor which cycled the samples.

Thermal-Vacuum Cycling and UV Exposure tests were divided into three one-week periods of UV exposure and three one-week periods of thermal-vacuum cycling. The testing sequence alternated between one week of UV and one week of thermal-vacuum cycling.

<u>DATES</u>	<u>CONDITIONS</u>
11/20/86 - 11/30/86	UV Exposure 218.5 ESH*
12/01/86 - 01/28/86	Thermal Cycling 222 Cycles
12/08/86 - 12/15/86	UV Exposure 135.2 ESH
12/15/86 - 12/22/86	Thermal Cycling 232 Cycles
12/22/86 - 12/29/86	UV Exposure 150.2 ESH
12/29/86 - 01/05/87	Thermal Cycling 223 Cycles

*Equivalent sun hours

Total UV Exposure	503.8 ESH
Average UV Exposure Rate	0.89 UV Suns
Total Number of Thermal Cycles	677
Cycle Time	42-45 Min
(Between -80°C and +80°C)	

Table 11: Test Parameters For The Combined Vacuum
Thermal Cycling/Ultraviolet Radiation Exposure,
Fall 1986

(THIS PAGE INTENTIONALLY LEFT BLANK)

VACUUM THERMAL CYCLE TESTING:

Total Number of Cycles:	811
Temperature Range:	-80°C + -3°C to +80°C + -3°C
Cycle Period:	39-41 minutes (typical)
Vacuum:	1.0 - 7.0 x 10 ⁻⁸ Torr

ULTRAVIOLET EXPOSURE:

Total UV Exposure:	796 ESH
Sample Temperature:	+109°C to +115°C (0.40 to 0.25 micron range):
Average UV Exposure Rate:	1.5 to 1.6 solar constants
Vacuum:	1.0 - 6.0 x 10 ⁻⁸ Torr

Table 12: Test Parameters for the Combined Vacuum Thermal Cycling/
Ultraviolet Radiation Exposure, Spring 1988

PRECEDING PAGE BLANK NOT FILMED

(THIS PAGE INTENTIONALLY LEFT BLANK)

Equivalent Sun Hours of UV	0	200	500	1000
35 Kev Proton Fluence/cm ²	0	1.1 x 10 ¹⁵	3.3 x 10 ¹⁵	6.0 x 10 ¹⁵
30 Kev Electron Fluence/cm ²	0	9 x 10 ¹⁴	2.5 x 10 ¹⁵	5.4 x 10 ¹⁵

Table 13: Parameters For Combined Effects Test Exposure, Spring 1987

(THIS PAGE INTENTIONALLY LEFT BLANK)

<u>Exposure Time</u> <u>Increments</u>	<u>Cumulative</u>	<u>Average</u> <u>uv Suns</u> 0	<u>%R</u> <u>Measurement</u>	<u>Lyman</u> <u>Alpha</u>	<u>Protons</u> 0	<u>Particle Fluences</u> <u>Electrons</u> 0
62 Hours	62 Hours	1.6	100 ESH	ON	3.5x10 ¹⁴	7.7x10 ¹⁴
60 Hours	122 Hours	1.6	200 ESH	OFF	7.1x10 ¹⁴	1.2x10 ¹⁵
104 Hours	226 Hours	1.5	360 ESH	ON	1.1x10 ¹⁵	2.2x10 ¹⁵
110 Hours	336 Hours	1.5	520 ESH	OFF	2.0x10 ¹⁵	3.3x10 ¹⁵
135 Hours	471 Hours	1.8	760 ESH	ON	2.5x10 ¹⁵	4.2x10 ¹⁵
135 Hours	606 Hours	1.8	1000 ESH	OFF	3.1x10 ¹⁵	4.9x10 ¹⁵
-100		0		ON	(p/cm ²)	(e/cm ²)

Table 14: Irradiation Parameters And Test Sequence
For Combined Effects Exposure: Mid-1988

The UV portion of the test was performed by moving the samples to the window area and adding a water window to the outside of the chamber (see figure 10). The UV source is a Spectrolab X25L solar simulator. The UV intensity was measured with a Hy-Them Pyrhelimeter manufactured by Hy-Cal Engineering. The UV content was set by mounting the pyrhelimeter on the sample plane and passing the X-25L beam through the water window. During the ultraviolet testing, the samples were moved to the thermal cycle "heat" position, a second quartz "water window" was attached to the vacuum chamber and the X-25 solar simulator was started. (The "water window" was necessary to reduce the infrared component of the solar simulator spectrum.)

The X-25 solar simulator was configured to provide a 1.0 solar constant simulated beam over a 12" diameter test plane at a distance of 72 inches in the absence of attenuating media.

The pyrhelimeter was then moved to a special mount which provides repeatable positioning outside the chamber and the UV content measured. This procedure allowed the UV measurements to be made outside the chamber during exposure. The exposure rate was at one UV sun.

The thermal cycling portion of the test was performed by moving the samples from the window position for heating to the liquid nitrogen cooled chamber for cooling. This process was automated under the control of a programmable temperature controller. The thermal cycle extremes were -80°C and $+80^{\circ}\text{C}$. Heating was accomplished by illuminating the samples through a quartz window with IR lamps. The temperature controller will adjust the IR intensity automatically to reach $+80^{\circ}\text{C}$.

The test fixture was illuminated by an array of infrared heating elements during the heating cycle, the IR energy being admitted to the vacuum chamber through a one inch quartz window. The fixture was then mechanically moved on

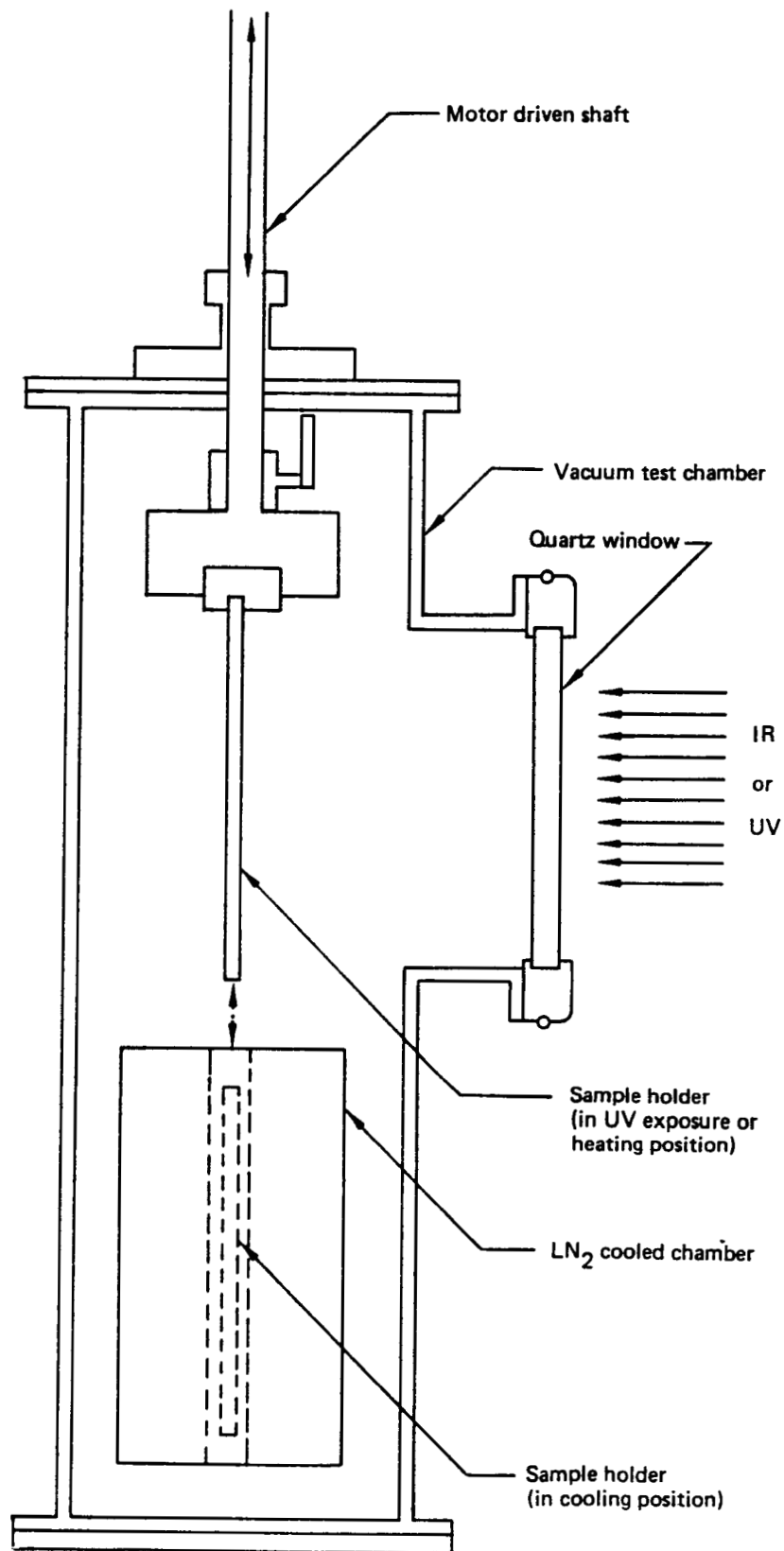


Figure 9: Thermal Vacuum Cycling and UV Exposure Test Chamber

(THIS PAGE INTENTIONALLY LEFT BLANK)

ORIGINAL PAGE IS
OF POOR QUALITY

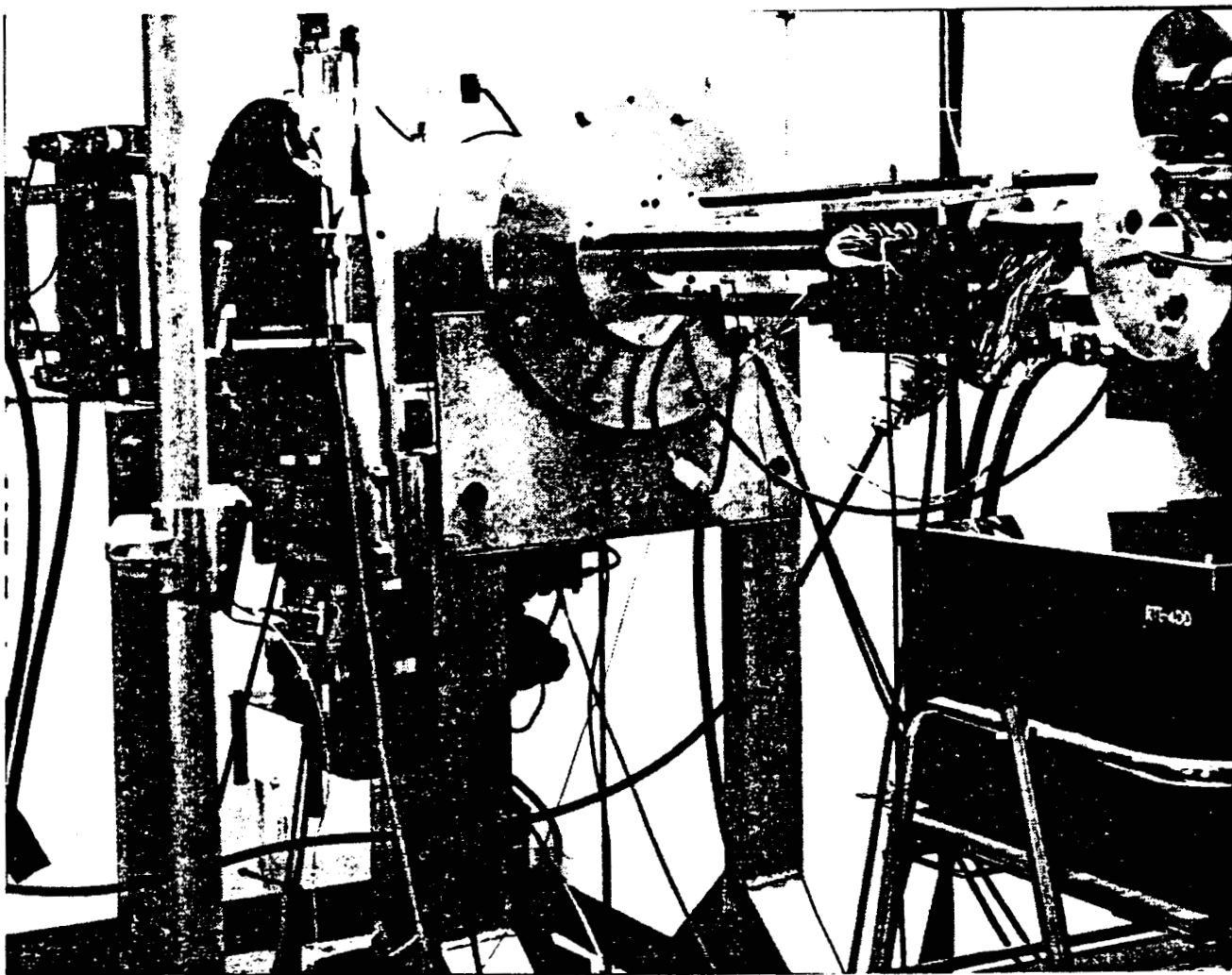


Figure 10: Vacuum Test Chamber With IR Lamp Array Used For
Thermal Cycling Test

PRECEDING PAGE, IMAGE NOT FILMED

a motor driven shaft into a slot in a liquid nitrogen filled cold trap for the cooling portion of the cycle. A microprocessor activated system of relays caused samples to change position after reaching the desired temperature. The limiting factor in sample cycle time was the rate of radiative loss to the walls of the liquid nitrogen cold trap. Data from the exposure during late 1986 is reported in tables 15 and 16.

<u>Material #</u>	<u>(± 0.03)</u>		<u>(± 0.02)</u>	
	<u>Initial</u>	<u>Post Exposure</u>	<u>Initial</u>	<u>Post Exposure</u>
50	0.145	0.19	0.57	0.61
52	0.15	0.20	0.55	0.55
58	0.145	0.24	0.74	0.65
65	0.15	0.22	0.60	0.72
66	0.165	0.23	0.69	0.72

Table 15: Optical Properties of Selected Samples Before and After Sample Exposure to Vacuum Thermal Cycling Conditions.
Data From Test Conducted in Late 1986.

	<u>Average Wt Loss (g)</u>	<u>(# of Samples)</u>
HMDS (50)	0.0001	(6)
HMDS/TFE (8/1) (52)	0.0000	(6)
Silicone CV1-1144-0 (65)	0.0002	(6)
Fluorosilicone CV1-3530 (66)	0.0001	(6)
Polyphosphazene X128 (58)	0.0009	(6)
IITRI S13/G/L0-1 on FC-Epoxy	0.0018	(4)
IITRI S13/G-L0-1 on Aluminum	0.0005	(3)

Table 16: Average Weight Loss of Materials Exposed to UV/Thermal Vacuum Cycling Conditions. Data From Test Conducted Late 1986.

A second combined vacuum thermal cycling/UV exposure test was performed on 37 samples of candidate Space Station surface materials in the space simulation test chamber located at Boeing Physical Sciences Research Center. Testing consisted of three one week periods of vacuum thermal cycling alternating with three one week periods of ultraviolet exposure. Tests were conducted beginning with vacuum thermal cycling on February 2, 1988. Alternating with one week periods of thermal cycle testing and commencing on the second week of the test, the samples were exposed to ultraviolet radiation at 1.5 to 1.6 solar constants for one week periods. The total exposure time period was six weeks.

Test requirements were for as much ultraviolet as could be provided. Calculations indicated that at a distance of 45 inches the test fixture could be covered with a relatively uniform beam at an intensity of 1.5 to 1.6 solar constants. This distance takes into account the attenuation in the ultraviolet and the correction factor from actual simulator output to the real solar spectrum in the wavelength region from 0.40 microns to 0.2 microns. Solar simulator output intensity was measured daily by rotating the Hy-CAL Engineering Model #P-8400-B-10-120 pyreheliometer into the simulator beam. This pyreheliometer was calibrated to a reference value which corresponded to 1.58 ultraviolet suns at the sample plane. Simulator output was maintained at that reference value throughout the test. Sample temperature during the ultraviolet exposure testing reached equilibrium in the range of 109°C to 115°C. The samples received 796.2 equivalent sun hours of exposure to the ultraviolet radiation. The test parameters are summarized in table 12.

One test requirement was to cycle the samples between +80°C and -80°C as many times as possible during the three weeks of testing. Cycle times were

typically 39 to 41 minutes with high temperature values ranging from 78°C to 81°C and low temperature values ranging from -80°C to -83°C.

The samples were protected by a system of interlocks and safety alarms which prevented the occurrence of any temperature extremes outside the range -85°C and +85°C during the thermal cycle testing. During thermal vacuum cycle #728 of the second set of exposures, it was discovered that the maximum temperature reached during cycles 725 through 728 was approximately 65°C to 75°C. A simple mechanical problem with the motor and shaft assembly was immediately corrected. The test samples were cycled a total of 811 times over the three week period.

Solar absorptance and thermal emittance were determined for the test specimens as follows. The infrared reflectance was measured on a Gier Dunkle DB 100 infrared reflectometer. A comparison was made between total normal reflectance and total hemispherical reflectance as measured by this instrument. The average difference was found to be 0.052; total hemispherical reflectance being higher. The infrared transmission was measured using a Digilab FTS 60 Fourier transform infrared spectrometer.

The ultraviolet reflectance and transmission measurements were carried out on a Perkin-Elmer Lambda 9 UV/VIS/near IR spectrophotometer, using a 60mm integrating sphere. Tables 17 through 19 show the results of measurements on control specimens, and the set of specimens which were previously exposed to the vacuum thermal cycling/UV radiation test environment, respectively. The ultraviolet reflectance measurements have been corrected for the fact that the black absorbing disc placed behind the samples actually has a reflectance of 0.043. A factor of $0.043 T^2$, where T is the ultraviolet transmission, must be subtracted from the measured reflectance. The T^2 factor results from the fact that light reflected from the background disc must pass through the sample material twice.

Combined Radiation Effects on Optical Properties

Two tests were carried to determine the effects of combined proton, electron and UV exposure on coating optical properties. The facility used is shown schematically in figure 11 and a photograph is shown in figure 12. Three elements of the low earth orbit radiation environment were simulated under vacuum. Absorptance measurements were made periodically under vacuum during the course of the test run. To make the absorptance measurements the radiation sources shown in figure 11 are shutdown and the specimen block holding

(THIS PAGE INTENTIONALLY LEFT BLANK)

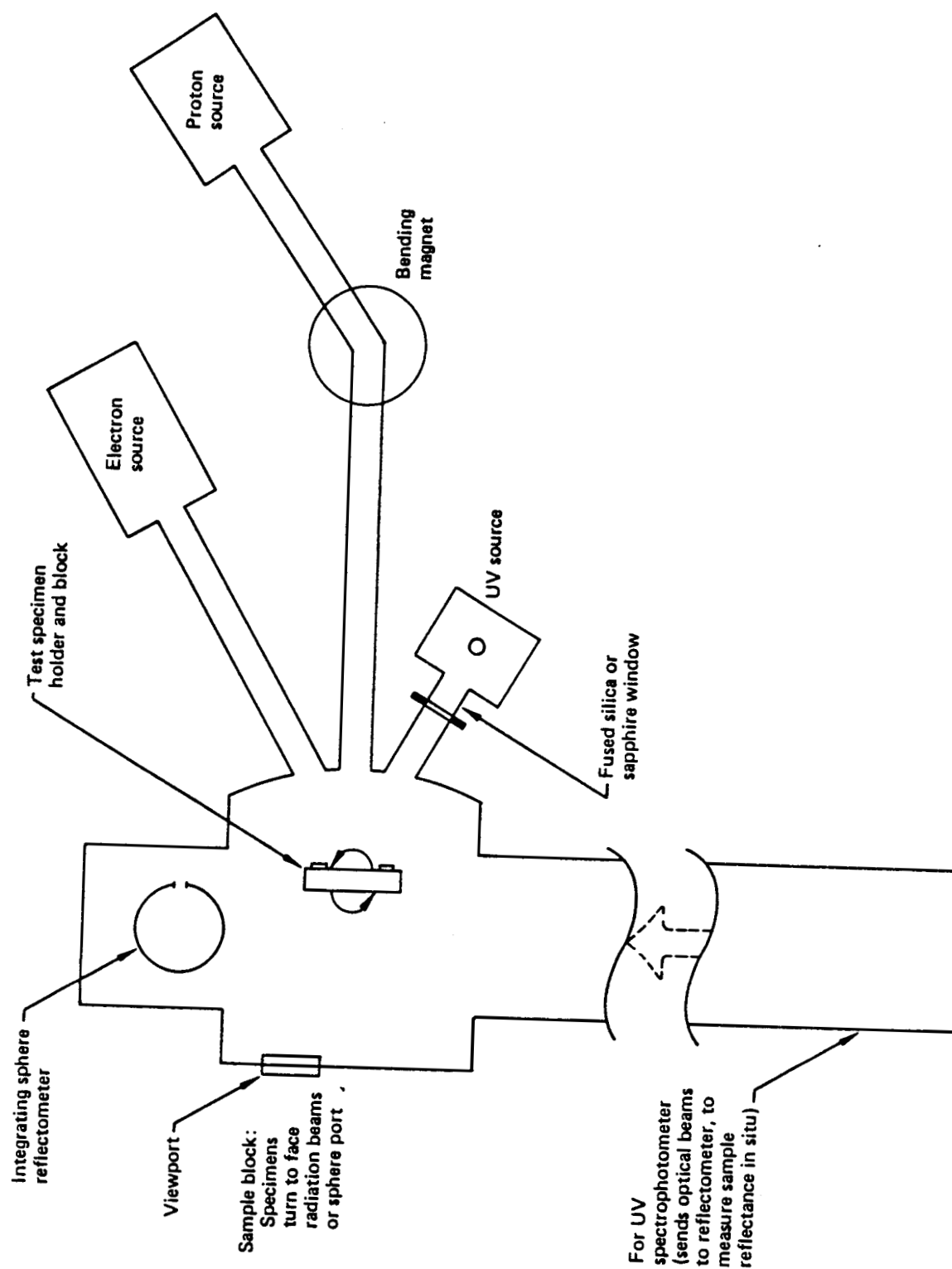


Figure 11: Schematic of Boeing Combined Radiation Effects Test Chamber (CRETC) II

PRECEDING PAGE BLANK NOT FILMED

(THIS PAGE INTENTIONALLY LEFT BLANK)

ORIGINAL PAGE IS
OF POOR QUALITY



Figure 12: Photo of Boeing Combined Radiation Effects Test Chamber II

(THIS PAGE INTENTIONALLY LEFT BLANK)

<u>Material</u>	<u>R_{IR}</u>	<u>T_{IR}</u>	<u>ε</u>	<u>R_{UV}</u>	<u>T_{UV}</u>	<u>α</u>
Kapton	0.183	0.260	0.557	0.126	0.598	0.276
Apical	0.182	0.259	0.559	0.119	0.562	0.319
Fluorinated Ethylene						
Propylene	0.145	0.175	0.680	0.090	0.626	0.284
Tetrafluoroethylene	0.142	0.346	0.512	0.182	0.839	---
Silicone (DSET)	0.137	0.001	0.862	0.842	0.076	0.082
Hexamethyl Disiloxane/ Tetrafluoroethylene (Large Demonstration Article-HMDS/TFE)						
HMDS/TFE (112)	0.168	0.314	0.518	0.085	0.664	0.251
Silicone-Polyimide						
Copolymer (93)	0.178	0.262	0.560	0.148	0.616	0.236
HMDS (110)	0.160	0.275	0.565	0.085	0.662	0.253
Fluorosilicone (RTV-GE)	0.149	0.109	0.742	0.298	0.165	0.537
HMDS (5000A)	0.193	0.401	0.406	0.100	0.658	0.242
Fluorophosphazene	0.147	0.199	0.654	0.100	0.656	0.244
Silicone (CV1-1144)	0.153	0.161	0.686	0.095	0.062	0.243
Fluorosilicone (CV-3530)	0.140	0.073	0.787	0.094	0.660	0.246

Table 17: Results of Optical Properties Measurements on Selected Materials. Coatings are Applied to Kapton. Specimens are Control Samples for Comparison With Samples From Combined Vacuum Thermal Cycling/UV Exposure Test of Early 1988.

PRECEDING PAGE BLANK NOT FILMED

(THIS PAGE INTENTIONALLY LEFT BLANK)

<u>Material</u>	<u># Specimens</u>	<u>R_{IR}</u>	<u>T_{IR}</u>	<u>ε</u>	<u>R_{UV}</u>	<u>T_{UV}</u>	<u>α</u>
HMDS (110)	3	0.156	0.281	0.563	0.086	0.662	0.252
Fluoro- silicone (CV-3530)	3	0.140	0.058	0.802	0.093	0.659	0.248
Kapton R Silicone (CV1-1144)	3	0.183	0.261	0.556	0.125	0.599	0.276
HMDS/TFE (112)	3	0.154	0.154	0.692	0.092	0.649	0.259
Fluorophos- phazene	2	0.170	0.302	0.528	0.082	0.659	0.259
Silicone (DSET)	3	0.176	0.042	0.782	0.089	0.519	0.392
Fluoro silicone (RTV-GE)	1	0.141	0.002	0.857	0.821	0.086	0.093
Apical R	1	0.153	0.134	0.713	0.285	0.183	0.532
HMDS (5000A)	2	0.183	0.259	0.558	0.120	0.561	0.319
TFE	3	0.194	0.407	0.399	0.103	0.659	0.238
FEP	3	0.142	0.347	0.511	0.178	0.767	0.055
S11G/LO	1	0.145	0.183	0.672	0.092	0.624	0.284
V10 S/LO	1	0.145	0.011	0.844	0.769	0.146	0.915
HMDS/TFE	1	0.146	0.088	0.756	0.083	0.613	0.304
(Large Demonstration Article)	1	0.161	0.288	0.551	0.099	0.649	0.252
Siloxane/ Polyimide Copolymer	3	0.157	0.632	0.211	0.114	0.587	0.309

Table 18: Results of Measurements of Optical Properties of Specimens
Exposed to the Combined Vacuum Thermal Cycling/UV Environment

C-2

(THIS PAGE INTENTIONALLY LEFT BLANK)

<u>Material</u>	<u>$\Delta\epsilon$</u>	<u>$\Delta\alpha$</u>
Fluorosilicone (GE-101)	-0.029	-0.005
HMDS (5000A Thick)	-0.008	-0.004
Apical R	-0.001	0.000
CV-3530	0.015	0.003
Fluorophosphazene (X-128)	0.128	0.166
Siloxane-Polyimide Copolymer	0.120	0.064
FEP	-0.012	0.000
SI1G/L0	-0.009	-0.002
TFE	-0.001	(Increase)
CV1-1144	0.006	0.016
Silicone (DSET)	-0.005	0.010
HMDS	-0.002	-0.002
HMDS/TFE	0.010	0.009
Kapton ^R	-0.002	-0.001
V10G/L0	-0.020	-0.010
HMDS/TFE (Large Demo Article)	0.024	0.012

Table 19: Average Change in Optical Properties of Selected Materials Due to Exposure to the Combined Thermal Vacuum Cycling/ Ultraviolet Radiation Environment.

PRECEDING PAGE BLANK NOT FILMED

(THIS PAGE INTENTIONALLY LEFT BLANK)

the test specimens is rotated so that it faces an integrating sphere within the vacuum chamber. The integrating sphere can be translated and maneuvered into position over selected portions of the specimen block. The irradiated portion of the specimen block is 3 inches in diameter.

The simulated space environment used in these test includes ultraviolet radiation, electrons, and protons and is summarized as follows:

- o The ultraviolet radiation rate is not more than 2 suns with a minimum of 1 sun and a probable rate of 1.5 suns. The total exposure time of 667 hours provides 1000 ESH (equivalent solar hours) of UV.
- o The spectrum used to simulate solar UV covers 200-400 nm, of approximately one sun total intensity. A water column is used to cool the UV source, thus producing an irradiance spectrum from 200 nm to 1400 nm (i.e., the longer IR wavelengths are cut off).
- o The electron flux was on the order of $1 \times 10^9 \text{e/cm}^2 - \text{sec}$, simulating typical fluxes but not the peak of the most intense substorms.
- o The electron energy was 30 keV.
- o The proton flux was slightly less than the electron flux. The protons had an energy of 35 keV.
- o The sample temperature during the first test was 20°C, measured in the block beneath the sample substrates. During the second test samples were maintained at 40°C.
- o The tests were carried out in a vacuum of 10^{-7} to 10^{-8} torr, pumped without organic fluids.

PRECEDING PAGE BLANK NOT FILMED

<u>Material</u>	Initial Values		Post Exposure		Post Exposure (In Situ)
	—	—	—	—	—
Silicone (CV1-1144-0)	0.324	0.816	0.32	0.79	0.41
Fluorosilicone (CV-3530)	0.322	0.794	0.39	0.81	0.44
S13 G/L0	0.097	0.843	0.21	0.83	0.44
Kapton R	0.259	0.574	0.36	0.64	0.49
Hexamethyl	0.344	0.641	0.35	0.66	0.42
Disiloxane/ Tetrafluoroethylene)(8:1)					
Fluorophosphazene	0.221	0.595	0.53	0.71	0.58

Table 20: Optical Properties of Materials Exposed to the Combined Radiation Effects Test Chamber Environment at the Boeing Radiation Effects Laboratory Results From Tests Conducted in early 1987.

Table 20 includes absorptivity and emissivity data for the materials which had been exposed to the combined radiation environment at the Boeing Radiation Effects Laboratory. In virtually every case the ex situ absorptance measurements showed a partial recovery toward the original values when the samples were exposed to atmosphere. Little net changes were observed for the emissivity values except for Kapton. In situ measurements of changes in absorptance as a function of fluence of particle and UV radiation are reported in table 21.

The Boeing Combined Radiation Effects chamber (CRETC) II was again used during July and August of 1988 to irradiate candidate coating materials with protons, electrons, solar continuum ultraviolet radiation, and Lyman-alpha 1216 Angstrom line UV radiation. The hemispherical spectral reflectance of

Material	Equivalent Sun Hours of UV	0			200			500			1000		
		35 kev portion fluence/cm ²			1.1 x 10 ¹⁴			3.3 x 10 ¹⁵			5.4 x 10 ¹⁵		
		30 kev electron fluence/cm ²			9 x 10 ¹⁴			2/5 x 10 ¹⁵			5.4 x 10 ¹⁵		
Witness OSR		0.070			0.072			0.076			0.081		
Kapton (#1)		0.360			0.394			0.441			0.489		
Battelle (#67)		0.363			0.380			0.397			0.416		
Battelle (#69)		0.362			0.379			0.396			0.419		
Ethyl (#82)		0.360			0.412			0.507			0.577		
IITRI SI3G-LO-1		0.234			0.288			0.378			0.445		
McGhan-NuSi1 CV1144		0.338			0.357			0.380			0.407		
McGhan-NuSi1 CV3530		0.334			0.356			0.400			0.444		

Table 21. Solar Absorptance Values for Selected Materials as a Function of Combined Radiation Effects Dose Level. Values are for In Situ Measurements From Test of Early 1987.

the test samples was measured at intervals throughout the experiment. This reflectance is a useful measure of material degradation for determining spacecraft thermal balance as a function of time in orbit. Most materials tested were damaged significantly by various types of radiation, especially protons. In addition, the Lyman-alpha far UV did have an observable effect, enhancing the damage in several materials.

A thin, opaque film of aluminum was evaporated onto the back surface of samples that were not already opaque. To bond specimens to the metal sample block, strips of 3M high-temp acrylic adhesive were laid down on the block. Samples were then applied to the adhesive strips in a close-pack pattern. Finally, a punch was used to separate excess adhesive from the block. Material type CV-3530 was found to be incompatible with CRETC equipment when the completed test array and sample block were mounted and checked out inside CRETC II, especially with regard to the close (10-20 mil) alignment of the integrating sphere. Smearing of the top, tacky layer of 2 CV-3530 specimens across several other samples occurred. Those had to be cleaned, and CV-3530 abandoned in favor of some other test materials.

Thermal Vacuum Cycling and UV Exposure Tests

The second set of samples exposed to UV, H+, and e- consisted of 30 specimens and two witness plates. The simulated solar UV reaches all or part of 11 specimens. The proton beam covers the identical areas of those 11 samples plus all or part of 9 additional samples. The electron beam covers a larger area so that some samples receive a dose of electrons only. Figures 13 and 14 show the arrangement of the samples on the test plate and the identify of each sample, respectively. Figure 13 also shows an outline of each area exposed to a particular type of radiation.

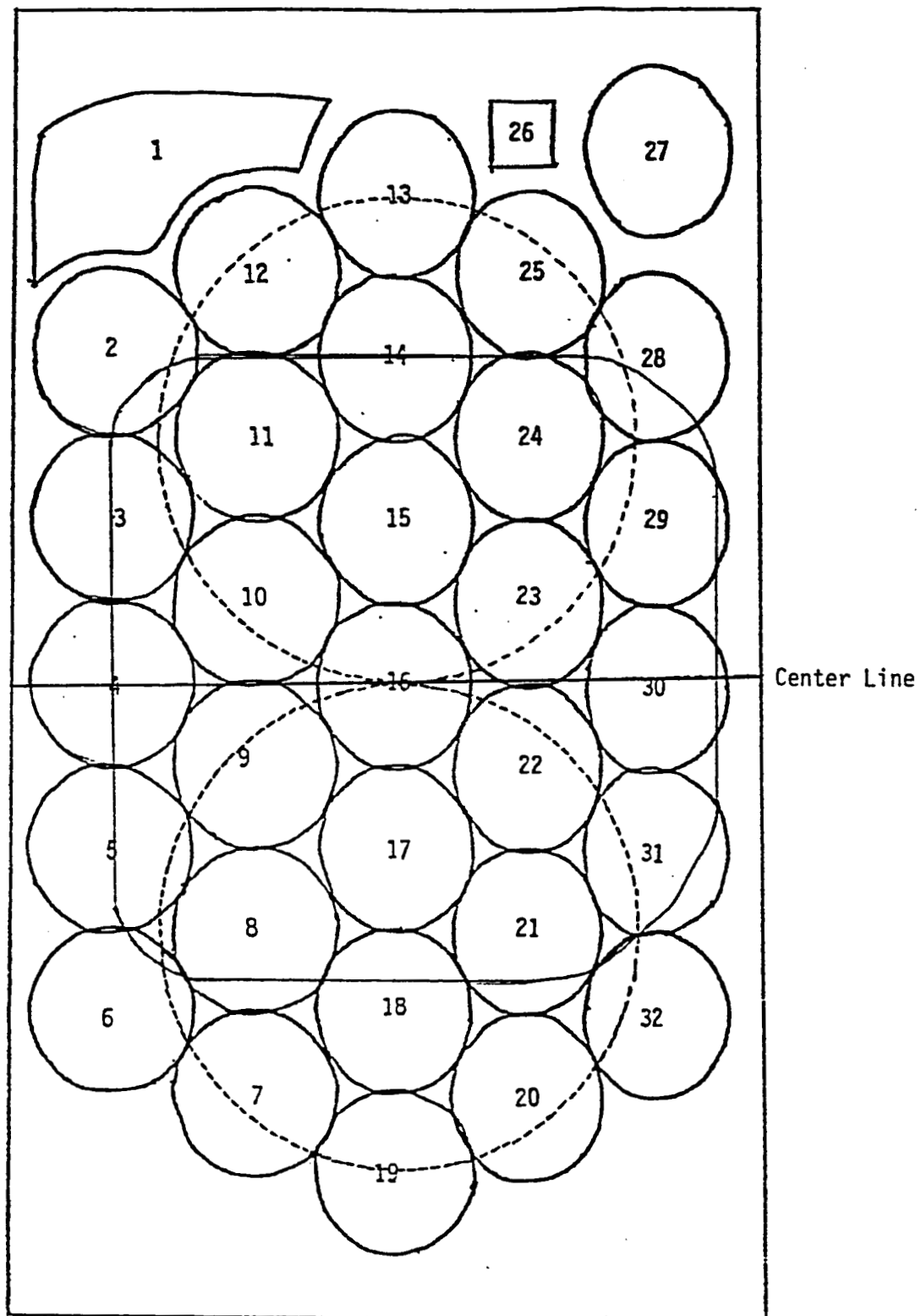


Figure 13: Sample Arrangement During The Latest Combined Effects Test, Showing The Areas Exposed To The Proton And UV Flux _____, And The Areas Exposed To The Vacuum UV Flux -----.

(THIS PAGE INTENTIONALLY LEFT BLANK)

<u>Location Number</u>	<u>Material</u>
1	Aluminum Foil
2	DSET Silicone
3	Apical
4	Fluorophosphazene
5	HMDS/TFE
6	CVI-1144 (Siloxane)
7	HMDS (Large Scale Demo)
8	DSET Silicone
9	Fluorophosphazene
10	S11 G/LO
11	HMDS
12	CVI-1144
13	FEP
14	HMDS
15	CVI-1144
16	Siloxane-Polyimide
17	CVI-1144 (No Aluminum Backing)
18	Kapton
19	Fluorophosphazene
20	Siloxane-Polyimide
21	HMDS/TFE
22	CVI-1144
23	Kapton
24	"Thin" HMDS
25	Kapton
26	Evaporated Aluminum (Witness Plate)
27	RTV Fluorosilicone
28	TFE
29	HMDS/TFE
30	"Thin" HMDS
31	S13 G/LO
32	V-10 S/LO

Figure 14: Identity of Each Material at Each
Location in the Test Chamber

PRELU TO PAGE PLANK NOT FILMED

The specimens receiving UV radiation were exposed to 1,000 equivalent sun hours of simulated solar UV. The vacuum ultraviolet sources used produce Lyman - α radiation ($\sim 122\text{m}$) and have a useful life of only about 500 hours. For this reason the lamps were turned on and off in the sequence 100 hours on, 100 hours off, 160 hours off, 240 hours on, 240 hours off. Each time the lamp was turned on or off, the absorbance of selected samples was measured in situ. These data show enhanced degradation during the first VUV exposure periods. This effect has been observed for materials tested on other programs. Absorptance data for all specimens as a function of exposure is listed in table 22.

One replacement was a sample of material #110, a non-opaque material. It was decided not to delay the test for the time necessary to evaporate aluminum on to the back surface of #110. Reflectance plots and solar absorptance values of #110, presented later, are affected by this. The CRETC measurement system received reflected energy from the sample's first surface, from its bulk properties, from the adhesive holding this specimen to the sample plate, and from the machined (but non-polished) aluminum sample plate itself. This sample assembly was a less efficient reflector than the other non-opaque materials were with their thin, specular film of evaporated aluminum.

Ex situ emissivity data is reported for materials exposed to the CRETC II environment in table 23.

Lyman-Alpha Far UV Lamps

These sources of 1216 A line radiation in the "far uv" provided a feature nearly unique to this test. Boeing performed a combined radiation test including similar Lyman-Alpha sources for COMSAT/INTELSAT in 1975. One or two other facilities may have performed occasional tests of this type, but any such tests could have used "Hinteregger-type" sources. There is no window to

Coating Material	Sample Location Number	Absorptance Vs. Time of Exposure (ESH*)			
		0	100	200	360
Witness Plates					
Aluminum Foil	1-1	0.117		0.123	
	1-2	0.116			
Evaporated Aluminum	26	0.094		0.102	0.099
Apical	3	0.434		0.469	
HMDS-TFE	5	0.365		0.394	
	21	0.365	0.392	0.395	0.404
	29	0.358		0.388	
HMDS	11	0.338	0.365	0.370	0.377
	14	0.350	0.373	0.375	0.386
"Thin" HMDS	24	0.355	0.403	0.416	0.439
	30	0.352		0.408	
CV1-1144	6			0.340	0.374
	12	0.359		0.373	
	15	0.345	0.386	0.398	0.419
	22	0.345	0.387	0.398	0.420
Kapton	18	0.389		0.427	
	23	0.389	0.423	0.433	0.451
	25	0.380		0.402	
FEP	13	0.374		0.384	
CV1-1144 No Aluminum Backing	17	0.572	0.588	0.589	0.592
GE RTV Fluorosilicone	27	0.636		0.648	
V10-S/LO IITRI Resin	32	0.396		0.403	

Table 22: In Situ Absorptance Measurements on Materials Under Simultaneous Exposure to Protons, Electrons, and Simulated Solar UV Radiation

*ESH (Equivalent Sun Hours)

(THIS PAGE INTENTIONALLY LEFT BLANK)

<u>Coating Material</u>	<u>Sample Location Number</u>	<u>Absorptance Vs. Time of Exposure (ESH*)</u>			
		0	100	200	360
Witness Plates					
Aluminum Foil	1-1	0.117		0.123	
	1-2	0.116			
Evaporated Aluminum	26	0.094		0.102	0.099
Apical	3	0.434		0.469	
HMDS-TFE	5	0.365		0.394	
	21	0.365	0.392	0.395	0.404
	29	0.358		0.388	
HMDS	11	0.338	0.365	0.370	0.377
	14	0.350	0.373	0.375	0.386
"Thin" HMDS	24	0.355	0.403	0.416	0.439
	30	0.352		0.408	
CV1-1144	6			0.340	0.374
	12	0.359		0.373	
	15	0.345	0.386	0.398	0.419
	22	0.345	0.387	0.398	0.420
Kapton	18	0.389		0.427	
	23	0.389	0.423	0.433	0.451
	25	0.380		0.402	
FEP	13	0.374		0.384	
CV1-1144 No Aluminum Backing	17	0.572	0.588	0.589	0.592
GE RTV Fluorosilicone	27	0.636		0.648	
V10-S/LO IITRI Resin	32	0.396		0.403	

*ESH (Equivalent Sun Hours)

Table 22: In Situ Absorptance Measurements on Materials Under Simultaneous Exposure to Protons, Electrons, and Simulated Solar UV Radiation

(THIS PAGE INTENTIONALLY LEFT BLANK)

<u>Coating Material</u>	<u>Sample Location Number</u>	<u>Absorptance Vs. Time of Exposure (ESH*)</u>		
		500	760	1000
Witness Plates				
Aluminum Foil	1-1	0.128		0.125
	1-2	0.129		0.124
Evaporated Aluminum	26	0.106	0.098	0.100
Apical	3	0.496		0.514
HMDS-TFE	5	0.413		0.424
	21	0.413	0.418	0.425
	29	0.403		0.411
HMDS	11	0.388	0.391	0.399
	14	0.397	0.401	0.408
"Thin" HMDS	24	0.460	0.479	0.498
	30	0.453		0.488
CV1-1144	6	0.391		
	12	0.378		
	15	0.443	0.464	0.486
	22	0.444	0.464	0.487
Kapton	18	0.452		0.456
	23	0.469	0.487	0.506
	25	0.406		0.403
FEP	13	0.386		0.384
CV1-1144 No Aluminum Backing	17	0.598	0.598	0.602
GE RTV Fluorosilicone	27	0.657		0.406
V-10-S/LO IITRI Resin	32	0.658		0.410

*ESH (Equivalent Sun Hours)

Table 22 (Continued): In Situ Absorptance Measurements on
Materials Under Simultaneous Exposure to Protons, Electrons,
and Simulated Solar UV Radiation

(THIS PAGE INTENTIONALLY LEFT BLANK)

Coating Material	Sample Location Number	Absorptance Vs. Time of Exposure (ESH*)							
		0	100	200	360	520	760	1000	
DSET (White Silicone)	2	0.191	0.225	0.241		0.237			
	8	0.190	0.279	0.315	0.375	0.425	0.460	0.491	
S11G/L0	10	0.197	0.284	0.322	0.377	0.424	0.455	0.485	
S13G/L0	31	0.195		0.314		0.412		0.466	
TFE	28	0.211		0.235		0.258		0.267	
GE 93	16	0.386	0.428	0.438	0.458	0.475	0.490	0.506	
X-128 (Fluoro-phosphazene)	4	0.476		0.492		0.539		0.573	
	9	0.397	0.446	0.471	0.507	0.538	0.565	0.591	
DSET (With H ⁺ Exposure)	2								0.433
DSET (Without H ⁺ Exposure)	2								0.224

*ESH (Equivalent Sun Hours)

Table 22: (Continued): In Situ Absorptance Measurements on Materials Under Simultaneous Exposure to Protons, Electrons, and Simulated Solar UV Radiation

PRECEDING PAGE BLANK NOT FILMED

(THIS PAGE INTENTIONALLY LEFT BLANK)

<u>Sample #</u>	<u>€</u>	<u>Sample #</u>	<u>€</u>
1	0.02	17	0.86
2	0.91	18	0.77
3	0.77	19	0.87
4	0.86	20	0.79
5	0.78	21	0.76
6	0.65	22	0.66
7	0.77	23	0.77
8	0.90	24	0.67
9	0.87	25	0.76
10	0.88	26	----
11	0.80	27	0.89
12	0.83	28	0.68
13	0.85	29	0.75
14	0.79	30	0.67
15	0.67	31	0.88
16	0.79	32	0.89

Table 23: Emissivity of Specimens Subsequent to Exposure in the Boeing Combined Effects Test Chamber.

isolate the test-sample area from the background gas (Hydrogen or other) in that class of lamps. Thus, there is very little comparative data.

The two lamps used arrived at Boeing with some basic test data by Artech, the manufacturer, to indicate their performance. No in situ 1216 A dosimetry equipment (principally sensors) was available during this test period, so we know nothing about rate of lamp output degradation. Artech stated that each lamp provides usable output over a discharge-current range of approximately 3 to 9 ma. Artech personnel made a verbal estimate that one "Sun" of the 1216 A Lyman-Alpha line of hydrogen would be provided at 6 ma. No particular beam size or projection distance was indicated by Artech.

During lamp check out starting at 3ma the Lyman-Alpha source outputs were very erratic, with a lot of intermittent discharges among the various elements (or discharge tubes) making up each source. After 10-12 hours we found that each lamp would usually provide stable output at 7-8 ma. To allow at least an estimate regarding how many samples would be exposed to Lyman-Alpha, we sketched the shape and size of the lavender light provided by the two lamp discharges operating together. This was done in a darkened room with the light projected onto vellum paper at the sample plane. The pattern is only a gross estimate. It features two areas of peak intensity, one due to each source, and lesser intensity across the center, top, bottom, and sides of the array of samples. All this was done in air, before final sample installation.

Near the end of the main (1000-hour) test, Lyman-Alpha lamp output was not always constant, even at 7-8 ma. At this point the sources had been used approximately 400 hours, and had resided in a hard vacuum with illumination at a fraction of one sun almost double that time. Artech had previously informed

Boeing that lamp lifetime is most prolonged in dark conditions, and is lessened by the presence of light.

At the end of the main test additional irradiation of some samples by both Lyman-Alpha lamps (but no other kinds of radiation) continued for about 100 hours while the principal test data was being processed. After this time the output of both lamps ceased altogether.

Dosimetry for Other Kinds of Radiation

The intensity of every other type of radiation (UV, protons, and electrons) was measured daily. The test was set up so that a nominal 1.5 uv suns would allow reaching the 1000-hour (called 1000 ESH, or equivalent uv sun-hour) level in 667 hours, roughly one month allowing for dosimetry and reflectance measurement downtimes.

The UV dosimetry consisted of measuring the solar uv output (from the xenon-arc discharge) with and without a uv-blocking filter. The difference, with scaling factors to account for chamber dimensions and the detector sensitivity, provided a measure of the actual sun intensity day by day. This varied from 1.5 to 1.8 suns, and cumulative exposure records kept track of overall progress.

Proton and electron dosimetry involved daily measurements of the individual positive and negative currents arriving at the sample plane from the respective sources. Conversion factors yielded the fluxes (particles per cm^2 per second) represented by these currents and allowed determination of the time-integrated fluences (particles per cm^2).

Test Sequence

Half of the total exposure time included Lyman-Alpha radiation, and the other excluded it, in alternating segments. This provided a test of the extent to which Lyman-Alpha radiation contributes to degradation. Reflectance

was measured after each segment of exposure. The conditions and duration of the exposure sequences are summarized in table 14.

To isolate Lyman-Alpha as a source of damage, or lack of it, every precaution that was in our hands to control was taken. For example, the solar-uv rate was closely controlled to 1.6 suns during the first 62 hours, therefore it was held very close to that level during the next segment. Increases in uv intensity took place only later in the test after the first two comparison periods were over.

It was not possible to maintain electron and proton fluxes at constant levels since there is a "black-box" aspect to such equipment, and since small changes of such things as line voltage and room temperature can strongly influence charged-particle output. Therefore, the electron and proton dosimetry values obtained must be carefully examined. From table 14 and figure 15 it can be seen that the time-integrated proton and electron (especially proton) fluences were not as well ordered as desirable when trying to isolate the effects Lyman-Alpha Radiation. Nevertheless, considering just the first two measurement/comparison periods (0 to 100 ESH and 100-200 ESH) the presence or absence of Lyman-Alpha appears to be a significant variable. Lyman-Alpha radiation appears to contribute to material degradation in the early portion of this test.

Uniformity of Radiation Exposure

Values used in this report are generally those measured at the center of the test-sample array. The size of the sample array in this test would have to be termed "very large" in any comparison with typical groups of samples irradiated in this kind of testing.

The solar UV beam illuminated the entire sample array, but not uniformly.

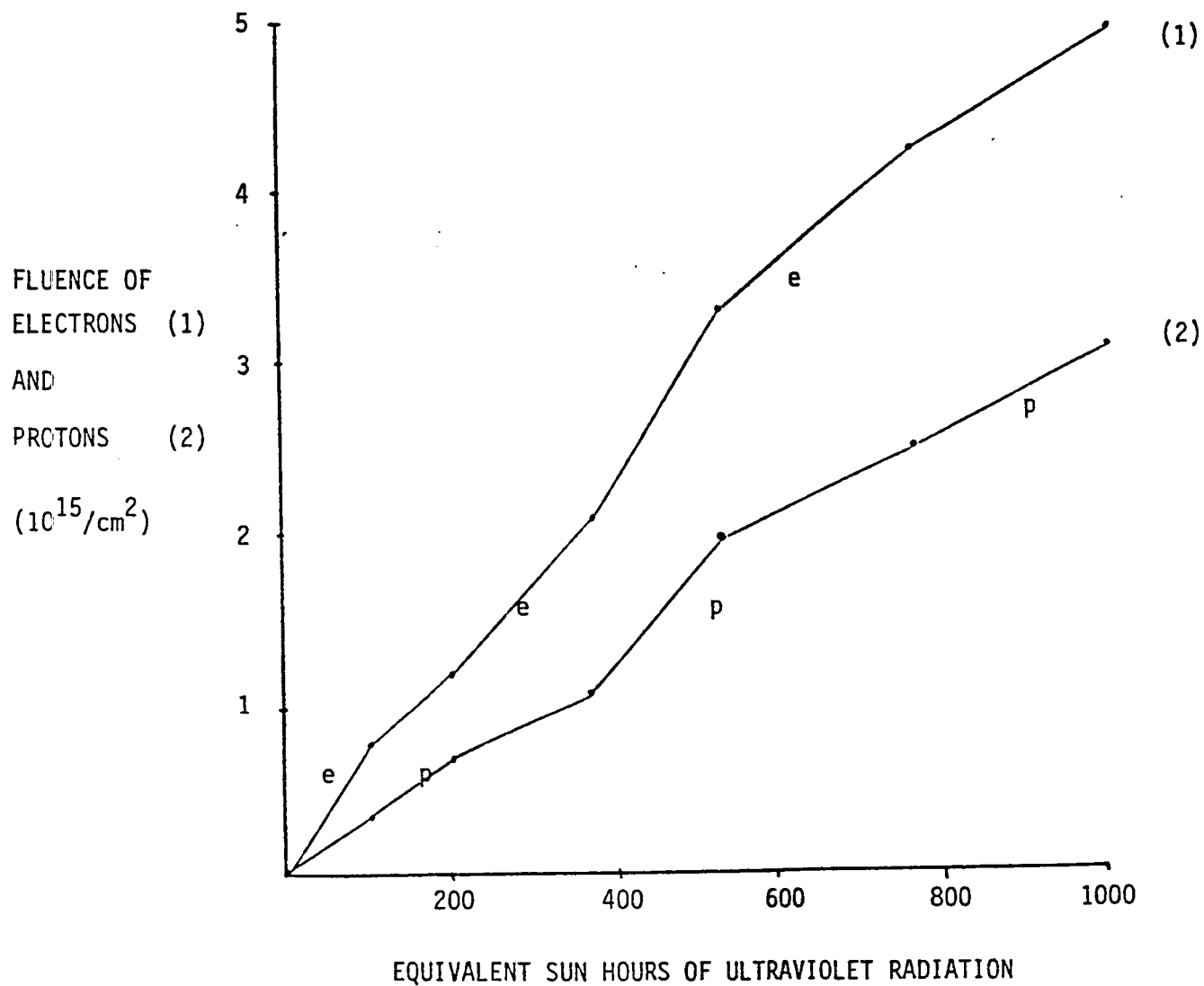


Figure 15: Proton And Electron Fluence As A Function Of UV Radiation Dose

Intensity fall off was approximately 10% compounded about every inch in a concentric pattern away from the center of the test array.

The shape of the vacuum uv (Lyman-Alpha) beam(s) was described earlier.

The protons, owing to the x-y raster method of generating a relatively large beam irradiated about 2/3 of the samples rather uniformly. The protons were blocked from irradiating any of the remainder of the samples. A relatively small number of samples, where the direction of the raster-scanning reverses, received a more intense flux of protons. Quantitatively, the proton fluences for samples 8 and 21 are perhaps 1.2 times those in table 14 and the fluence values for sample 14 are approximately 1.5 times those in table 14.

Electrons irradiated all the samples after traversing a thin scattering foil near their source. Most samples received at least 80% of the central fluence figures. The top and bottom rows in the sample array received perhaps only half the electron fluence levels measured at the center.

Notes Specific to Certain Samples or Materials

Specimens at location numbers 4, 5, 12, 16, 24, and 25 were exposed to the combined vacuum thermal cycling/UV exposure environment prior to exposure to the combined proton, electron, and UV/VUV environment.

At the end of the main test, Sample 2 (DSET #16) was examined to see if the regular measurement spot was at all in the "proton zone" (tanned pattern). Measurements of reflectance after 1000 ESH (end of main test) indicated that one very small area in the corner of the measurement beam did extend into the proton zone. Table 22 shows the full range of alpha values measured for DSET #16.

Changes in solar absorptance in the four white-paint samples were plotted in figure 16. The data suggest but do not conclusively demonstrate that Lyman-Alpha radiation may contribute to damage. The white paints were heavily

damaged by protons, especially in the visible wave length region that is important in determining alphas. This means variations in incremental proton and/or electron exposure levels (table 14) may effectively mask changes due to VUV.

Infrared-region damage in some materials is associated with exposure to electrons. Nearly 20 years ago at the Boeing Radiation Effects Laboratory, it was discovered that such infrared-region damage can recover with time in vacuum (see Progress in Astronautics and Aeronautics, 1970). During the current test, about 22 hours elapsed before measurements were started after the 1000 ESH, compared to previous measurements after 760 ESH or 520 ESH. Earlier in the test, reflectance measurements were begun much sooner after interrupting irradiation. In some samples there was very little change in alpha after 1000 ESH, compared to previous measurements after 760 ESH or 520 ESH. The time lapse may account for this observation.

Tables 24, 25a, and 25b show results of surface analysis by X-ray photoelectron spectroscopy and mass loss measurements of better candidate materials after various exposures to atomic oxygen and/or combined vacuum thermal cycling and UV radiation.

(THIS PAGE INTENTIONALLY LEFT BLANK)

α_s

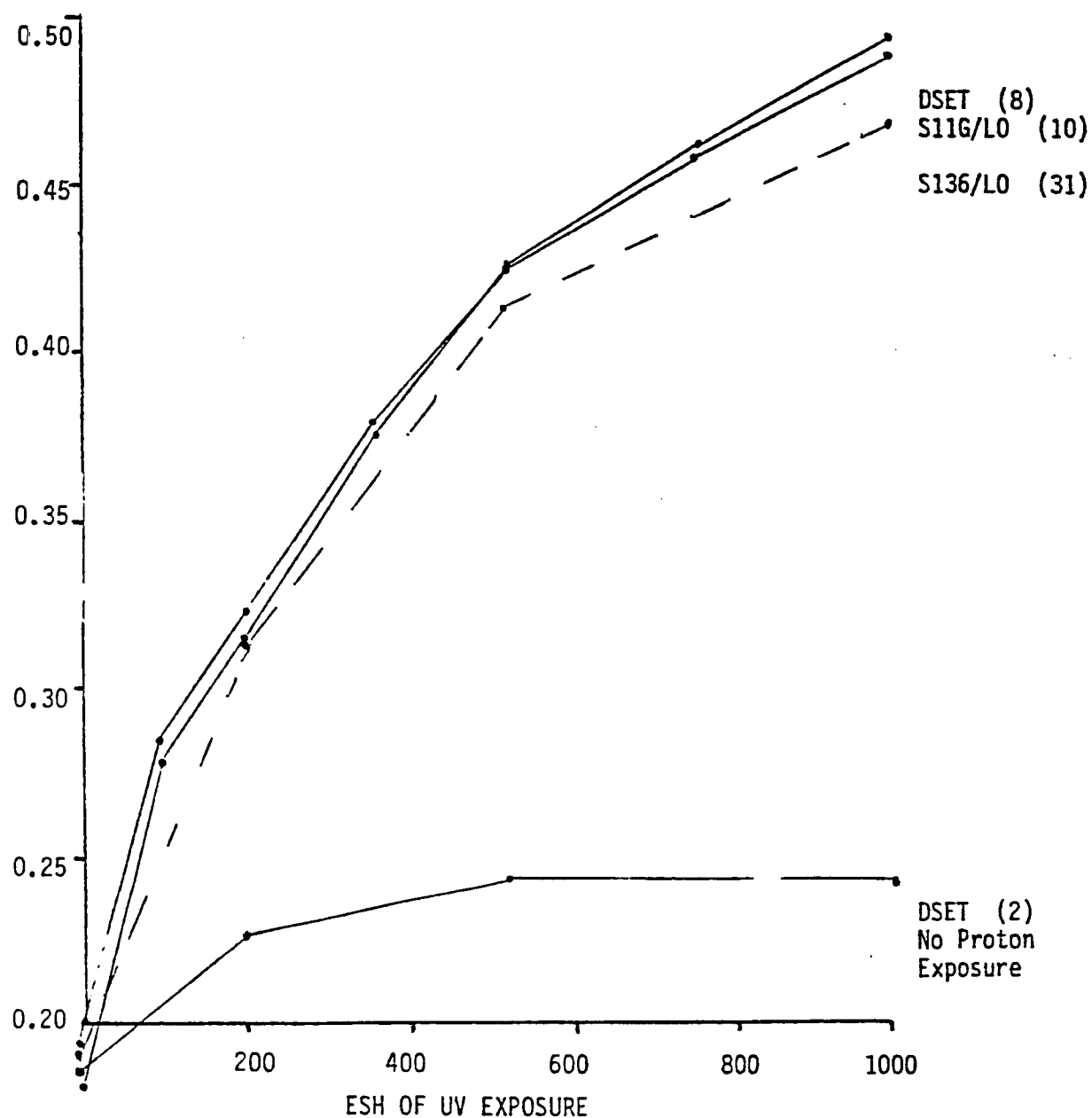


Figure 16: Changes In Absorptance Of White Pigmented Coatings As A Function Of Combined Proton, Electron, UV and VUV Exposure. Sample Locations Are In Parentheses. Sample At Location 31 Was Exposed To Slightly Reduced Levels Of All Radiation Types.

(THIS PAGE INTENTIONALLY LEFT BLANK)

<u>Material #</u>	<u>Element</u>	<u>MOL Fraction</u>	<u>Ratio Relative To Carbon</u>
HMDS (110)	F	0.003	0
	O	0.208	0.4
	C	0.543	1.0
	Si	0.247	0.45
HMDS (110)	F	0.002	0
	O	0.206	0.4
	C	0.541	1.0
	Si	0.251	0.45
X-128	F	0.454	1.55
	O	0.126	0.4
	C	0.294	1.0
	Si	0.017	0.05
	N	0.050	0.2
	P	0.059	0.2
TFE	F	0.661	2.0
	C	0.339	1.0
FEP (31)	F	0.078	0.1
	O	0.055	0.05
	C	0.849	1.0
	N	0.017	0
Siloxane-Polyimide (93)	O	0.231	0.45
	C	0.508	1.0
	Si	0.261	0.5
DSET (White Pigmented Silicone)	C	0.48	1.0
	O	0.23	0.5
	Si	0.29	0.6
HMDS/TFE (#112)	F	0.014	0
	O	0.216	0.4
	C	0.525	1.0
	Si	0.245	0.45
CV-3530 (Large Scale Article #151)	F	0.267	0.5
	O	0.108	0.2
	C	0.519	1.0
	Si	0.107	0.2
"Thin" HMDS (#26)	F	0.028	0.05
	O	0.191	0.33
	C	0.574	1.0
	Si	0.208	0.35

Table 24: Results of XPS Analysis of Specimens Previously Exposed to the Combined Vacuum Thermal Cycling, Simulated Solar UV Environments During Test of Early 1988.

(THIS PAGE INTENTIONALLY LEFT BLANK)

<u>Material</u>	<u>Mass Loss</u> (mg)	<u>Average Flux</u> ($10^{16}/\text{cm}^2\text{-sec}$)
Siloxane-Polyimide (#93) (BREL)	0.62	4.1
#93	0.53	
Kapton	1.47	
	1.77	
CV1-1144 (BREL)	0.60	4.1
CV1-1144	0.43	
Kapton	2.27	
	1.98	
CV-3530 (BREL)	0.55	
CV-3530	0.67	
Kapton	1.81	
	2.22	
HMDS (#110) (BREL)	0.22	4.2
HMDS	+0.08 (GAIN)	
Kapton	1.62	
	1.65	
DSET Silicone (BREL)	0.82	4.8
DSET	0.55	
Kapton	1.55	
	1.64	
FEP (#31) (BREL)	0.46	4.4
FEP (#31)	0.83	
Kapton	0.82, 0.83	
TFE (BREL)	+0.04 (GAIN)	4.2
TFE	+0.18 (GAIN)	
Kapton	0.81, 0.80	

Table 25a: Mass Loss of Selected Materials After Exposure to Atomic Oxygen for 24 Hours. Samples Designated (BREL) Were Previously Exposed to a Combined Vacuum Thermal Cycling Ultraviolet Radiation Environment During Test of Early 1988. Samples Were Held at 85°C During Exposure to Atomic Oxygen.

(THIS PAGE INTENTIONALLY LEFT BLANK)

<u>Material</u>	<u>Exposure Time</u> (Hours)	<u>Mass Loss</u> (mg)	<u>Average Flux</u> ($10^{16}/\text{cm}^2\text{-sec}$)
FEP (BREL)	57	0.99	4.4
FEP		1.41	
Kapton		2.66	
		2.71	
TFE	65	0.02	4.2
		0.00	
		+ 0.22 (GAIN)	
		+ 0.19 (GAIN)	
Kapton		1.97, 3.92	
		3.90, 3.66	
CV-1144	3.5	0.20, 0.08	5.3
		0.05, 0.17	
Kapton		0.51, 0.72	
		0.52, 0.68	
CV1-1144	27.5	0.82, 0.41	4.2
		0.32, 0.22	
Kapton		1.03, 1.55	
		1.71, 1.54	
TFE (BREL)	72	+ 0.03 (GAIN)	4.2
	96	+ 0.03 (GAIN)	
	120	0.00	
	185	0.00	
TFE	72	+ 0.23 (GAIN)	
	96	+ 0.21 (GAIN)	
	120	+ 0.10 (GAIN)	
	185	+ 0.05 (GAIN)	
Kapton	72	3.10, 3.65	4.2
	96	4.06, 4.76	
	120	5.11, 5.79	
	185	8.27, 9.55	

Table 25b: Mass Loss of Selected Materials, Held at 85°C, After Varying Periods of Exposure to Atomic Oxygen.

Peel Tests

Tests were conducted on several materials to determine their auto adhesion tendencies. Results of the initial test are reported in table 26.

A one square inch specimen of coated Kapton was placed in contact with another specimen of coated Kapton such that the coatings were in contact. The second specimen was also one inch wide but was 1-1/4 inch long so that a clamp could be attached to the 1/4" tab when the peel test was conducted. Ten individual specimen pairs were prepared, and placed on an aluminum block. A second aluminum block, weighing 10.18 lbs, was placed on the samples. It was assumed that the load was evenly distributed between the ten sample pairs. The sample pairs were left under compression for 8 days. The weight was then removed. The uncoated Kapton side of each 1 square inch sample was fastened to the aluminum block with a spray adhesive and the block was then turned upside down. Four 1" x 1-1/4" specimens did not adhere and fell immediately under the force of gravity. Each of the other six specimen pairs peeled when the clamp assembly, weight 4.45g, was fastened to the tab and allowed to hang freely. The time required to peel the one square inch was less than five seconds in all cases except one. One test required 30 seconds because a small amount of the spray adhesive adhered to the sides of the test specimens.

<u>Materials</u>	<u>Results</u>
HMDS/TFE Copolymer (#52)	Did Not Adhere
Silicone Polyimide Copolymer (#93)	Did Not Adhere
CVI-1144 Silicone (#65)	Peeled By 4.4557g Weight
CVI-3530 Fluorosilicone (#66)	Peeled By 4.4557g Weight
RTV Fluorosilicone (#101)	Peeled By 4.4557g Weight

Table 26: Summary of Results of Peel Tests. Sample Contact Area
Were 1 Inch Square. Ten Samples Were Held Under A Total
Weight Of 10.18 Lbs. For 8 Days.

A second set of specimens were put through the same conditions; for these samples the addition of weights was done with increased care. Results of this peel test are reported in table 27. Duplicate samples were run on each material. For one sample of each material weights were added in rather large increments (several grams at a time). One to two minutes were allowed between addition of weights to give ample opportunity for the specimen to peel. For the other sample of each material, weights were added in much smaller increments (0.3-0.5g). Thus, the values obtained for sample #2 of each material are probably the most reliable. For comparison purposes, the blocking requirement for the solar array panels on the space telescope is a maximum of 100 grams of force to peel a 10cm by 10cm specimen. This is about 25g per linear inch. The CV-3530 fluorosilicone clearly blocks less than the silicone material. This is the clearest advantage which we have observed for a fluorosilicone over a silicone material. The fluorophosphazene was very tacky and was not successfully peeled.

<u>Material</u> (Specimen #)	<u>Weight Required To Peel Surfaces</u> (g)	<u>Time Required</u> (Sec)
CV-1144 (1)	10.69	5
(2)	13.35	10
CV-3530 (1)	4.46	20
(2)	4.15	90
Fluorophosphazene (1)	37.63 (Adhesive failed,	--
(2)	35.62 did not peel)	--

Table 27: Results of 90° Peel Test on Selected Specimens

A additional series of blocking/peel tests was run on selected material samples. Samples of silicone, fluorosilicone and fluorosphazene materials

were exposed to an oxygen plasma discharge (80 watts), in a March Instruments Plasmod, for 10, 20, and 30 minutes. Following this exposure, samples were placed in compression under a load of 6.2 lbs/in² for 7 days. Peel tests were then conducted on each sample by applying a force at 90° to the surface of the material. The McGhan-Nusil CV-1144-0 (unfilled, clear siloxane) and the IITRI S13G/L0 tested did not block at all. Specimens of these materials separated immediately upon being released from compression.

A decrease in the force required to peel specimens of fluorophosphazene and fluorosilicone was observed after exposure to atomic oxygen. The numerical results are reported in table 28. For each test weights were added in small increments. After each addition of weight, samples were observed for one to two minutes before the next weight increment was added to the load. The peel times reported are times under maximum load required for peeling to occur.

	Time In Plasmod (Minutes)			
	<u>0</u>	<u>10</u>	<u>20</u>	<u>30</u>
CV1-1144-0				
Load (g)	0	0	0	0
Peel Time (Sec.)	-	-	-	-
S13-G/L0				
Load	0	0	0	0
Peel Time	-	-	-	-
CV-3530				
Load	7.83	1.25	1.71	1.71
Peel Time	123	25	7	4
X-128				
Load	10.06	6.07	2.25	2.25
Peel Time	87	41	39	7

Table 28: Results of 90° Peel Test on Selected Specimens

Duplicate specimens of the same four materials were exposed to a flux of atomic oxygen for 10 hours in our Material Screening Chamber. These specimens

were then placed under compression for 7 days under identical condition to the previous specimens. Once again the CV-1144-0 and S13 G/L0 did not block. The X-128 specimens peeled partially under a load of about 1.1g and then required considerable additional force to completely peel. The thickness of this coating may have varied over the area of the test specimens causing unevenness in the distribution of the compressive load on these specimens.

Table 29 shows values of the maximum loads required to peel the X-128 and CV-3530.

	<u>LOAD</u> (g)	<u>TIME</u> (Sec)
X-128		
Specimen # (1)	4.43	60
(2)	3.93	40
CV-3530		
Specimen # (1)	1.16	10
(2)	1.18	12

Table 29: Results of Peel Tests for Specimens Previously Exposed to Atomic Oxygen in the Materials Screening Chamber

<u>Material</u>	<u>Bend Diameter D = 15 Mils</u>	<u>Bend Diameter D = 40 Mils</u>	<u>Comments</u>
#58: Ethyl X-128 Fluorophosphazene	No Cracking	No Cracking	Virgin Material and BREL (Vac/Thermal Cycling/Solar UV) Tested Material
#65: McGhan-MuSIL CVI-1144-0 Silicone	Cracks	Cracks	
#65	No Cracking	No Cracking	BREL-Tested Material
#66: McGhan-NuSIL CVI-3530 Fluorosilicone	Cracks	Cracks	
#66	Single Crack	Cracks	BREL-Tested Material
#50: Battelle Plasma Polymerized HMDS/TFE	No Cracking	No Cracking	
#50	Single Crack	Single Crack	BREL-Tested Material
#52: Battelle Plasma Polymerized HMD/TFE (Ratio 8/1)	No Cracking	No Cracking	
#52	No Cracking	No Cracking	BREL-Tested Material
#49: Battelle Plasma Polymerized HMDS/TFE, Ratio 4/1	Cracks	No Cracking	
#51: Battelle Plasma Polymerized HMDS/TFE, Ratio 20/1	No Cracking	No Cracking	
#70: McGhan-NuSil CVI-3530 Fluoro- silicone (Prepared by Sheldahl)	Slight Cracking	No Cracking	
#71: McGhan-NuSil CVI-1144-0 Silicone (Prepared by Sheldahl)	No Cracking	No Cracking	
NASA-LeRC 51386 Siloxane	No Cracking	No Cracking	

Table 30: Results of Bend Radius Tests on Selected Materials

Bend Radius Testing

To characterize the flexibility of the candidate coatings, a "bend radius" test was developed. An aluminum sheet rounded on one edge to a selected diameter was used. Aluminum sheets 15 and 40 mils thick were used for this test.

A strip of the material to be tested is bent over the rounded edge of the aluminum sheet chosen for the test. The material is then taped in place. The bend region is examined for evidence of cracking through the use of scanning electron microscopy (SEM). The orientation of the coating material relative to the SEM is sketched in figure 17. Results of this test is summarized in table 30.

Outgassing Tests

NASA-SP-R-0022 is a generally accepted rapid outgassing screening test for materials for spacecraft use. NASA-SP-R-0022A is used to measure the total mass loss (TML) and collectable volatile condensible materials (CVCM) of a material exposed to 125°C and 1×10^{-6} torr or less for 24 hours. The volatile condensible material condenses on a collector plate held at 25°C.

Maximum outgassing limits for spacecraft, established in NASA-SP-R-0022, are 1.0% TML and 0.1% CVCM when the sample is held under a vacuum of at least 1×10^{-6} torr and 125°C for 24 hours. Deviations from these limits may be allowed because of the anticipated temperature environment, the expected life or the mass or location of the material on the spacecraft. Results of outgassing measurements are shown in table 31.

Flatwise Tension Tests

A set of measurements was carried out to measure the adhesion of selected table 32. Duplicate samples were run in all cases except for HMDS/TFE (8:1)

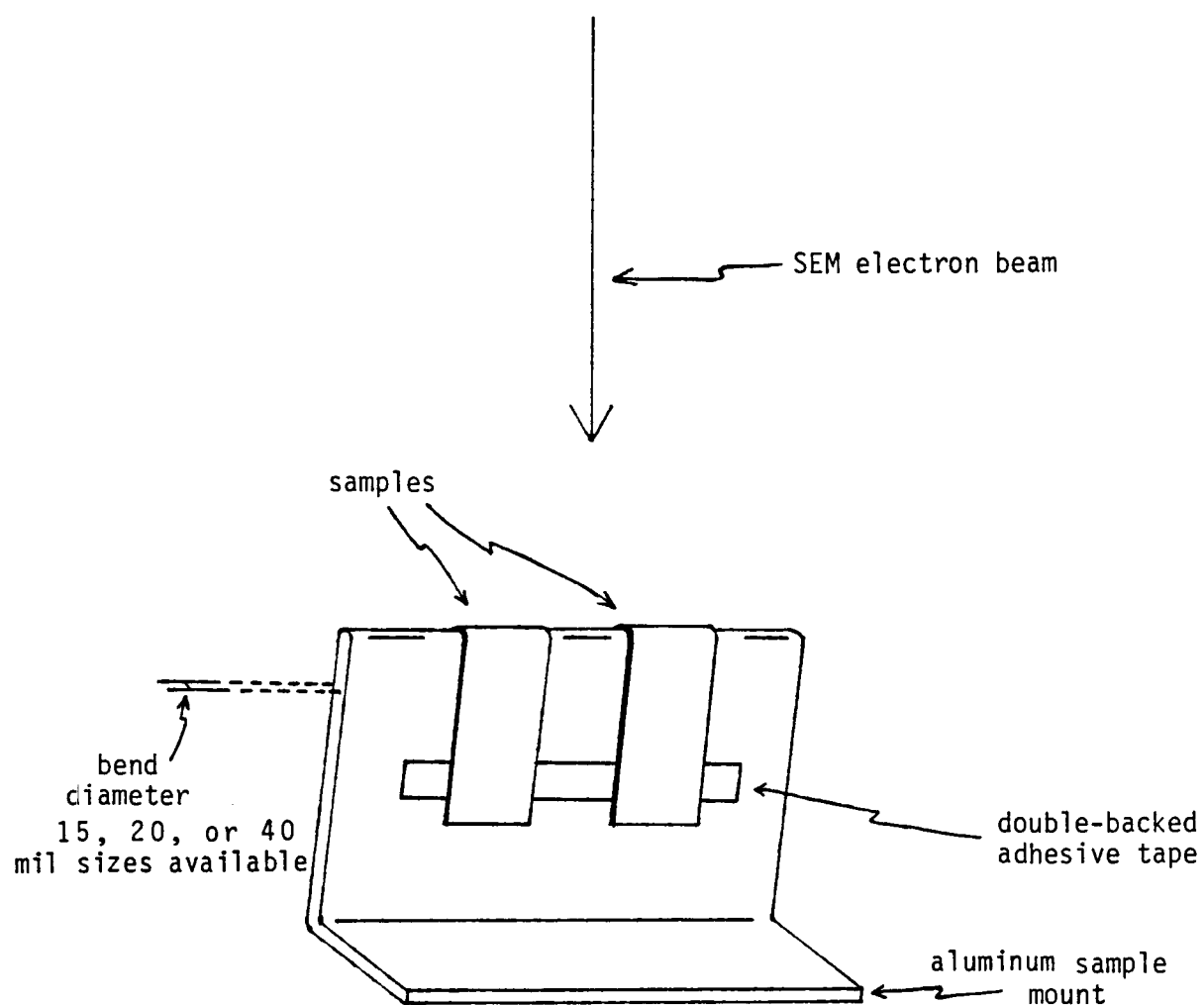


Figure 17: Bend Radius Test Sample Configuration

(THIS PAGE INTENTIONALLY LEFT BLANK)

<u>Material (#)</u>			<u>% Total Mass Loss</u>	<u>% Collectable Volatile Condensable Materials</u>
Kapton (1)			0.19	0.02
Apilcal (106)			0.046	0.013
Silicone (65)			0.21	0.09
CV-1144 (15)			0.26	0.03
Fluorosilicone CV-3530 (66)			0.16	0.03
Room Temperature				
Vulcanized Fluorosilicone (100)			0.90	0.016
Room Temperature				
Vulcanized Diphenyl				
Dimethyl Silicone (100)			0.16	0.0
Siloxane-Polyimide Copolymer (93)			0.70	0.0
Fluorinated Ethylene-Propylene (FEP)				
On Kapton (31)			0.11	0.0004
On Apical			0.11	0.011
Hexamethyl Disiloxane/ Tetrafluoroethylene Copolymer				
Ratio	(8:5)	(10)	0.26	0.02
	(8:1)	(52)	0.14	0.016
	(9:5)	(11)	0.31	0.02

Table 31: Results of Outgassing Tests on Selected Materials

(THIS PAGE INTENTIONALLY LEFT BLANK)

<u>Material (#)</u>	<u>Ultimate Load (lbs)</u>
S13 G/L0-1 FG-Epoxy (62)	103.5 139
Plasma Polymerized HMDS or 1 mil Kapton (50)	430 475
Plasma Polymerized HMDS/TFE (8:1) 1 mil Kapton (52)	340 0
McGhan NuSil CV1-1144-0 on 1 mil Kapton Using SP-120 Primer (65)	287 328
McGhan NuSil CV1-3530 on 1 mil Kapton Using CF1-135 Primer (66)	387 403

Table 32: Results of Flatwise Tension Tests on Selected Materials

PRECEDING PAGE BLANK NOT FILMED

coatings to particular substrates. The results of these tests are reported in on 1 mil Kapton. One sample of HMDS/TFE (8:1) on 1 mil Kapton was twisted to testing, causing failure.

Kapton test samples coated on one side, were bonded with an adhesive between two blocks, (1 square inch, $\pm 1\%$). The test configuration is left until the adhesive has cured at room temperature and then any excess sample is trimmed. The test is then carried out using an Instron Tensile Tester. In each test, failure occurred between the adhesive and the Kapton. The test results indicate the adhesion between the Kapton and the coating material was greater than the adhesion between the Kapton and the adhesive holding the sample to the block. This test configuration is shown in figure 18.

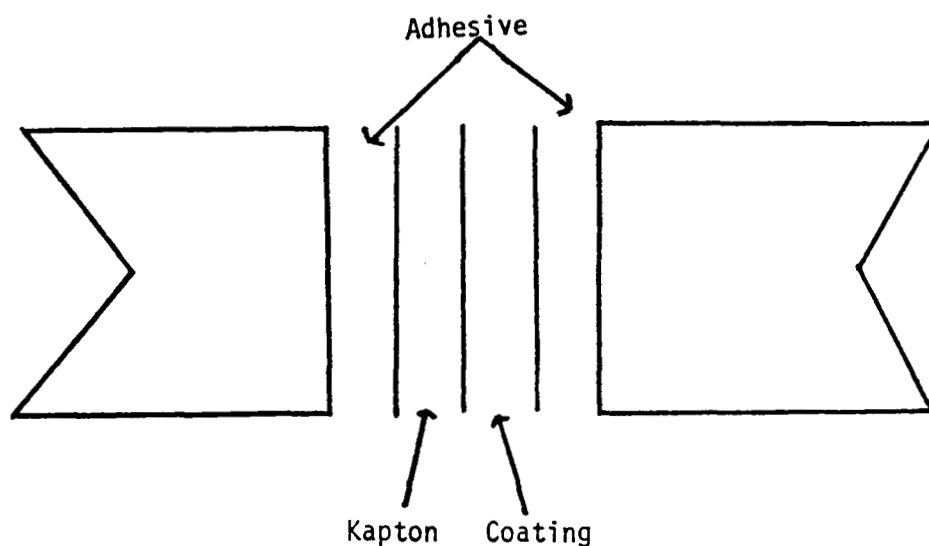


Figure 18: Flatwise Tension Test Sample Configuration

Similar McGhan-NuSil materials, tested previously, had cracked severely. The current samples contained less filler than previous samples and are thus more flexible. The use of filler was an attempt to solve the surface tackiness of these materials. The samples which cracked contained about 20% filler by weight, the others about 10%.

Stress Effects on Atom Oxygen Degradation

A test specimen holder, designed to hold a film sample under a fixed tensile strain while undergoing atomic oxygen exposure, was fabricated by NASA-MSFC personnel. Trial runs were attempted using the holder with Kapton H film. One of the tests runs was made with zero stress. Two test runs were attempted at approximately 5% and 10% strain. In both of these later tests, the Kapton film separated before the four hour run was completed.

Results of SEM Measurements

Extensive investigations of the surfaces of many coating specimens were carried out using the scanning electron microscope and the Energy Dispersive Analysis by X-rays (EPAX) technique. Results of the observations are shown in figures 19 through 130 and discussed in the paragraphs below. Each set of measurements are labeled by Electron Microscopy experiment number and date of measurement for identification.

Specimens of coated Kapton which had been previously exposed to the combined radiation effects environment have been examined under a scanning electron microscope (SEM). Figures 19-24 show SEM photographs for these samples. Figure 19 shows SEM photographs of uncoated Kapton to allow comparison with the coated specimens. There are few surface features identifiable on the Kapton, and only at high resolution. Figure 20 shows the SEM photographs of hexamethyldisiloxane. This coating does exhibit some cracking and the higher resolution picture appears to show that small sections of the coating have flaked off. Figure 21 shows SEM photographs of S13 G/L0-1. This coating appears to have a granular, porous structure with some small cracks particularly visible in the higher resolution photograph. Figure 22 shows an SEM photograph of fluorophosphazene and of HMDS/TFE. The HMDS/TFE coating appears

ORIGINAL PAGE IS
OF POOR QUALITY

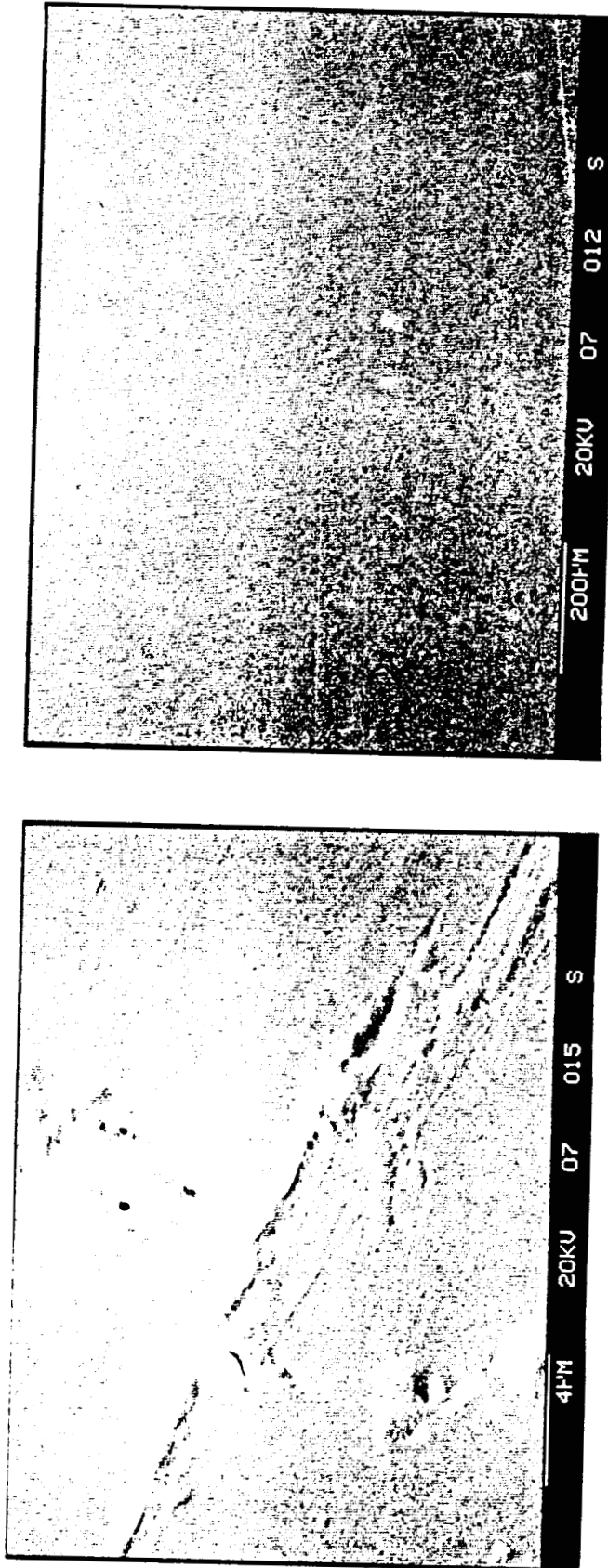


Figure 19: Results of Scanning Electron Microscopy of Kapton
After Exposure to Combined Radiation Effects Test Environment

(THIS PAGE INTENTIONALLY LEFT BLANK)

ORIGINAL PAGE IS
OF POOR QUALITY

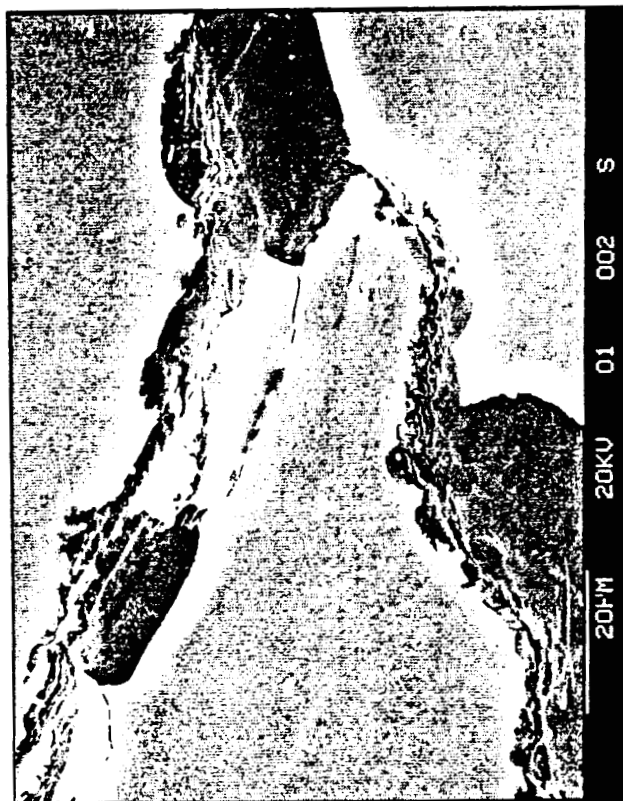
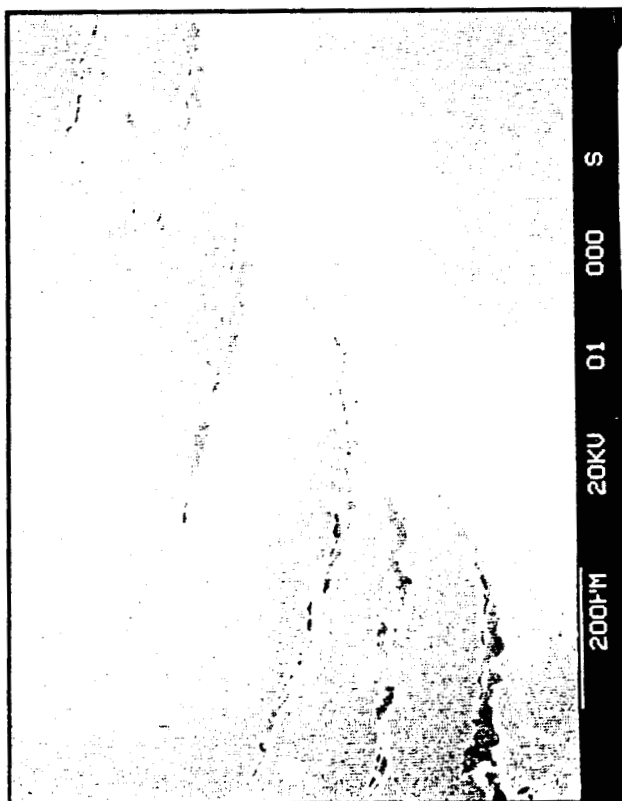


Figure 20: Results of Scanning Electron Microscopy of HMDS Coating
After Exposure to Combined Radiation Effects Test Environment

(THIS PAGE INTENTIONALLY LEFT BLANK)

ORIGINAL PAGE IS
OF POOR QUALITY

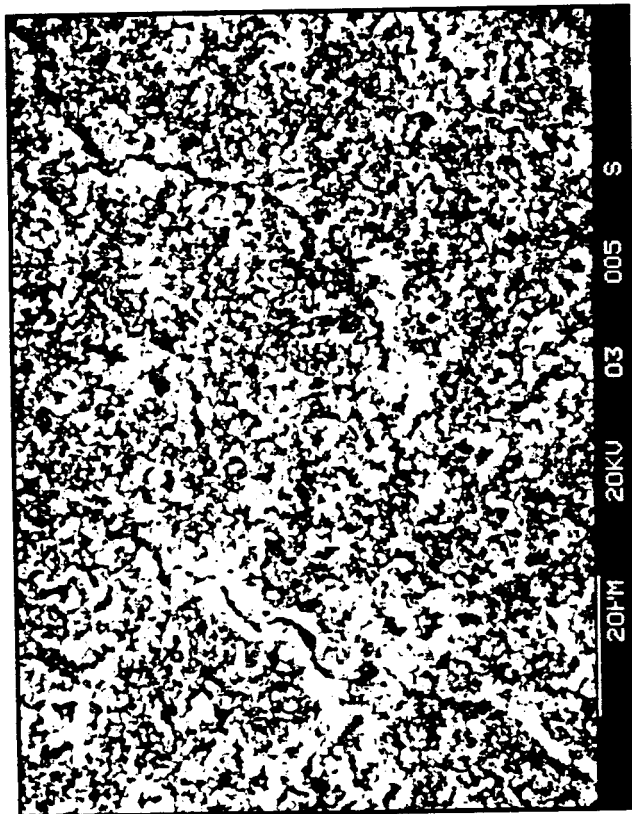
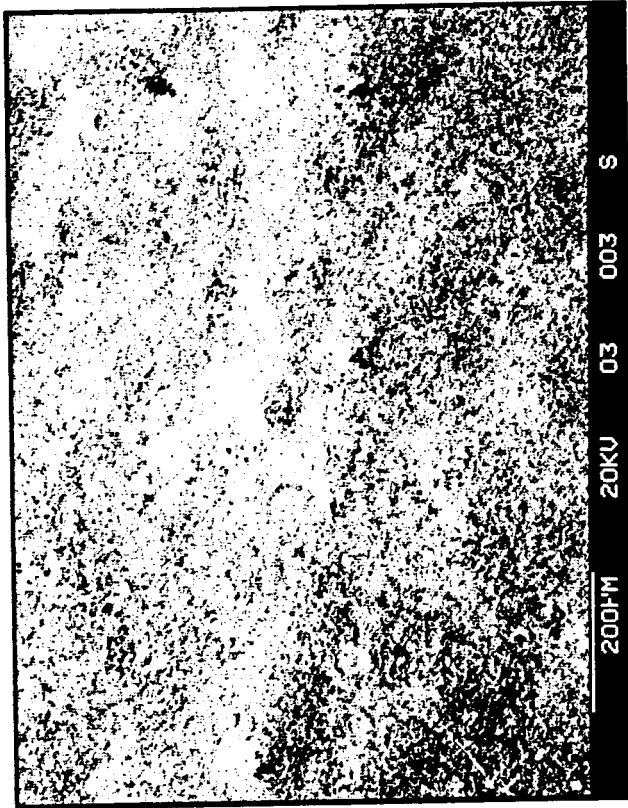


Figure 21: Results of Scanning Electron Microscopy on S13-G/L0-1 Coating
After Exposure to Combined Radiation Effects Test Environment

(THIS PAGE INTENTIONALLY LEFT BLANK)

ORIGINAL PAGE IS
OF POOR QUALITY

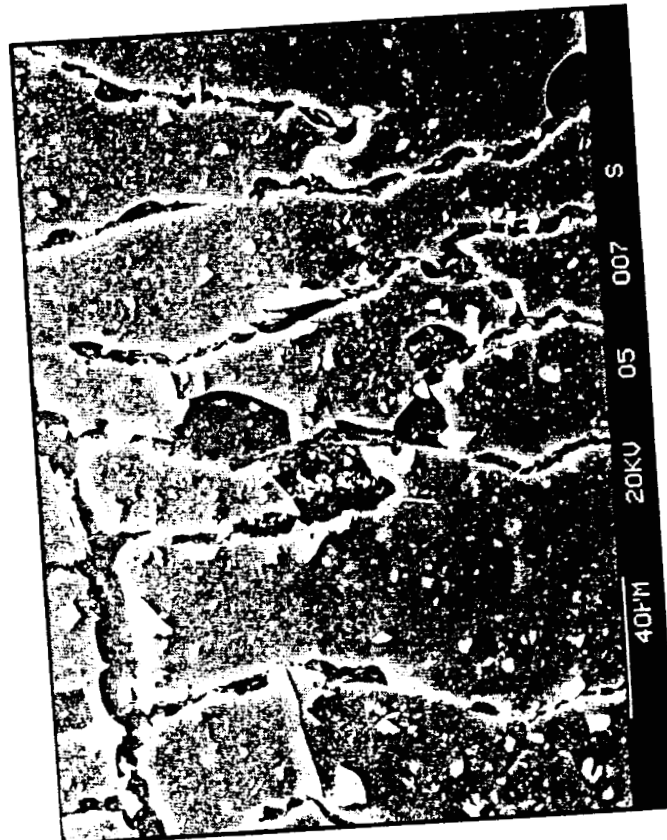
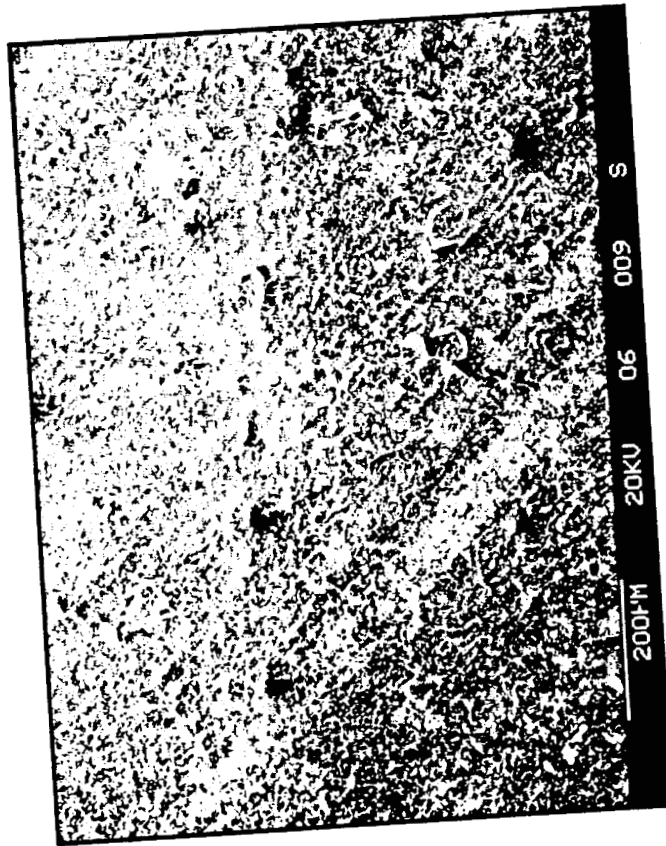


Figure 22: Results of Scanning Electron Microscopy of HMDS/TFE and
Fluorophosphazene Coatings After Exposure to Combined Radiation
Effects Test Environment

(THIS PAGE INTENTIONALLY LEFT BLANK)

ORIGINAL PAGE IS
OF POOR QUALITY

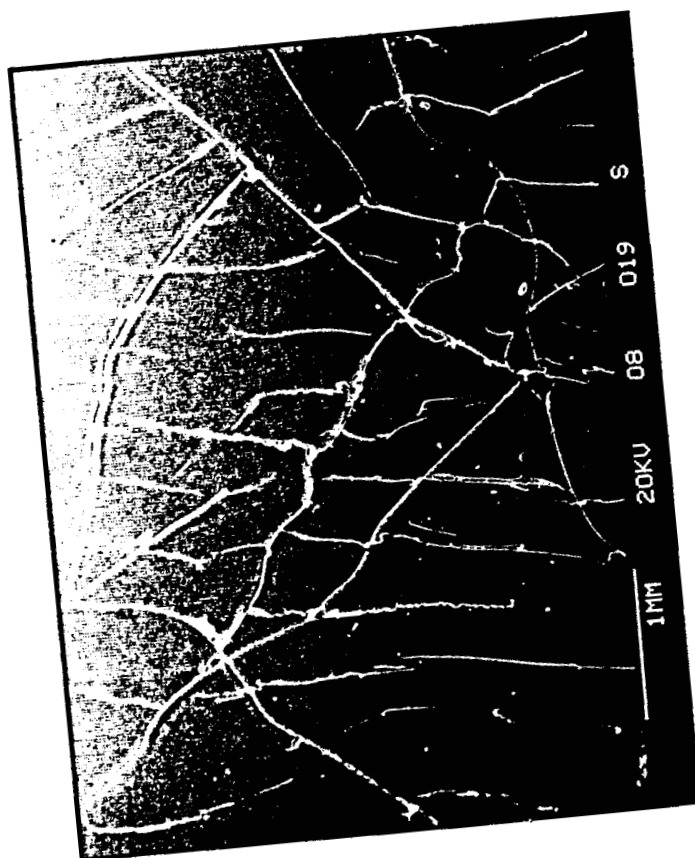
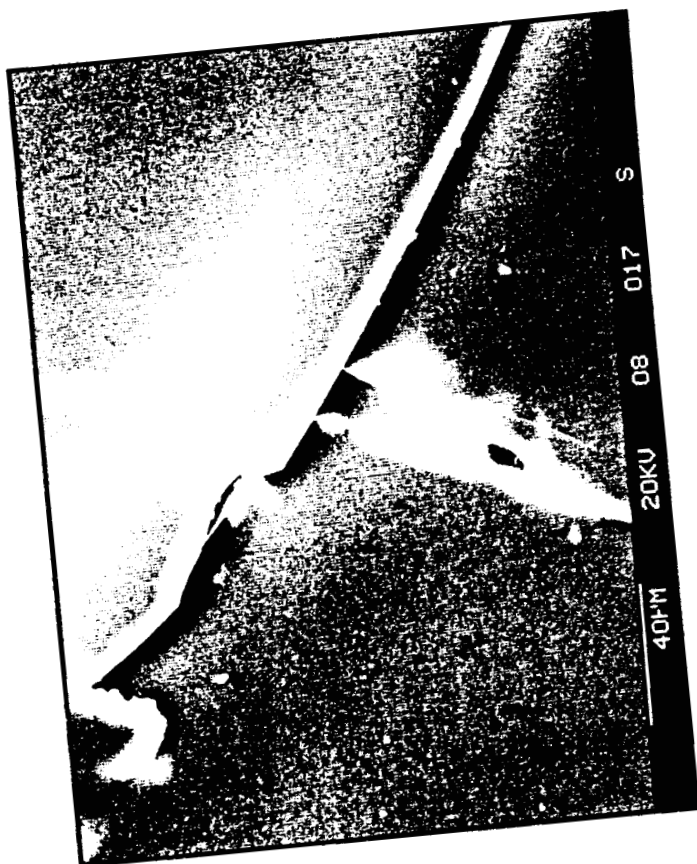


Figure 23: Results of Scanning Electron Microscopy of Silicone
(CV-1144) Coating After Exposure to Combined
Radiation Effects Test Environment

(THIS PAGE INTENTIONALLY LEFT BLANK)



Figure 24: Results of Scanning Electron Microscopy of Fluorosilicone
(CV-3530) Coating After Exposure to Combined Radiation
Effects Test Environment

to have flaked off in certain areas, much like the similar coating in figure 20. The fluorophosphazene coating has a textured appearance but few surface features otherwise. Figure 23 shows many cracks in the CV-1144 coating visible even at low resolution. Figure 24 shows a similar, but less extensive distribution of cracks for the CV-3530 coating.

Figures 25-28 shows SEM photographs of materials which have been exposed to atomic oxygen. These photos show extensive cracking, areas where the coating has been removed, and indicate that oxygen atoms are undercutting the coatings. Thin, bright areas around the cracked areas indicate the possibility of attack by oxygen atoms at the adhesive bonds between the coatings and the Kapton substrate. Certain areas in figure 28 shows no coating remaining and the Kapton has a topography depending on the degree of exposure.

Figures 29 through 32 show X-ray photoelectron spectra of a fluorophosphazene, a siloxane-polyimide co-polymer after two different exposures, and a siloxane (CV-1144). Table 33 summarizes the surface elemental analysis for each specimen.

Figure 29 shows that the fluorophosphazene sample contains some silicon peaks, indicating cross-contamination from a siloxane sample being run simultaneously. Because of this evidence of cross-contamination, different material types should not be simultaneously exposed to atomic oxygen. Figures 30 and 31 show the siloxane-polyimide co-polymer after short and long term exposure to atomic oxygen (6 and 51 hours, respectively, December 87-January 88). The data in table 33 show the expected increase in oxygen and silicon relative to carbon. Figure 32 shows results of a repeat of earlier measurements on CV-1144 and shows the expected surface oxidation.

ORIGINAL PAGE IS
OF POOR QUALITY

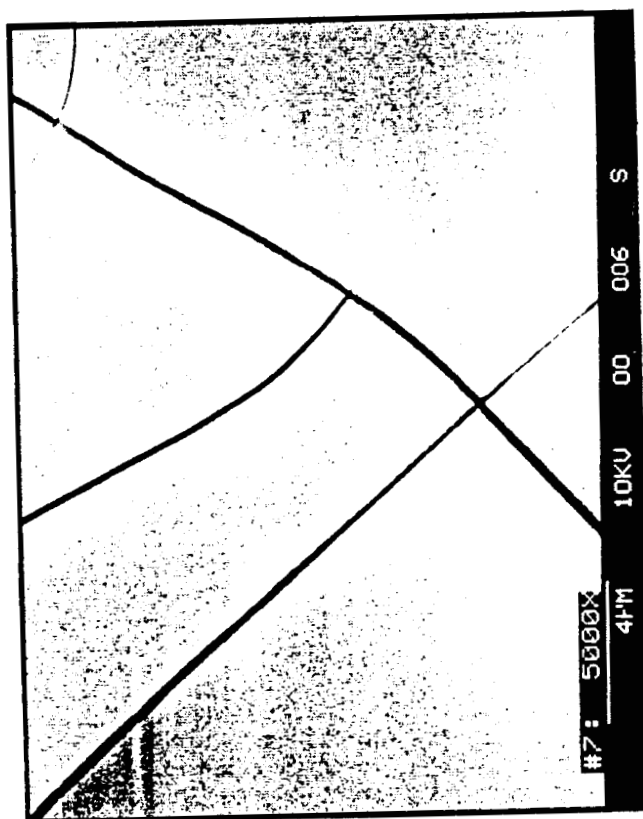
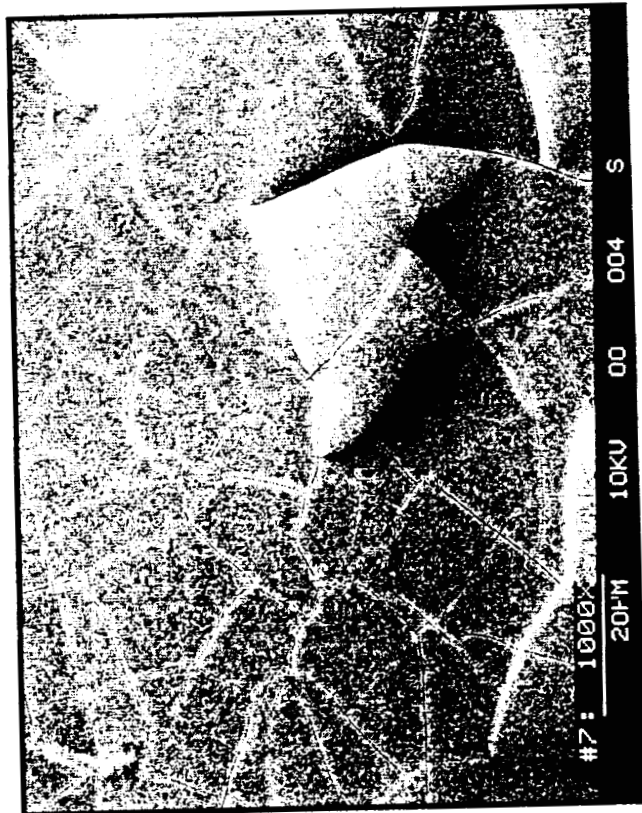
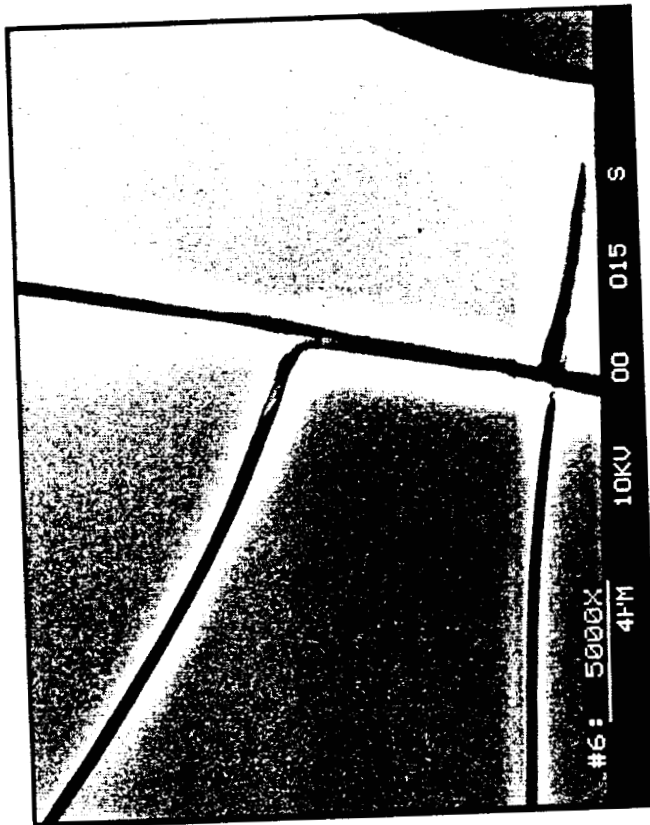
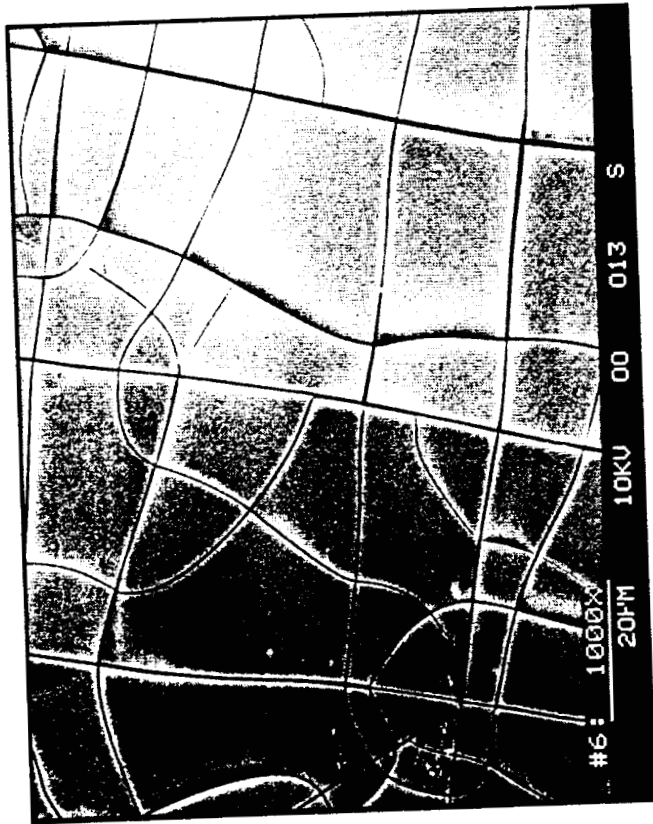


Figure 25: Results of Scanning Electron Microscopy on HMDS Coating.
The Sample was Previously Exposed to Atomic Oxygen for 25 Hours.

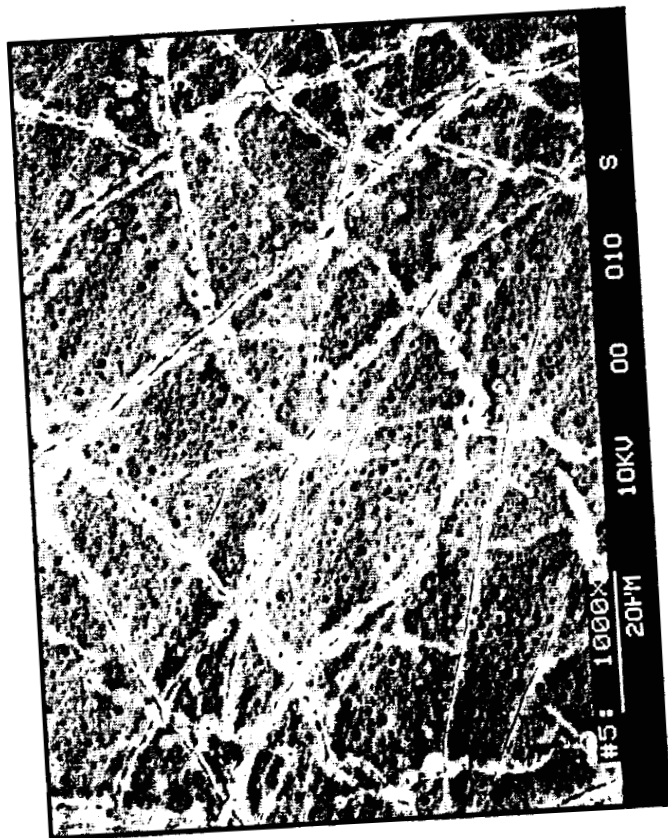
(THIS PAGE INTENTIONALLY LEFT BLANK)



ORIGINAL PAGE IS
OF POOR QUALITY

Figure 26: Results of Scanning Electron Microscopy on HMDS Coating.
The Sample was Previously Exposed to Atomic Oxygen for 48 Hours.

(THIS PAGE INTENTIONALLY LEFT BLANK)



ORIGINAL PAGE IS
OF POOR QUALITY

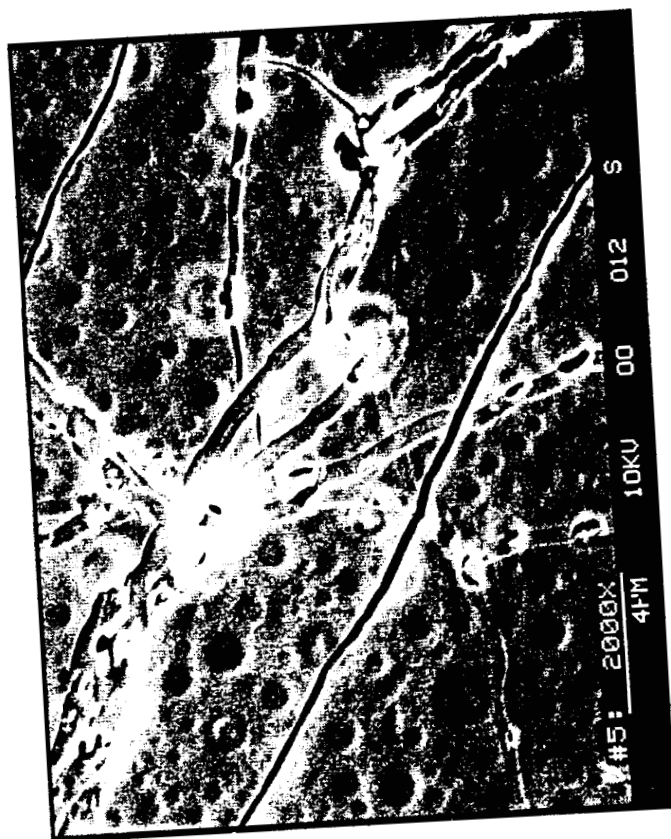


Figure 27: Results of Scanning Electron Microscopy on Polyimide-Siloxane Coating. The Sample was Previously Exposed to Atomic Oxygen for 93 Hours.

(THIS PAGE INTENTIONALLY LEFT BLANK)

ORIGINAL PAGE IS
OF POOR QUALITY

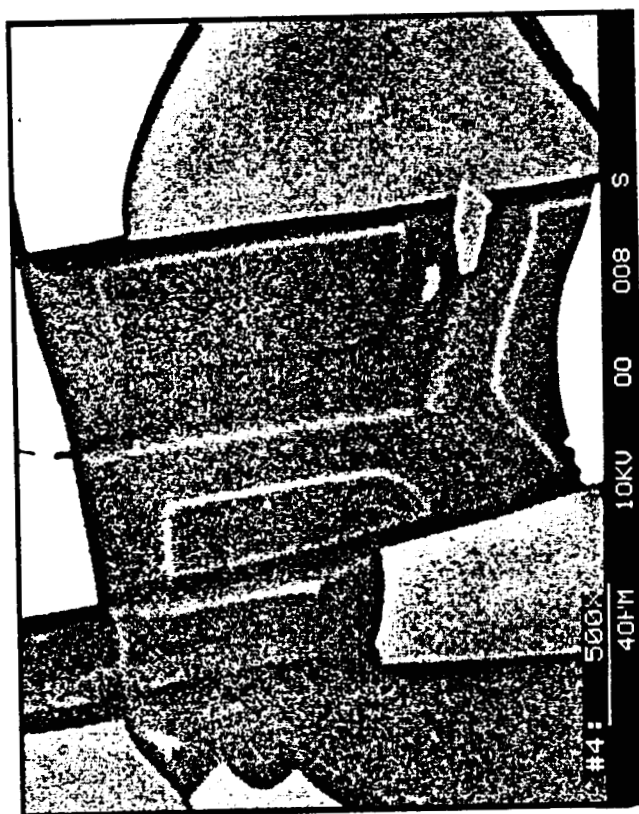
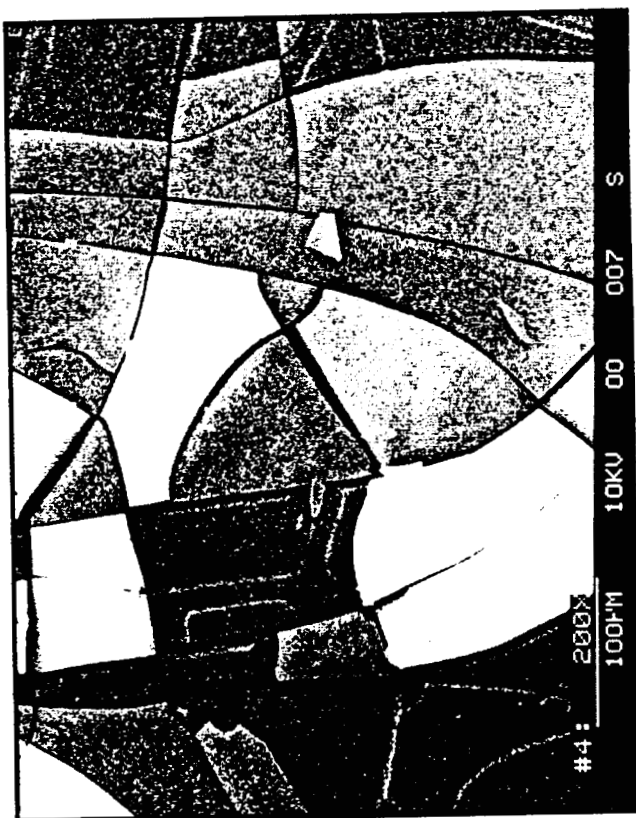


Figure 28: Results of Scanning Electron Microscopy on HMDS/TFE Coating.
The Sample was Previously Exposed to Atomic Oxygen for 96 Hours.

(THIS PAGE INTENTIONALLY LEFT BLANK)

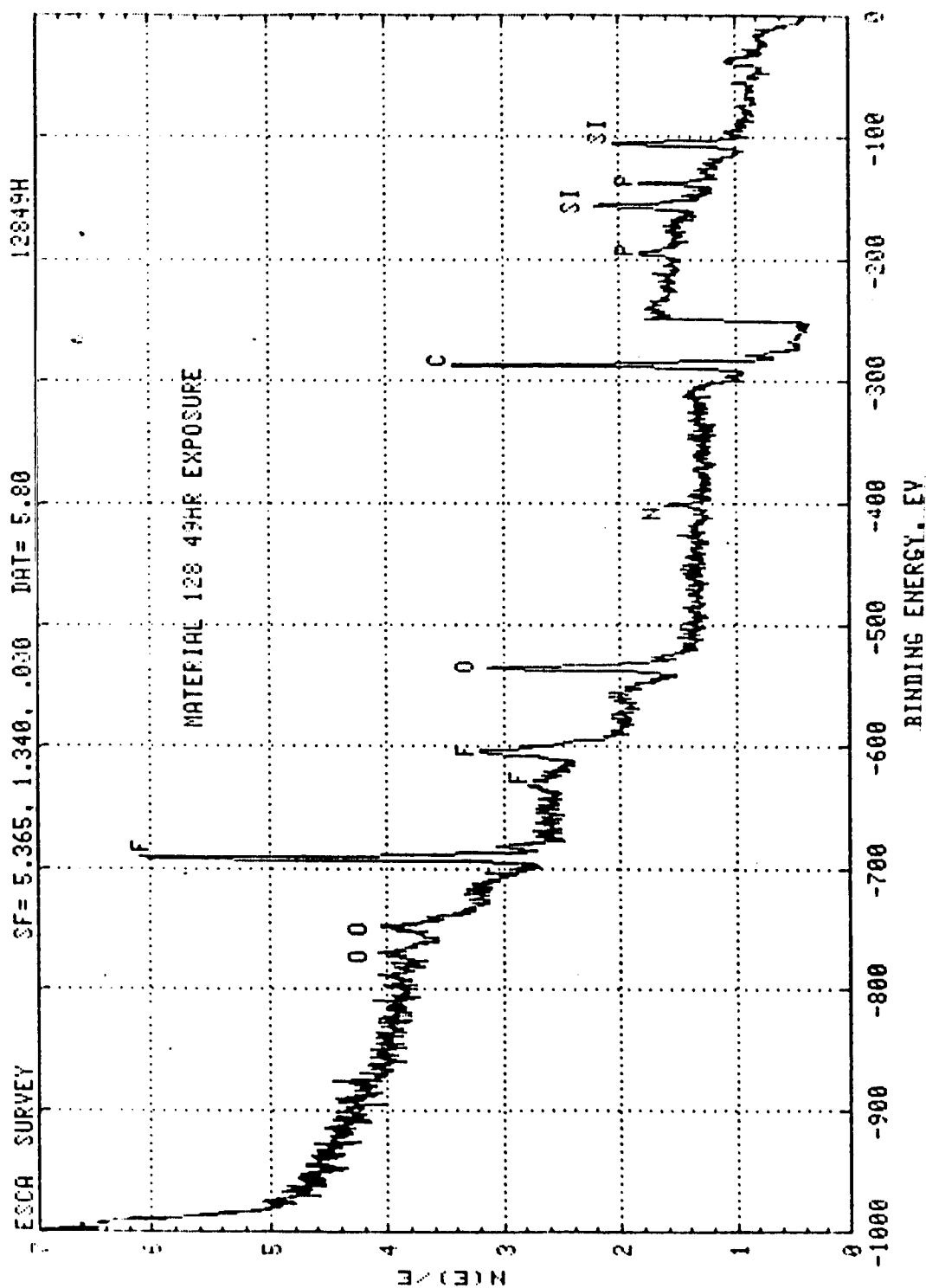


Figure 29: X-Ray Photoelectron Spectrum of Fluorophosphazene Coating on Kapton. The Sample was Previously Exposed to Atomic Oxygen for 49 Hours.

(THIS PAGE INTENTIONALLY LEFT BLANK)

ORIGINAL PAGE IS
OF POOR QUALITY

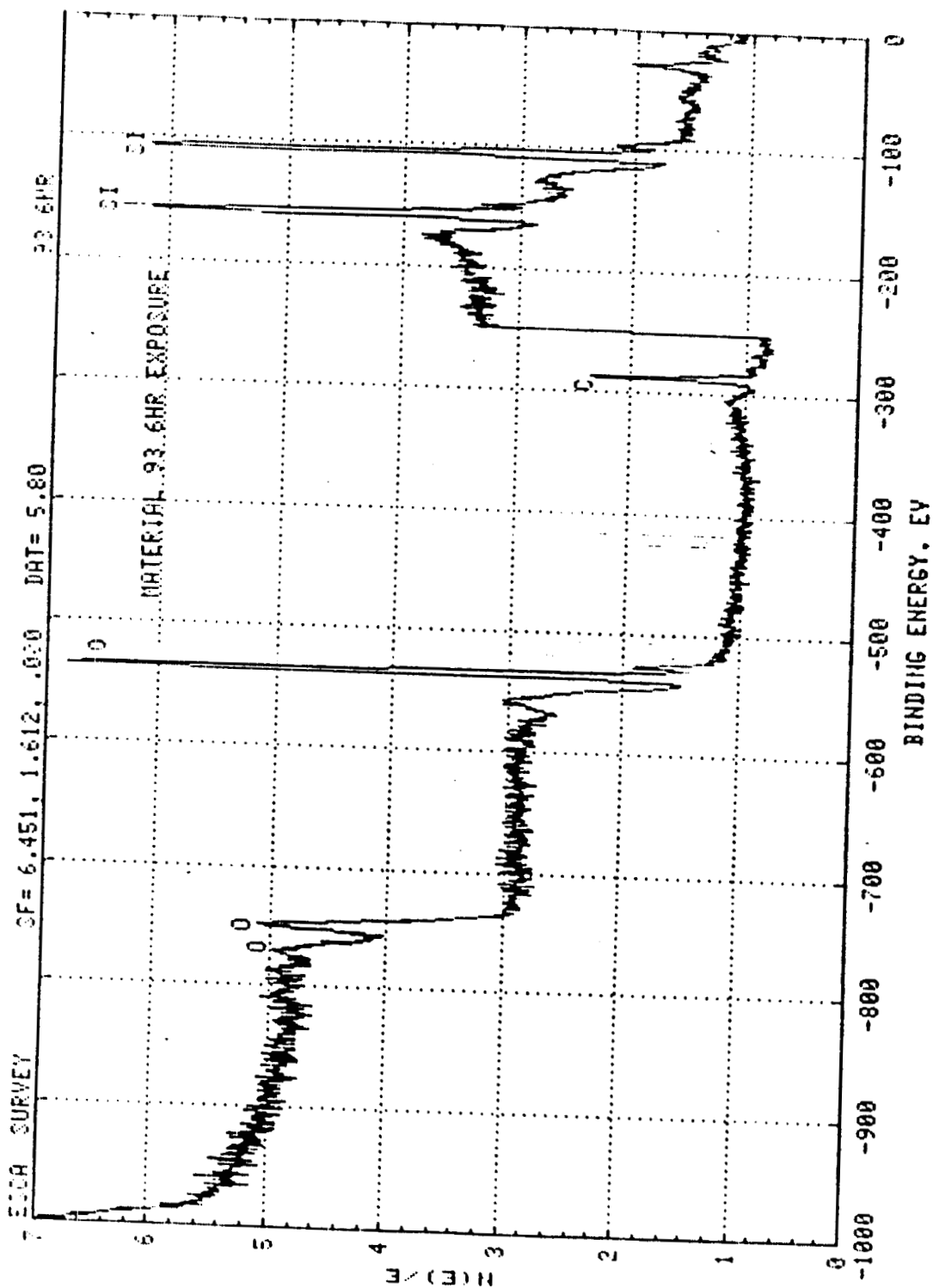


Figure 30: X-Ray Photoelectron Spectrum of Siloxane-Polyimide Co-Polymer Coating on Kapton. The Sample was Previously Exposed to Atomic Oxygen for 6 Hours.

(THIS PAGE INTENTIONALLY LEFT BLANK)

ORIGINAL PAGE IS
OF POOR QUALITY

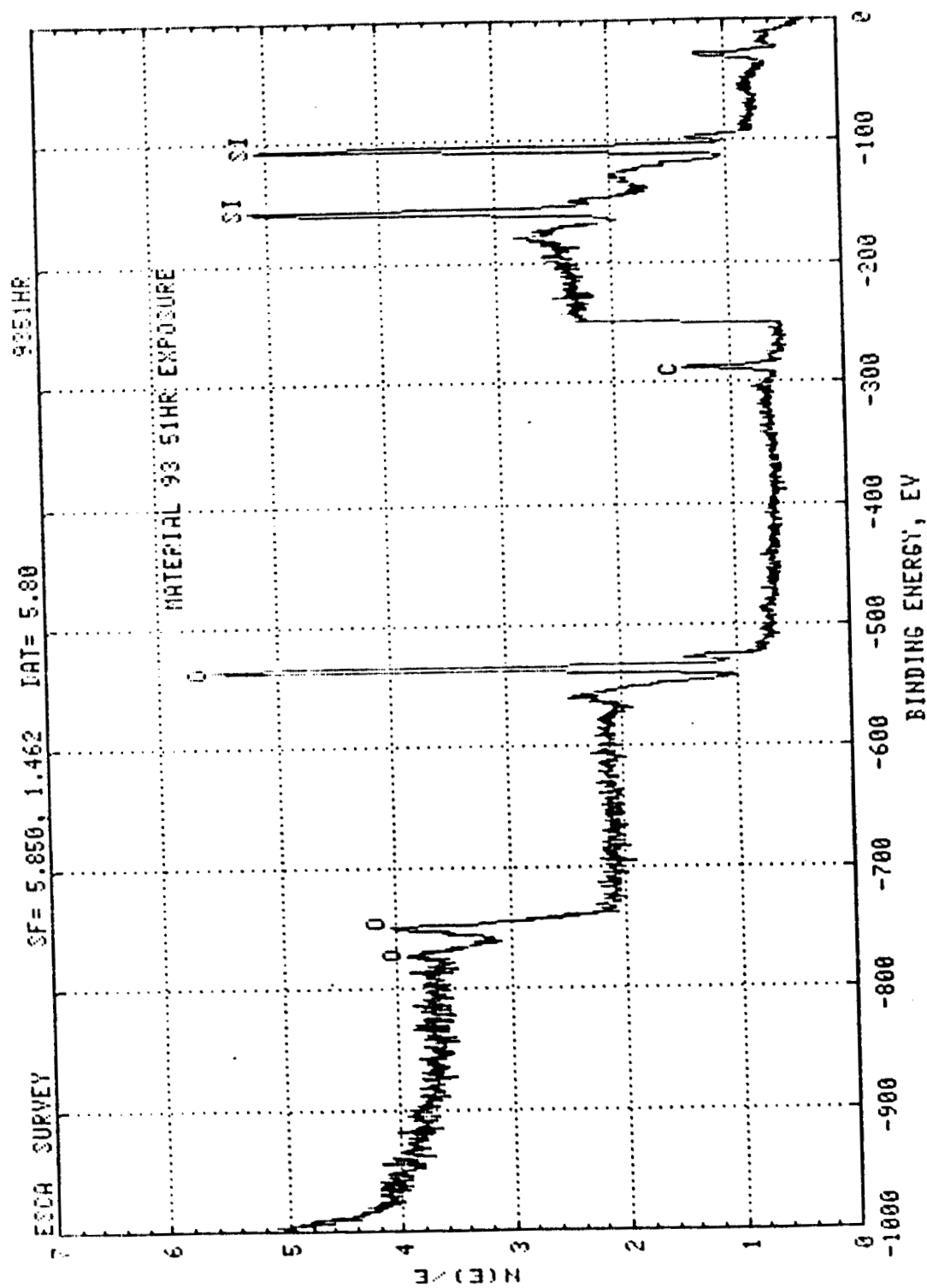


Figure 31: X-Ray Photoelectron Spectrum of Siloxane-Polyimide Co-Polymer Coating on Kapton. The Sample was Previously Exposed to Atomic Oxygen for 51 Hours.

(THIS PAGE INTENTIONALLY LEFT BLANK)

ORIGINAL PAGE IS
OF POOR QUALITY

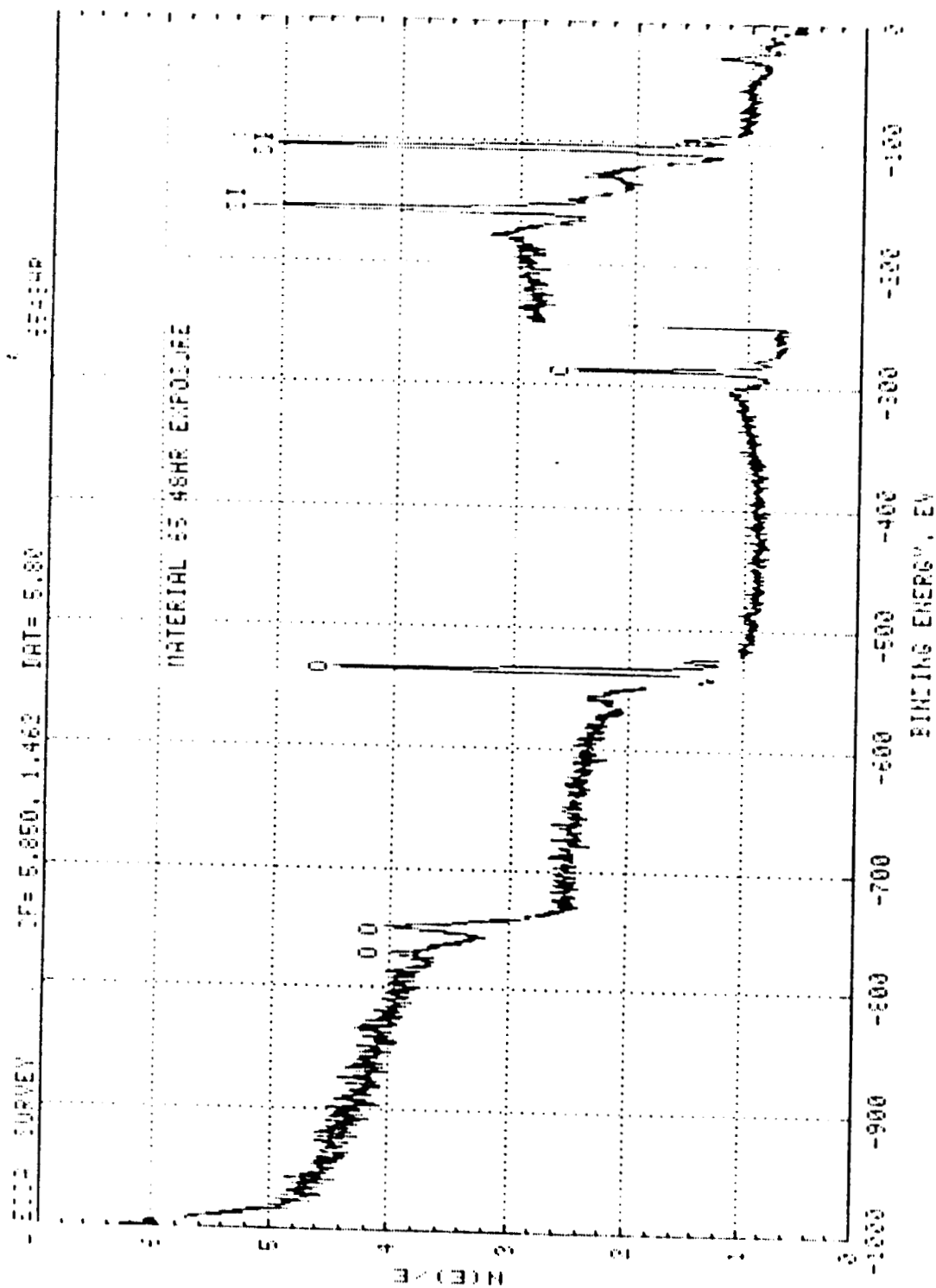


Figure 32: X-Ray Photoelectron Spectrum of Silicone (CV-1144) Coating on Kapton. The Sample was Previously Exposed to Atomic Oxygen for 48 Hours.

(THIS PAGE INTENTIONALLY LEFT BLANK)

<u>SPECIMEN</u>	<u>AO EXPOSURE (Hours)</u>	<u>ELEMENT</u>	<u>MOL PERCENT</u>	<u>RATIOS RELATIVE TO CARBON</u>
#65	48	O	28.6	0.73
		C	39.4	1.0
		Si	32.0	0.81
#128	49	O	15.9	0.23
		C	67.8	1.0
		Si	8.5	0.13
		F	0.9	0.1
		N	3.7	0.005
#93	6	P	3.1	0.05
		O	38.1	1.28
		C	29.8	1.0
		Si	32.0	1.07
#93	51	O	43.4	2.14
		C	20.3	1.0
		Si	36.3	1.79

Table 33. Results of X-Ray Photoelectron Spectroscopy
Surface analysis On Selected Coating Specimens

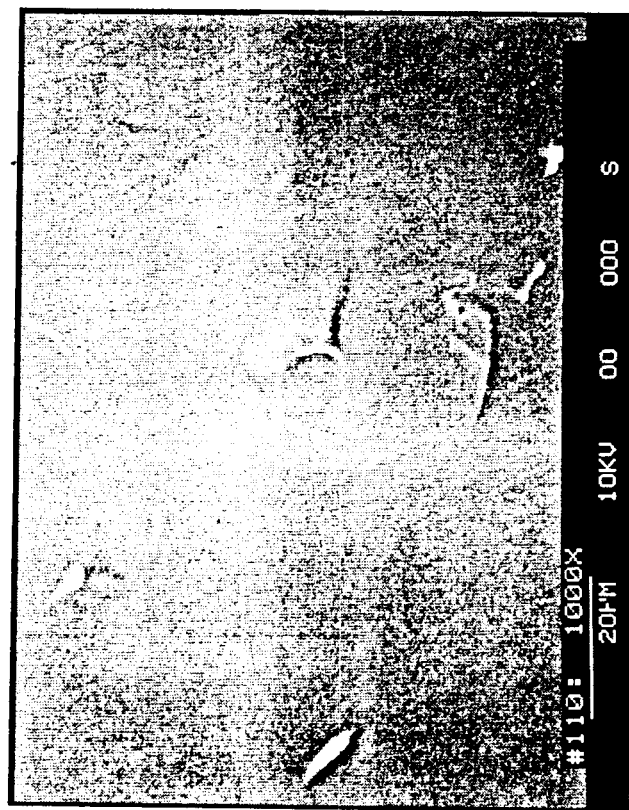
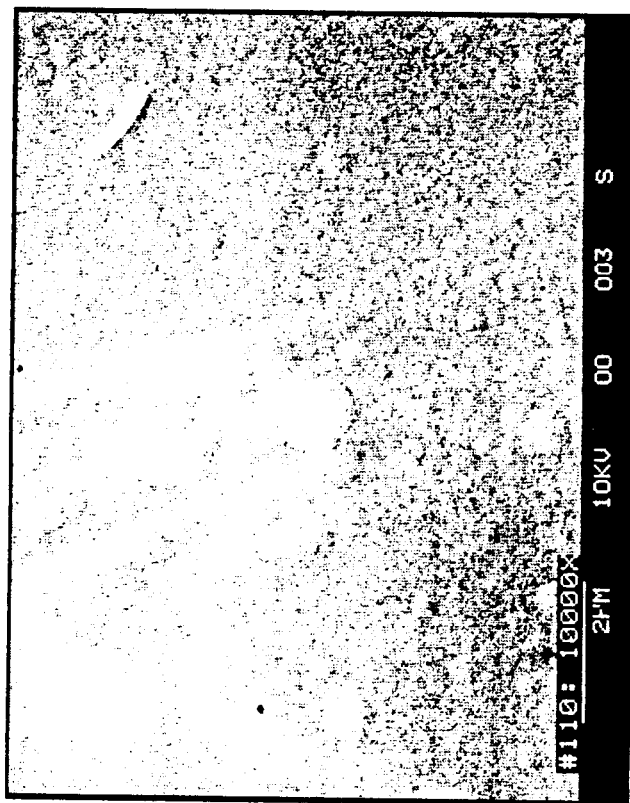
PRECEDING PAGE BLANK NOT FILMED

Figure 33 shows photographs scanning electron microscope (SEM) examination of Battelle's Plasma Polymerized hexamethyldisiloxane coating on Kapton. These pictures are typical of many of the better candidate materials. There are few features apparent, the coatings are uniform and there is no evidence of cracking.

Figures 34 and 35 are SEM's of Battelle HMDS coatings on Kapton after exposure to a combined radiation effects environment (protons, electrons, simulated solar UV) and subsequent exposure to atomic oxygen for 48 hours, at a flux of about $4-5 \times 10^{16}$ atoms/cm²-sec. These photographs were taken at different resolutions and were made at relatively low electron voltage. There are regions where the coating is gone, areas with cracks which are roughly parallel to one another, and clear evidence of attack on the underlying Kapton. The photograph taken with the electron beam at 2.5 Kilovolts shows electron charging along the cracks, indicating areas where the coating is especially thin. These are the extremely light areas along the cracks.

Several material specimens, previously exposed to the combined simulated solar ultraviolet radiation and vacuum thermal cycling environments, were analyzed by X-ray photoelectron spectroscopy (XPS). The samples included coatings of Hexamethyl disiloxane (HMDS), fluorophosphazene, tetrafluoroethylene (TFE), fluorinated ethylene propylene, siloxane-polyimide co-polymer, fluorosilicone, white pigmented silicone, and a plasma polymerized HMDS/TFE, each on a Kapton substrate.

Table 34 shows the elements identified on the surface of each specimen and the mol fraction of each element.



ORIGINAL PAGE IS
OF POOR QUALITY

Figure 33: Scanning Electron Micrograph of Plasma Polymerized
Hexamethyldisiloxane

(THIS PAGE INTENTIONALLY LEFT BLANK)

ORIGINAL PAGE IS
OF POOR QUALITY

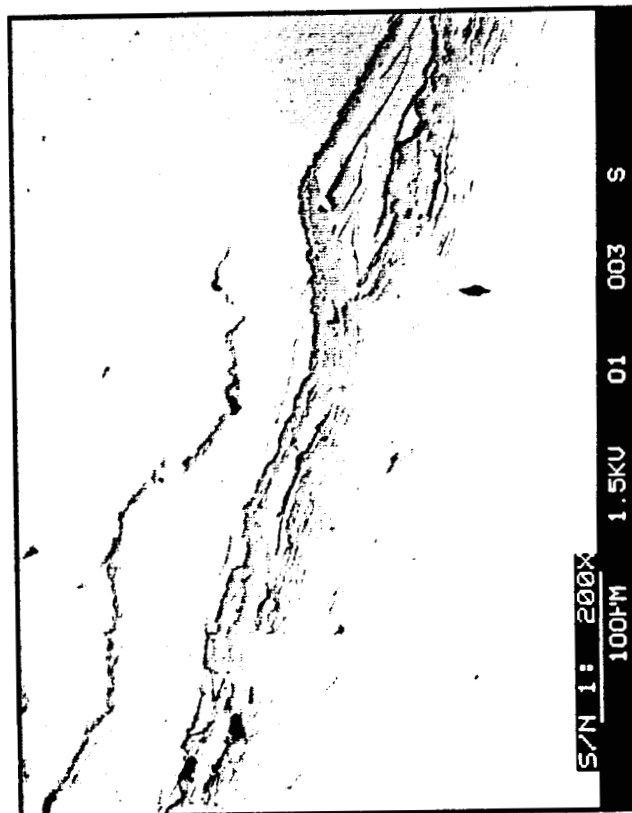


Figure 34: Scanning Electron Micrograph (SEM) of Plasma Polymerized HMDS After Exposure to a Combined Radiation Effects Environment (Electrons, Protons, Simulated Solar UV) and Subsequent Exposure to Atomic Oxygen for 48 Hours.

(THIS PAGE INTENTIONALLY LEFT BLANK)

ORIGINAL PAGE IS
OF POOR QUALITY

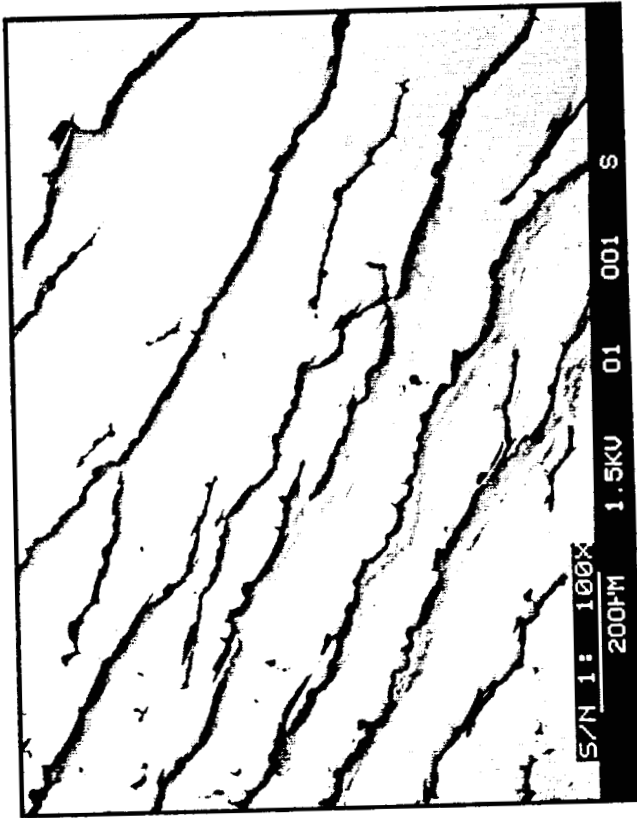


Figure 35: SEM of Plasma Polymerized HMDS After Exposure to a Combined
Radiation Effects Environment and Subsequent Exposure to Atomic
Oxygen for 48 Hours.

(THIS PAGE INTENTIONALLY LEFT BLANK)

<u>MATERIAL #</u>	<u>ELEMENT</u>	<u>MOL FRACTION</u>	<u>RATIO RELATIVE TO CARBON</u>
HMDS (110)	F	0.003	0
	O	0.208	0.4
	C	0.543	1.0
	Si	0.247	0.45
HMDS (110)	F	0.002	0
	O	0.206	0.4
	C	0.541	1.0
	Si	0.251	0.45
X-128	F	0.454	1.55
	O	0.126	0.4
	C	0.294	1.0
	Si	0.017	0.05
	N	0.050	0.2
	P	0.059	0.2
TFE	F	0.661	2.0
	C	0.339	1.0
FEP (31)	F	0.078	0.1
	O	0.055	0.05
	C	0.849	1.0
	N	0.017	0
Siloxane-Polyimide (93)	O	0.231	0.45
	C	0.508	1.0
	Si	0.261	0.5
DSET (White Pigmented Silicone)	C	0.48	1.0
	O	0.23	0.5
	Si	0.29	0.6
HMDS/TFE (#112)	F	0.014	0
	O	0.216	0.4
	C	0.525	1.0
	Si	0.245	0.45
CV-3530 (Large Scale Article #151)	F	0.267	0.5
	O	0.108	0.2
	C	0.519	1.0
	Si	0.107	0.2
26	F	0.028	0.005
	O	0.191	0.33
	C	0.574	1.0
	Si	0.208	0.35

Table 34: Results of XPS Analysis of Specimens Previously Exposed to the Combined Vacuum Thermal Cycling, Simulated Solar UV Environments

The mol fractions of the constituent elements are as expected for each of these materials. There is no indication of preferential degradation of any particular functional group on any of these samples, with one exception. The FEP sample shows relatively small amounts of fluorine. However, this sample has a small crease and the presence of nitrogen indicates that the probe was detecting Kapton in addition to the coating. The fluorophosphazene sample also shows a small smount of silicone contamination. All the siloxane based samples show similar carbon to silicon elemental ratios; changes in these materials due to this exposure are physical; microcracking, annealing, rather than chemical.

Figure 36 shows an SEM of Kapton after combined radiation effects and subsequent atomic oxygen exposure. The pattern of peeling in the surface layer is of questionable origin. It could be due to peeling along processing marks. It could also be due to surface contamination from coatings on samples exposed simultaneously, although we do not observe this pattern with any coatings which we have examined. It could also be an artifact since an extremely thin palladium coating is applied to the samples to improve the contrast in the SEM.

Figures 37 and 38 are a sequence of SEM photographs from low to high resolution, showing the cracking, peeling, and loss of distinct regions of a fluorophosphazene coating. This sequence also shows evidence of attack by oxygen atoms through cracks in the coating followed by undercutting along the adhesive bonds between the Kapton and the coating.

Figure 39 shows cracking in the S13-G/LO-1 coating after combined radiation effects and atomic oxygen exposure. The porosity of this coating is shown in the higher resolution photograph.

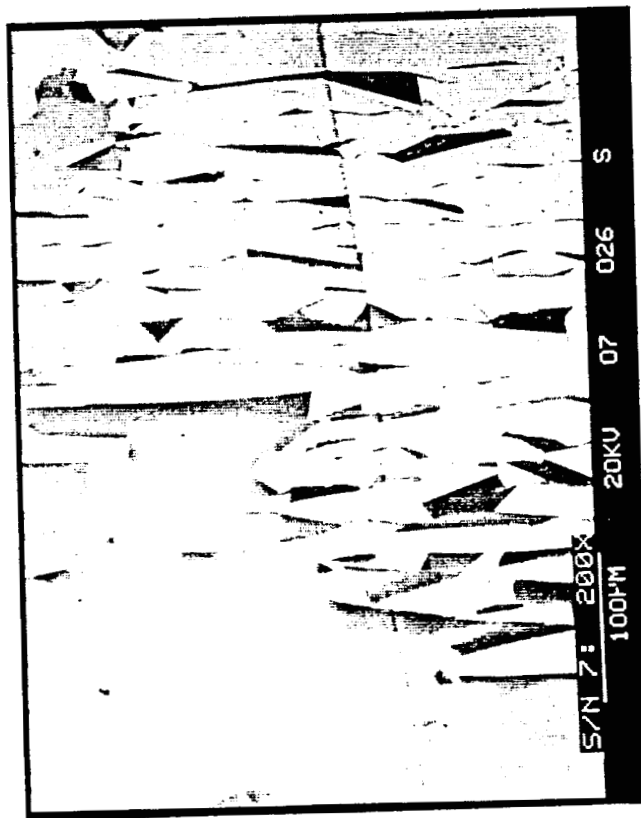
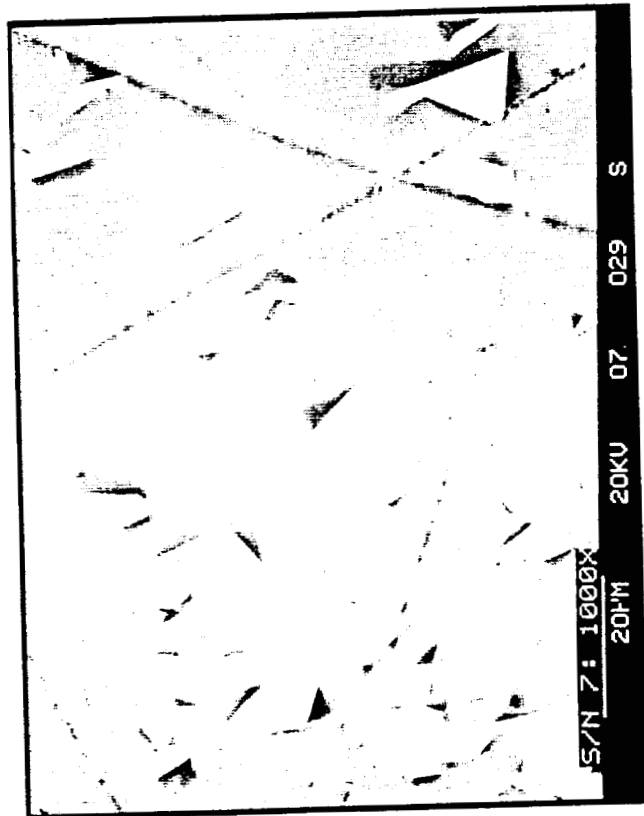


Figure 36: SEM of Kapton After Exposure to a Combined Radiation Effects Environment and Subsequent Exposure to Atomic Oxygen for 48 Hours.

(THIS PAGE INTENTIONALLY LEFT BLANK)

ORIGINAL PAGE IS
OF POOR QUALITY

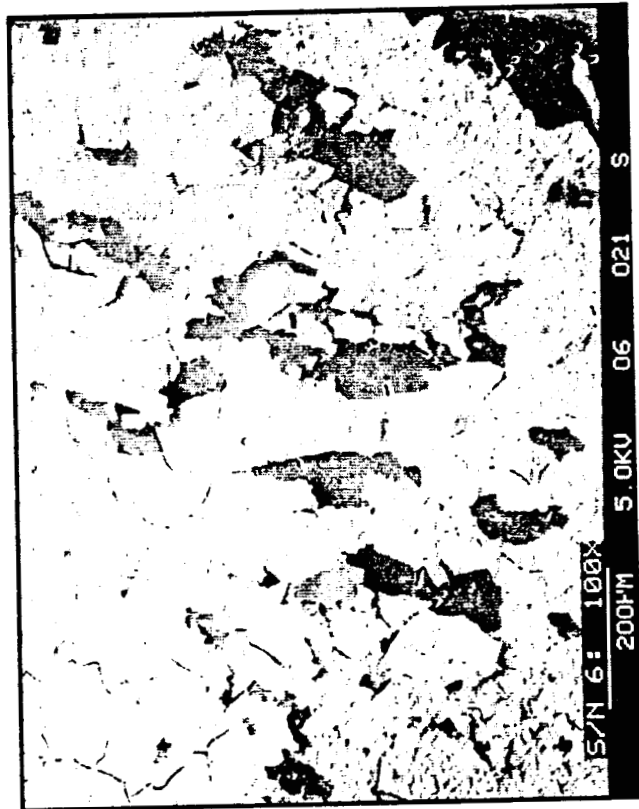


Figure 37: SEM of Fluorophosphazene After Exposure to a Combined Radiation Effects Environment and Subsequent Exposure to Atomic Oxygen for 48 Hours.

(THIS PAGE INTENTIONALLY LEFT BLANK)

ORIGINAL PAGE IS
OF POOR QUALITY

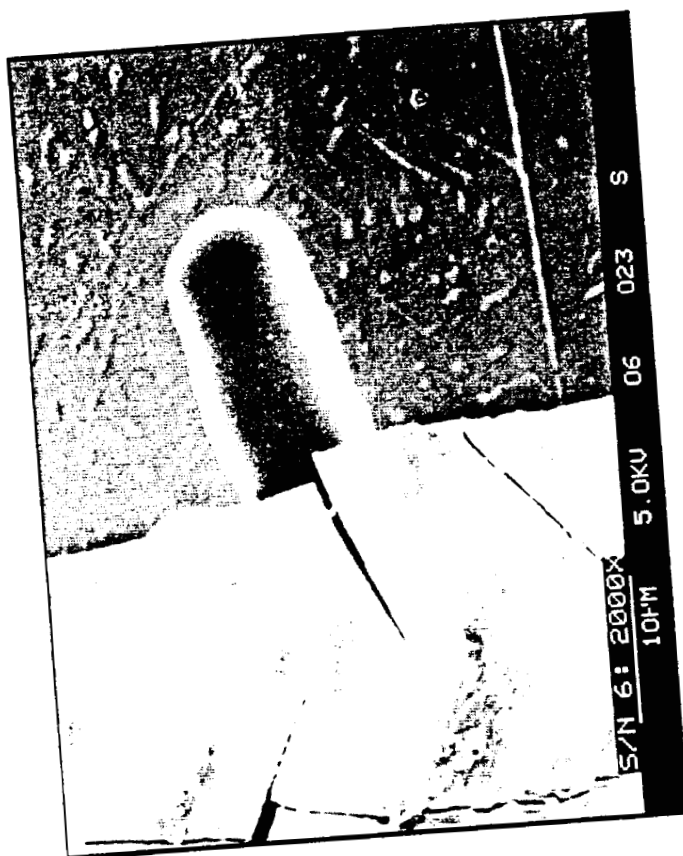


Figure 38: SEM of Fluorophosphazene After Exposure to a Combined Radiation Effects Environment and Subsequent to Atomic Oxygen for 48 Hours.

(THIS PAGE INTENTIONALLY LEFT BLANK)

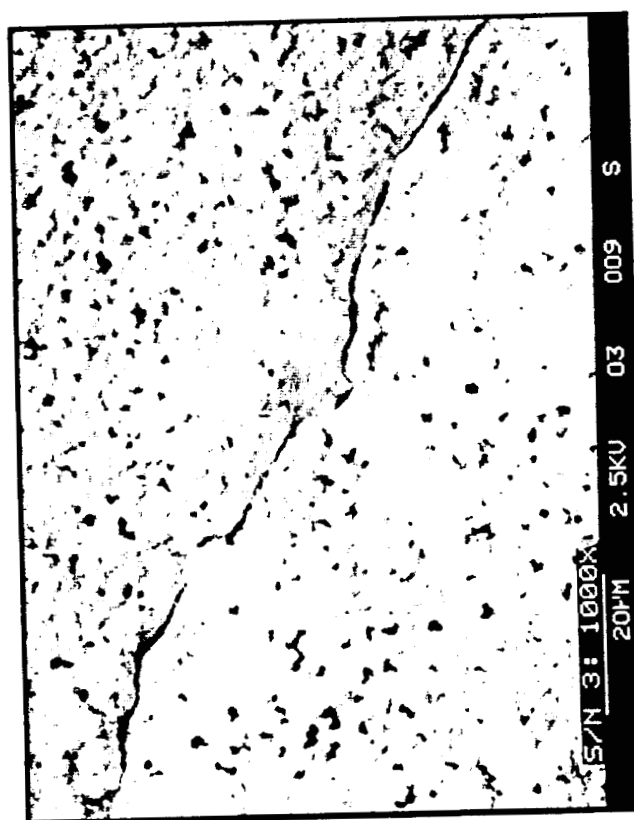
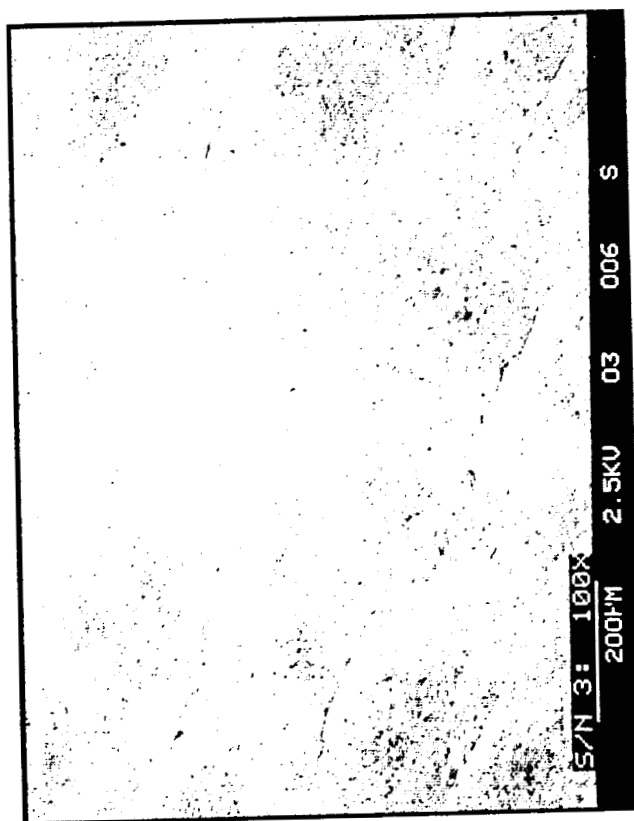


Figure 39: SEM of S13-G/L0 After Exposure to a Combined Radiation Effects Environment and Subsequent Exposure to Atomic Oxygen for 48 Hours.

Figures 40 and 41 show SEM's of McGhan-NuSil's Silicone and Fluorosilicone coatings, respectively. Cracks are apparent in both these coatings, but especially in the fluorosilicone. The high resolution pictures of both these coatings show electron charging along the cracks just under the coating edges.

Figures 42 and 43 are SEM photographs of Battelle's plasma polymerized hexamethyldisiloxane/tetrafluoroethylene coating after combined radiation effects and atomic oxygen exposure. One photo shows blistering, cracking and peeling of this coating. The remaining photographs in these figures are a sequence, each showing the same location, with the electron beam energy being increased. As the electron energy goes up, undercutting beneath the coating, as well as severe degradation of the Kapton substrate are clearly seen.

In summary, there is some cracking on most of the coatings after exposure to the combined radiation effects environment. However, virtually all of the mass loss, the flaking off of the coating, the severe undercutting of the coating and etching of the substrate is observed after exposure to atomic oxygen.

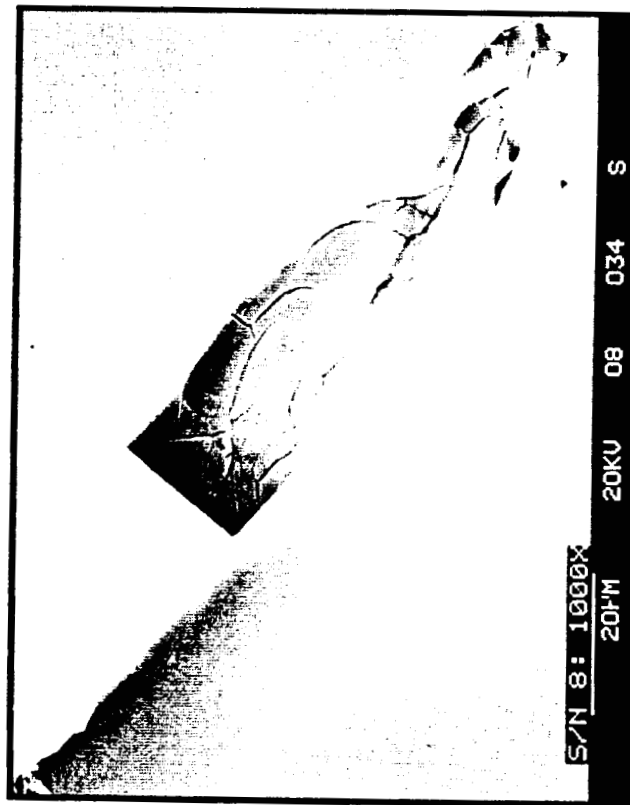
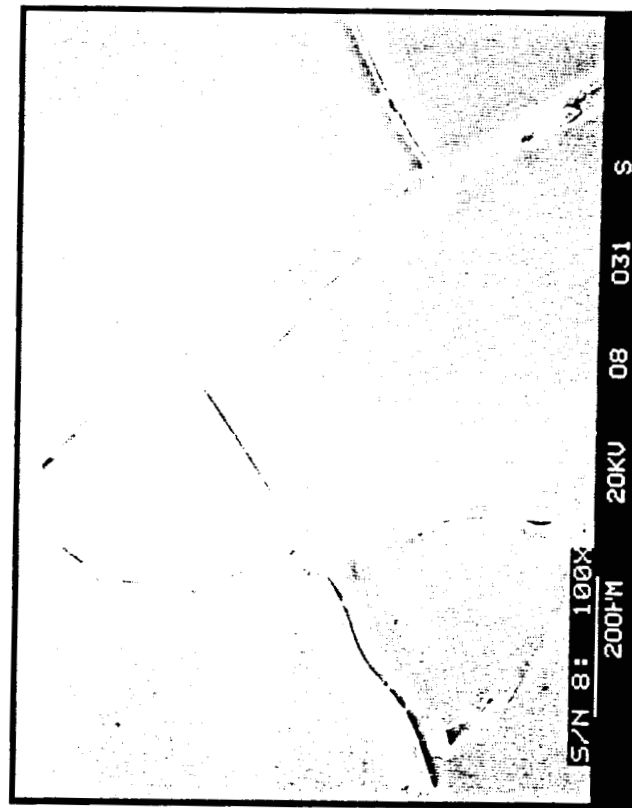


Figure 40: SEM of a Silicone (CV-1144) After Exposure to a Combined Radiation Effects Environment and Subsequent Exposure to Atomic Oxygen for 48 Hours.

(THIS PAGE INTENTIONALLY LEFT BLANK)

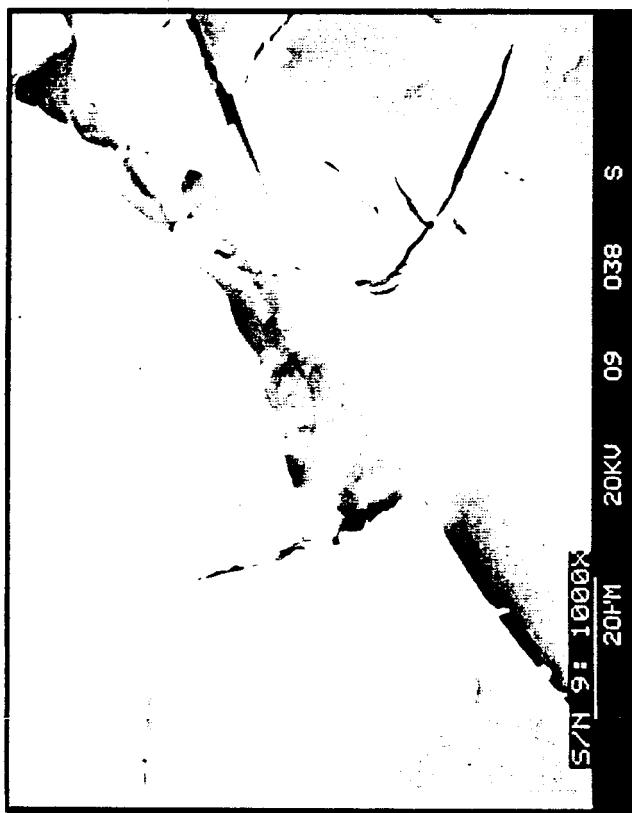


Figure 41: SEM of a Fluorosilicone (CV-3530) After Exposure to a Combined Radiation Effects Environment and Subsequent Exposure to Atomic Oxygen for 48 Hours.

ORIGINAL PAGE IS
OF POOR QUALITY

(THIS PAGE INTENTIONALLY LEFT BLANK)

ORIGINAL PAGE IS
OF POOR QUALITY

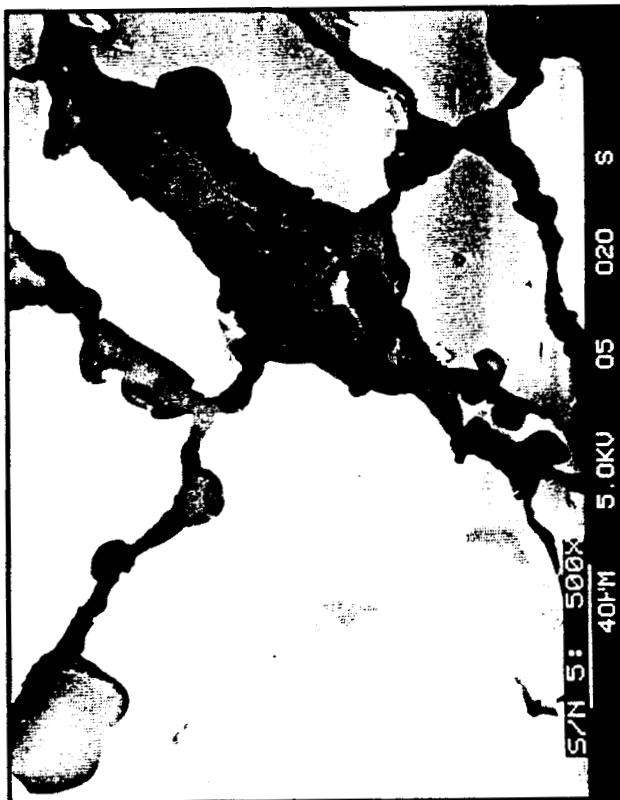
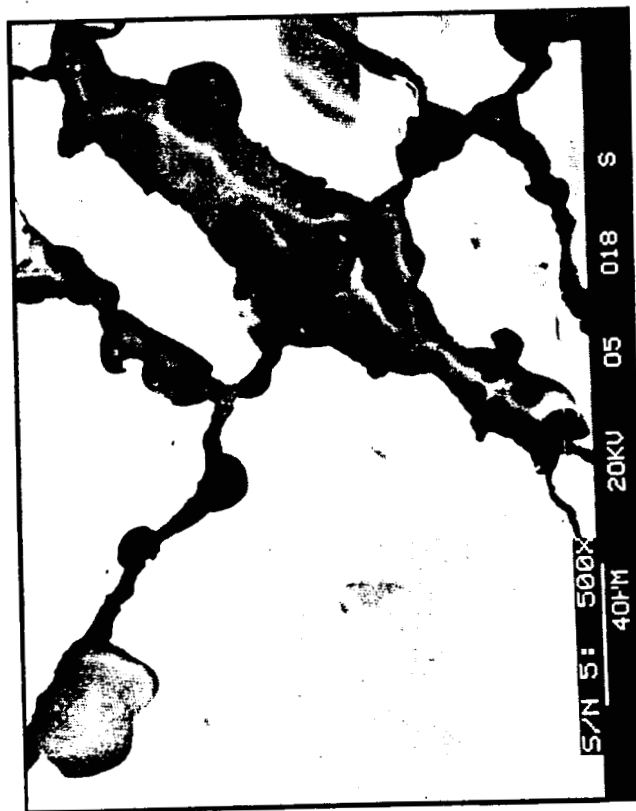
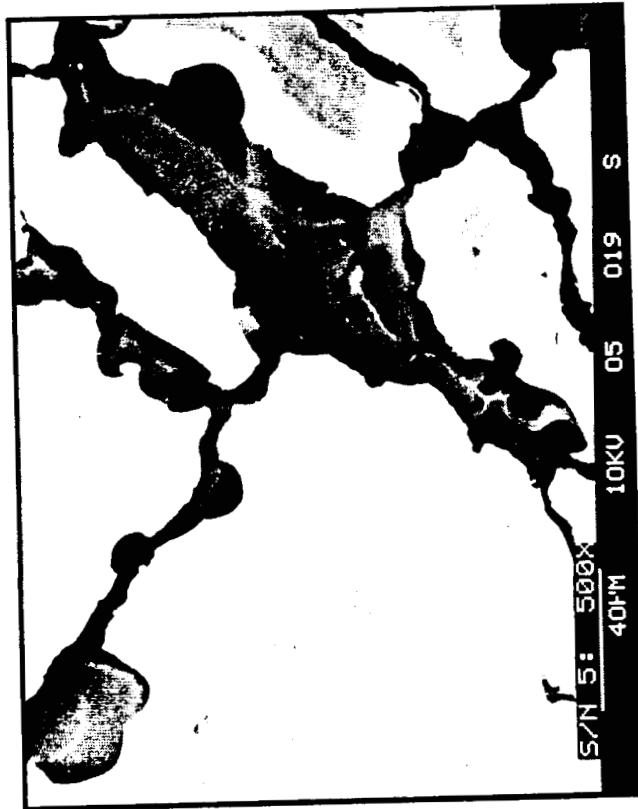


Figure 42: SEM of Plasma Polymerized Hexamethylcyclotrisiloxane/Tetrafluoroethylene (8:1), After Exposure to a combined Radiation Effects Environment and Subsequent Exposure to Atomic Oxygen for 48 Hours.

(THIS PAGE INTENTIONALLY LEFT BLANK)



ORIGINAL PAGE IS
OF POOR QUALITY

Figure 43: SEM of Plasma Polymerized HMDS/TFE After Exposure to a Combined
Radiation Effects Environment and Subsequent Exposure to Atomic
Oxygen for 48 Hours.

The following data are from an extensive group of observations of surfaces of a large number of specimens. The text is a discussion for each figure.

SET 1 (10/16/86)

Figure 44:

Material #46: As received; Type: plasma-polymerized HMDS on 1-mil Kapton film; Au/Pd-coated for SEM analysis. Title: MTL-46-PreX. Magnification: 1500X. Legend: Striation Patterns, Surface Debris, and Pits in Plasma Polymerized Coating. Description: Typical surface features observed at low power over the approximately one square centimeter of as-received coated material. The striated patterns are seen occasionally, the surface pits are more common, but randomly distributed. Random surface debris was scattered lightly over the sample's surface.

Figure 45:

Material #46: exposed to atomic oxygen (run #36, position 5) 4 hours at 350 watts; Au/Pd-coated for SEM analysis. Title: MTL-46-36-5. Magnification: 100X. Legend: Surface Defects on Atomic Oxygen Exposed Coating. Description: Typical surface defect features resulting from BAC plasma atomic oxygen testing. Note the cracked and peeling surface coating, which exposes the Kapton substrate. The feature at center right shows cracking occurring in the exposed substrate material. Many such defects similar to these were observed over the central region of this sample.

Figure 46:

Title: MTL-46-36-5. Magnification: 42X. Legend: Detail of Outer Ring Damage (Material #46). Description: This is a view of the region where the lip of the aluminum sample holder holds the outer rim edge of the disc material

ORIGINAL PAGE IS
OF POOR QUALITY

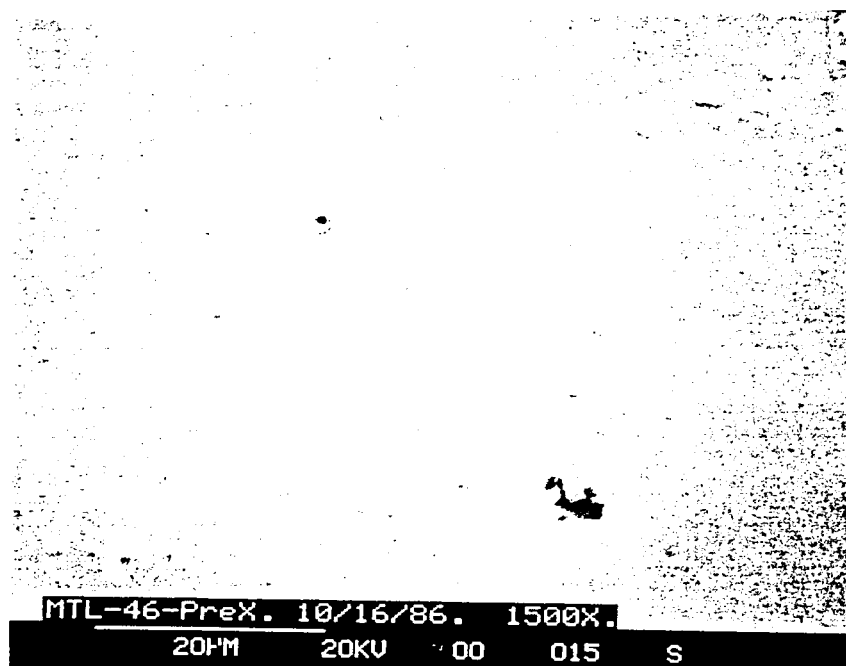


Figure 44: Plasma Polymerized HMDS (#46) on 1-Mil Kapton

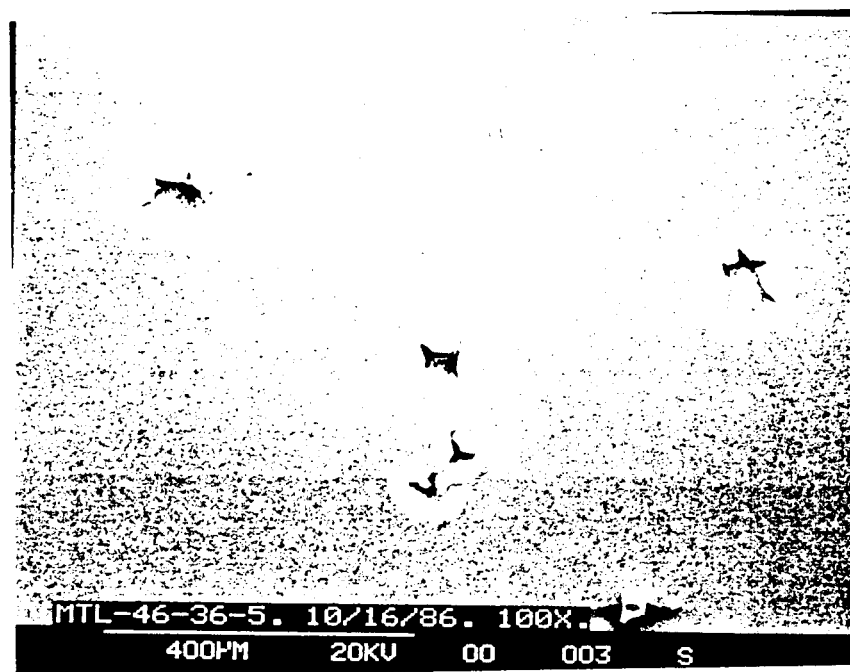


Figure 45: HMDS Coating (#46) on Kapton. Sample Exposed to Atomic Oxygen for 4 Hours.

sample. The splitting of the remnants of the protective coating is more severe on the side held by the aluminum lip, the substrate erosion patterns in the central exposed band region, and the circular pits in the exposed Kapton substrate to the lower center right. The unevenness of the splitting from the exposed side of the band as compared to the aluminum held side is unique, and may be the results of mechanical (compression) or thermal differences.

Figure 47:

Title: MTL-46-36-6. Magnification: 160X. Legend: Detail of Pit Cluster Area and Surface Erosion Features (Material #46). Description: A close-up showing pits and erosion patterns. Note especially the pits in the lower part of the picture, which appear to have formed after the erosion patterns. If this has occurred, then the pits cannot be the result of surface defects originally in the coating prior to atomic oxygen exposure, but must be due to preferential erosion of the Kapton substrate upon removal of the protective coating and formation of the typical surface erosion patterns.

SET 2 (11/05/86)

Figure 48:

Standard Material: Kapton polyimide 2-mil film, unexposed; Au/Pd-coated for SEM analysis. Title: Kapton Std. PreX. Photo #001. Magnification: 5KX. Legend: Surface of As-Received Kapton Polyimide Film. Description: photo of a typical region of the film surface. Note uniformity and general cleanliness of the film, with only traces of surface debris (probably dust particles), and the shallow horizontal groove. No pits and few other surface defects were observed in the Kapton samples examined.

Figure 49:

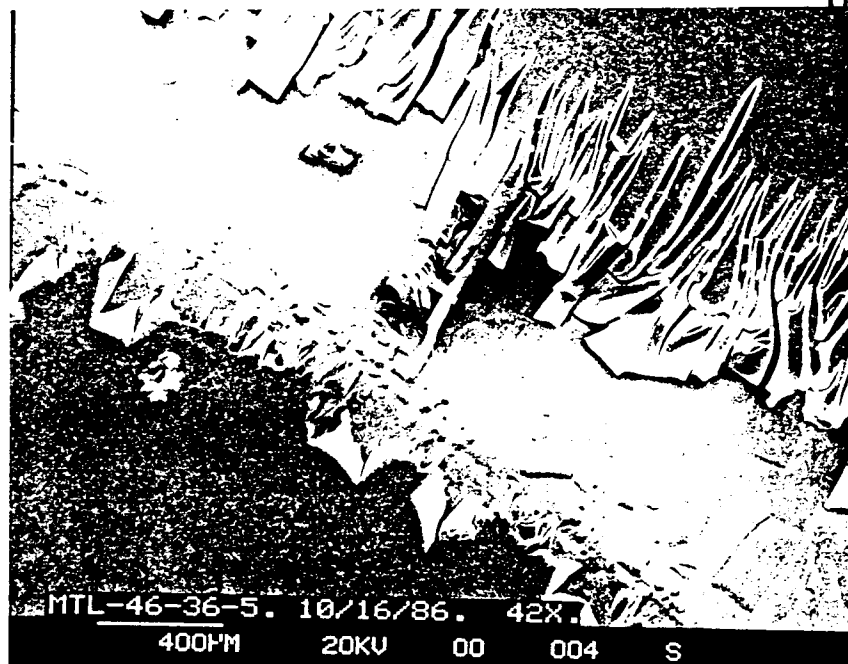


Figure 46: Detail of Damage at Boundary of Exposed and Covered Regions of HMDS Coating After 4 Hours Exposure to Atomic Oxygen.

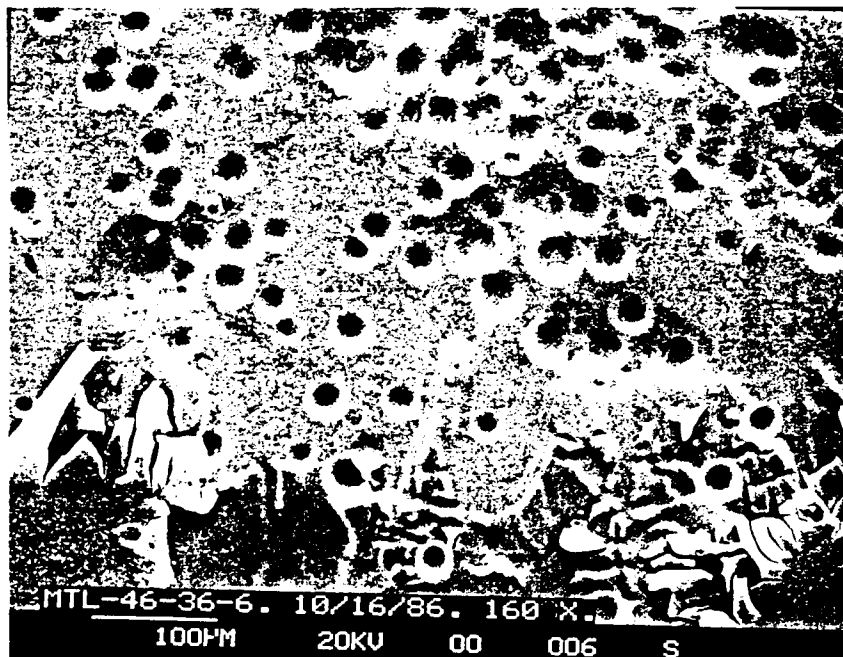


Figure 47: Detail of Area Near Edge of Exposed Region Showing Attack of Kapton Substrate by Atomic Oxygen Upon Coating Loss.

(THIS PAGE INTENTIONALLY LEFT BLANK)

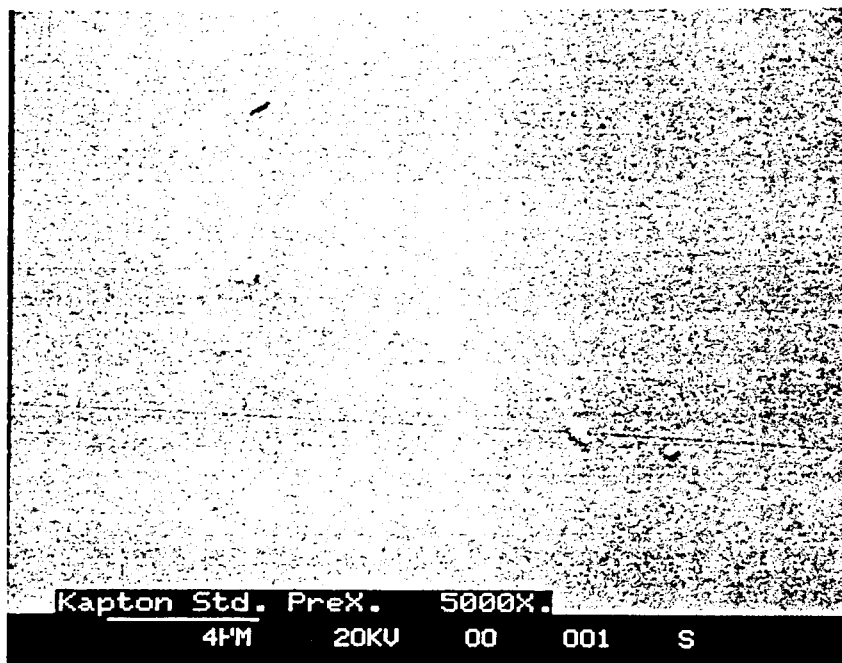


Figure 48: Uncoated 2-Mil Kapton Film

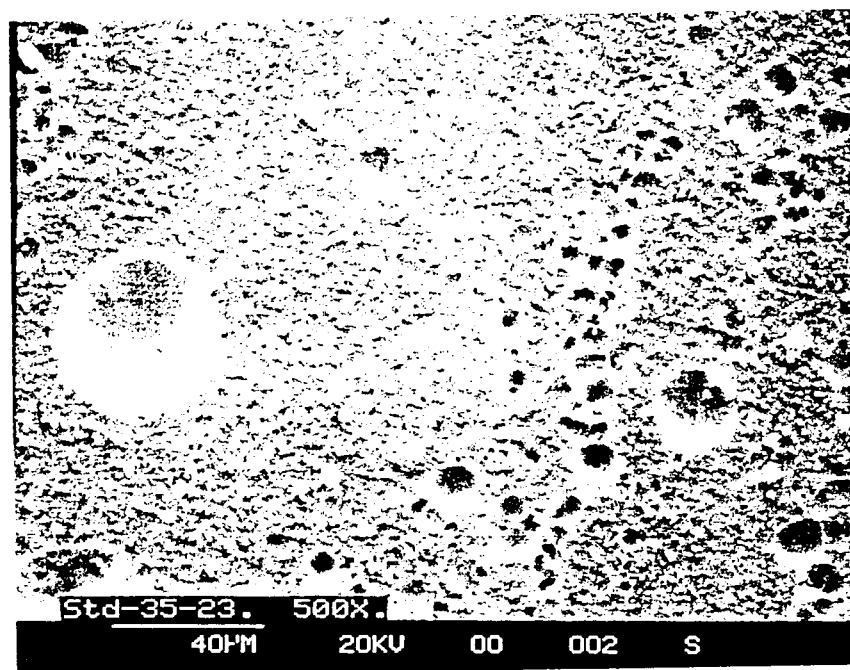


Figure 49: Uncoated 2-Mil Kapton Film After 4 Hours of Exposure to Atomic Oxygen

Standard Material: Kapton 2-mil film, exposed to atomic oxygen (run #35, position 23) for 4 hours at 350 watts; Au/Pd-coated for SEM analysis. Title: Std-35-23. Photo #002. Magnification: 500X. Legend: Typical Surface Features of Kapton Film Standard Material Exposed to Atomic Oxygen in the BAC Plasma Materials Screening Facility. Description: There is a random distribution of pit sizes, and a non-uniform distribution of pits located over the sample, indicating preferential pit initiation sites. There is a uniform scattering of surface debris particles over the sample, which was not observed in the pre-exposure Kapton samples. The atomic oxygen appears to attack the Kapton surface in two separate but simultaneous methods: (1) a general, even surface recession, resulting in a uniform thickness loss over the entire exposed region, and (2) preferential attack and rapid erosion at certain more susceptible sites, resulting in pits and, eventually, hole formation. EDAX (Energy Dispersive X-ray Analysis) spectra were obtained of certain surface features have been obtained. Figure 50 is an EDAX spectrum of a relatively clear, bare area towards the center of the atomic oxygen exposed sample--in the region seen in photo #002- and shows the material in this region to be essentially carbon and oxygen, with slight tracer of aluminum, silicon and zinc (impurities). The gold and palladium peaks are due to the conductive coating sputtered onto the sample for SEM analysis. Figure 51 is an EDAX spectrum taken of the unexposed (protected) rim material of the Kapton sample. Traces of aluminum and silicon are seen as in Figure 50. Comparison of the ratio of peak heights of carbon to oxygen of both figures indicates that the two regions, exposed and unexposed, are essentially the same, with no oxygen enrichment or carbon depletion occurring in the exposed region. Figure 52 is an EDAX spectrum of a large debris particle on the surface, with the exposed area.

KAPTON, S/N 35-23.

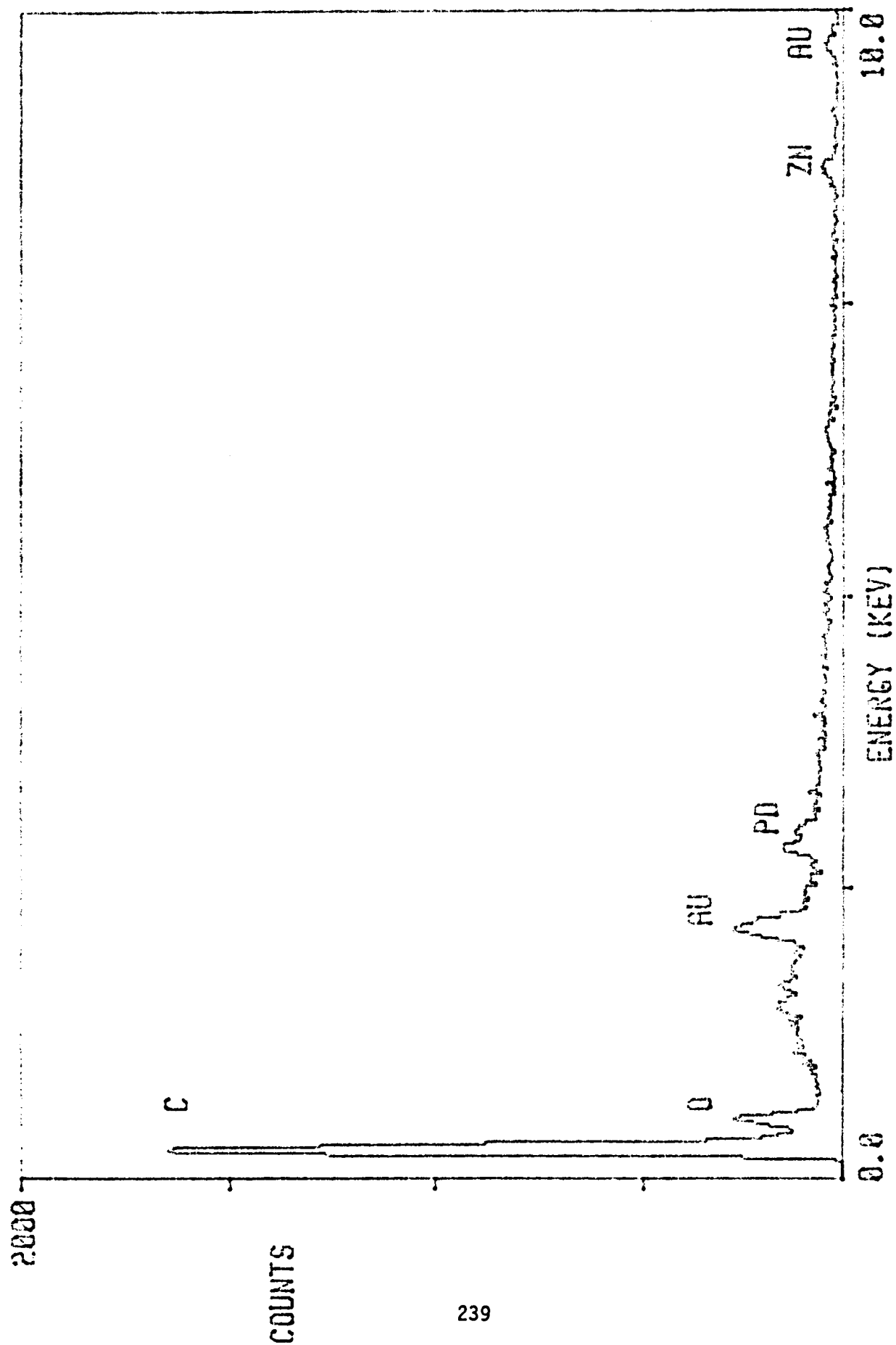


Figure 50: EDAX Spectrum of Kapton Exposed to Atomic Oxygen For 4 Hours

(THIS PAGE INTENTIONALLY LEFT BLANK)

KAPTON A111, 35-23.



Figure 51: EDAX Spectrum of Unexposed Edge Area of Kapton. Region of Sample Under Lip of Specimen Holder.

(THIS PAGE INTENTIONALLY LEFT BLANK)

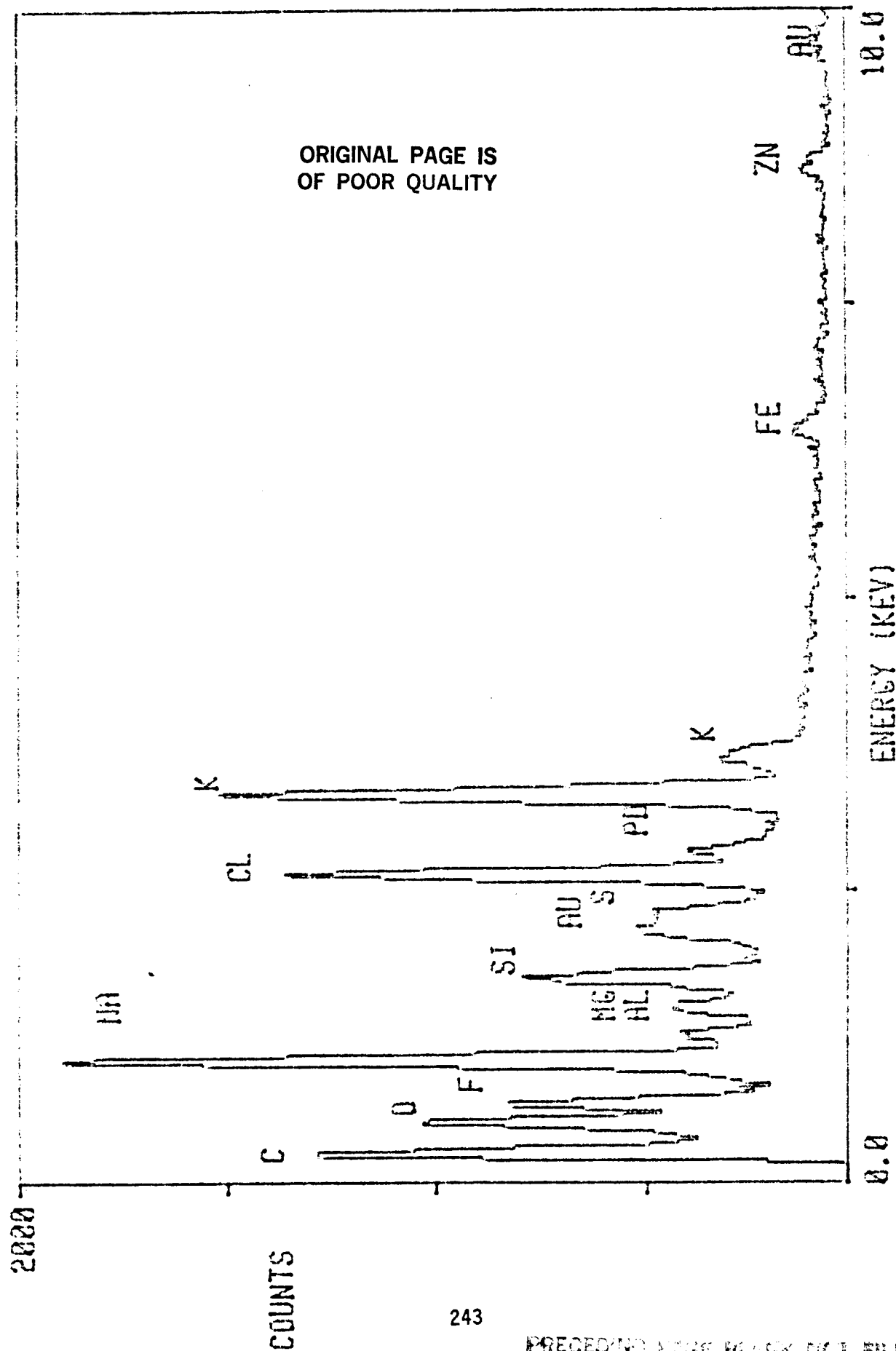


Figure 52: EDAX Spectrum of Large Debris Particle on Surface of Kapton Exposed to Atomic Oxygen for 4 Hours.

(THIS PAGE INTENTIONALLY LEFT BLANK)

Figure 53:

Title: Std-35-23. Photo #006. Magnification: 250X. Legend: Pit Patterns in Atomic Oxygen Exposed Kapton Film. Description: An observed feature of the exposed Kapton film was pit formation. Many of these pits are conical with a dark spot/apex. Others are shallow hemispherical pits. Surface debris, fairly uniform in particle size, is distributed evenly over the surface except where pits have formed. At these sites debris rims a pit but generally no debris is present within the pit. The debris in the pits could not have simply reacted with oxygen atoms and been eroded away as this is not observed for the surface debris present between the pits.

Figure 54:

Material #57: Ethyl Eypel-X129 coating on 1-mil Kapton film; exposed to atomic oxygen (run #44, position 9) for 2 hours at 350 watts; Au/Pd-coated for SEM analysis. Title: Mtl-57-44-9. Photo #012. Magnification: 100X. Legend: Interface Region Between Exposed (Left) and Unexposed (Right) Coating. Description: Blistering is observed on the atomic oxygen exposed coating material, with a random distribution of blister size and location. This was observed over the entire rim interface of the sample. The outer rim material (to the right) was protected by the lip of the aluminum sample holder during exposure to atomic oxygen. No blistering was observed in this protected rim region over the entire circumference of the sample.

Figure 55:

Material #58: Ethyl Eypel-X128 Fluorosphozene coating on 1-mil Kapton film; exposed to atomic oxygen (run #44, position 5) for 2 hours at 350 watts; Au/Pd-coated for SEM analysis. Title: MTL-58-44-5. Photo #016. Magnification: 160X. Legend: Splits in Eypel-X128 Fluorophosphazene Coating Upon Exposure to

(THIS PAGE INTENTIONALLY LEFT BLANK)

ORIGINAL PAGE IS
OF POOR QUALITY

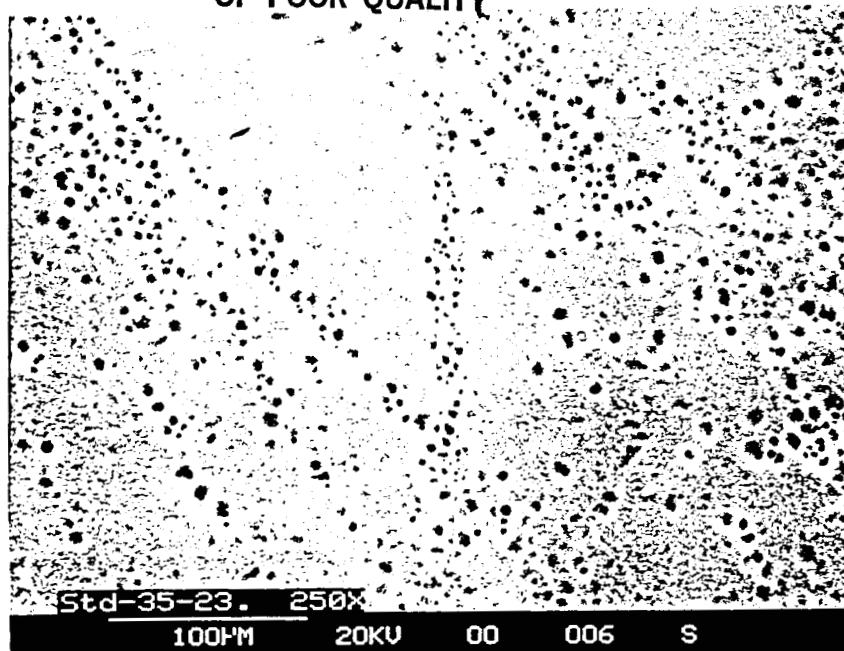


Figure 53: Texture of Uncoated Kapton Film After 4 Hours Atomic Oxygen Exposure

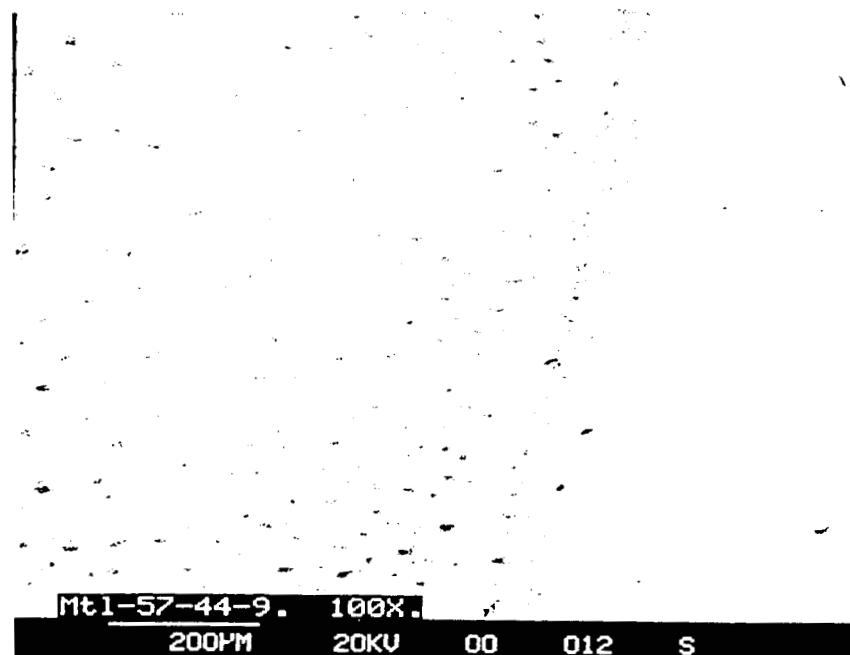


Figure 54: Ethyl Epe1 (X-129) Coating on Kapton. Sample was Exposed to Atomic Oxygen for 2 Hours.

(THIS PAGE INTENTIONALLY LEFT BLANK)

ORIGINAL PAGE IS
OF POOR QUALITY

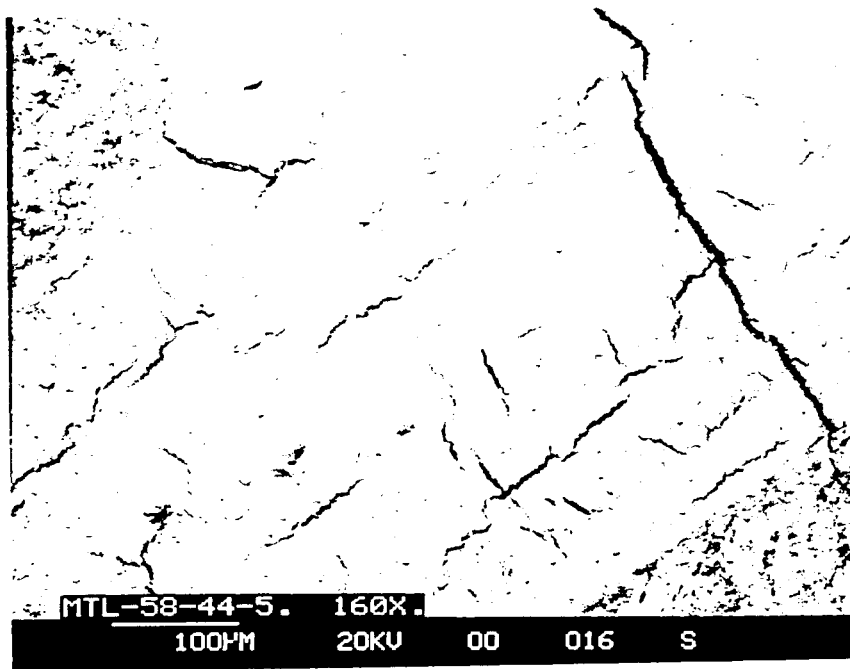


Figure 55: Eypel [®]-Type Coating (X-128) on Kapton. Sample Exposed to Atomic Oxygen Plasma for 2 Hours.

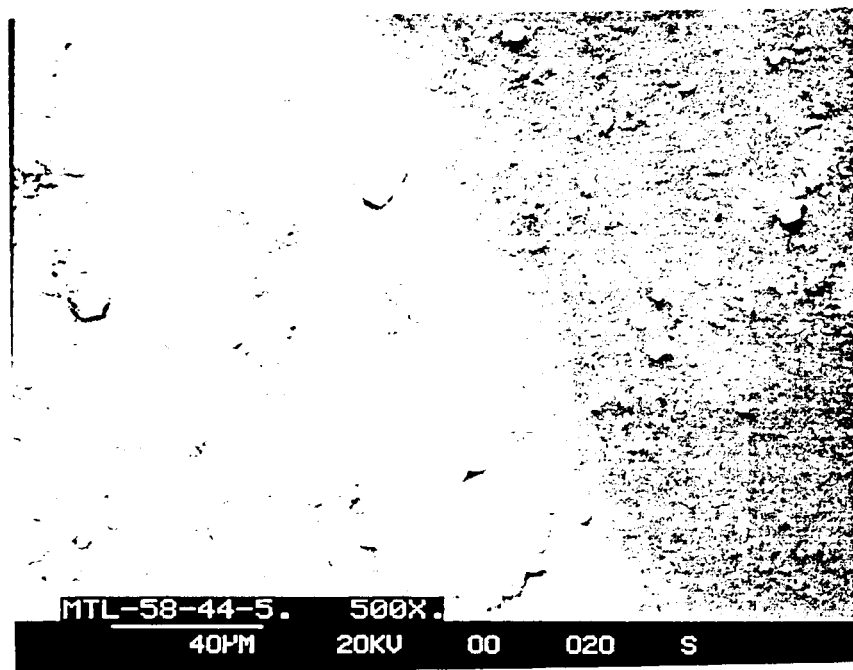


Figure 56: Interface Between X-128 Coating Exposed to Atomic Oxygen (Left) and Unexposed (Right).

Atomic Oxygen. Description: Typical view of the surface of exposed Material #58. Note uneven distribution of surface debris, and splits in the coating which reveal the Kapton substrate below.

Figure 56:

Title: MTL-58-44-5. Photo #020. Magnification: 500X. Legend: Interface Region Between Atomic Oxygen Exposed (Left) and Unexposed (Right) Eypel-X128 Fluorophosphazene Coating (Material #58). Description: Note lightening of exposed region due to uncovering of filler materials by surface recession. Also, while small splits are present at the interface, no splits in the coating are visible on the unexposed (protected) rim material.

SET 3 (11/07/86)

Figure 57:

Material #58: Ethyl Corporation. Eypel-X128 fluorophosphazene coating on 2-mil Kapton film; unexposed: Au/Pd-coated for SEM analysis. Title: MTL-58. PreX. Photo #028. Magnification: 10KX. Legend: Relatively debris-free region of surface of as-received Eypel X-128 Fluorophosphazene Coating (Material #58). Description: A clean area of this sample. The grainy texture suggests a relatively high level of filler in this coating. EDAX spectrum of this region is shown in figure 58.

Figure 59:

Material #59: ITTRI silicone glass coating on 1-mil Kapton film, from ITT Research Institute; unexposed; Au/Pd-coated for SEM analysis. Title: MTL-59. PreX. Photo #030. Magnification: 1500X. Legend: Pit or Pinhole Defects in the Surface of As-Received Coating Description: A close-up of the coating showing a dimpled surface with an embedded particle and two pits or pinholes. The pits/pinholes and surface dimpling are probably artifacts of the spray

ORIGINAL PAGE IS
OF POOR QUALITY

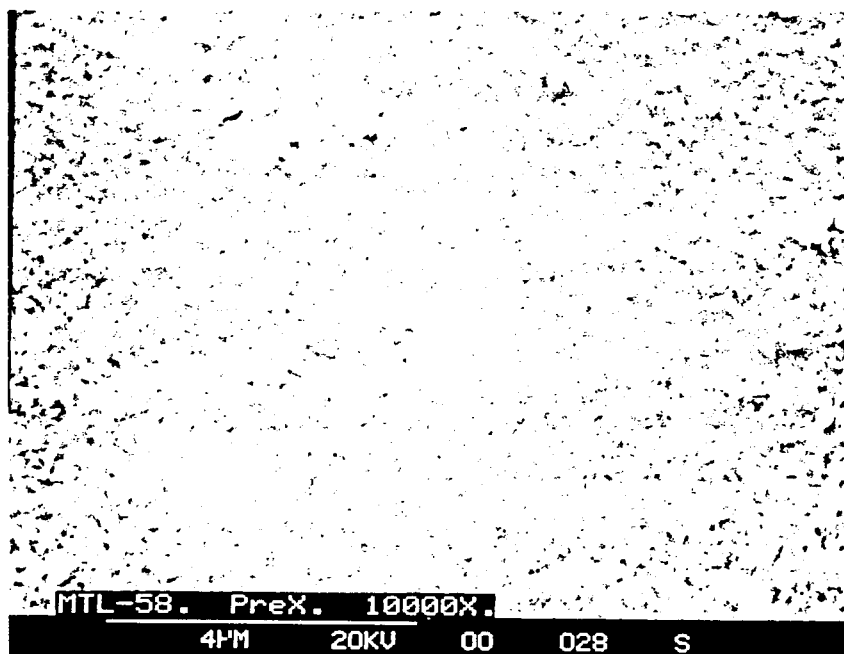


Figure 57: Ethyl X-128 (#58) Coating on 2-Mil Kapton Film

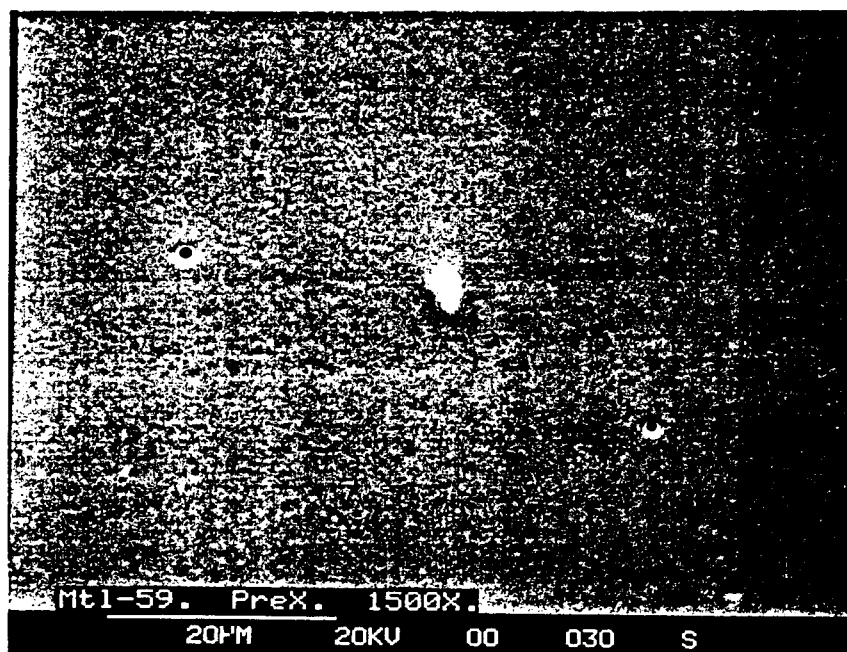


Figure 59: IITRI Silicone Glass Coating on 1-Mil Kapton Film

(THIS PAGE INTENTIONALLY LEFT BLANK)

SPT. KAP20

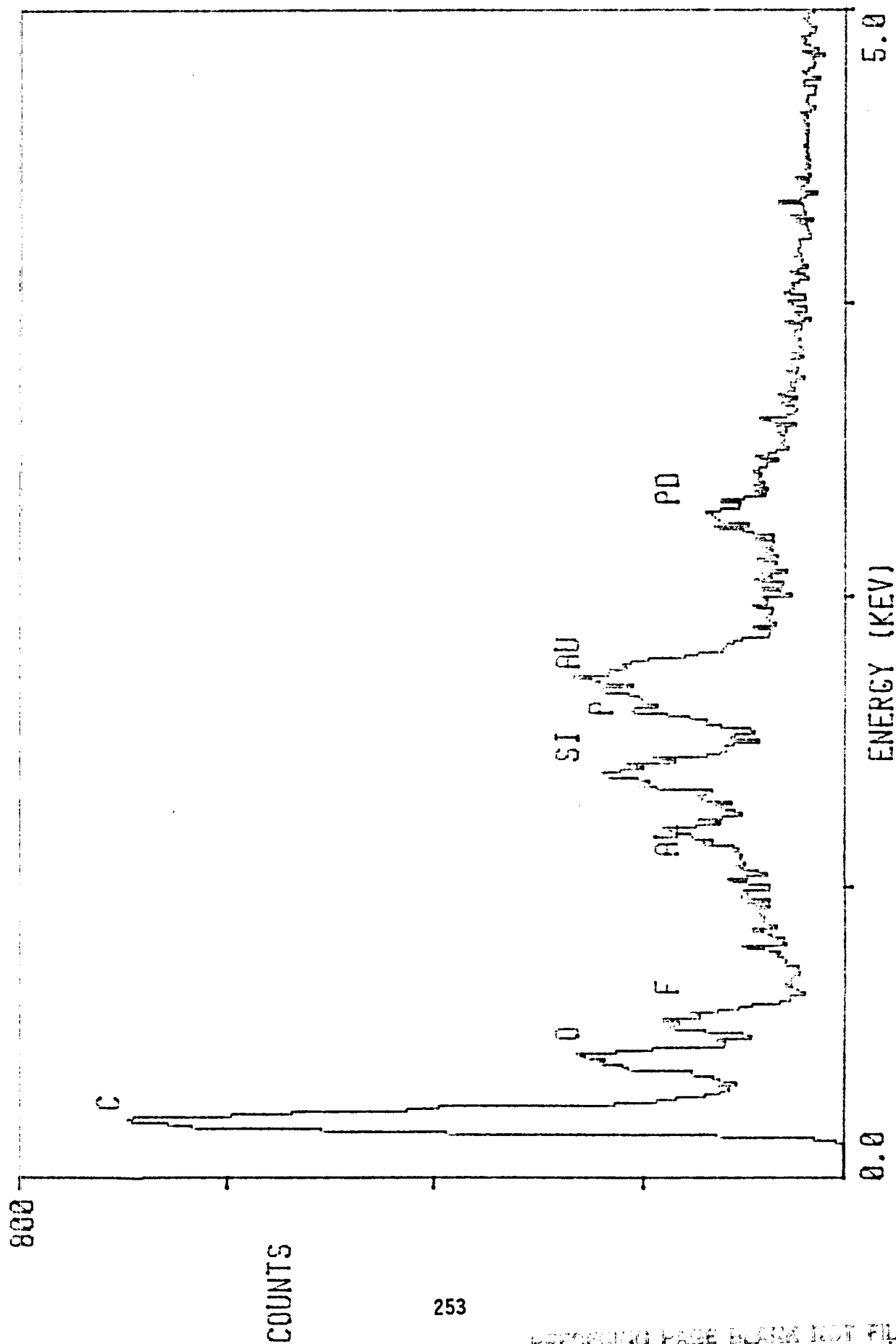


Figure 58: EDAX Spectrum of Unexposed Ethyl X-128 Fluorophosphazene

application of the coating to the substrate. An EDAX spectrum of the dimpled background is shown in figure 60, and the coating's silicone base is reflected by the strong silicon peak. Traces of zinc and carbon were observed. The carbon may have been present in the silicone used, while the zinc may have been a contaminant from the lab where this sample was sprayed up.

Figure 61:

Material #62: ITTRI S13G/L0-1 zinc oxide-filled silicone coating on 40-mil glass fiber/epoxy substrate; unexposed; Au/Pd-coated for SEM analysis. Title: Mtl-62. PreX. Photo #033. Magnification: 1000X. Legend: Typical View of Surface of As-Received S13G/L0-1 Coating on Glass/Epoxy Substrate (Material #62). Description: View of the granular surface of this coating, which is a heavily filled silicone material. The surface appears porous. An EDAX spectrum of the surface is shown in Figure 62, and exhibits strong zinc, and oxygen peaks as expected.

Figure 63:

Material #3: Battelle plasma polymerized silica (HMDS) on 1-mil Kapton film; unexposed; Au/Pd-coated for SEM analysis. Title: Mtl-3. PreX. Photo #036. Magnification: 450X. Legend: Typical View of Surface of As-Received Plasma Polymerized Silica on Kapton Film. Description: A general view of this coating's surface. An EDAX spectrum of a relatively clear, bare area is shown in figure 64, and the spectrum of a group of spherical surface debris particles is shown in figure 65.

Material #3: Battelle plasma polymerized silica (HMDS) on 1-mil Kapton film; exposed to atomic oxygen (run #20.2, position R9) for 2 hours at 300 watts; Au/Pd-coated for SEM analysis.

Figure 66:

Title: Mtl-3-X. Photo #037. Magnification: 9KX. Legend: Surface Features

SPT. KAP2P.

MTL-59, PREX.

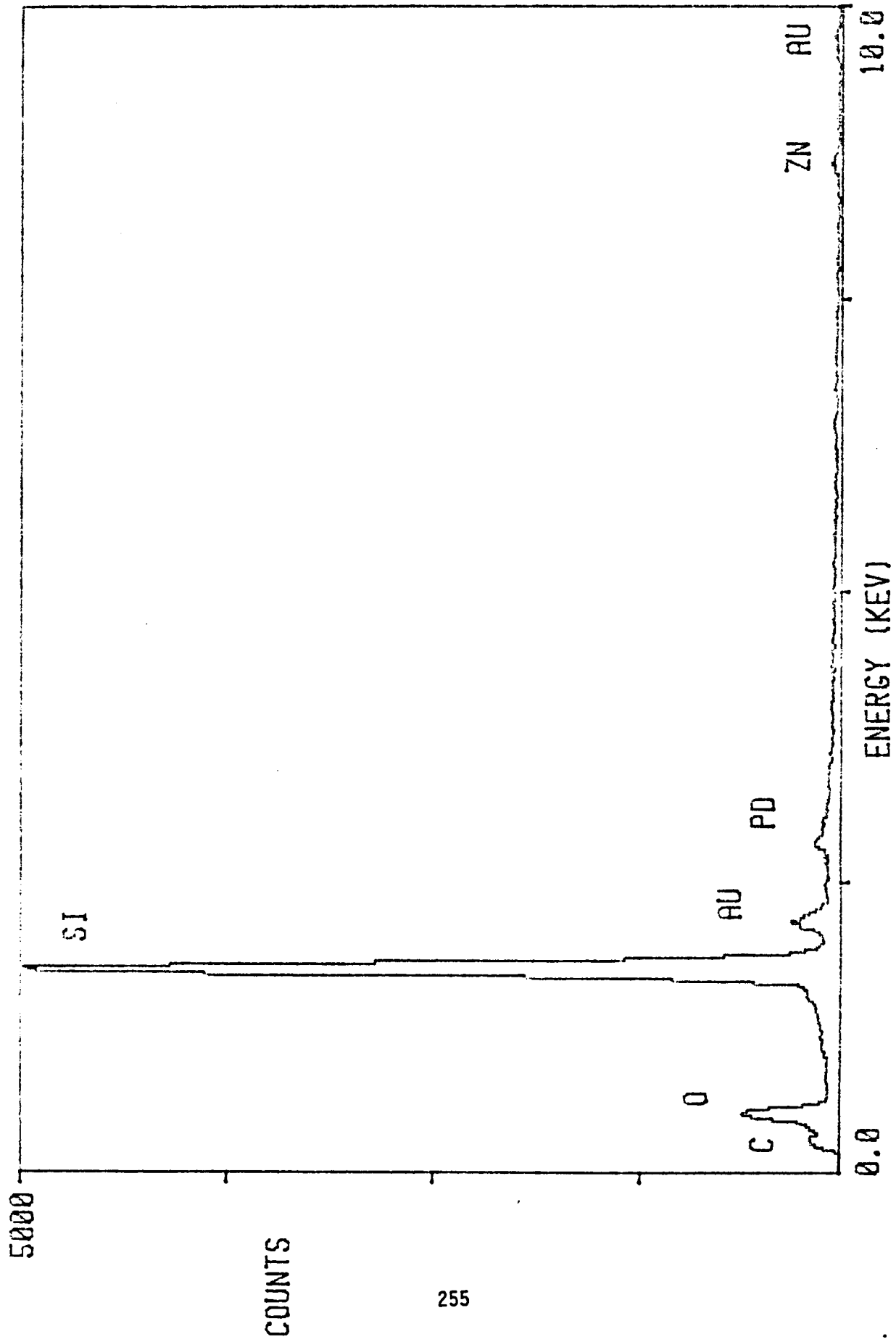


Figure 60: EDAX Spectrum of Unexposed IITRI Silicone Glass coating

(THIS PAGE INTENTIONALLY LEFT BLANK)

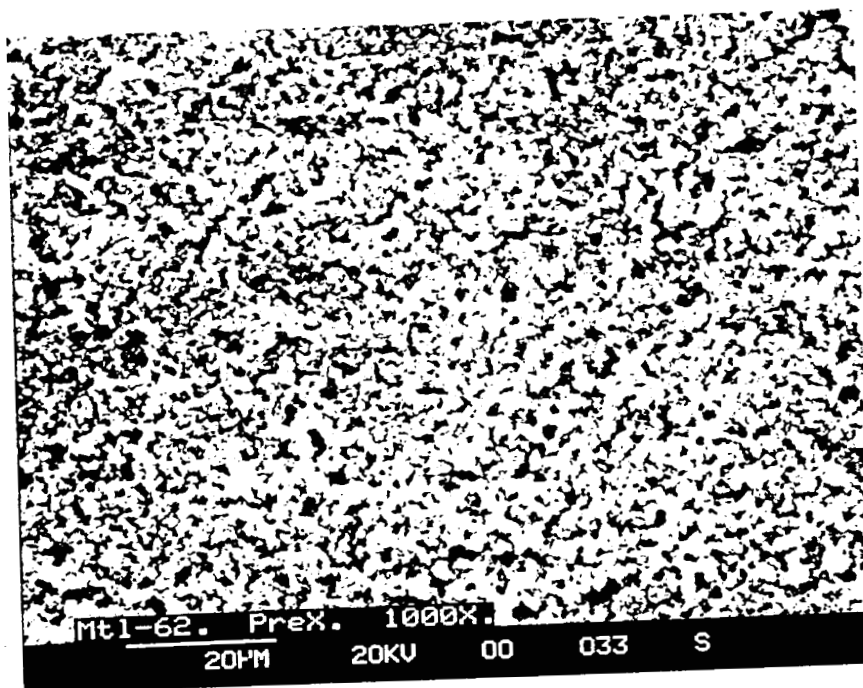


Figure 61: IITRI S13G/L0-1 on Glass Fiber/Epoxy Substrate

ORIGINAL PAGE IS
OF POOR QUALITY

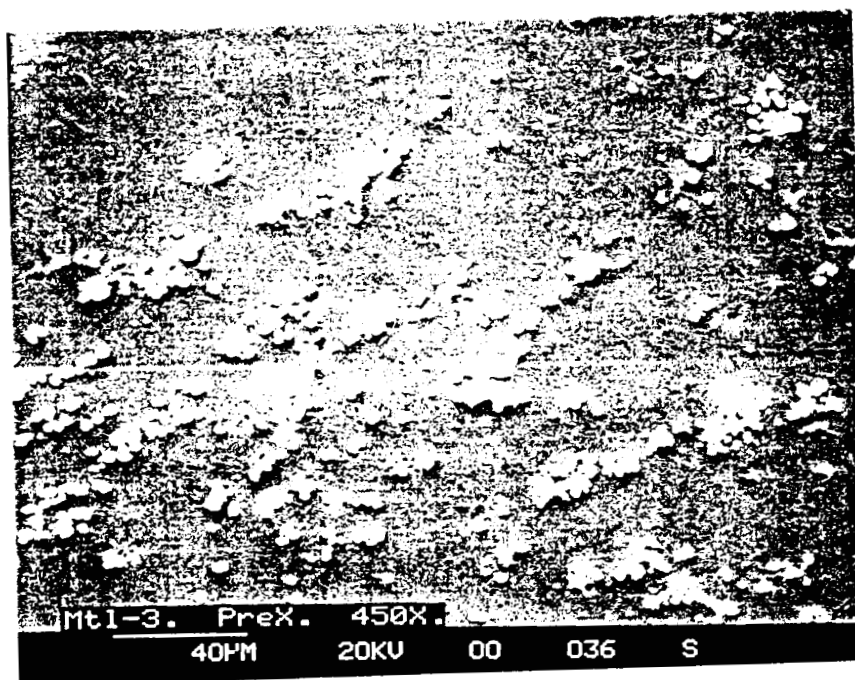


Figure 63: HMDS (#3) on 1-Mil Kapton Film

(THIS PAGE INTENTIONALLY LEFT BLANK)

SPT. KAP20.

MTL-62. FILLER.

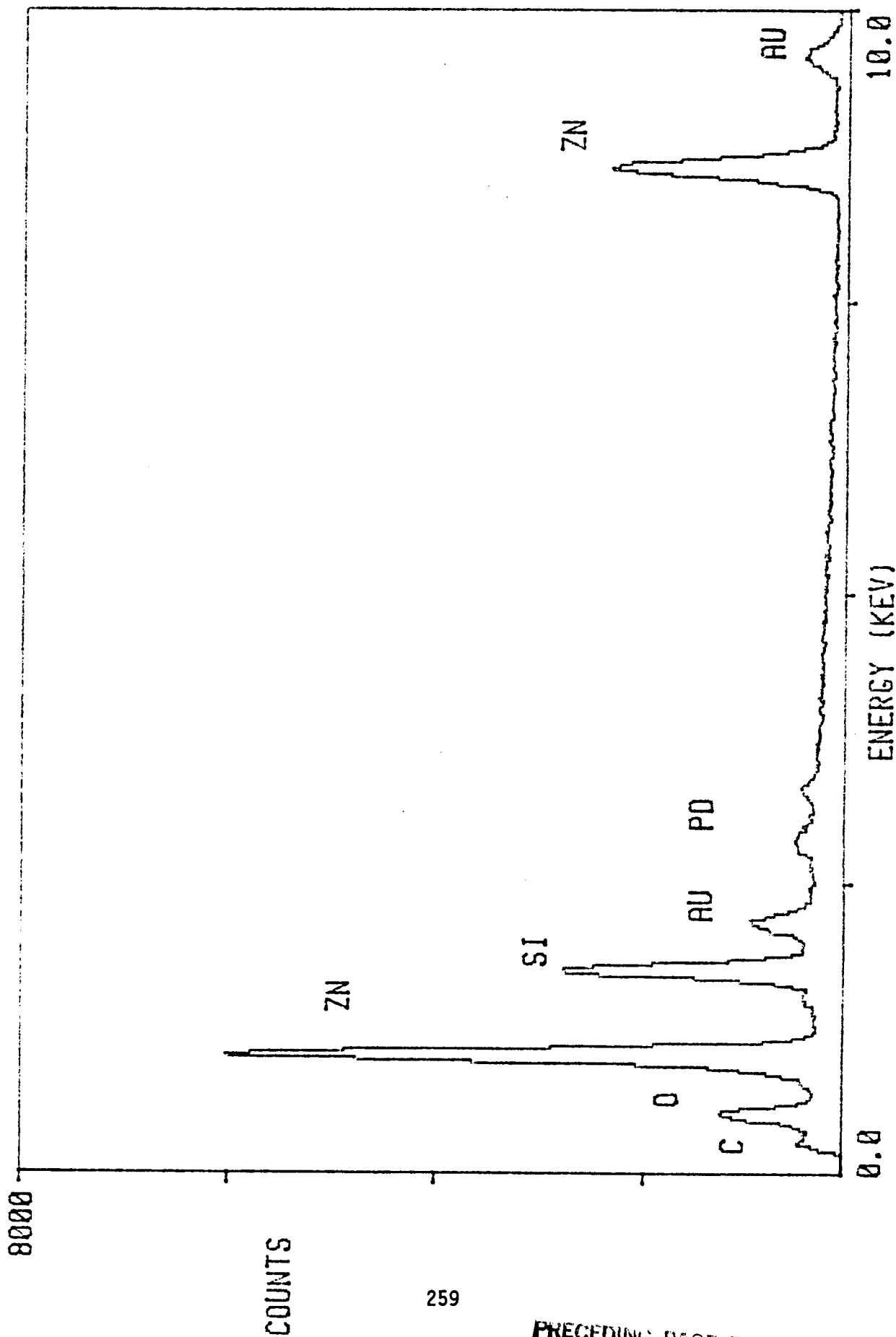


Figure 62: EDAX Spectrum of IITRI S13G/L0-1 on Glass Fiber/Epoxy Substrate

(THIS PAGE INTENTIONALLY LEFT BLANK)

MTL-3, PREX.

SPT. KAP1A.

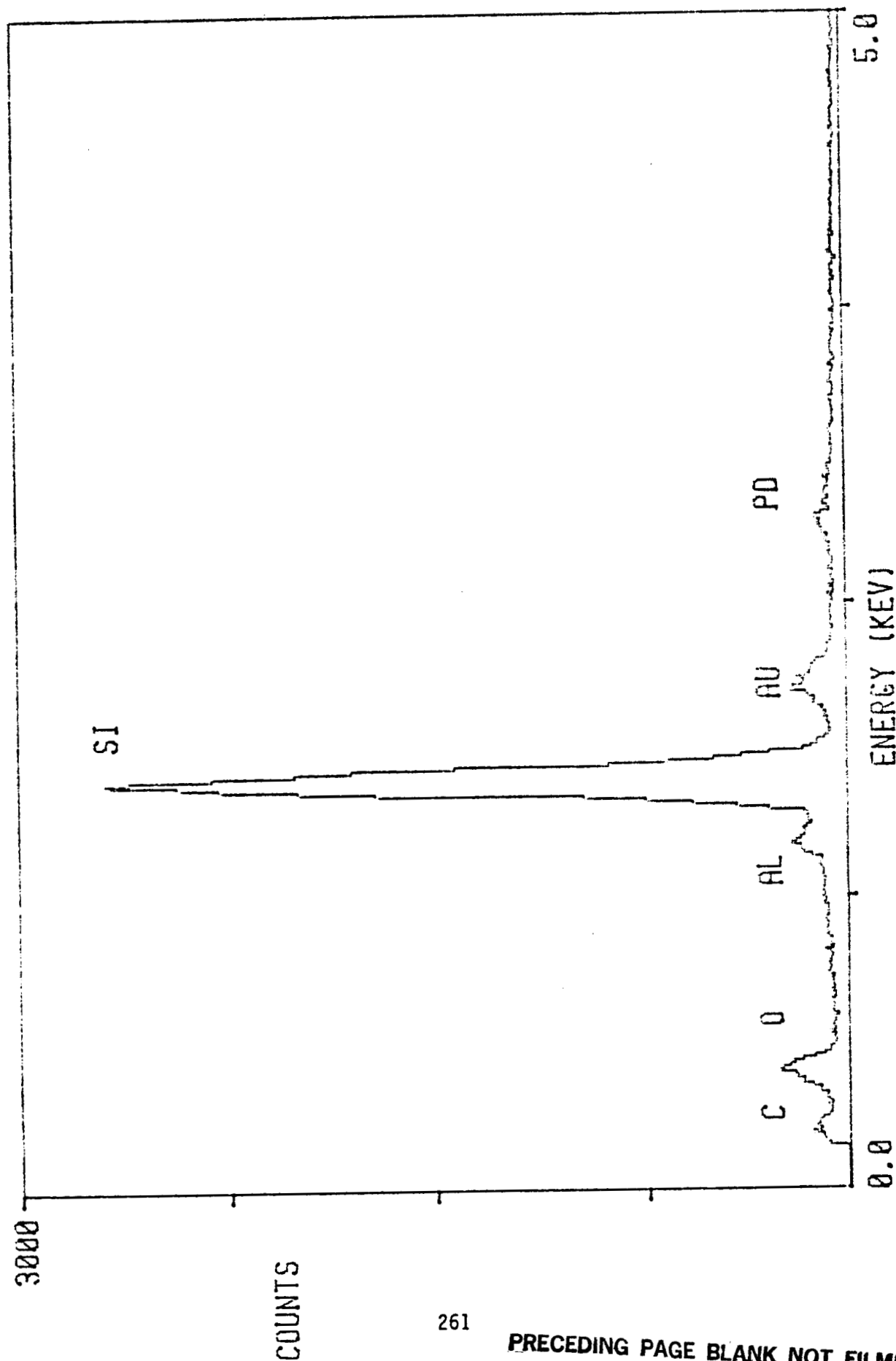


Figure 64: EDAX Spectrum of HMDS Coating on Kapton

(THIS PAGE INTENTIONALLY LEFT BLANK)

SPT. KAP1B.

MTL-3, PREX, DEBRIS.

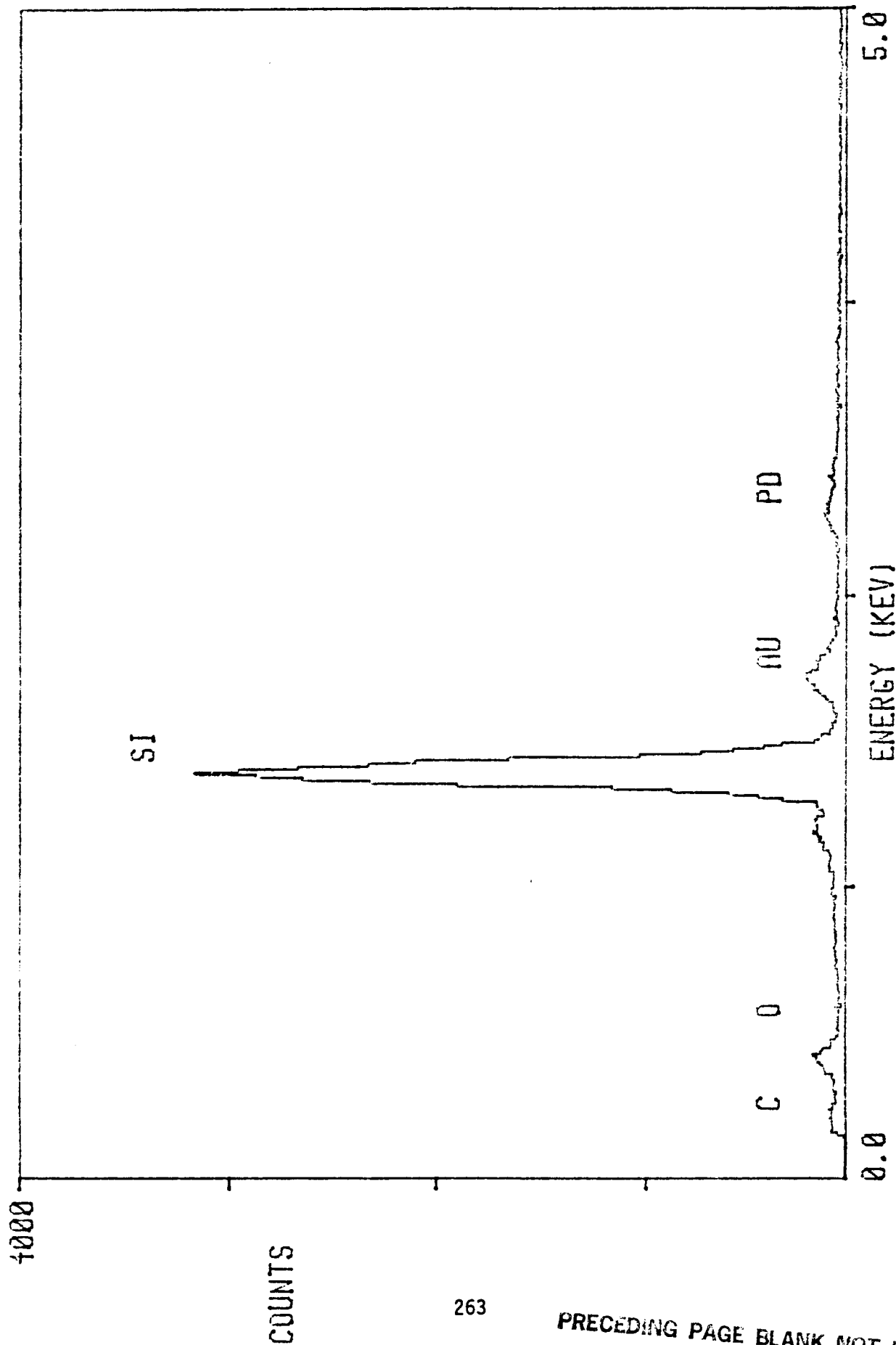


Figure 65: EDAX Spectrum of Debris Particles on HMDS Coating

of Atomic Oxygen Exposed Plasma Polymerized Silica on Kapton Film (Material #3). description: Close-up of atomic oxygen exposed coating surface shows presence of small blister-like features. The blister-like formations may be filler particles in the process of being exposed by surface recession. The diameters of these features are much smaller than the debris particles observable on the coating surface.

Figure 67:

Title: Mtl-3-X. Photo #039. Magnification: 6KX. Legend: Pit Defect in Surface of Atomic Oxygen Exposed Plasma Polymerized Silica Coating (Material #3). Description: A close-up of a pit defect showing an apparent oxygen attack site in the right side of the pit. While it is not conclusive that the hole was caused by oxygen atom attack, no similar pit feature was observed while examining unexposed Material #3 coating samples.

Figure 68:

Title Mtl-52. PreX. Photo #46. Magnification: 10KX. Legend: Surface of Plasma Polymerized HMDS/TFE (Ratio 8/1) Coating on Kapton Film (Material #52). Description: A view of the surface of this coating showing a smooth, uniform surface. The slight amount of surface debris in this photo is actually rare, and the blister-like object was the only such feature observed. An EDAX spectrum of this coating is shown in Figure 69. Traces of zinc and aluminum are seen, besides the expected strong silicon peak. There is no fluorine peak apparent; fluorine should be present due to the TFE monomer used to produce the coating. The strong carbon peak may be due to either monomer.

SET 4 (11/10/86)

Material #59: ITTRI glassy silicone coating on 2-mil Kapton film; exposed to atomic oxygen (run #46, position 24) for 2 hours at 350 watts; Au/Pd-coated

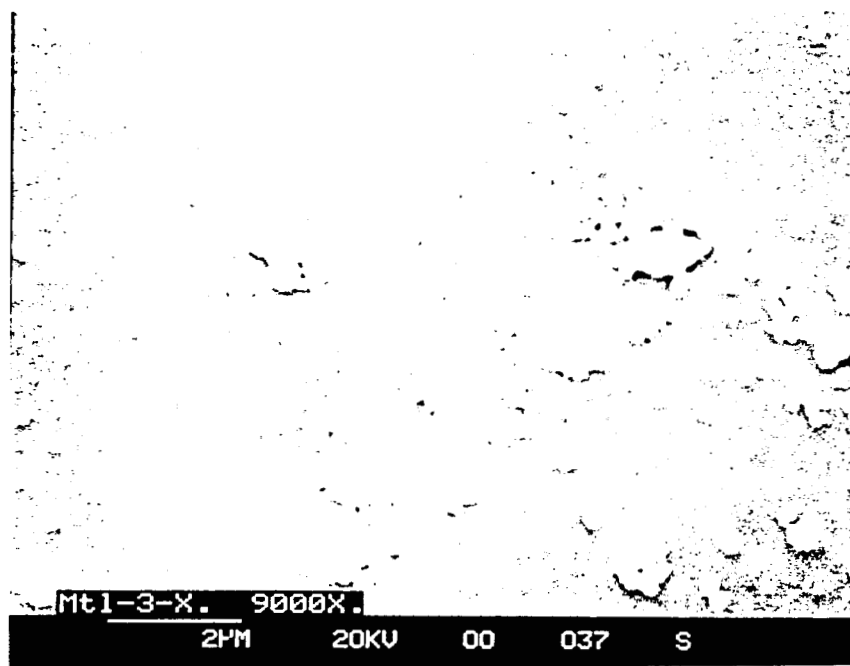


Figure 66: HMDS Coating on Kapton. Sample Exposed to Atomic Oxygen for 2 Hours.

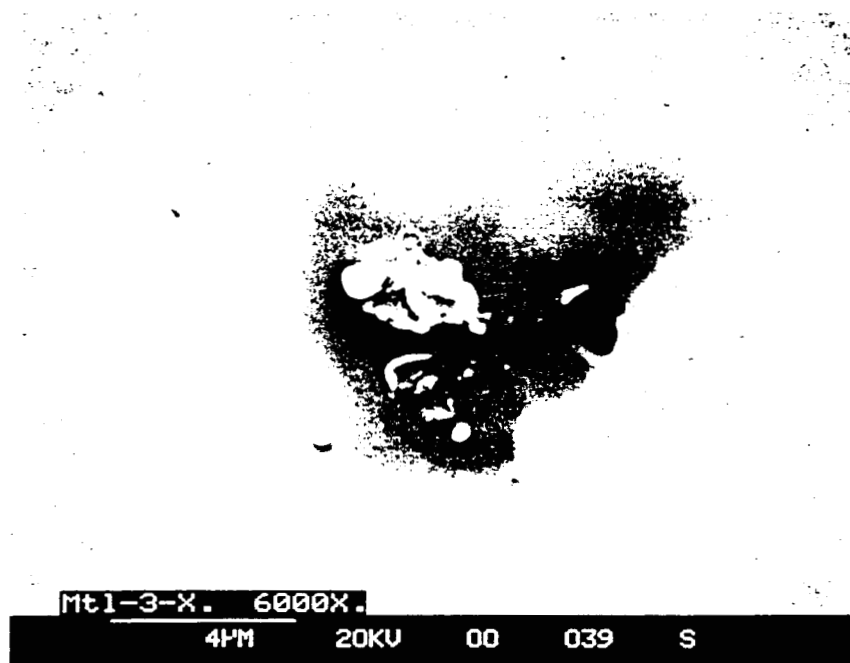


Figure 67: Surface Feature of HMDS on Kapton. Sample Previously Exposed to Atomic Oxygen.

(THIS PAGE INTENTIONALLY LEFT BLANK)

ORIGINAL PAGE IS
OF POOR QUALITY

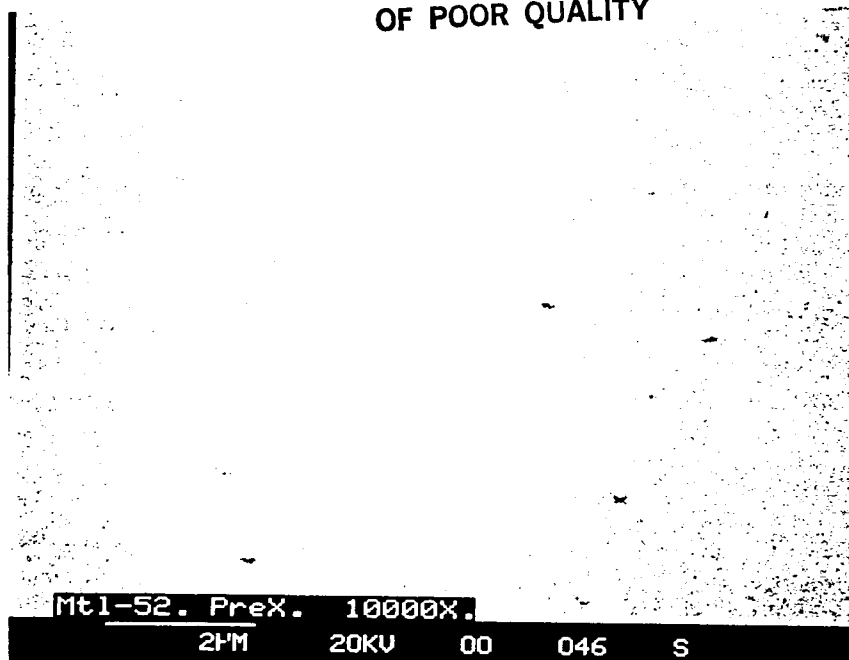


Figure 68: Plasma Polymerized HMDS/TFE (#52) Coating on Kapton.

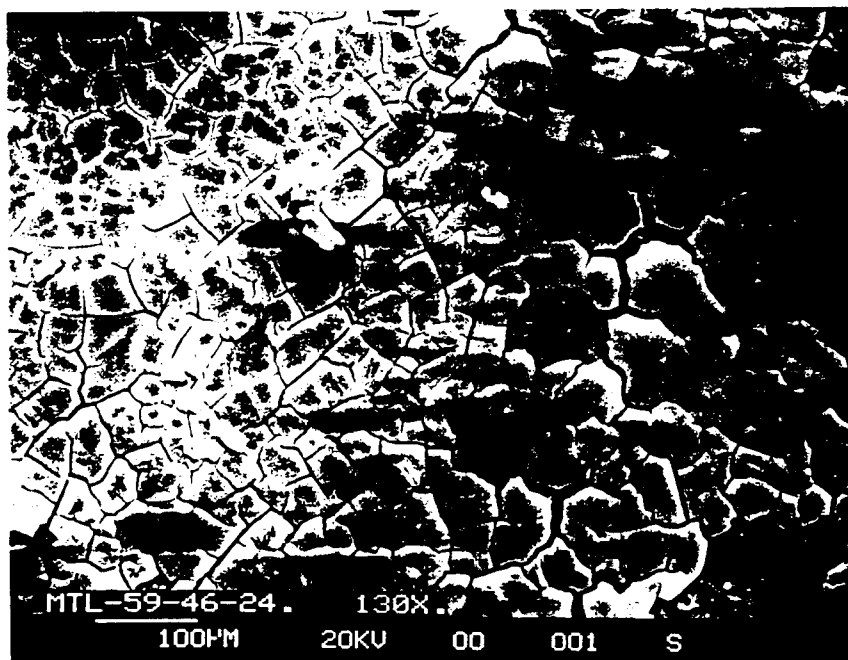


Figure 70: ITTRI Glassy Silicone Coating (#59) on Kapton. Sample Exposed to Atomic Oxygen for 2 Hours.

(THIS PAGE INTENTIONALLY LEFT BLANK)

SPT. KAP3C.

MTL-52. BACKGROUND.

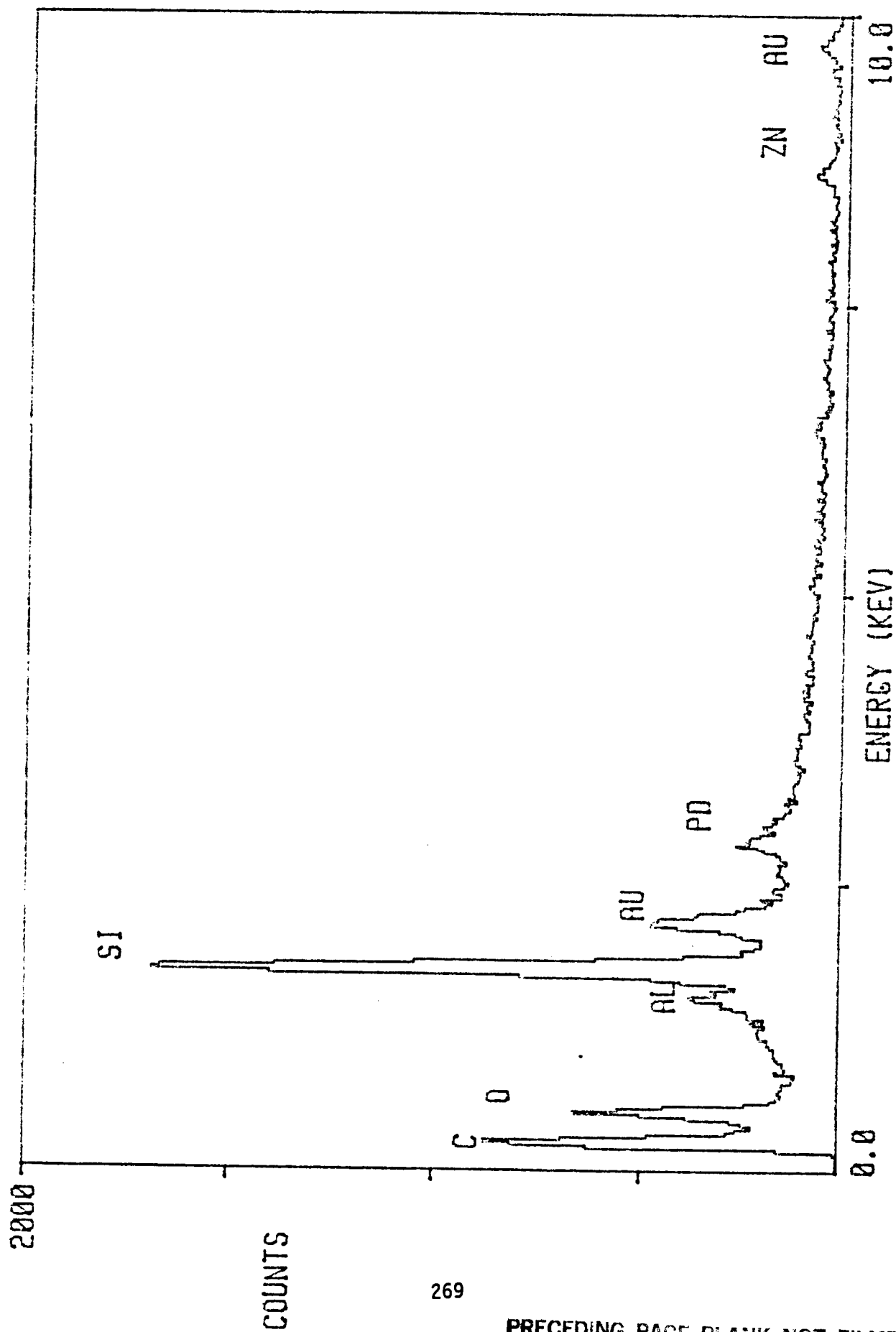


Figure 69: EDAX Spectrum of Plasma Polymerized HMDS/TFE Coating on Kapton

for SEM analysis.

Figure 70:

Title MTL-59-46-24. Photo #001. Magnification: 130X. Legend: Surface of Atomic Oxygen exposed ITTRI Glassy Silicone Coating (Material #59). Description: A typical view of the surface, showing severe cracking and/or splitting of the coating, and exposed areas of Kapton substrate exhibiting erosion patterns.

Figure 71:

Title: MTL-59-46-24. Photo #002. Magnification: 500X. Legend: Area of Kapton Substrate Exposed to Oxygen Atom Attack by Loss of Coating (Material #59). Description: An area where the coating has been removed either by oxygen degradation or by handling after exposure. Note the erosion patterns in the Kapton material indicating the locations of splits or cracks in the original surface coating prior to coating removal. Note formation of pits in the exposed substrate.

Figure 72:

Title: MTL-59-46-24. Photo #007. Magnification: 700X. Legend: Localized Charging on Exposed Coating Surface Showing Initial Crack Formations (Material #59). Description: Although sputter-coated with gold/palladium for analysis, localized charging from the SEM electron beam was observed. This charging, seen here as contrast changes, revealed the presence of very fine cracks or fractures in the larger segments of coating material. The EDAX spectrum of an exposed coating specimen is shown in figure 73, and can be compared to the spectrum of the unexposed coating shown in figure 60. The exposed coating contains a significantly higher level of oxygen, with no other changes in composition apparent. This indicates a silicone-to-silica oxidation process has occurred.

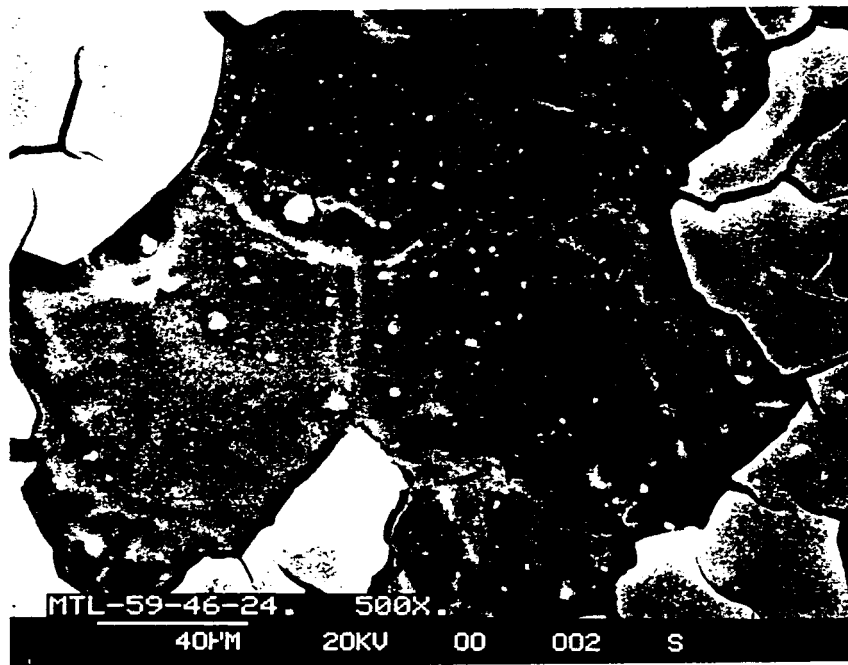


Figure 71: Area of Coating (#59) Loss and Kapton Exposure to Atomic Oxygen Attack

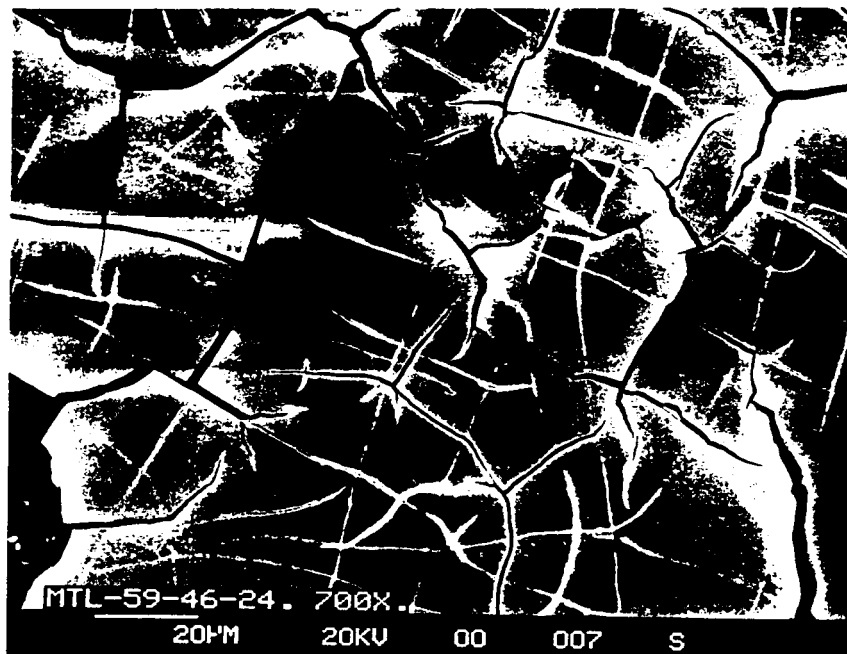


Figure 72: Localized Charging Along Cracks in Coating Material (#59) Subsequent to Atomic Oxygen Exposure

(THIS PAGE INTENTIONALLY LEFT BLANK)

SPT. KAP4B.

MTL-62-46-5. RIM, BG.

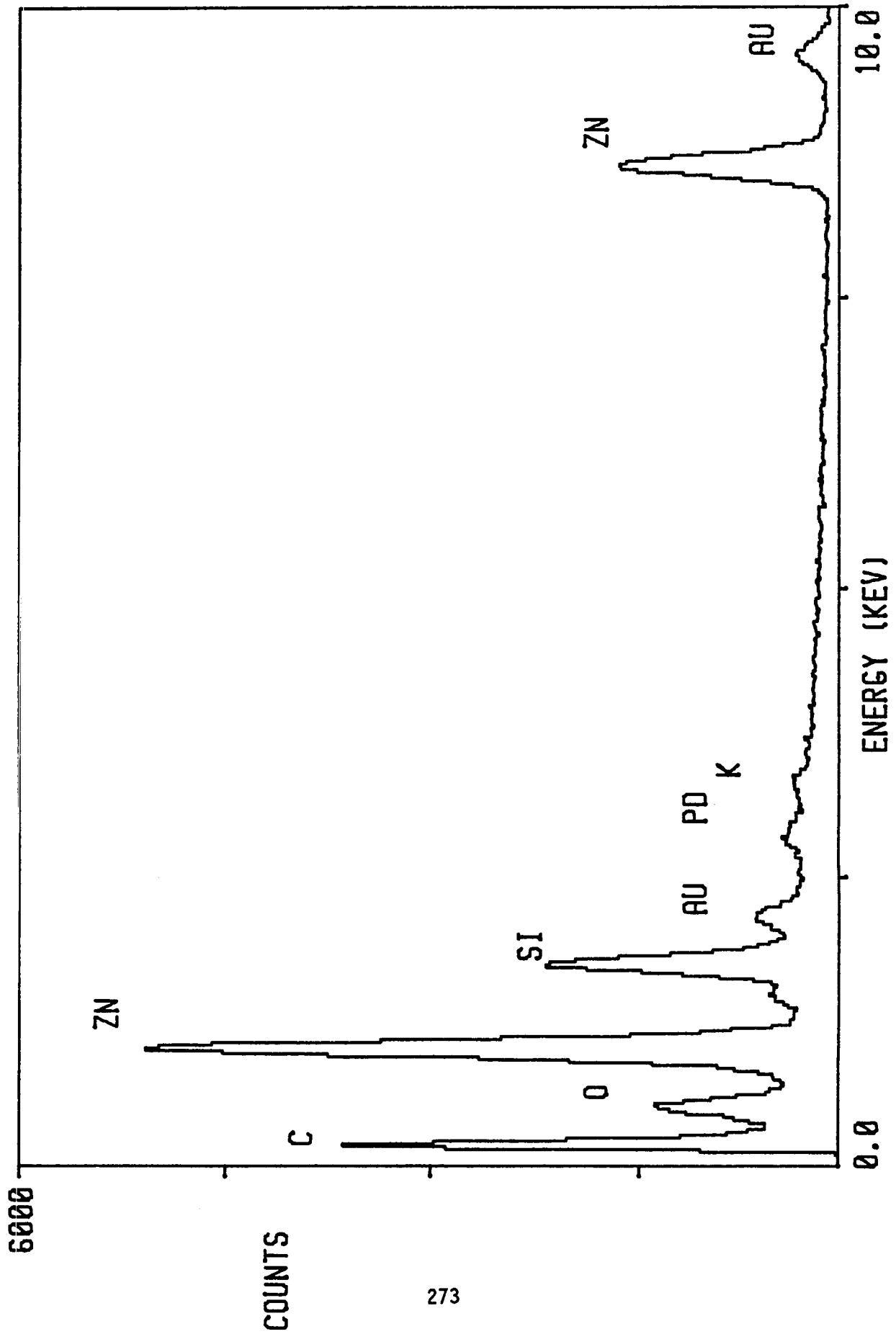


Figure 73: EDAX Spectrum of IITRI Glass Resin on Kapton Subsequent to Atomic Oxygen Exposure

SET 5 (11/14/86)

Material #54: Battelle plasma polymerized HMDS/TFE (ratio 8/1) on 1-mil Kapton film; unexposed; Au/Pd-coated for SEM analysis.

Figure 74:

Title: Mtl-54. PreX. Photo #001. Magnification: 1000X. Legend: Surface Features of As-Received Plasma Polymerized HMDS/TFE (Ratio 8/1) Coating on Kapton Film (Material #54). Description: This coating was generally very uniform and defect-free. Depressions were rarely observed, and the amount of surface debris was significantly lower than had been observed on previously examined plasma polymerized HMDS/TFE coatings.

Figure 75:

Title: Mtl-54-45-24. Photo #005. Magnification: 350X. Legend: Surface of Clouded Region on Plasma polymerized HMDS/TFE (Ratio 8/1) Coating (Material #54). Description: Streaks of clouded areas could be observed on this sample at low magnification. Examination of one of these streaks reveals the cloudiness to be high levels of particulate debris on and in the coating surface. EDAX analysis of the debris and the bare (clean) coating surface (figures 76 and 77, respectively) showed the elemental compositions to be similar, with the debris having a slightly higher level of carbon. No traces of fluorine are observed. Fluorine should be present due to the TFE (tetrafluoroethylene) component of the coating. Fourier Transform Infrared (FTIR) spectrometry (figure 78) of the coating also failed to unambiguously detect fluorine-containing species in the coating's molecular structure. The coating's IR spectrum is similar to that of a typical commercial dimethyl silicone formulation, and lacks the peaks present in the spectrum of a typical TFE formulation. While the TFE content of this coating is low, according to the supplier's data, the FTIR and EDAX should have easily detected the fluorocarbon

ORIGINAL PAGE IS
OF POOR QUALITY

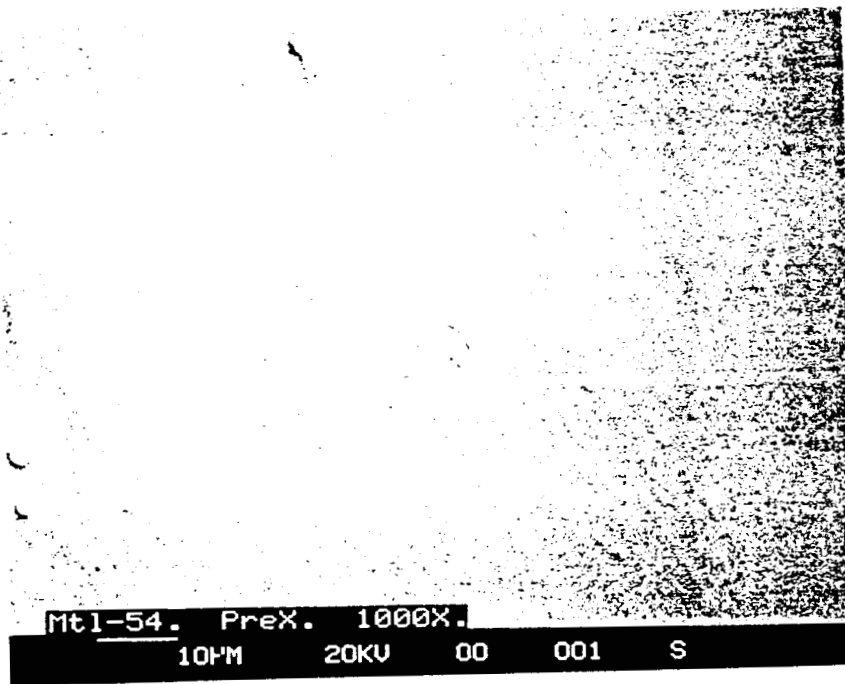


Figure 74: HMDS/TFE (#54) Coating on Kapton

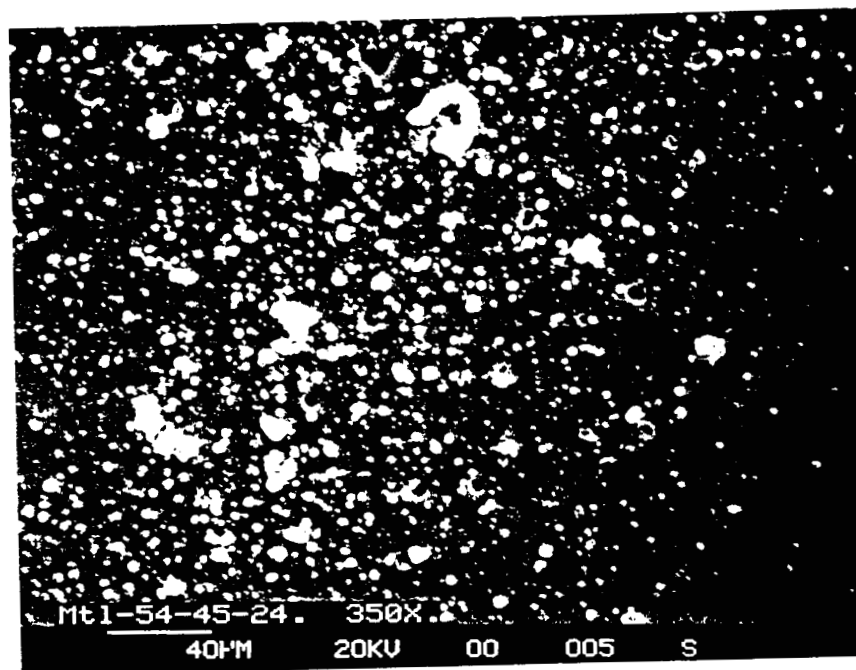


Figure 75: Clouded Region of HMDS/TFE Coating (#54) on Kapton

c-3

(THIS PAGE INTENTIONALLY LEFT BLANK)

KAP5A

MTL-54-45-24. DEBRIS.

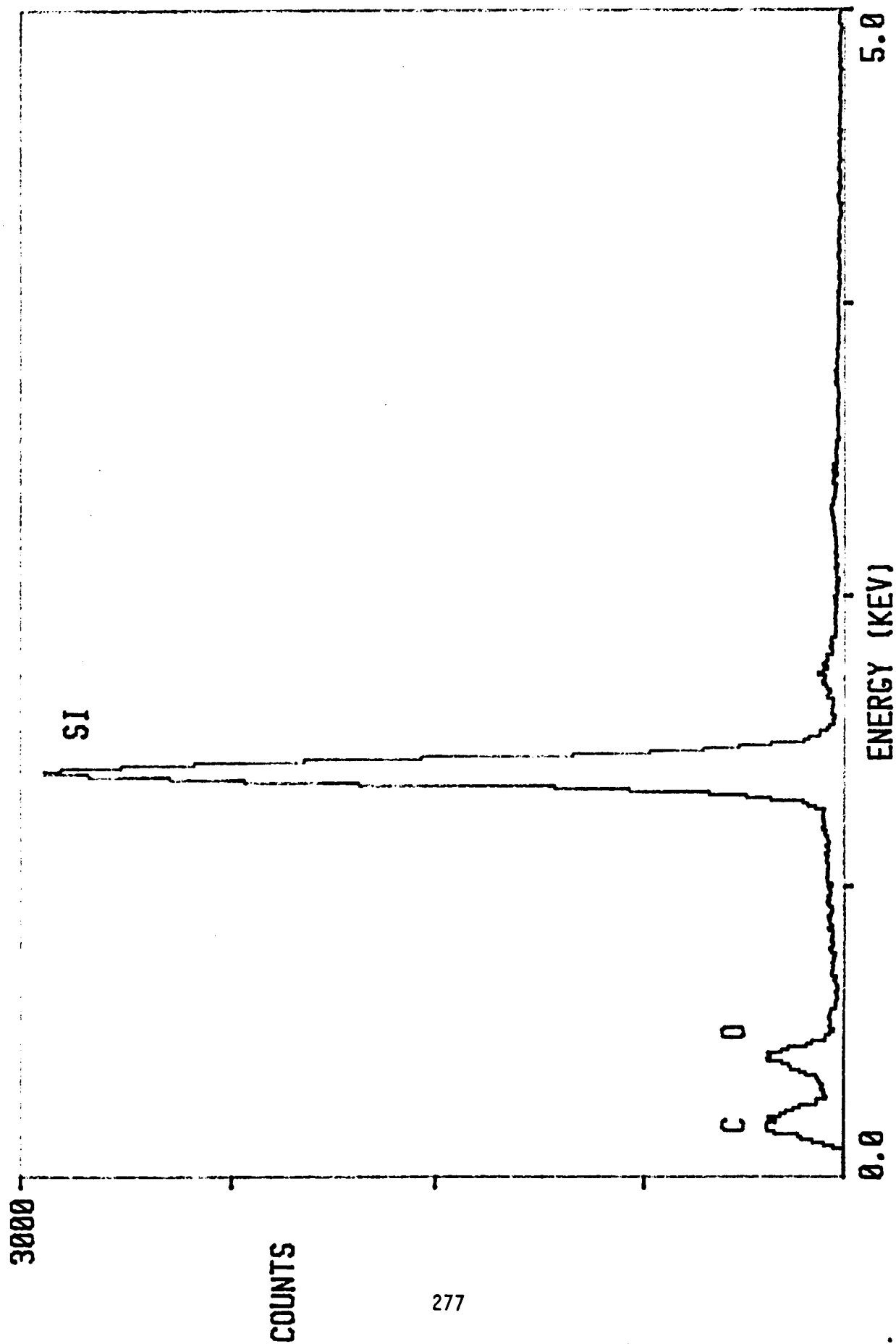


Figure 76: EDAX Spectrum of Debris on Surface of HMDS/TFE Coating

(THIS PAGE INTENTIONALLY LEFT BLANK)

KAP58

MTL-54-45-24 X BACKGROUND.

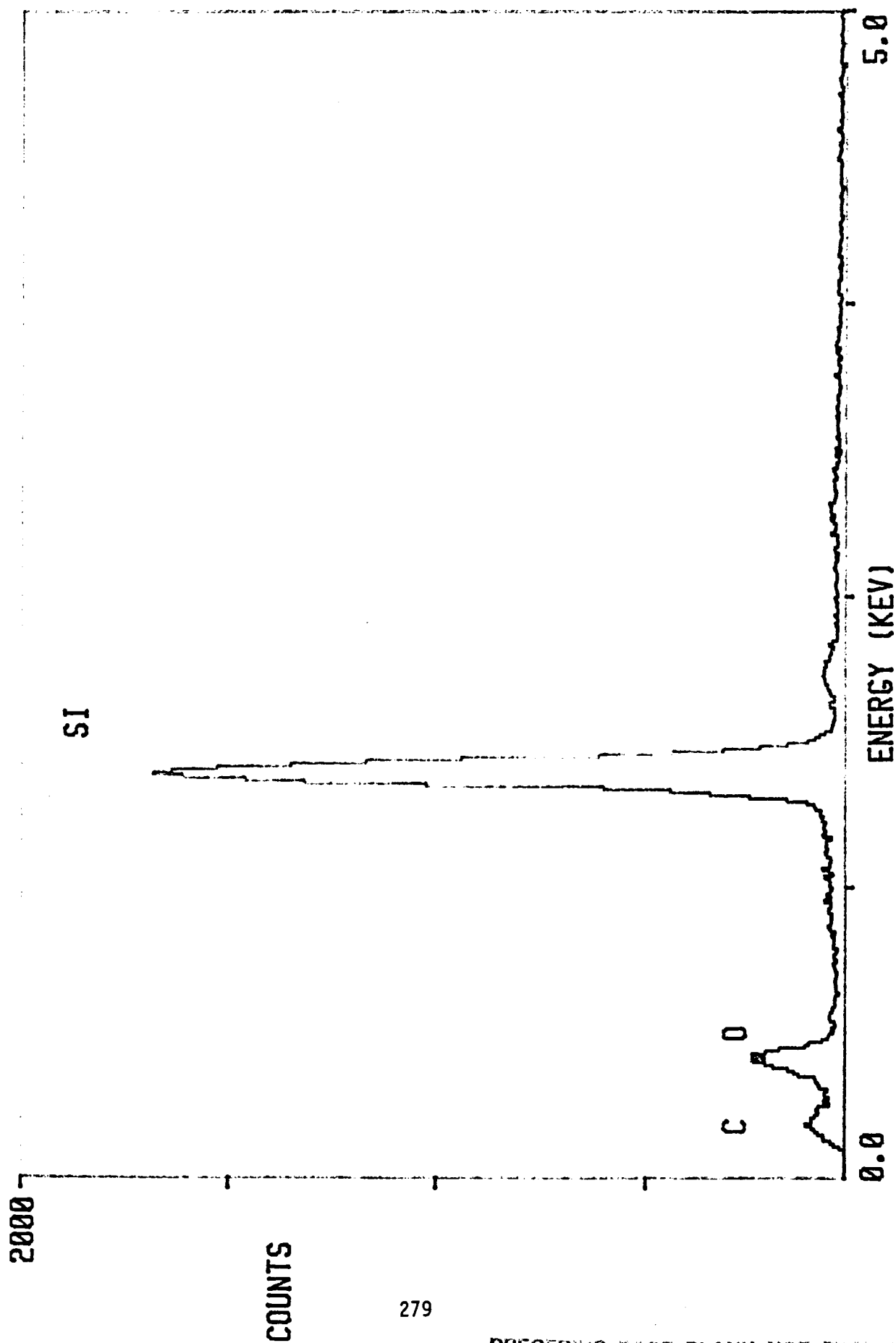


Figure 77: EDAX Spectrum of Plasma Polymerized HMDS/TFE Coating

(THIS PAGE INTENTIONALLY LEFT BLANK)

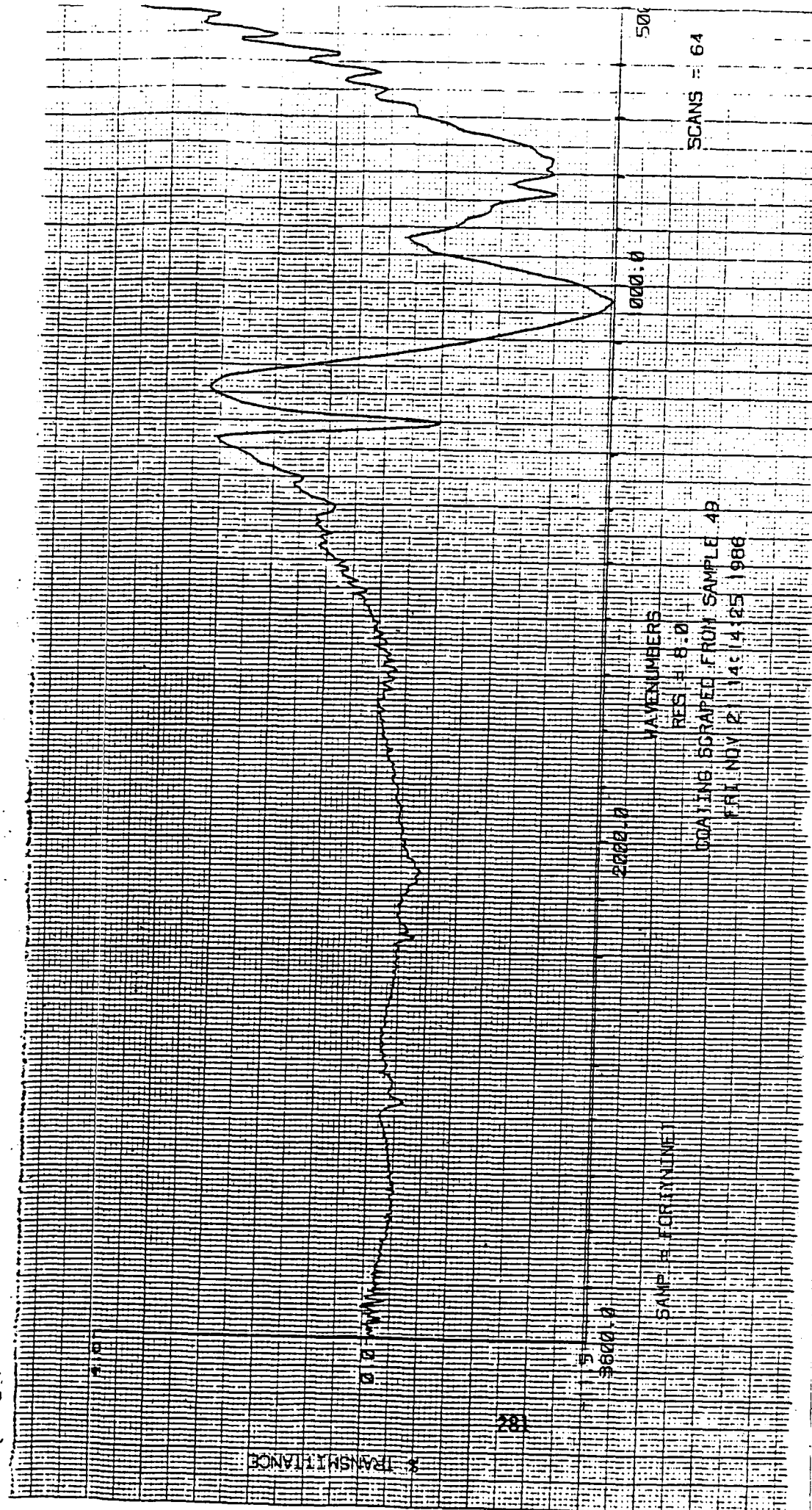


Figure 78: IR Spectrum of Battelle Plasma-Polymerized HMDS/TFE (Ratio 4/1)
Coating Material (Unexposed) Scraped Off Kapton Film Substrate

ORIGINAL PAGE IS
OF POOR QUALITY

PRECEDING PAGE BLANK NOT FILMED

component. From the EDAX and FTIR data therefore, it appears that no TFE is present in any form in this coating material. From previous EDAX analysis of similar plasma polymerized coatings from the same supplier, similar failures to detect the presence of fluorine in the coatings indicates that none of these plasma prepared materials contain significant levels of fluorocarbon components.

Figure 79:

Material #55: Battelle plasma polymerized HMDS/TFE (ratio 20/1) on 1-mil Kapton film; exposed to atomic oxygen (run #43, position 5) for 2 hours at 350 watts; Au/Pd-coated for SEM analysis.

Title: Mtl-55-43-5. Photo #011. Magnification: 1300X. Legend: Same as for 10. Description: An area with pinhole damage. Note the more extensive damage in the lower center pit.

SET 6 (11/18/86)

Material #1: DuPont Kapton H polyimide film: exposed to atomic oxygen (run #40, position 13) for 4 hours at 350 watts; Au/Pd-coated for SEM analysis.

Figure 80:

Title: Mtl-1. HX. Photo #000. Magnification: 25X. Legend: Rim Region of Heavily Atomic Oxygen Degraded Kapton H Film (Material #1). Description: Various degradation features at the rim region of a sample of heavily atomic oxygen - damaged Kapton film. The streaked region of pitting in the exposed area are oriented in the same direction as streaks in the rim-protected outer area (upper right). A random distribution of larger pits are visible in the exposed region. More extensive damage is seen at the former rim position, suggesting the aluminum rim lip of the sample holder acts to increase the degradation rate at this lip boundary. This may be due to mechanical stress or

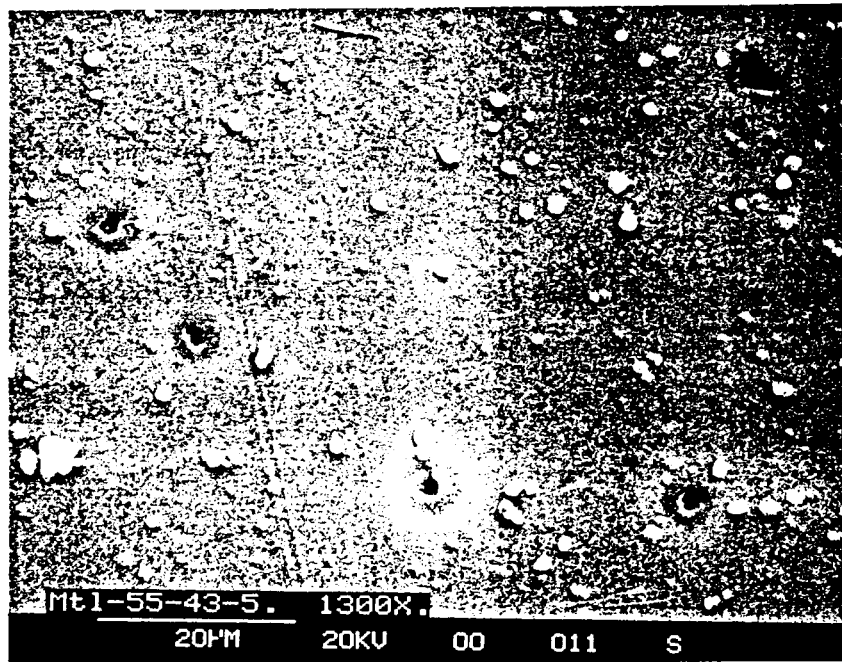


Figure 79: Plasma Polymerized HMDS/TFE Coating (#55) on 1-Mil Kapton. Sample Exposed to Atomic Oxygen Plasma for 2 Hours

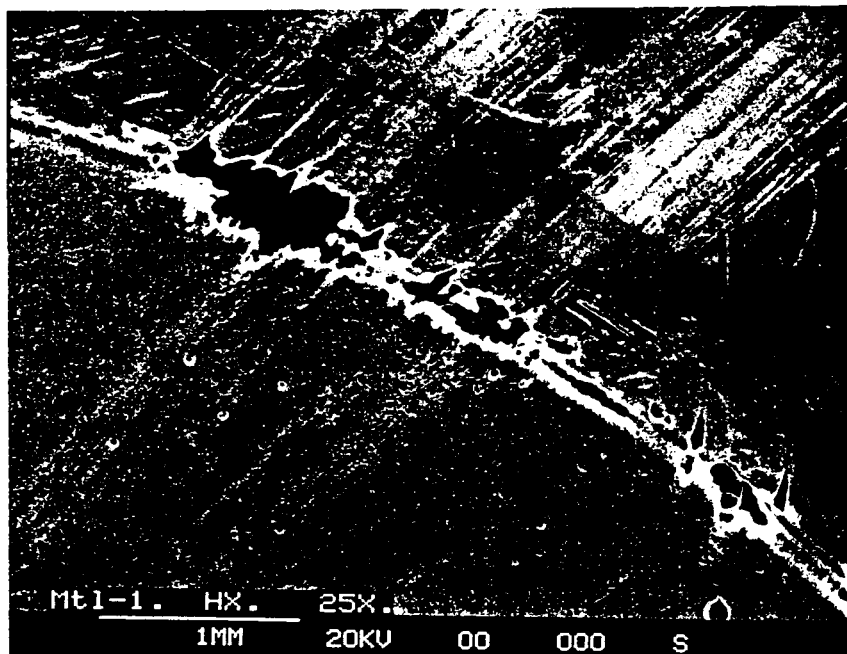


Figure 80: Kapton Film Heavily Degraded by Atomic Oxygen Exposure

damage to the sample by the metal lip.

Figure 81:

Title: Mtl-1. HX. Photo #010. Magnification: 200X. Legend: Surface Features of Heavily Atomic Oxygen Damaged Kapton Film (Material #1). Description: A typical view at the center region of this sample.

SET 7 (12/9/86)

The "bend radius" testing of candidate coating materials on Kapton polyimide film substrate was accomplished by taping strips of the coated film over a rounded metal edge of a known diameter (thickness). The diameters used were 15 and 40 mils. The strips, fastened to the metal sample mount, were then sputter coated with gold/palladium for examination under the scanning electron microscope (SEM). The specimens were examined for evidence of cracking of the coating in the bend region. The specimens were viewed edge-on to the bend region at a 0 to 20 degree angle to the SEM electron beam. The specimens (5-8mm wide by 20-40mm long) were cut from as-received sheet stock, one end of a strip attached to one side of the sample mount by double-backed adhesive tape, and the specimen bent over the rounded edge of the mount and fastened on the other side of the mount with tape. A minimum of tensile force was applied to the specimen as it was bent over the rounded edge. Two to three separate specimens could be placed on each sample mount. The mounted specimens were then coated with gold/palladium, and fastened to an SEM sample stub for mounting in the SEM sample chamber.

Material #59: ITTRI glassy silicone on 1 mil Kapton; Au/Pd-coated for SEM analysis.

Figure 82:

Title: Mtl-59. R = 15. Photo #010. Magnification: 200X. Legend: Detail of

ORIGINAL PAGE IS
OF POOR QUALITY

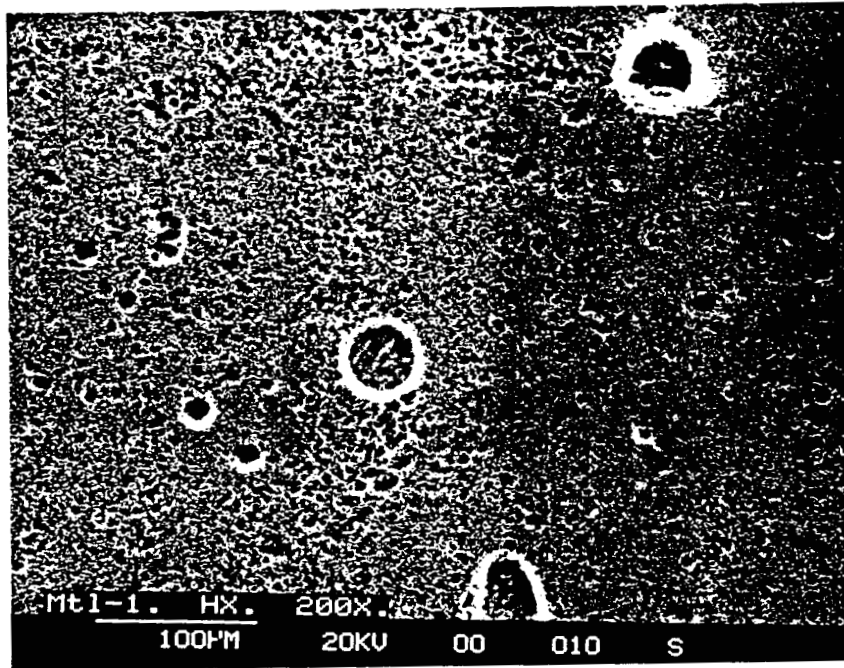


Figure 81: Kapton Film After Atomic Oxygen Exposure for 4 Hours

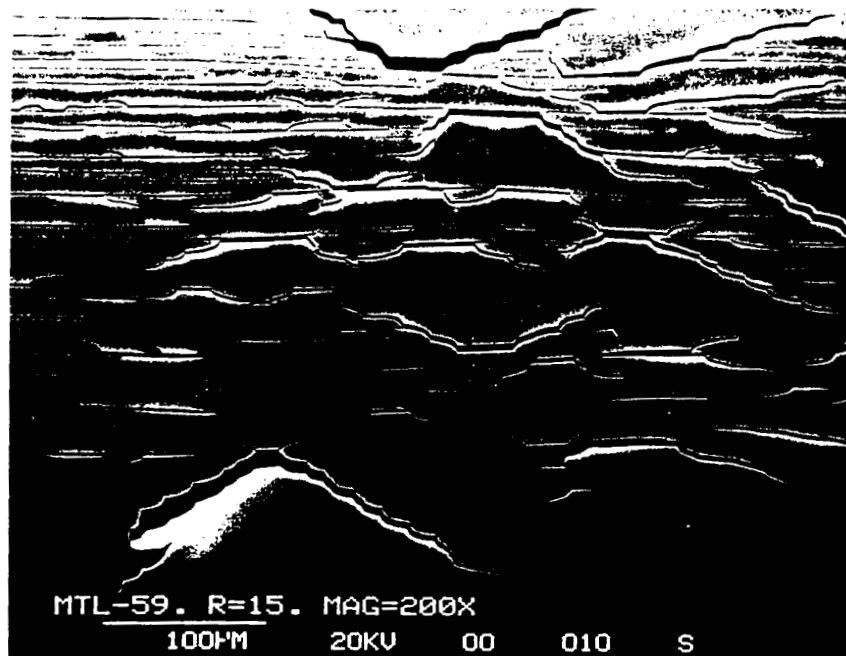


Figure 82: IITRI Glassy Silicone Bent Over a 15-Mil Radius

(THIS PAGE INTENTIONALLY LEFT BLANK)

Cracking in ITTRI Glassy Silicone Coating, Over a 15 mil bend diameter (Material #59). Description: Close-up of cracking in the center of the bend region. There is extensive lateral cracking, with some diagonal cracking and coating delamination.

Material #LERC-52286: NASA-LeRC 8% PTFE-SiO on 1 mil Kapton film; unexposed; Au/Pd-coated for SEM analysis.

Figure 83:

Title: LERC-52286. R = 40. Photo #004. Magnification: 200X. Legend: Bend Region of NASWA-LeRC 8% PTFE-SiO Coating, Over a 40 mil Bend Diameter (Material #LERC-52286). Description: A view of the bend region of this sample. The parallel grooves are probably due to the coating application process. Close examination at higher magnifications show these to be shallow grooves and not cracks or splits. No cracking was observed for this coating material over this bend diameter.

Figure 84:

Title: Mtl-59. This photo is incorrrectly labeled. It is actually material #LERC-52286, NOT material #59). R = 15. Photo #006. Magnification: 300X. Legend: Bend Region of NASA-LeRC 8% PTFE-SiO Coating. Over a 15 mil Bend Diameter. Description: A typical view of the bend region surface of this coating. No cracking was observed over the entire region, even at higher magnifications.

Material #56: Battelle plasma polymerized HMDS coating on 1 mil Kapton film; unexposed; Au/Pd-coated for SEM analysis.

Figure 85:

Title: Mtl-56. R = 40. Photo #013. Magnification: 20X. Legend: Bend

(THIS PAGE INTENTIONALLY LEFT BLANK)

ORIGINAL PAGE IS
OF POOR QUALITY

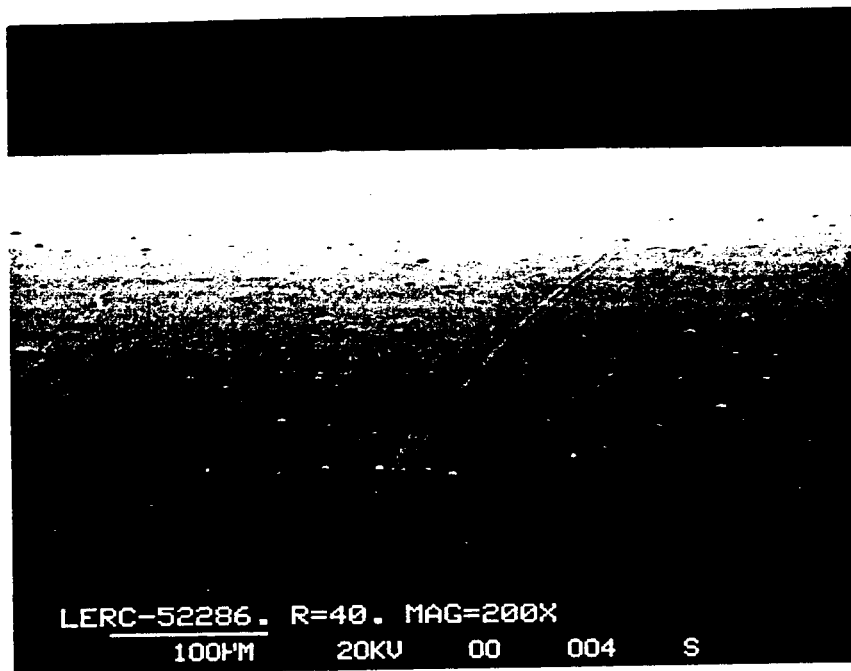


Figure 83: NASA LeRC 8% PTFE-SiO₂ Coating on 1-Mil Kapton Bent Over a 40-Mil Radius

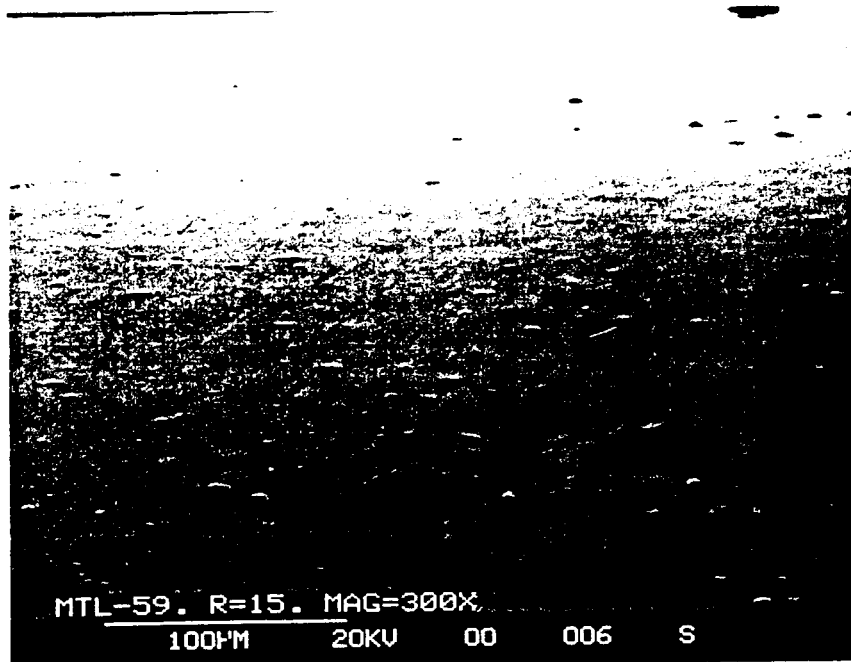


Figure 84: NASA LeRC 8% PTFE-SiO₂ Coating on 1-Mil Kapton Bent Over a 15-Mil Radius

Region of Battelle Plasma Polymerized HMDS Coating, Over a 40 mil Bend Diameter (Material #56). Description: A view of entire bend region of this sample. No cracking was observed, even at higher magnifications.

Figure 86:

Title Mtl-56. R = 15. Photo #018. Magnification: 15X. Legend: Bend Region of Battelle Plasma Polymerized HMDS Coating, Over a 15 mil Bend Diameter (Material #56). Description: A view of the entire bend region of this specimen, showing a smooth bend with no cracking. Cracking could not be detected even at higher magnification levels.

Material #65: McGhan-NuSil CV1-1144-0 silicone coating on 1 mil Kapton film, prepared by Sheldahl; unexposed; Au/Pd-coated for SEM analysis.

Figure 87:

Title Mtl-65. R = 40. Photo #012. Magnification: 20X. Legend: Bend Region with Cracks Visible in McGhan-NuSIL CV1-1144-0 Silicone Coating, Over a 40 mil Bend Diameter (Material #65). Description: A view of the entire bend region, showing lateral cracks across the specimen.

Figure 88:

Title Mtl-65. R = 15. Photo #016. Magnification: 20X. Legend: Bend Region with Cracks Visible in McGhan-NuSil CV1-1144-0 Silicone Coating, Over a 15 mil Bend Diameter (Material #65). Description: A view of the entire bend region of this specimen, showing extensive cracking. Comparing this photo to photo #012, the cracking here is more random in orientation.

Material #66: McGhan-NuSil CV1-3530 fluorosilicone coating on 1 mil Kapton film, prepared by Sheldahl; unexposed; Au/Pd-coated for SEM analysis.

Figure 89:

Title: Mtl-66. R = 40. Photo #015. Magnification: 13X. Legend: Bend Region of McGhan-NuSil CV1-3530 Fluorosilicone Coating, Over a 40 mil Bend

ORIGINAL PAGE IS
OF POOR QUALITY

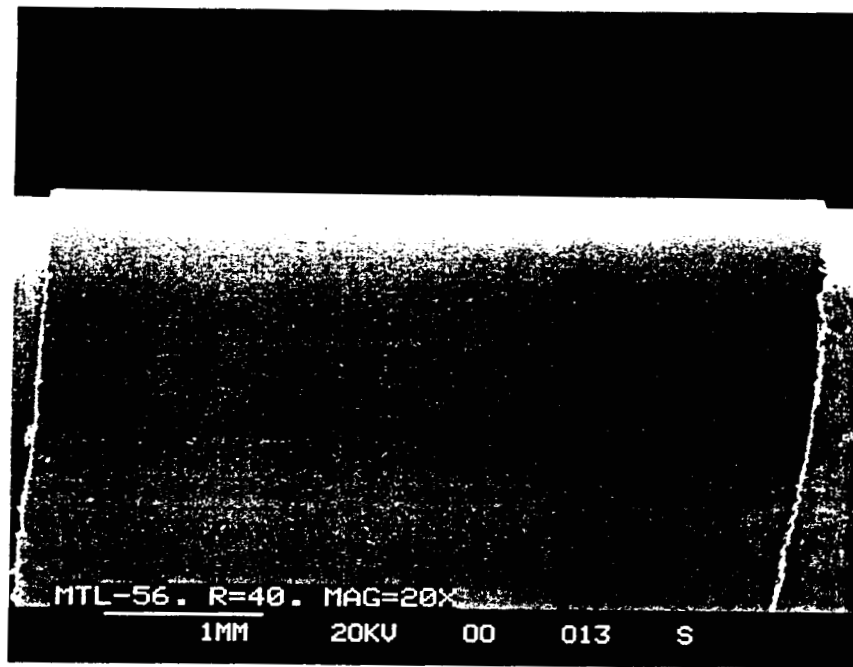


Figure 85: HMDS Coating (#56) on Kapton Bent Over 40-Mil Radius

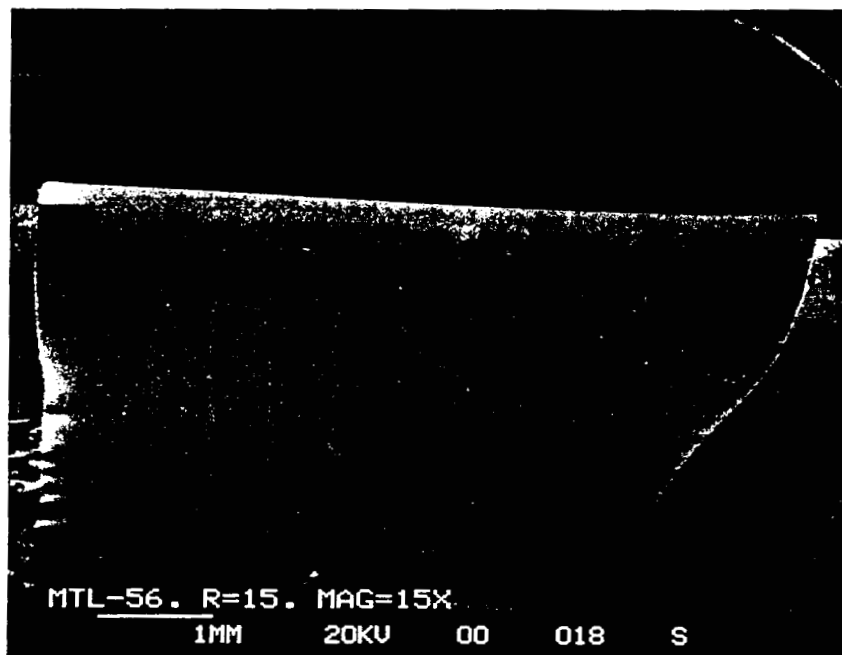


Figure 86: HMDS Coating (#56) on Kapton Bent Over 15-Mil Radius

(THIS PAGE INTENTIONALLY LEFT BLANK)



Figure 87: CVI-1144-0 Siloxane Coating (#65) on Kapton Bent Over a 40-Mil Radius



Figure 88: CVI-1144-0 Siloxane Coating (#65) on Kapton Bent Over a 15-Mil Radius

Diameter (Material #66). Description: Extensive cracking is clearly visible over the entire bend region and down the sides of the specimen.

Figure 90:

Title: Mtl-66. R = 15. Photo #017. Magnification: 20X. Legend: Bend Region of McGhan-NuSil CV1-3530 Fluorosilicone Coating. Over a 15 mil Bend Diameter (Material #66). Description: Extensive cracking can be seen over the entire specimen.

SET 8 (12/12/86)

Material #49: Battelle plasma polymerized HMDS/TFE (ratio 4/1) on 1 mil Kapton film; unexposed; Au/Pd-coated for SEM analysis.

Figure 91:

Title: Mtl-49. R = 40. Photo #006. Magnification: 2KX. Legend: Pit Defects in Surface of As-Received Battelle Plasma Polymerized HMDS/TFE (Ratio 4/1) Coating on Kapton Film, Over a 40 mil Bend Diameter (Material #49). Description: A view of the bend region of this sample. No cracking was observed, but many small pits in the coating surface can be seen.

Figure 92:

Title: Mtl-49. R = 15. Photo #000. Magnification: 1800X. Legend: Lateral Cracks in Battelle Plasma Polymerized HMDS/TFE (Ratio 4/1) Coating. Over a 15 mil Bend Diameter (Material #49). Description: Long parallel cracks along the bend axis were observed for this sample over the 15 mil bend diameter.

Material #51: Battelle plasma polymerized HMDS/TFE (ratio 20/1) coating on 1 mil Kapton film; unexposed; Au/Pd-coated for SEM analysis.

Figure 93:

Title: Mtl-51. R = 40. Photo #007. Magnification: 200X. Legend: Edge of

ORIGINAL PAGE IS
OF POOR QUALITY

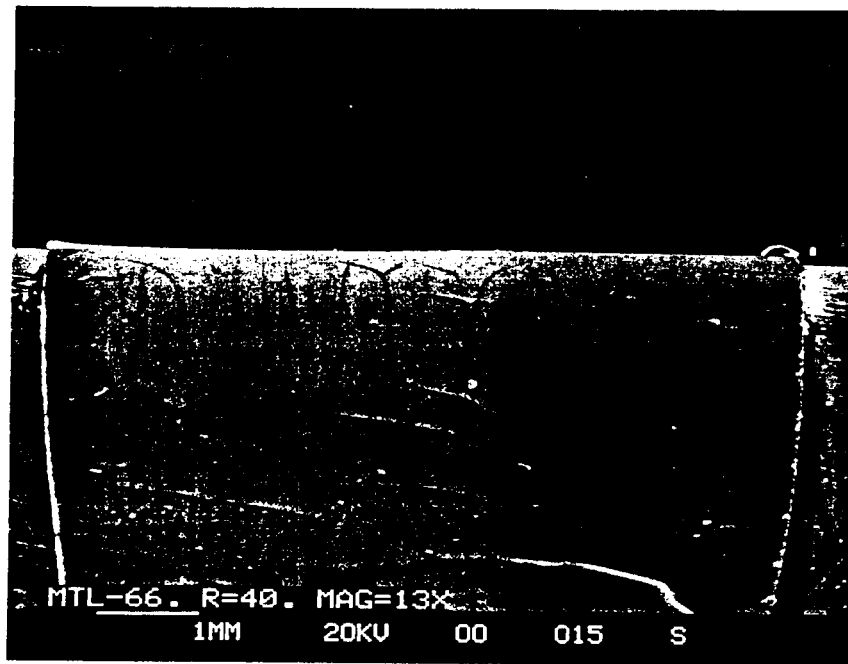


Figure 89: CVI-3530 Fluorosilicone Coating (#66) on Kapton Bent Over a 40-Mil Radius

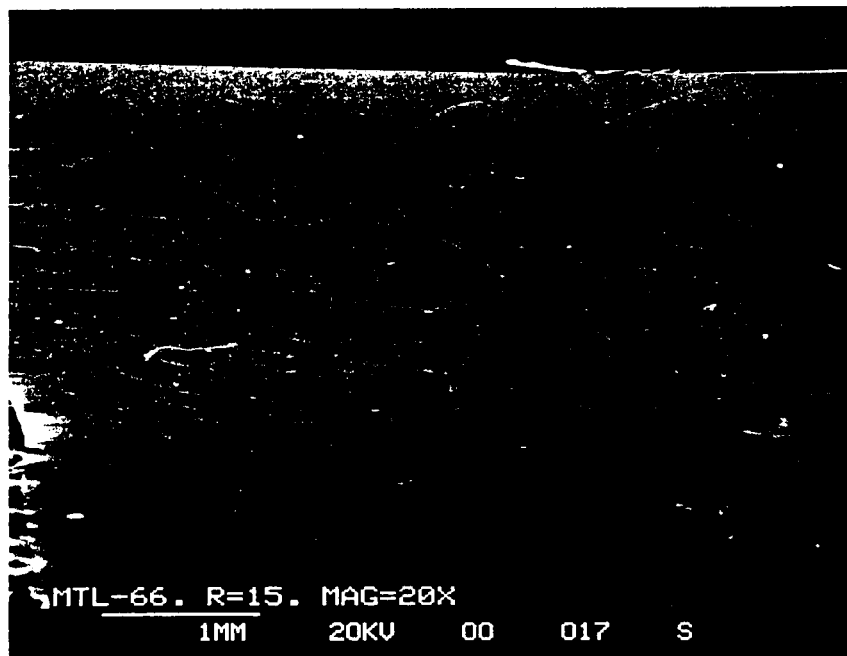


Figure 90: CVI-3530 Fluorosilicone Coating (#66) on Kapton Bent Over a 15-Mil Radius

(THIS PAGE INTENTIONALLY LEFT BLANK)

ORIGINAL PAGE IS
OF POOR QUALITY

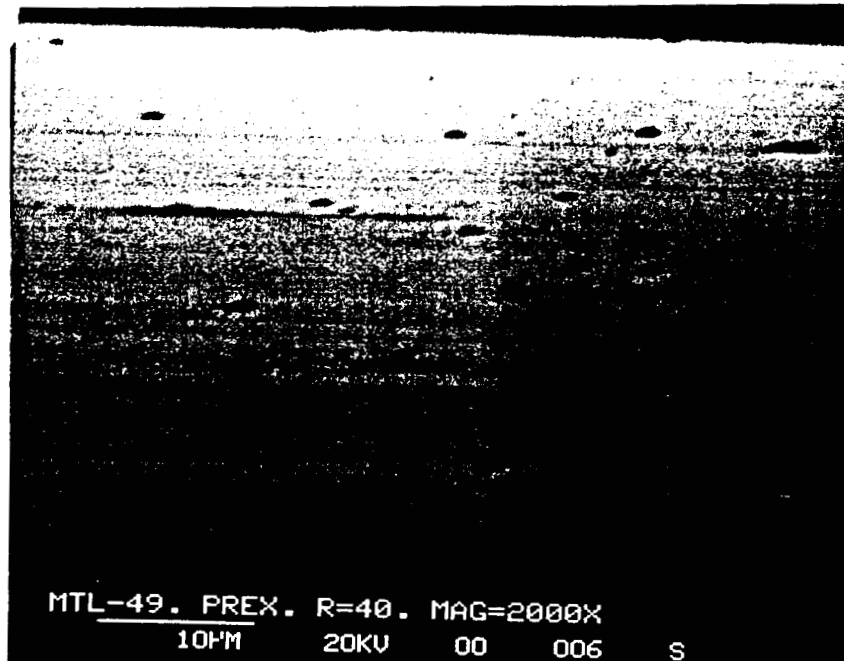


Figure 91: HMDS/TFE Coating (#49) on Kapton Bent Over a Radius of 40-Mil

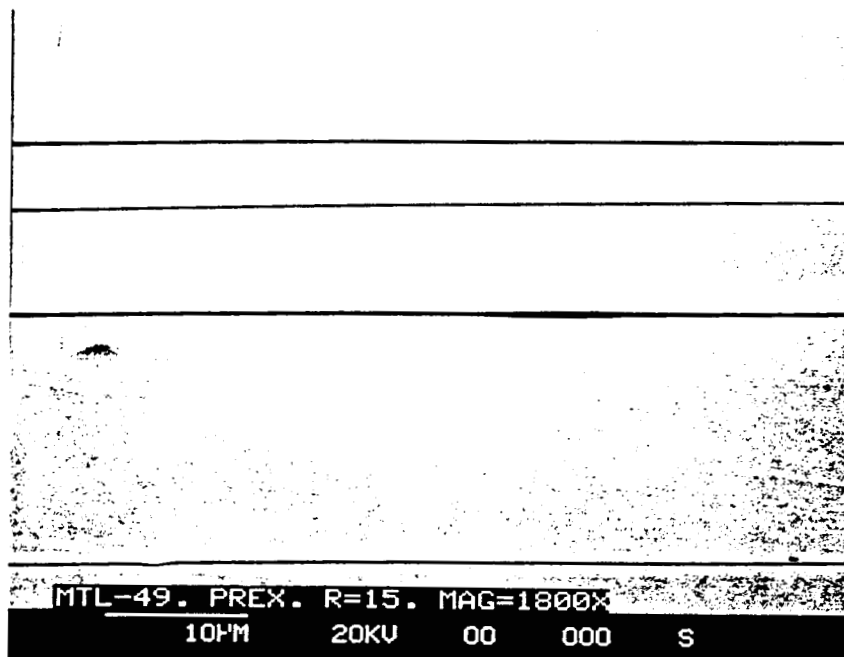


Figure 92: HMDS/TFE Coating (#49) on Kapton Bent Over a Radius of 15-Mil

Bend Region of Battelle Plasma Polymerized HMDS/TFE (Ratio 20/1) Coating, Over a 40 mil Bend Diameter (Material #51). Description: No cracking was observed in this sample. This is a view of the edge of the bend region, showing damage caused by cutting the sample from sheet stock.

Material #58: Ethyl X-128 fluorophosphazene coating on 1 mil Kapton film; unexposed; Au/Pd-coated for SEM analysis.

Figure 94:

Title: Mtl-58. R = 15. Photo #003. Magnification: 1000X. Legend: Surface of Ethyl X-128 Fluorophosphazene Coating, Over a 15 mil Bend Diameter (Material #58). Description: Typical view of the bend region of this sample. No cracking was observed in this coating.

Material #70: McGhan-NuSil CV1-3530 fluorosilicone coating on 1 mil Kapton film, prepared by Sheldahl; unexposed; Au/Pd-coated for SEM analysis.

Figure 95:

Title: Mtl-70. R = 40. Photo #012. Magnification: 510X. Legend: Defect Formation in Surface of McGhan-NuSil CV1-3530 Fluorosilicone Coating, Over a 40 mil Bend Diameter (Material #70). Description: While no general cracking was observed in this coating, this large surface defect does have a crack formed along the upper left in this photo. Note the surface striations through and above the defect, which may be cracks just forming (especially the striation to the upper right) or processing artifacts (in particular the horizontal striation). No other defect of this type was observed in the bend region of this sample.

Figure 96:

Title: Mtl-70. R = 15. Photo #016. Magnification: 1900X. Legend: Crack and Unusual Surface Features of McGhan-NuSIL CV1-3530 Fluorosilicone Coating, Over a 15 mil Bend Diameter (Material #70). Description: Wide areas of

ORIGINAL PAGE IS
OF POOR QUALITY

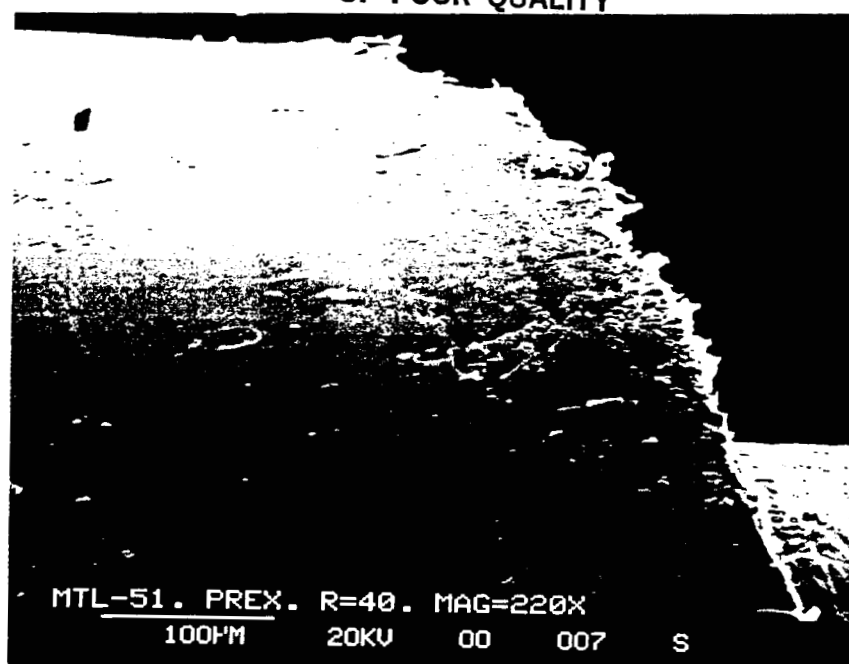


Figure 93: Plasma Polymerized HMDS/TFE Coating (#51) on Kapton Bent
Over a 40-Mil Radius

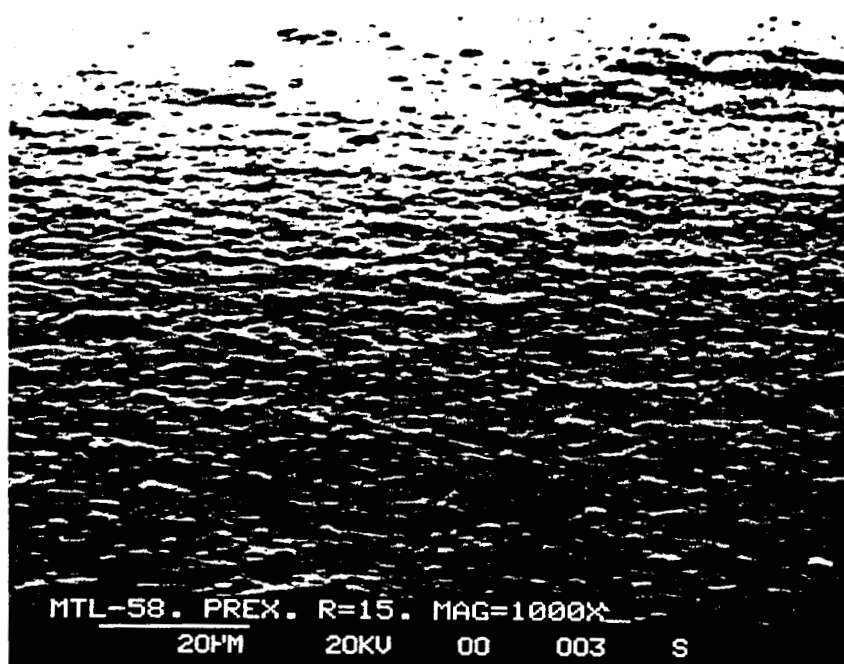


Figure 94: Ethyl X-128 (#58) Coating on 1-Mil Kapton Bent Over a
Radius of 15-Mil

(THIS PAGE INTENTIONALLY LEFT BLANK)

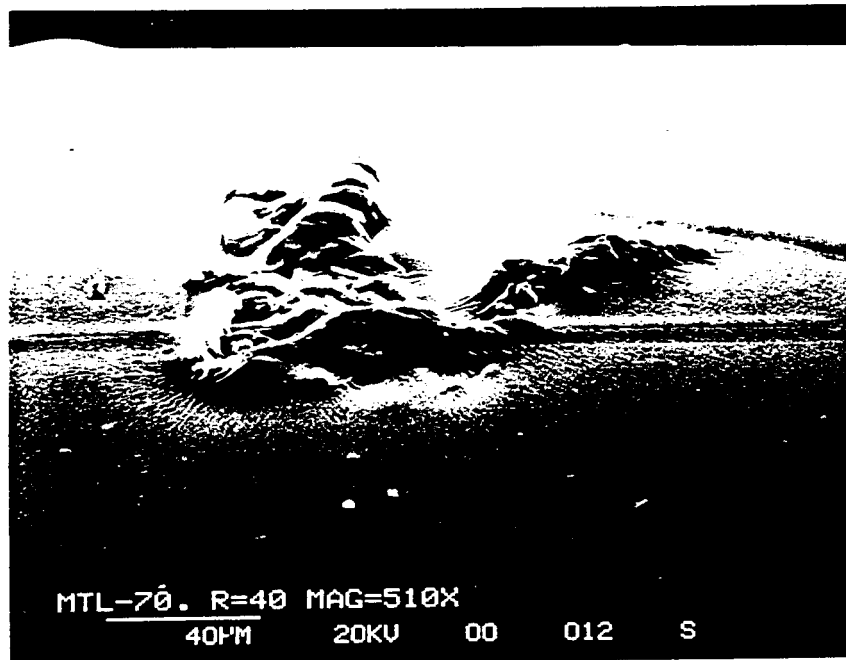


Figure 95: CVI-3530 Fluorosilicone Coating (#70) on Kapton Bent Over 40-Mil Radius

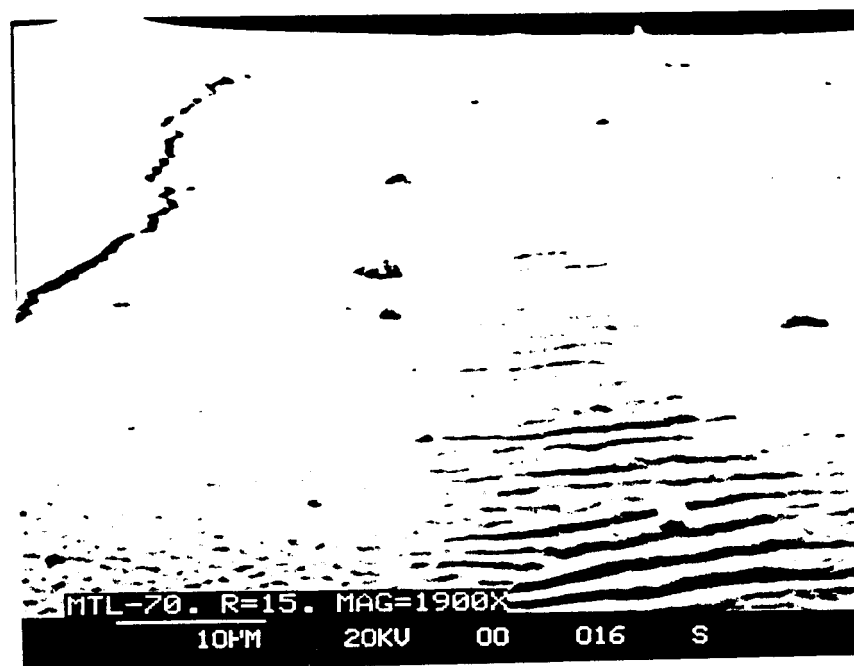


Figure 96: CVI-3530 Fluorosilicone Coating (#70) on Kapton Bent Over 15-Mil Radius

parallel grooves or ridges were observed in places on this sample. Note rough crack to upper left.

Figure 97:

Title: Mtl-70. R = 15. Photo #018. Magnification: 190X. Legend: Same as for 10. Description: These were the largest cracks observed in this sample.

Material #71: McGhan-NuSIL CV1-1144-0 silicone coating on 1 mil Kapton film, prepared by Sheldahl; unexposed; Au/Pd-coated for SEM analysis.

Figure 98:

Title: Mtl-71. R = 15. Photo #014. Magnification: 1000X. Legend: Bend Region of the McGhan-NuSIL CV1-1144-0 Silicone Coating, Over a 15 mil Bend Diameter (Material #71). Description: No cracking was observed in this sample. This is a typical view of the bend region surface.

Material #LERC-51386: NASA-LeRC siloxane (SiO) coating on 1 mil Kapton film; unexposed; Au/Pd-coated for SEM analysis.

Figure 99:

Title: LERC-51386. R = 40. Photo #010. Magnification: 600X. Legend: Bend Region of NASA-LeRC Siloxane (SiO) Coating, Over a 40 mil Bend Diameter (Material #LERC-51386). Description: No cracking was observed in this sample. This is a typical view of the bend region surface.

Figure 100:

Title: LERC-51386. R = 15. Photo #013. Magnification: 1000X. Legend: Bend Region of NASA LeRC Siloxane (SiO) Coating, Over a 15 mil Bend Diameter (Material #LERC-51386. Description: No cracking was observed in this sample. This is a typical view of the bend region surface.

SET 9 (2/2-3/87)

Material #58: Ethyl X-128 fluorophosphazene coating on 1 mil Kapton film;

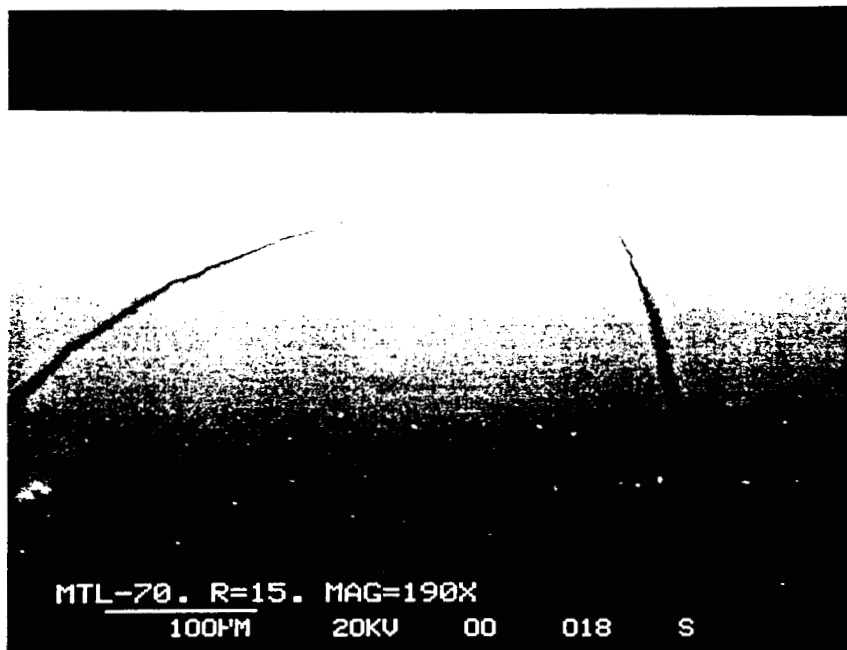


Figure 97: Largest Cracks Observed in CVI-3530 Fluorosilicone Coating (#70)
When Bent Over 15-Mil Radius

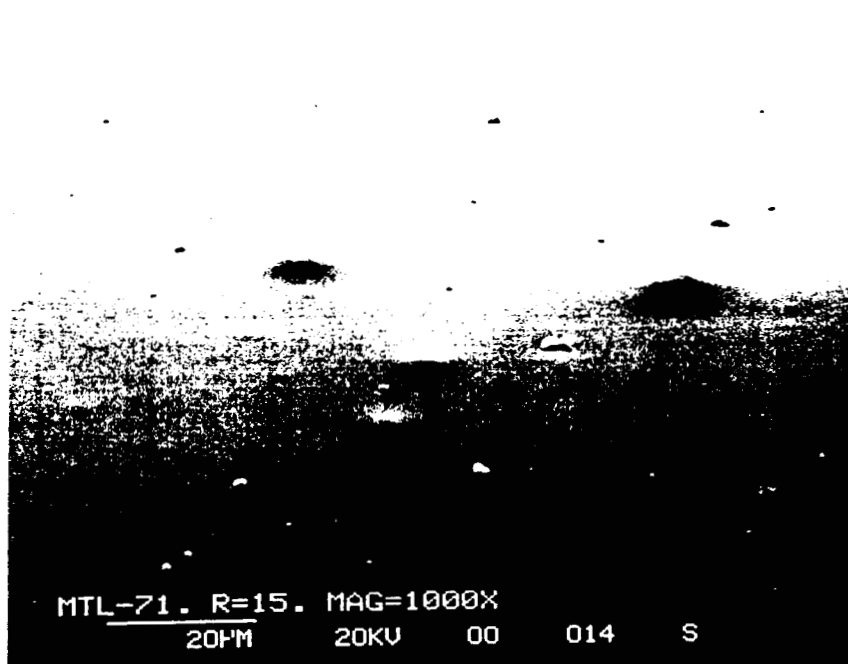


Figure 98: CVI-1144-0 Silicone Coating (#71) on Kapton Bent Over a
15-Mil Radius

(THIS PAGE INTENTIONALLY LEFT BLANK)

ORIGINAL PAGE IS
OF POOR QUALITY

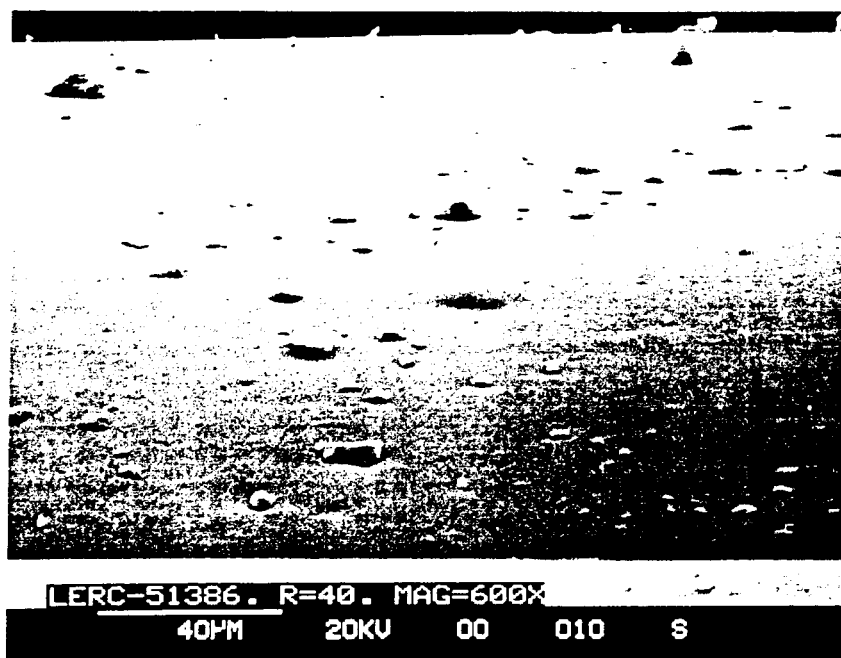


Figure 99: LeRC Siloxane Coating on Kapton Bent Over 40-Mil Radius

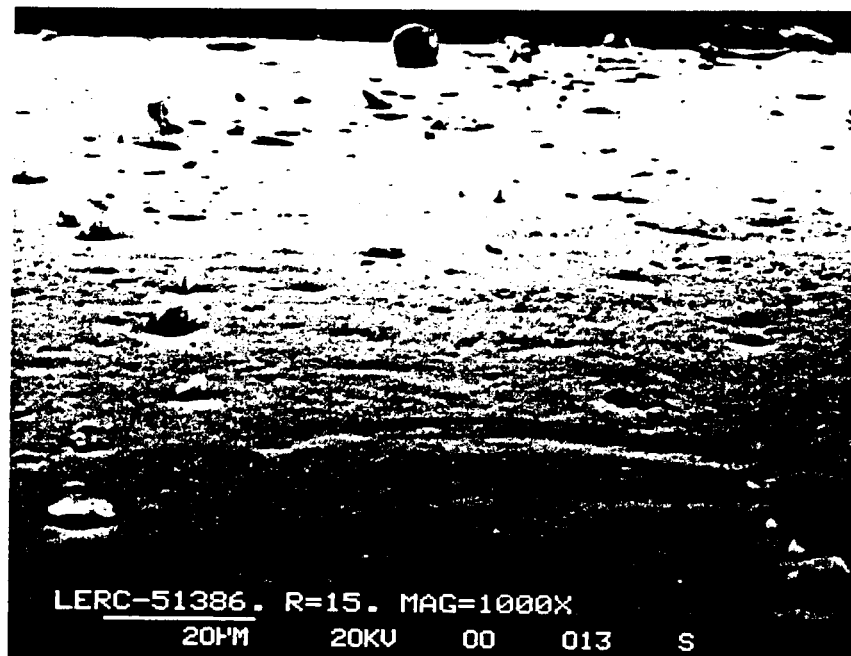


Figure 100: LeRC Siloxane Coating on Kapton Bent Over 15-Mil Radius

BREL test #1; Au/Pd-coated for SEM analysis.

Figure 101:

Title: Mtl-58. BREL. R = 15 ("R" = bend diameter in mils). Photo #000. Magnification: 50X. Legend: Bend Region of Vacuum Cycled sample, Over a 15 mil Bend Diameter (Material #58). Description: No cracking was observed over the bend region of this sample. The streaks/lines seen in this photo are due to an auto-tracking contrast function on the SEM, which was used to adjust for widely varying contrast levels across the sample; the lines are artifacts of the SEM, and not physical features on the coating surface. EDAX analysis of virgin and BREL-tested (figure 103) Material #58 indicates a slight loss of O, F, Al and Si upon Brel testing. This may indicate some loss of fluoroalkyl side groups from the material surface, possibly by UV-induced P-O bond disruption.

Figure 102:

Title: Mtl-58. BREL. R = 40. Photo #006. Magnification: 50X. Legend: Same as for previous figure, except over a 40 mil bend diameter. Description: No cracking of the surface was observed for this sample. Note the high level of surface debris, which was not observed previously on virgin samples of this material.

Material #65: McGhan-NuSil CV1-1144-0 silicone coating on 1 mil Kapton film; BREL test #1; Au/Pd-coated for SEM analysis.

ORIGINAL PAGE IS
OF POOR QUALITY

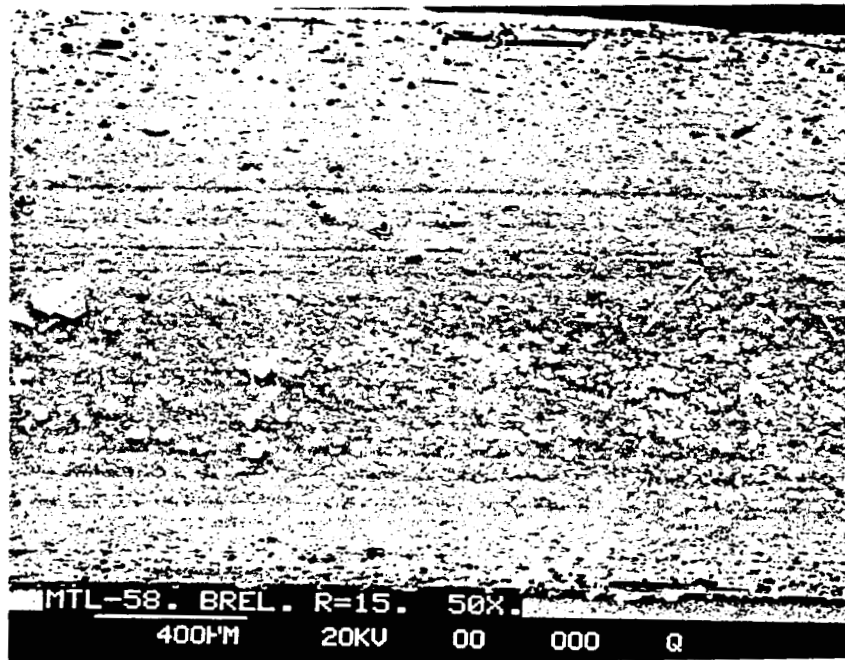


Figure 101: X-128 Coating (#58) on Kapton Bent Over 15-Mil Radius. Sample Previously Exposed to Combined Vacuum Thermal Cycling/UV Radiation

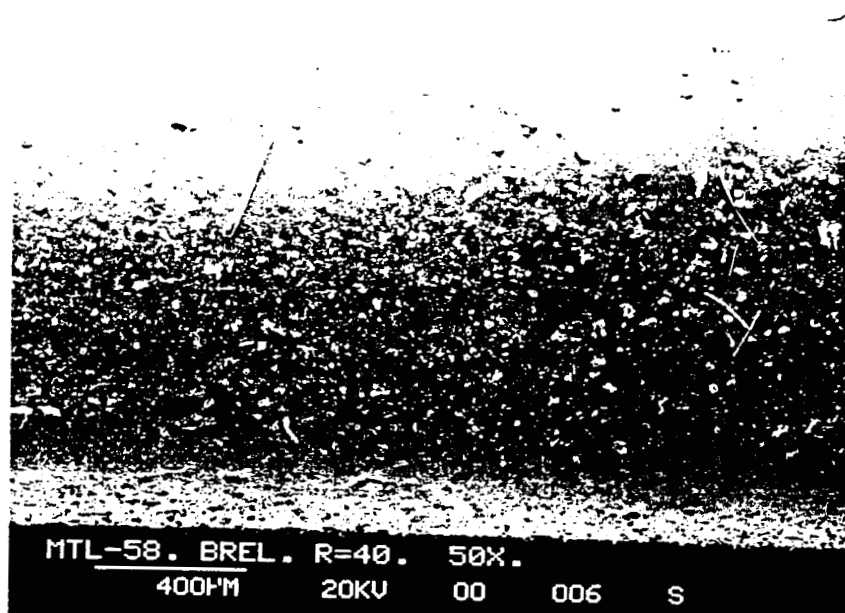


Figure 102: X-128 Coating (#58) on Kapton Bent Over 15-Mil Radius. Sample Previously Exposed to Combined Vacuum Thermal Cycling/UV Radiation

(THIS PAGE INTENTIONALLY LEFT BLANK)

KAP7A.

MTL-58. BREL.

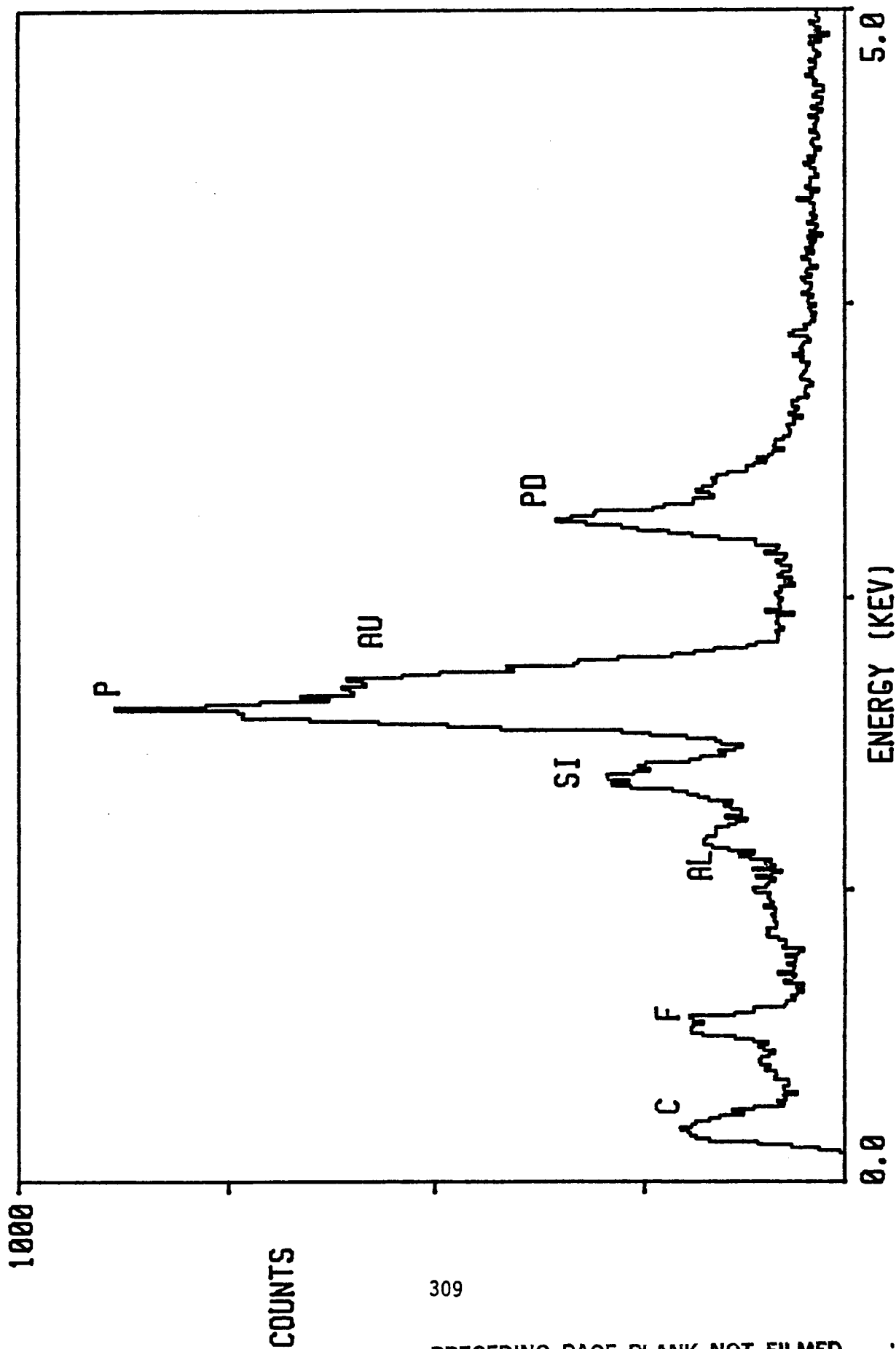


Figure 103: EDAX Spectrum of X-128 Coating. Sample Was Previously Exposed to Combined Vacuum Thermal Cycling/UV Radiation

Figure 104:

Title: Mtl-65. BREL. R = 15. Photo #001. Magnification: 50X. Legend: Bend Region of McGhan-NuSil CV1-1144-0 Silicone Coating, after Solar UV/Thermal Vacuum Cycling, Over a 15 mil Bend Diameter (Material #65). Description: No cracking could be observed over this region. This was surprising because cracks were observed in the virgin material.

Figure 105:

Title: Mtl-65. BREL. R = 40. Photo #004. Magnification: 50X. Legend: Same as above, except over a 40 mil bend diameter. Description: No cracks were observed in the surface of this coating, while cracking was extensive in the virgin material. The lateral lines in this photo are due to the SEM auto-track function, and are not real physical features.

Material #65: As above; virgin material; Au/Pd-coated for SEM analysis.

Figure 106:

Title: Mtl-65. PREX. R = 15. Photo #002. The photo is incorrectly labeled as photo #000). Magnification: 50X. Legend. Cracks in Surface of As-Received McGhan-NuSil CV1-1144-0 Silicone Coating, Over a 15 mil Bend Diameter (Material #65). Description: Cracks as seen in this photo were observed over the entire bend region. EDAX analysis indicates an increase in C, O and Al, and a decrease in Si upon BREL testing. These EDAX spectra are shown in figures 108 and 109.

Figure 107:

Title: Mtl-65. PREX. R = 40. Photo #003. Magnification: 50X. Legend: Same as above, except over a 40 mil bend diameter. Description: Cracks as seen in this photo were observed over the entire bend region.

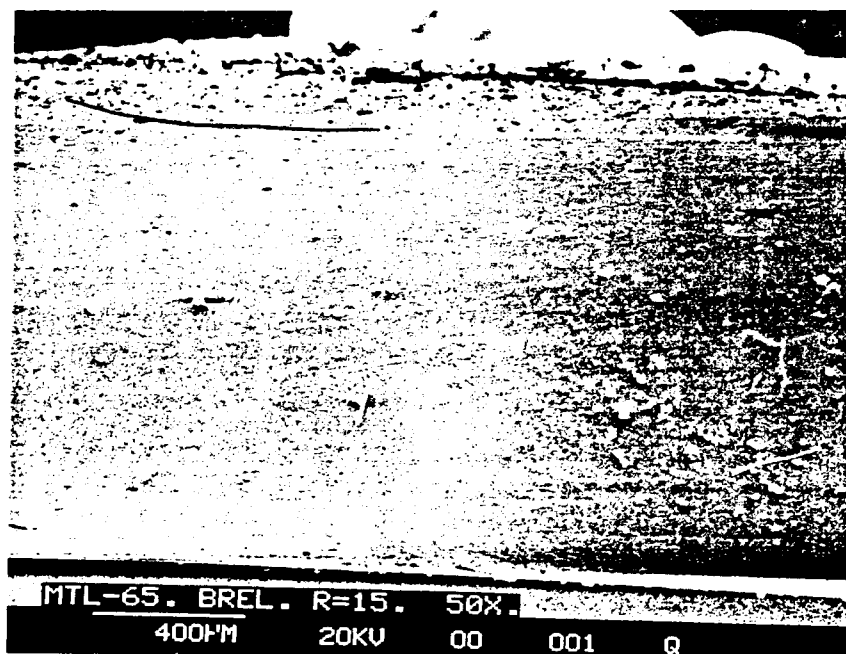


Figure 104: CV1-1144-0 Silicone Coating (#65) on Kapton Bent Over 15-Mil Radius. Sample Previously Exposed to Combined Vacuum Thermal Cycling/UV Radiation.

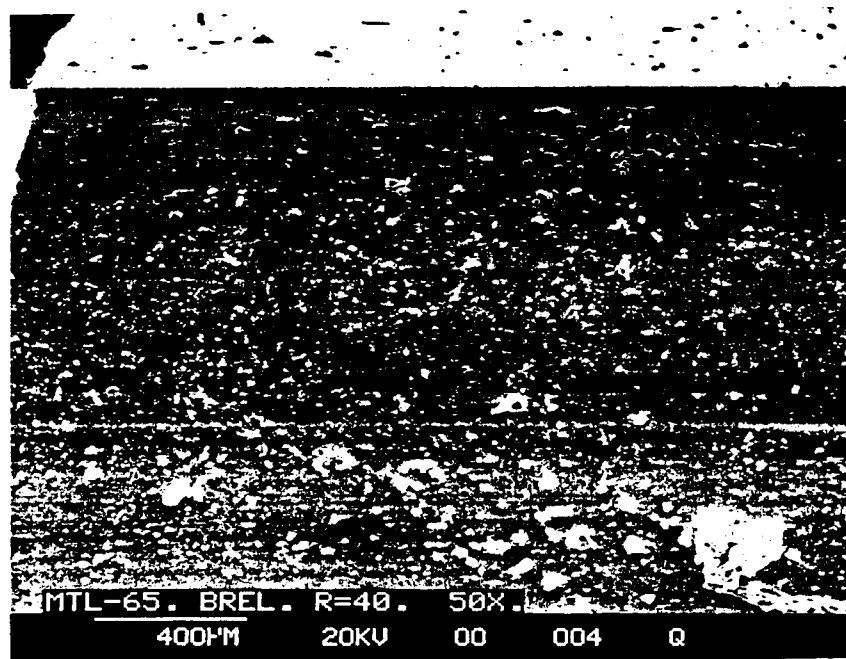


Figure 105: CV1-1144-0 Silicone Coating (#65) on Kapton Bent Over 15-Mil Radius. Sample Previously Exposed to Combined Vacuum Thermal Cycling/UV Radiation.

(THIS PAGE INTENTIONALLY LEFT BLANK)

ORIGINAL PAGE IS
OF POOR QUALITY

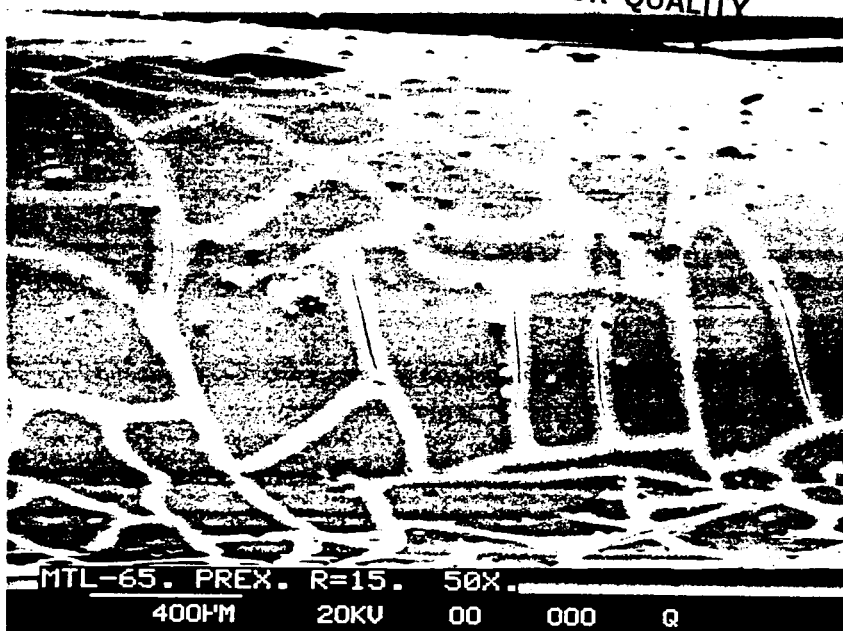


Figure 106: CVI-1144-0 Siloxane Coating (#65) on Kapton Bent Over a 15-Mil Radius

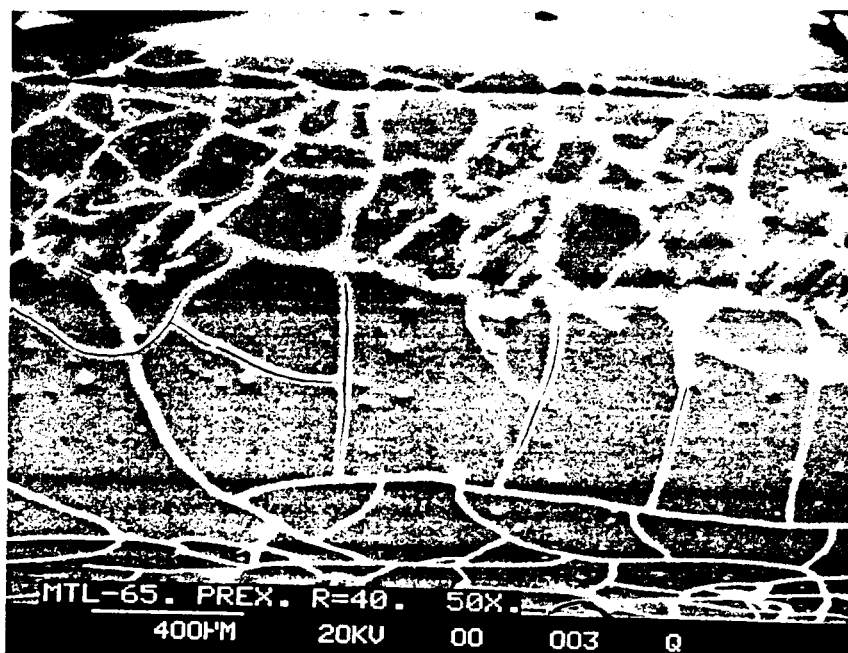


Figure 107: CVI-1144-0 Siloxane Coating (#65) on Kapton Bent Over a 40-Mil Radius

(THIS PAGE INTENTIONALLY LEFT BLANK)

KAP7C.

MTL-65. PREX.

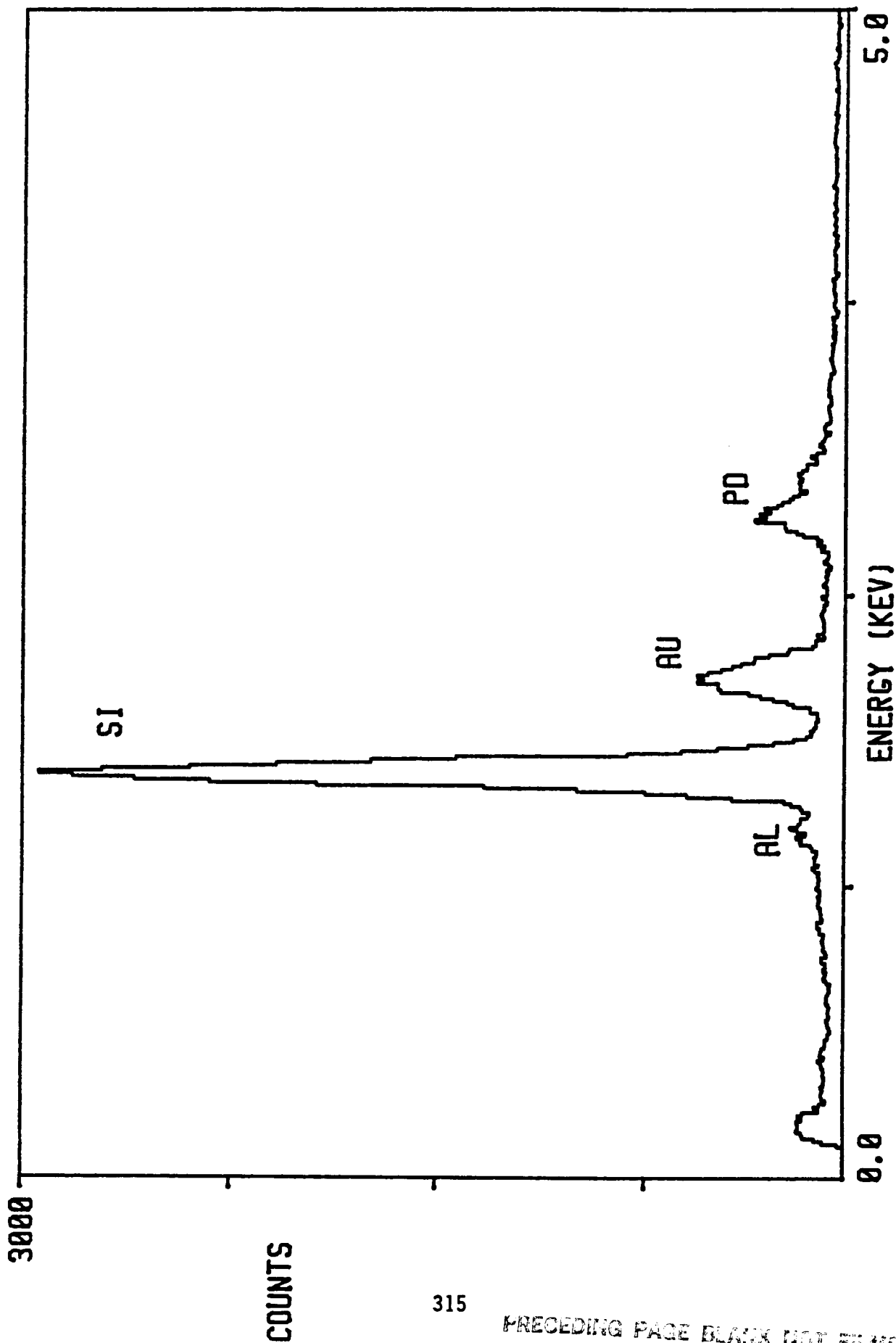


Figure 108: EDAX Spectrum of CVI-1144-0 Siloxane Coating on Kapton

(THIS PAGE INTENTIONALLY LEFT BLANK)

KAP7B.

MTL-65. BREL.

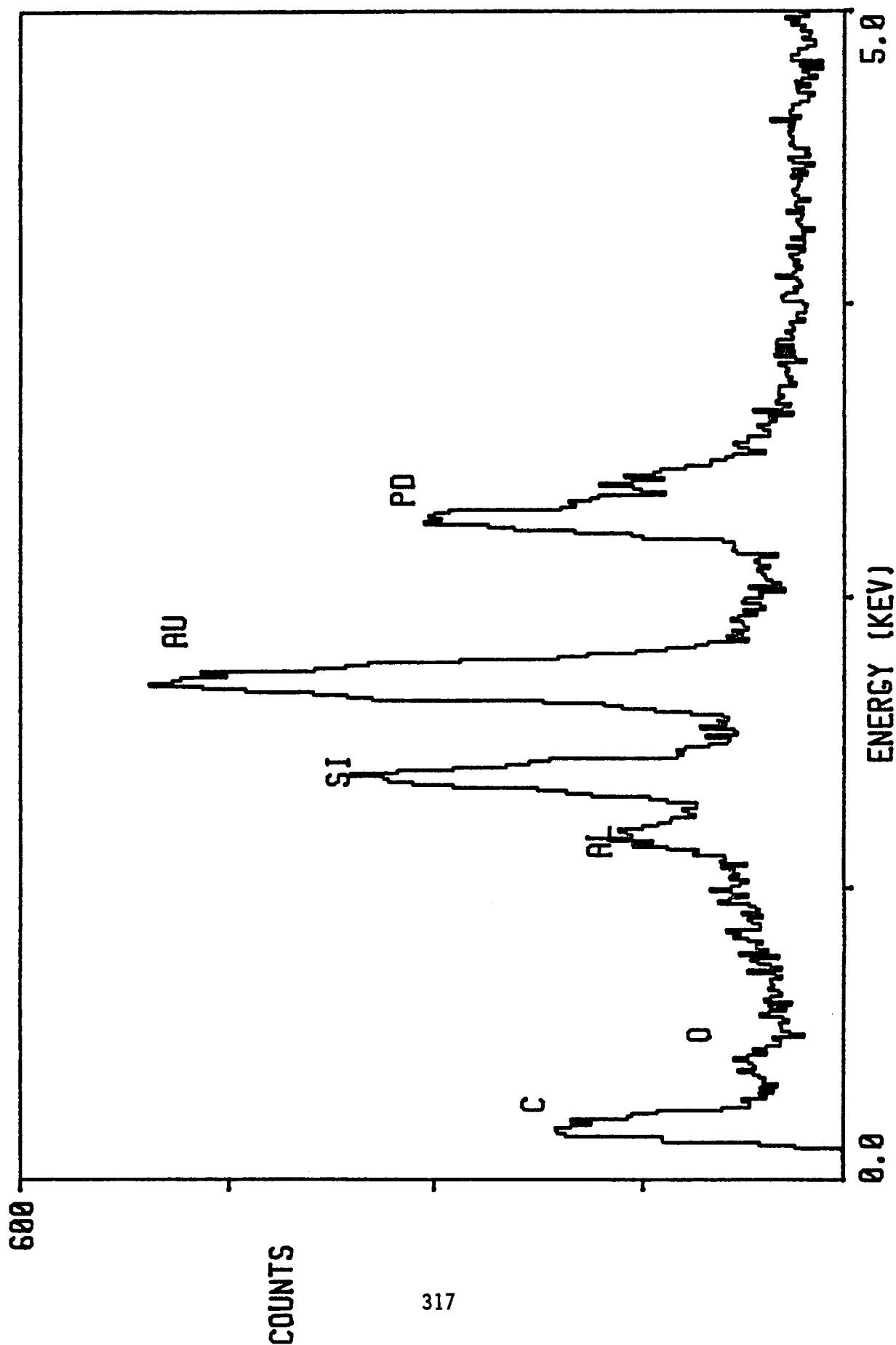


Figure 109: EDAX Spectrum of CVI-1144-0 Siloxane Coating on Kapton Sample Previously Exposed to Combined Vacuum Thermal Cycling/UV Radiation

Material #50: Battelle plasma polymerized HMDS coating on 1 mil Kapton film; BREL test #1; Au/Pd-coated for SEM analysis.

Figure 110:

Title: Mtl-50. BREL. R = 15. Photo #012. Magnification: 1000X. Legend: Single Crack in Surface of Battelle HMDS Coating, After BREL Solar UV/Thermal Vacuum Cycling, Over a 15 mil Bend Diameter (Material #50). Description: This is a picture of the only crack observed in the surface of this coating material. No other cracks were observed.

Figure 111:

Title: Mtl-50. BREL. R = 15. Photo #013. Magnification: 50X. Legend: Bend Region of Battelle HMDS After BREL Solar UV/Thermal Vacuum Cycling, Over a 15 mil Bend Diameter (Material #50). Description: Typical view of bend region of this sample. The solitary crack seen in photo #012 cannot be seen easily in this picture. EDAX analysis indicates a possible slight increase in Si and O levels in the BREL-tested material when compared to the as-received virgin material. These EDAX spectra are shown in figures 112 and 113

Figure 114:

Title: Mtl-50. BREL. R = 40. Photo #007. Magnification: 180X. Legend: Same as for 8, except over a 40 mil bend diameter. Description: A single, crack-like feature was observed in this sample, similar to what was seen in 7 over a smaller bend diameter. No other cracks were observed.

Material #50: As above, but virgin, as-received material; Au/Pd-coated for SEM analysis.

Figure 115

Title: Mtl-50. PREX. R = 15. Photo #014. Magnification: 50X. Legend: Bend Region of Battelle HMDS Over a 15 mil Bend Diameter (Material #50). Description: No cracks were observed in this coating material.

ORIGINAL PAGE IS
OF POOR QUALITY

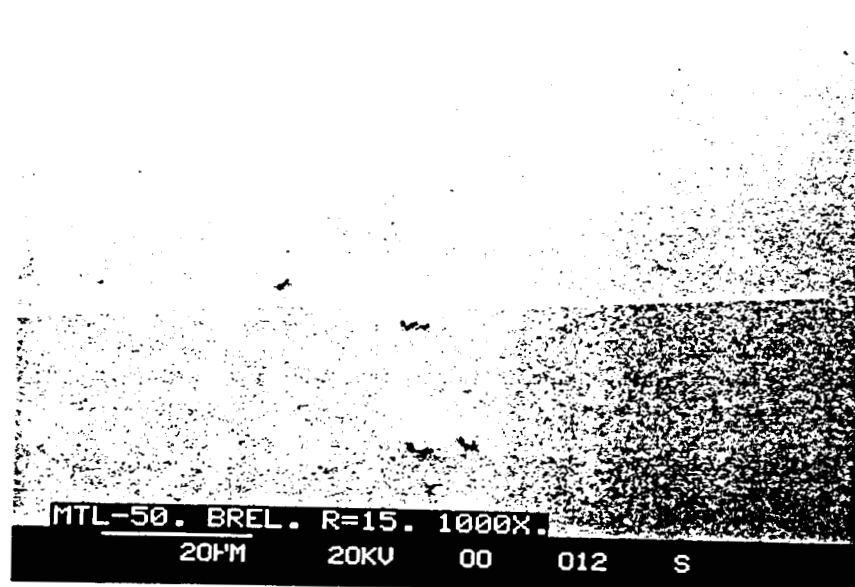


Figure 110: Region of HMDS Coating (#50) on Kapton Showing a Crack When Bent Over a 15-Mil Radius. Sample Previously Exposed to Combined Vacuum Thermal Cycling/UV Radiation

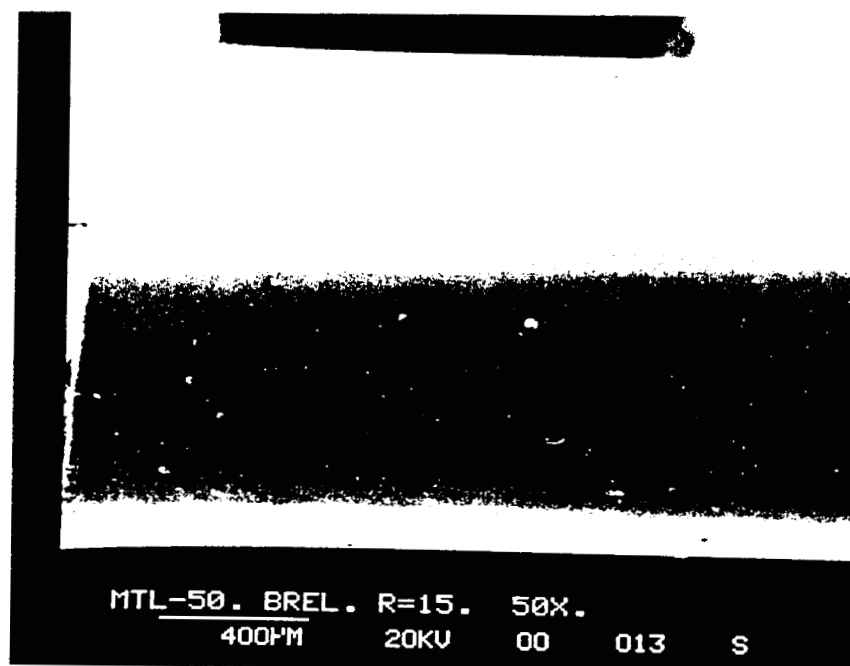


Figure 111: HMDS Coating (#50) on Kapton. Sample Previously Exposed to Combined Vacuum Thermal Cycling/UV Radiation.

(THIS PAGE INTENTIONALLY LEFT BLANK)

KAP7E.

MTL-50. PREX.

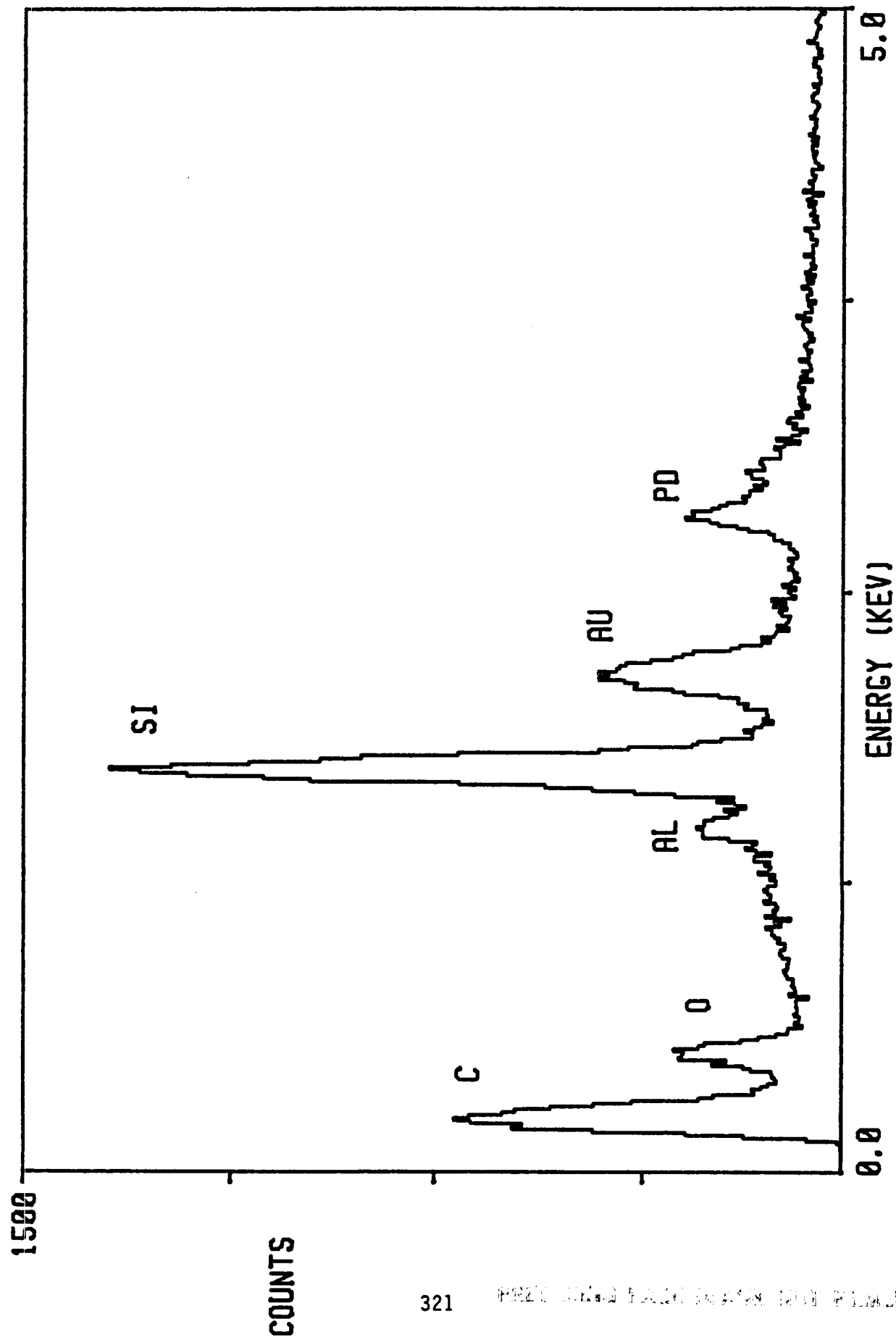


Figure 112: EDAX Spectrum of HMDS Coating (#50) on Kapton

(THIS PAGE INTENTIONALLY LEFT BLANK)

KAP7D.

MTL-50. BREL.

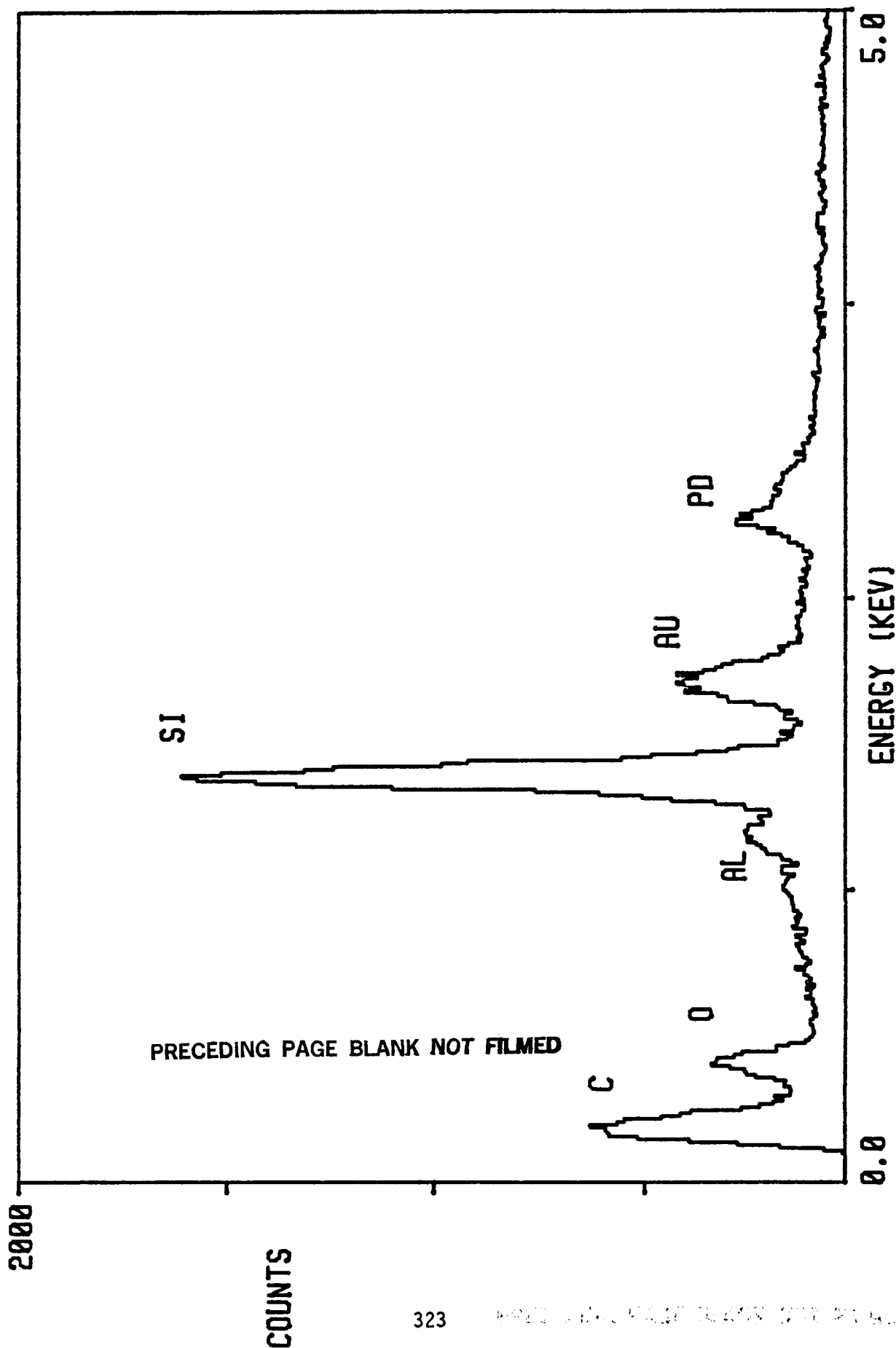


Figure 113: EDAX Spectrum of HMDS Coating on Kapton. Specimen Previously Exposed to Combined Vacuum Thermal Cycling/UV Radiation

(THIS PAGE INTENTIONALLY LEFT BLANK)

ORIGINAL PAGE IS
OF POOR QUALITY

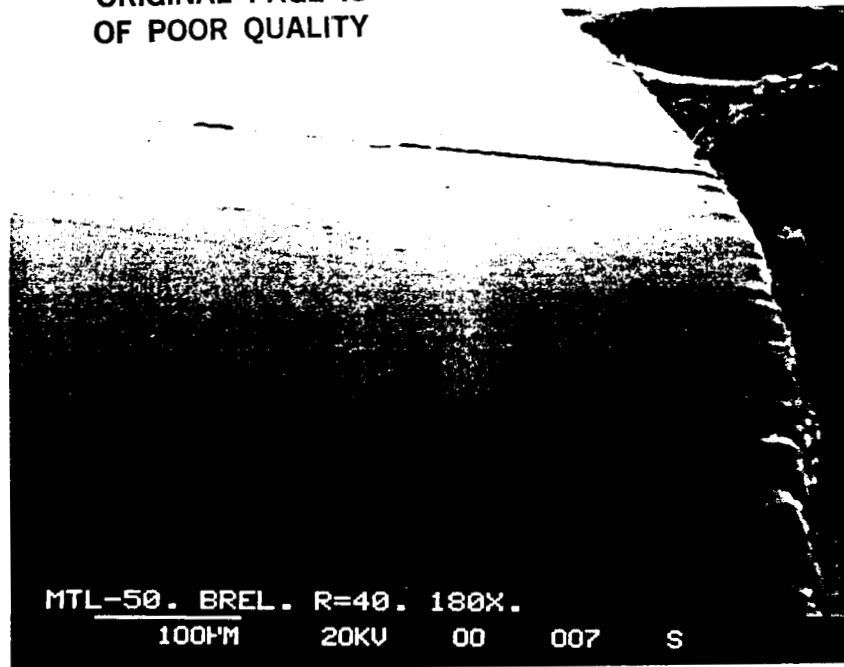


Figure 114: HMDS Coating (#50) on Kapton Bent Over 40-Mil Radius. Sample Exposed to Combined Vacuum Thermal Cycling/UV Radiation.

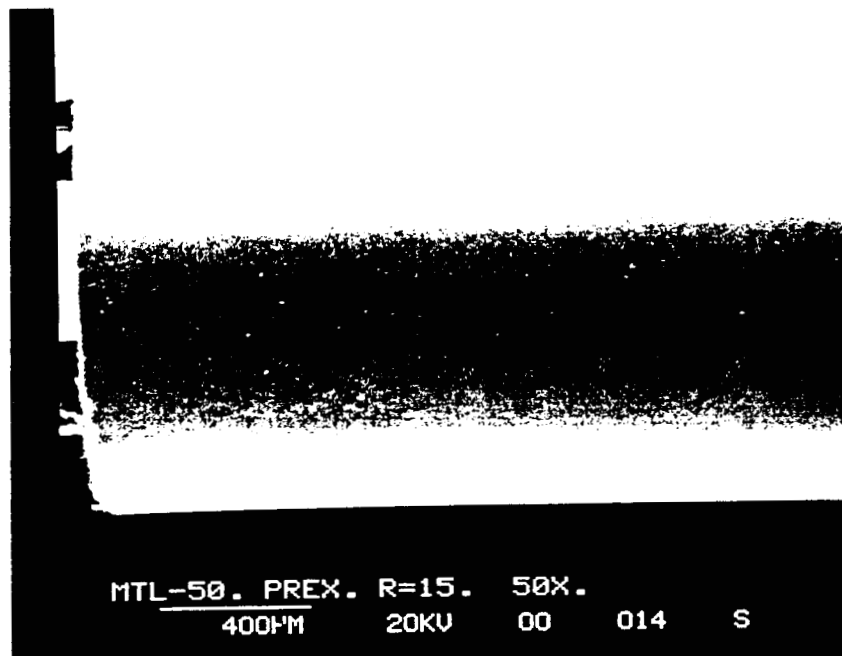


Figure 115: HMDS Coating (#50) on Kapton Bent Over 15-Mil Radius

Figure 116:

Title: Mtl-50. PREX. R = 40. Photo #008. Magnification: 50X. Legend: Same as for 10, except over a 40 mil bend diameter. Description: No cracks were observed in this coating material.

Material #52: Battelle plasma polymerized HMDS/TFE (ratio 8/1) coating on 1 mil Kapton film; BREL test #1; Au/Pd-coated for SEM analysis.

Figure 117:

Title: Mtl-52. BREL. R = 15. Photo #015. Magnification: 50X. Legend: Bend Region of Battelle Plasma Polymerized HMDS/TFE (Ratio 8/1) Coating, After Solar UV/Thermal Vacuum Cycling, Over a 15 mil Bend Diameter (Material #52). Description: No cracks were observed in the surface of this material, even at much higher magnification levels. The horizontal line seen at the top of this photo is the actual edge of the curved surface, similar to that seen at the bottom. EDAX analysis indicates a slight decrease in C and a slight increase in Si upon BREL testing. This may reflect some silicone to silica conversion in the coating's surface. These EDAX spectra are shown in figures 118 and 119.

Figure 120:

Title: Mtl-52. BREL. R = 40. Photo #010. Magnification: 50X. Legend: Bend Region of Battelle Plasma Polymerized HMDS/TFE (Ratio 8/1) Coating, After Solar UV//Thermal Vacuum Cycling, Over a 40 mil Bend Diameter (Material #52). Description: No cracks were observed in the surface of this material.

Material #52: Same as above but virgin, as-received material; Au/Pd-coated for SEM analysis.

Figure 121:

Title: Mtl-52. PREX. R = 15. Photo #16. Magnification: 50X. Legend: Bend Region of As-Received Battelle Plasma Polymerized HMDS/TFE (Ratio 8/1),

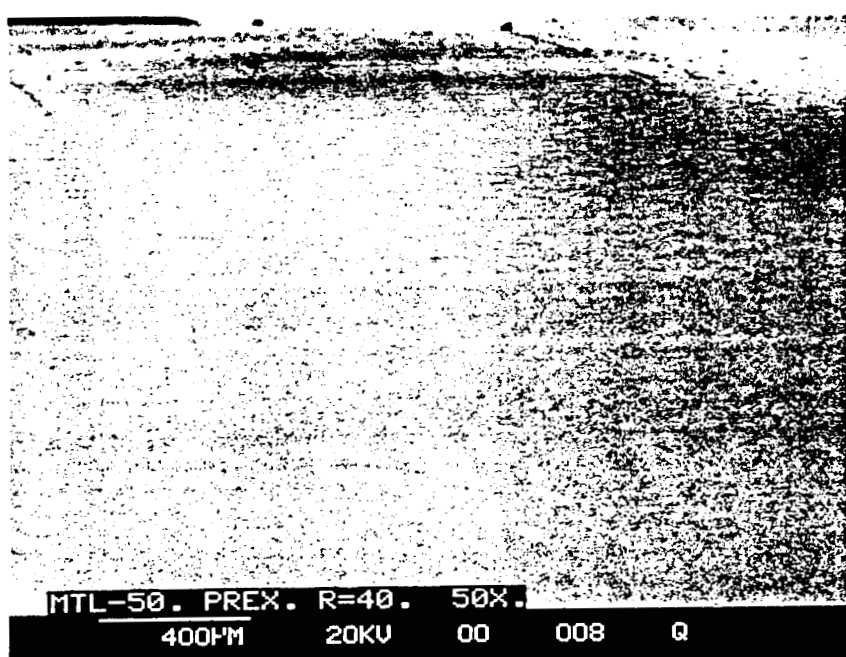


Figure 116: HMDS Coating (#50) on Kapton Bent Over a 40-Mil Radius

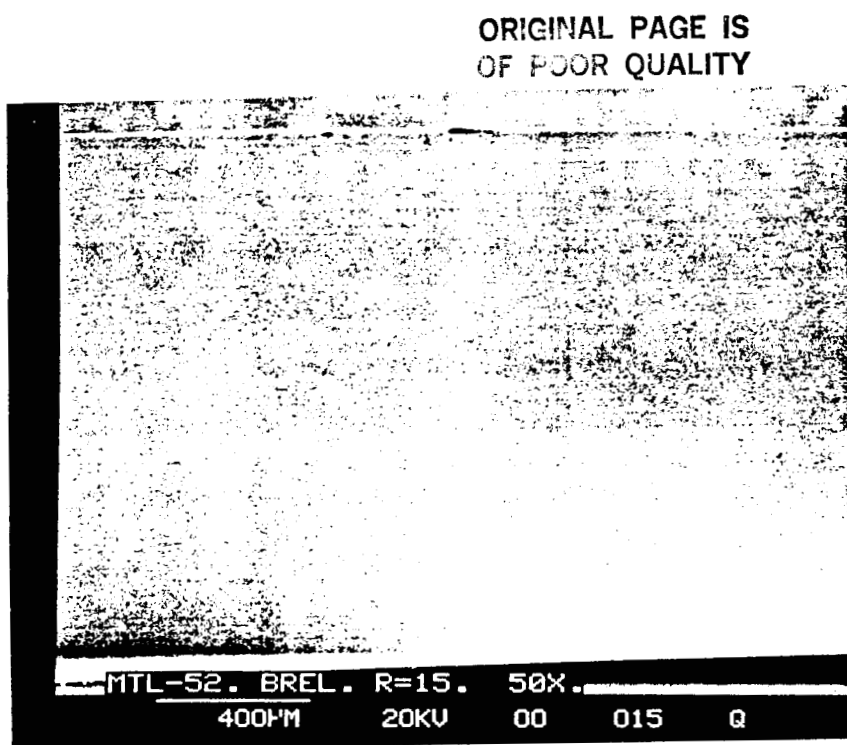


Figure 117: Plasma Polymerized HMDS/TFE Coating on Kapton Bent Over a 15-Mil Radius. Sample Previously Exposed to Combined Vacuum Thermal Cycling/UV Radiation.

(THIS PAGE INTENTIONALLY LEFT BLANK)

KAP76.

MTL-52. PREX.

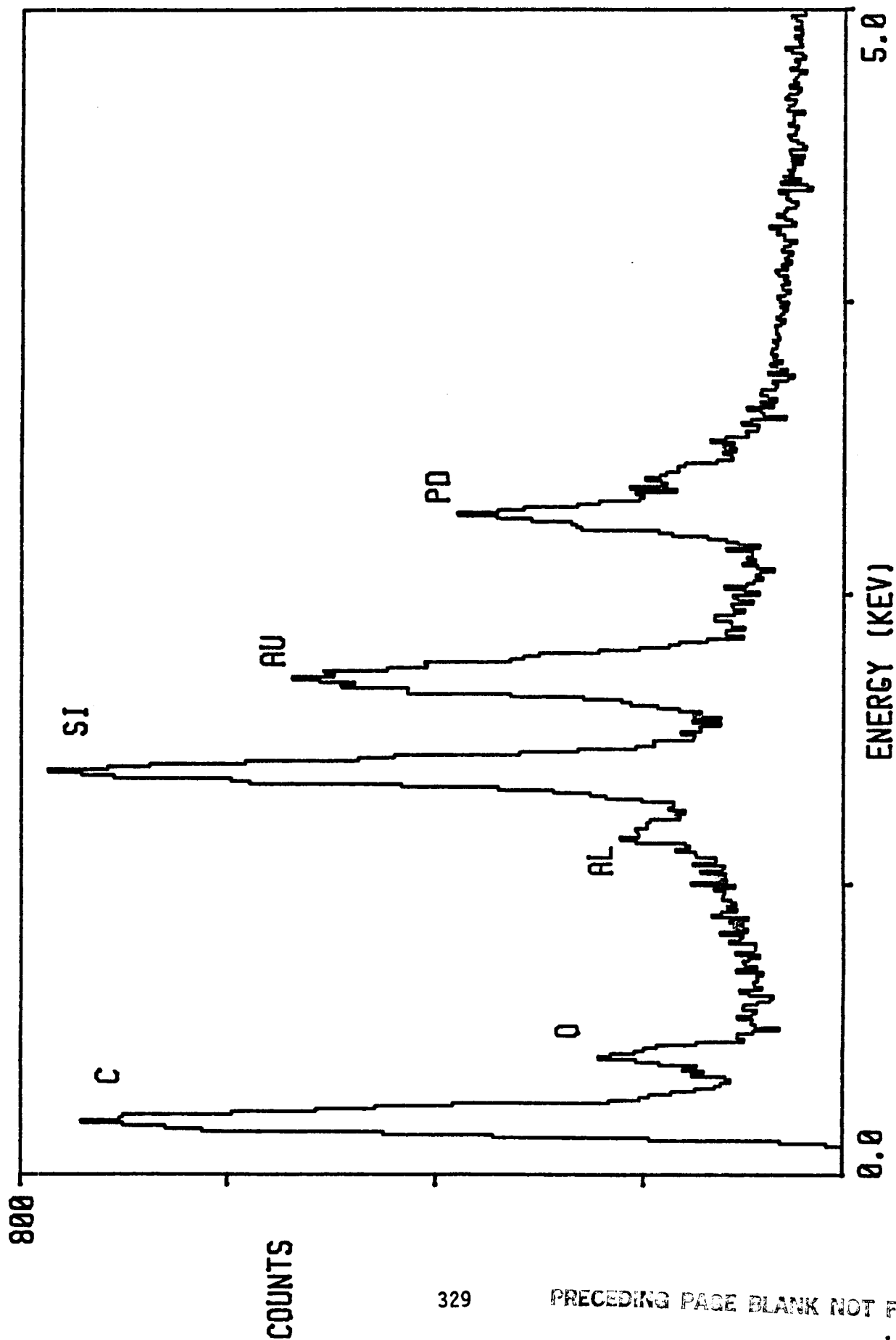


Figure 118: EDAX Spectrum of HMDS/TFE Coating on Kapton

(THIS PAGE INTENTIONALLY LEFT BLANK)

KAP7F.

MTL-52. BREL.

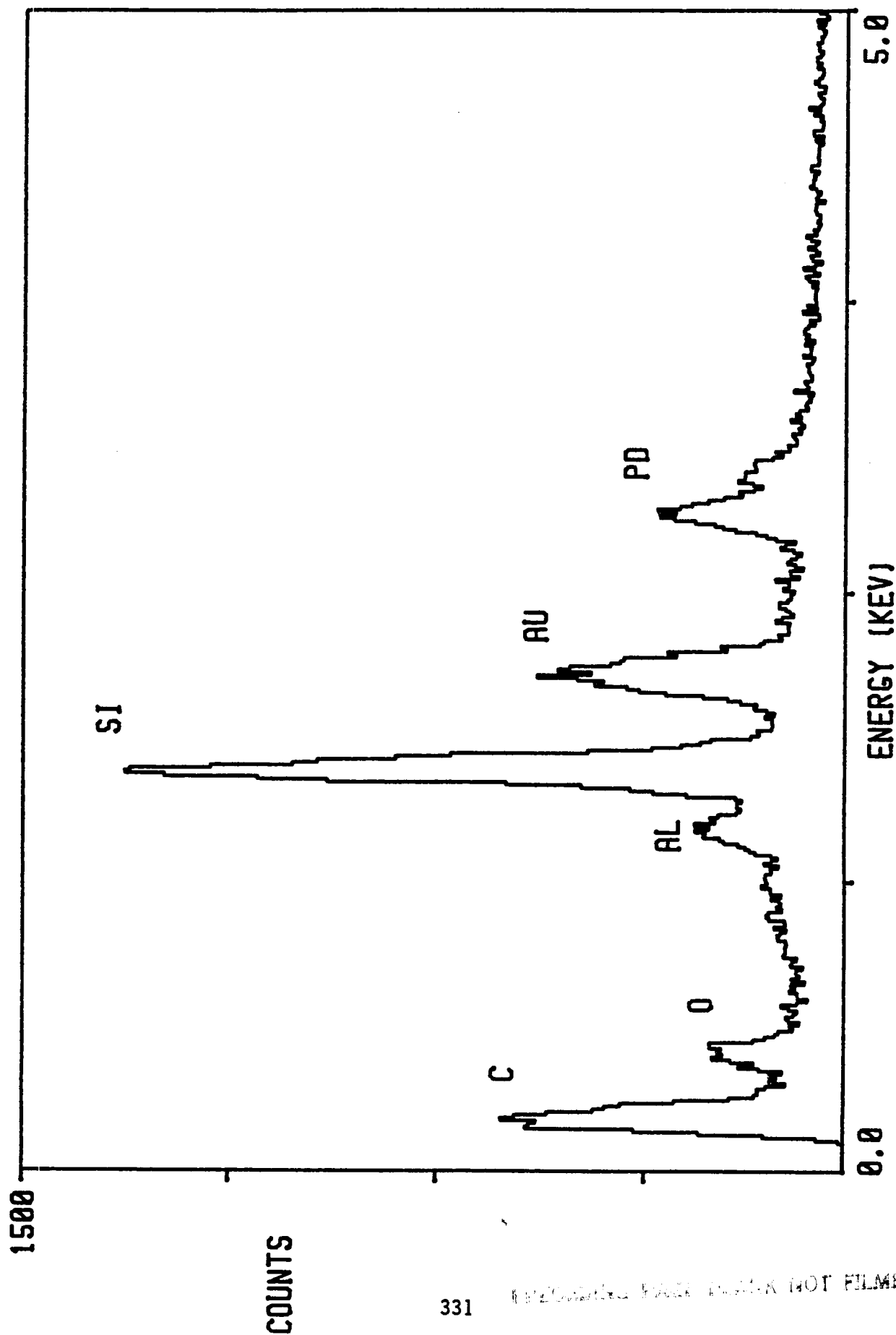


Figure 119: EDAX Spectrum of HMDS/TFE Coating on Kapton. Sample Previously Exposed to Combined Vacuum Thermal Cycling/UV Radiation

(THIS PAGE INTENTIONALLY LEFT BLANK)

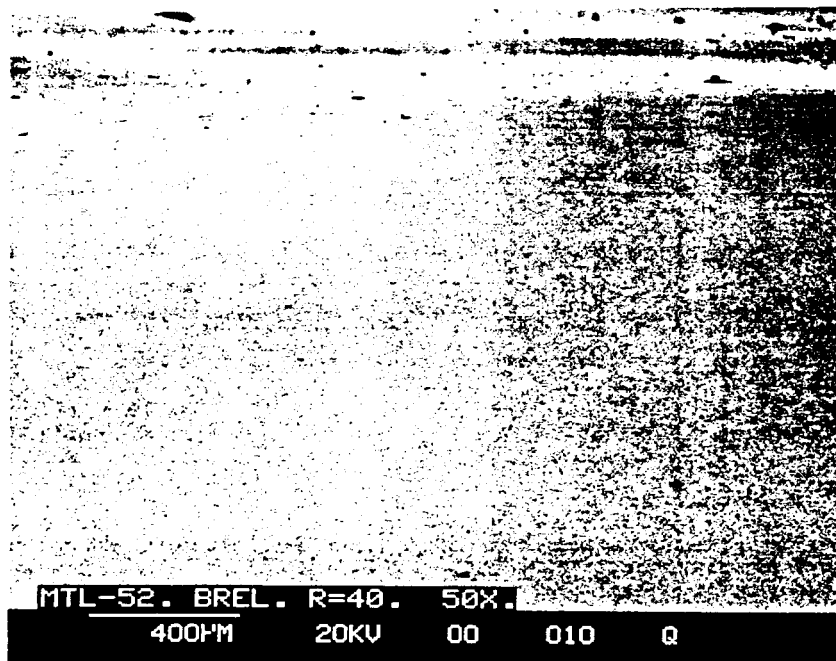


Figure 120: HMDS/TFE on Kapton Bent Over 40-Mil Radius. Sample Previously Exposed to Combined Vacuum Thermal Cycling/UV Radiation.

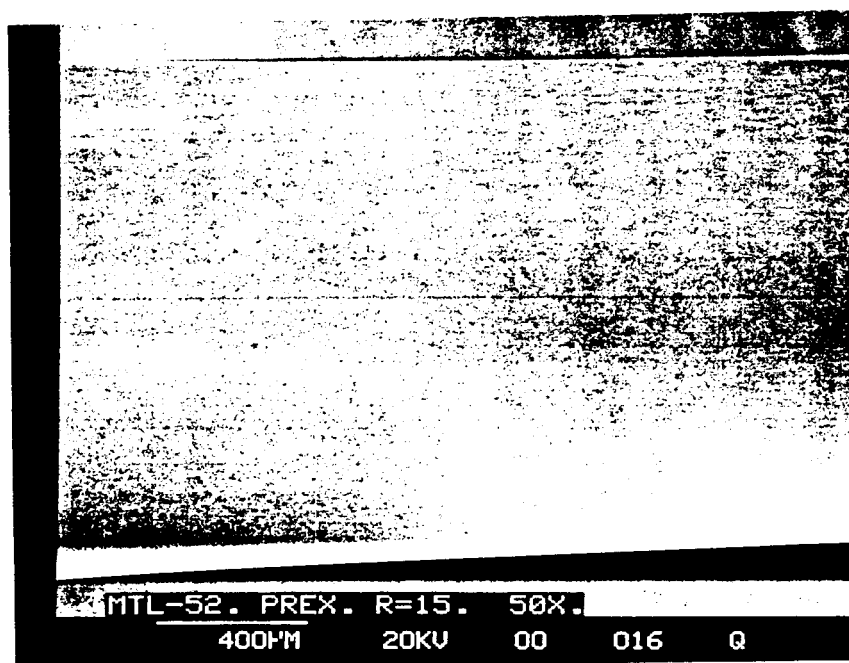


Figure 121: HMDS/TFE Coating on Kapton Bent Over 15-Mil Radius

Over a 15 mil Bend Diameter (Material #52). Description: No cracks were seen in the surface of this material. The horizontal lines seen in this picture are due to the auto-tracking contrast function of the SEM.

Figure 122:

Title: Mtl-52. PREX. R = 40. Photo #011. Magnification: 50X. Legend: Same as for 15, except over a 40 mil bend diameter. Description: Same as for 15.

Material #66: McGhan-NUSil CV1-3530 fluorosilicone coating on 1 mil Kapton film; BREL test #1; Au/Pd-coated for SEM analysis.

Figure 123:

Title: Mtl-66. BREL. R = 15. Photo #020. Magnification: 50X. Legend: Single Crack in Surface of McGhan-NuSil CV1-3530 Fluorosilicone Coating, After solar UV/Thermal Vacuum Cycling, Over a 15 mil Bend Diameter (Material #66). Legend: A single solitary crack was observed in the bend region of this sample. No other cracks were seen. EDAX analysis indicates a slight decrease in O and F, but not C, levels in the BREL tested material. These results are shown in figures 124 and 125.

Figure 126:

Title: Mtl-66. BREL. R = 40. Photo #017. Magnification: 200X. Legend: Cracks in Surface of McGhan-NuSil CV1-3530 Fluorosilicone Coating, After Solar UV/Thermal Vacuum Cycling, Over a 40 mil Bend Diameter (Material #66). Description: Many such cracks were in the coating as seen in this picture. The fact that similar cracking was not seen for the smaller bend diameter test of this material is not understood. The cracks observed in this sample may be an artifact due to handling.

Material #66: Same as above, but virgin as-received material; Au/Pd-coated for SEM analysis.

Figure 127:

Title: Mtl-66. PREX. R = 40. Photo #018. Magnification: 50X. Legend: Same as for 20, except over a 40 mil bend diameter. Description: Cracks over one side of this sample are seen here. Similar cracking occurred over the entire bend region.

Figure 128:

Title: Mtl-66. PREX. R = 15. Photo #022. Magnification: 600X. Legend: SEM Electron Beam Damage to McGhan-NuSil CV1-3530 Fluorosilicone Coating, Over a 15 mil Bend Diameter (Material #66).

Figure 129:

Title: Mtl-66. PREX. R = 15. Photo #021. Magnification: 50X. Legend: Cracks in Surface of As-Received McGhan-NuSIL CV1-3530 Fluorosilicone Coating, Over a 15 mil Bend Diameter (Material #66). Description: A view of two large, typical cracks seen in the surface of this coating. Note the auto-tracking contrast function was not used in this photo, resulting in wide contrast differences in the resulting picture.

Figure 130:

Title: Mtl-66. PREX R = 15. Photo #022. Magnification: 600X. Legend: SEM Electron Beam Damage to McGhan-NuSil CV1-3530 Fluorosilicone Coating, over a 15 mil bend diameter (Material #66).

X-Ray photoelectron spectroscopy is used to identify elements and provides a measurement of their relative abundance on the surface of a material to a depth of about 40 angstroms. Tables 35 and 36 show the relative abundance of species on coated surfaces after each particular exposure to atomic oxygen. Figures 131 through 143 show the spectra from which the surface composition data were obtained.

(THIS PAGE INTENTIONALLY LEFT BLANK)

ORIGINAL PAGE IS
OF POOR QUALITY

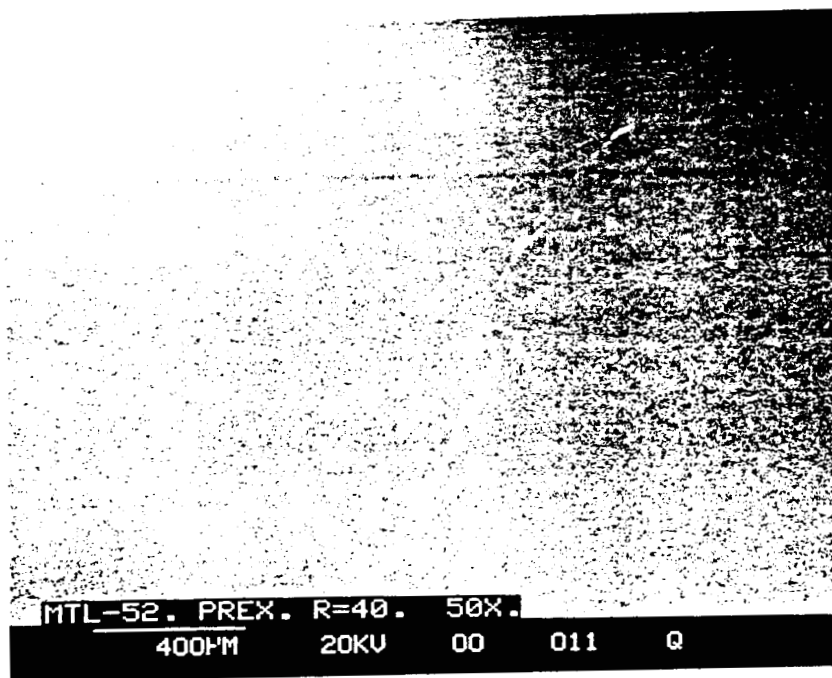


Figure 122: HMDS/TFE Coating on Kapton Bent Over 40-Mil Radius

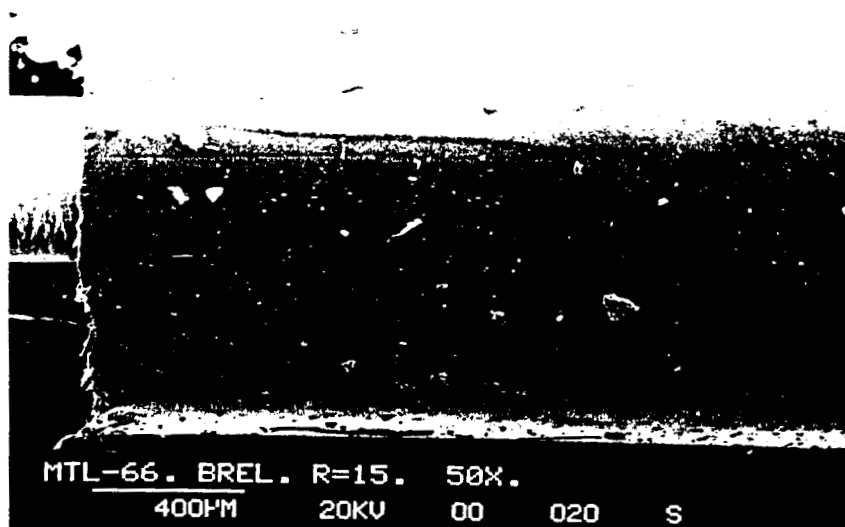


Figure 123: CVI-3530 Fluorosilicone Coating (#66) on Kapton Bent Over 15-Mil Radius. Sample Previously Exposed to Combined Vacuum Thermal Cycling/UV Radiation.

(THIS PAGE INTENTIONALLY LEFT BLANK)

KAP71.

MTL-66. PREX.

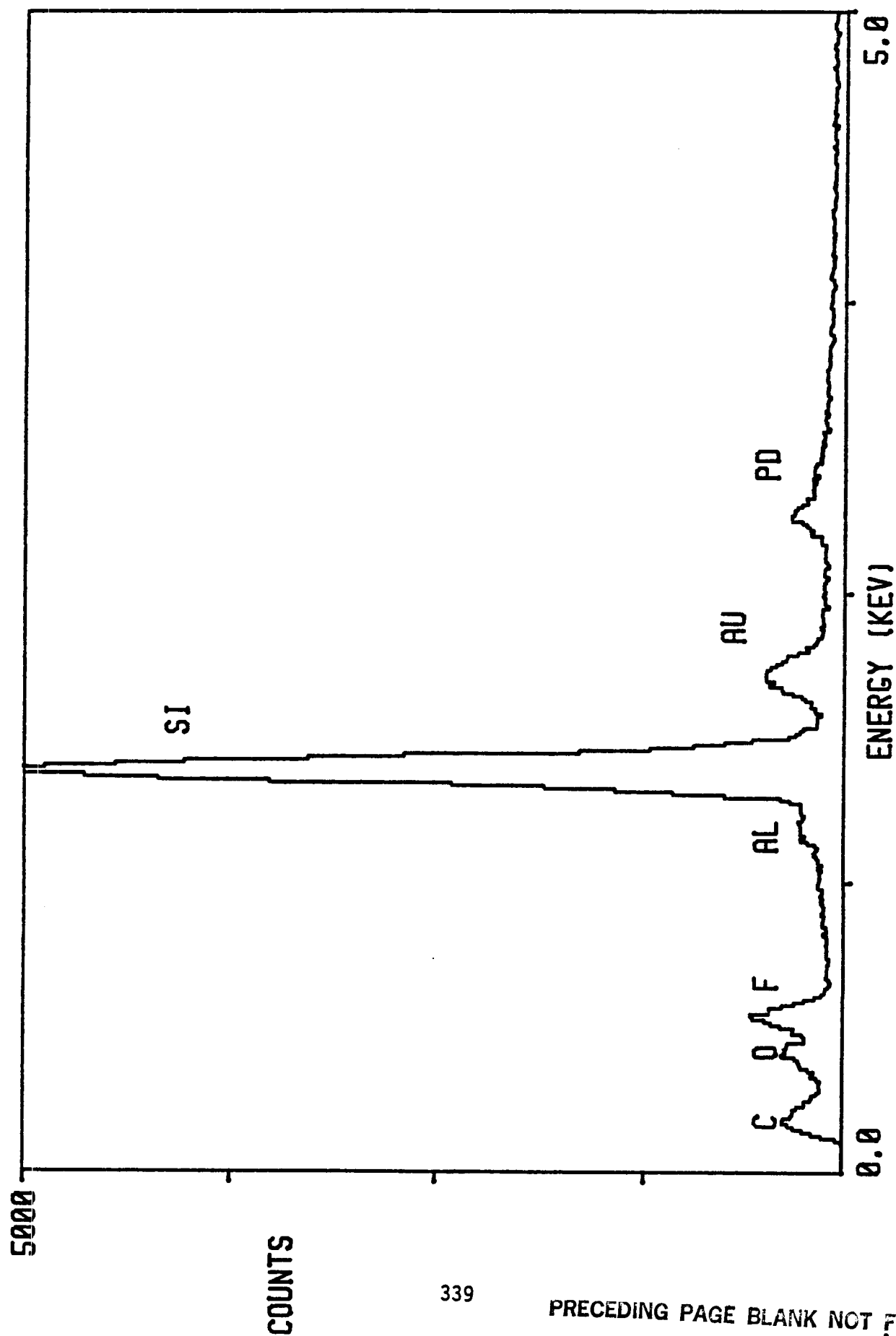


Figure 124: EDAX Spectrum of CV1-3530 Fluorosilicone Coating (#66) on Kapton

(THIS PAGE INTENTIONALLY LEFT BLANK)

KAP7H.

MTL-66. BREL.

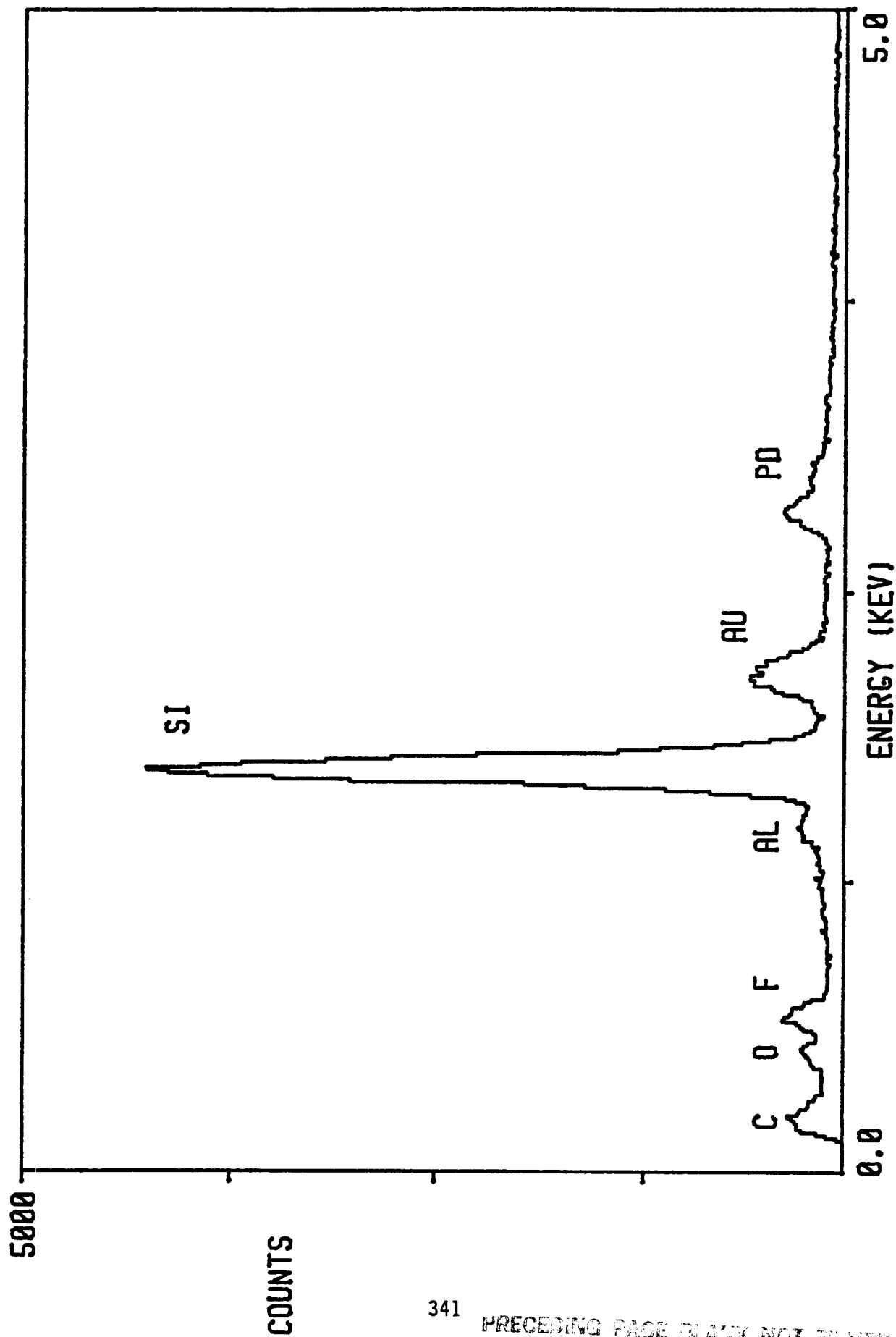


Figure 125: EDAX Spectrum of CVI-3530 Coating on Kapton. Sample Previously Exposed to Combined Vacuum Thermal Cycling/UV Radiation

(THIS PAGE INTENTIONALLY LEFT BLANK)

ORIGINAL PAGE IS
OF POOR QUALITY

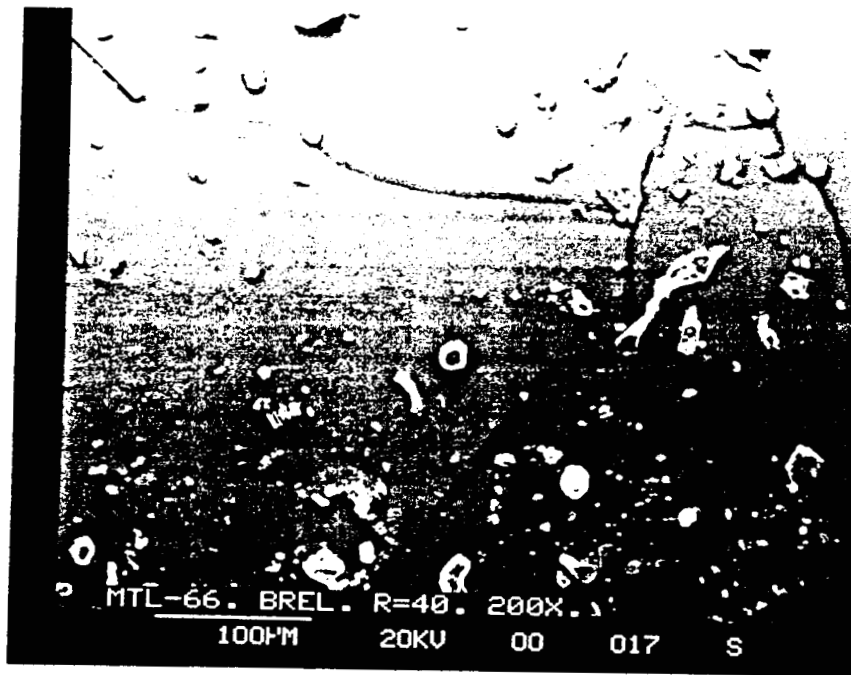


Figure 126: CVI-3530 Fluorosilicone Coating on Kapton Bent Over a 40-Mil Radius. Sample Previously Exposed to Combined Vacuum Thermal Cycling/UV Radiation.



Figure 127: CVI-3530 Fluorosilicone Coating on Kapton Bent Over 40-Mil Radius

(THIS PAGE INTENTIONALLY LEFT BLANK)

ORIGINAL PAGE IS
OF POOR QUALITY

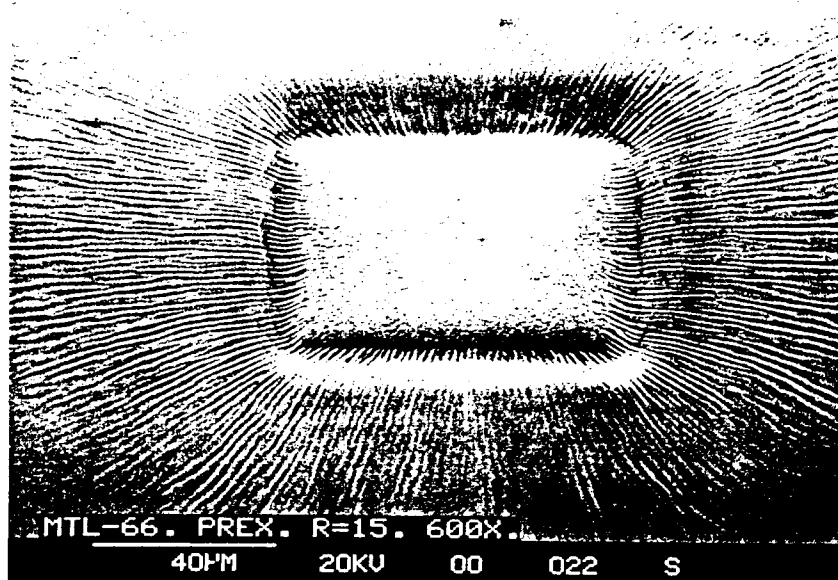


Figure 128: SEM Beam Damage to Previously Identified Region of CVI-3530 Fluorosilicone Coating (#66) on Kapton Bent Over 15-Mil Radius

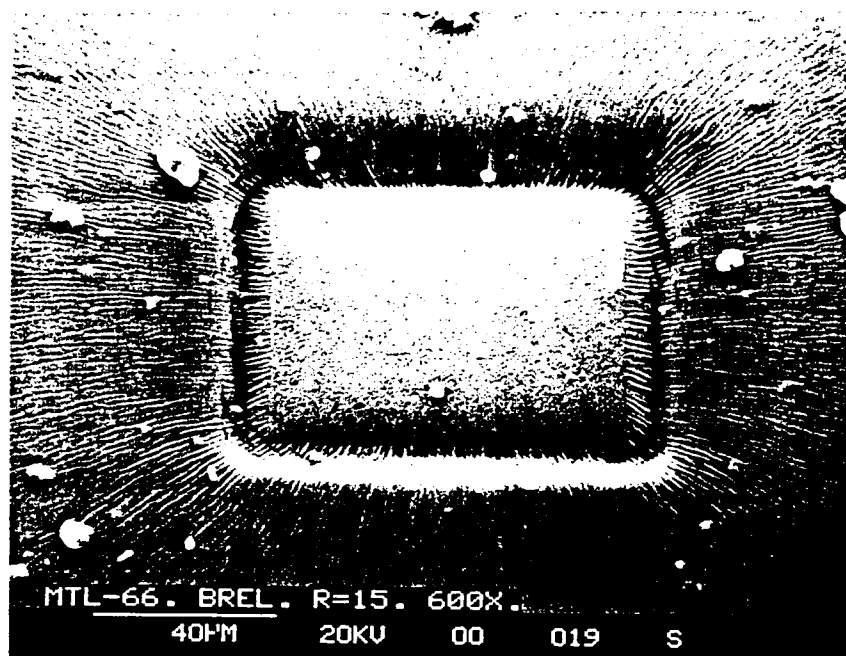


Figure 129: SEM Beam Damage to Previously Identified Region of CVI-3530 Fluorosilicone Coating (#66) on Kapton Bent Over 15-Mil Radius. Sample Previously Exposed to Combined Vacuum Thermal Cycling/UV Radiation

(THIS PAGE INTENTIONALLY LEFT BLANK)

ORIGINAL PAGE IS
OF POOR QUALITY

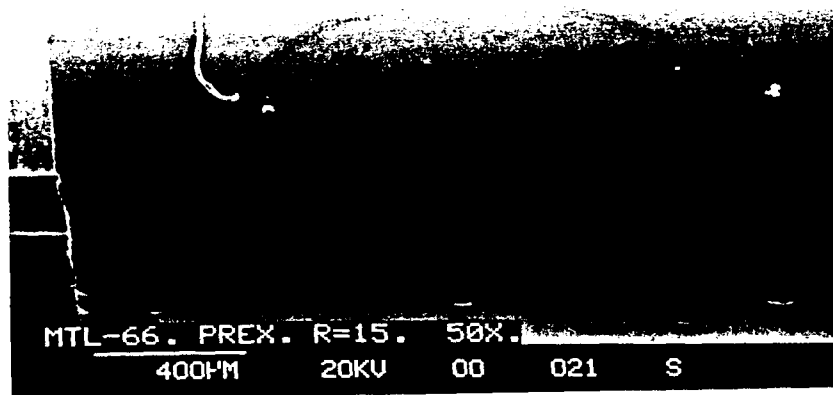


Figure 130: CVI-3530 Fluorosilicone Coating on Kapton Bent Over 15-Mil Radius

PRECEDING PAGE BLANK NOT FILMED

(THIS PAGE INTENTIONALLY LEFT BLANK)

Upon examination of the spectra the following points become evident. First, of all the unexposed specimens only the phosphazene coating has a peak which signifies the presence of nitrogen.

This result is as expected, none of the other coatings contain nitrogen. Second, after exposure to atomic oxygen for various times, no nitrogen can be observed in the spectra of the specimens of materials 65 and 66. These coatings are greater than 0.1 mil thick and again the results are expected. However, the spectra of coatings of materials numbers 110 and 112, which are very thin (<20000 A), plasma polymerized coatings from Battelle, do show small nitrogen peaks, after exposure to atomic oxygen. This fact is significant because neither of these coatings materials contains nitrogen. The presence of nitrogen, coupled with the fact that this analysis technique probes at most only to 50 A depth means that a source of nitrogen has reached the surface of this material. The Kapton polyimide substrate, over which the coatings are deposited, contains about 5 mole percent nitrogen. The data for these specimens indicates that the ultra thin coatings have at least partially failed and that the Kapton is exposed in places. There is no step in the plasma polymerization process which would cause nitrogen to be introduced into the coatings. There is no step in the exposure to atomic oxygen that would cause nitrogen to be added to some coatings and not others. The point is while the Battelle coatings are excellent on a lifetime per unit weight basis, they are 50 to 250 times thinner than the other coatings we are examining. Third, each material shows a clear increase in the fraction of oxygen on the surface subsequent to exposure to atomic oxygen. This is expected, the oxygen atoms are very reactive. Furthermore, the ratio of silicone to carbon increases upon exposure, the carbon based product species are more volatile than the silica which is formed upon oxidation of the silicone.

For several of the polymers being examined here, the carbon containing groups are primarily side groups and are more readily available to be attacked by the incoming oxygen atoms.

In the Battelle coatings produced by the plasma polymerization process, the carbon and silicone species are more highly crosslinked than in the linear chain polymers. The carbon atoms are not necessarily in clearly distinguishable side groups. The fact that the silicone to carbon ratio in these polymers does not increase upon exposure to atomic oxygen indicates that removal of carbon disrupts the essential structure of the polymer leading to simultaneous loss of silicone. Whether the species leave together or as separate independent events is not clear.

Table 37 provides the results of a repeat measurement on the effects of atomic oxygen exposure on the surface of a material. The results of XPS analysis again show nitrogen present on the surface.

Table 38 shows results of XPS analysis of the materials whose XPS spectra are shown in figures 131 through 143.

<u>SPECIMEN</u>	<u>ATOMIC OXYGEN EXPOSURE (HOURS)</u>	<u>ELEMENT</u>	<u>MOLE PERCENT</u>	<u>RATIOS RELATIVE TO CARBON</u>
#65	-	O	21.1	0.41
		C	51.6	1.0
		Si	27.2	0.53
#65	48	O	32.7	0.88
		C	37.2	1.0
		Si	30.1	0.81
#66	-	O	13.9	0.31
		C	44.9	1.0
		Si	15.1	0.34
		F	26.0	0.58
#66	24	O	33.5	1.32
		C	25.3	1.0
		Si	24.3	0.96
		F	17.0	0.67
#128	-	O	19.8	0.47
		C	42.0	1.0
		Si	7.4	0.18
		F	27.3	0.65
		P	3.6	0.09
#128	49	O	23.1	0.58
		C	39.7	1.0
		Si	13.6	0.34
		F	17.6	0.44
		N	2.7	0.07
		P	3.2	0.08

Table 35: Results of X-Ray Photoelectron Spectroscopy Surface Analysis on Coating Specimens Coating Thickness Greater Than 0.1 Mil.

(THIS PAGE INTENTIONALLY LEFT BLANK)

<u>SPECIMEN</u>	<u>ATOMIC OXYGEN EXPOSURE (HOURS)</u>	<u>ELEMENT</u>	<u>MOLE PERCENT</u>	<u>RATIOS RELATIVE TO CARBON</u>
#110	0	O	19.9	0.42
		C	47.1	1.0
		Si	32.8	0.70
#110	48	O	42.4	1.43
		C	29.7	1.0
		Si	27.7	0.92
#110	25	O	47.4	2.25
		N	0.3	0.01
		C	21.1	1.0
		Si	31.1	1.47
#112	0	O	18.4	0.38
		C	48.9	1.0
		Si	29.7	0.61
		F	3.0	0.06
#112	95.75	O	31.5	0.17
		C	46.9	1.0
		Si	20.9	0.45
		F	0.8	0.02
#112	95.75	O	29.9	0.59
		N	2.0	0.04
		C	50.4	1.0
		Si	17.7	0.35

Table 36: Results of X-Ray Photoelectron Spectroscopy
Surface Analysis on Ultrathin (20000 Å)
Coatings From Battelle

PRECEDING PAGE BLANK NOT FILMED

(THIS PAGE INTENTIONALLY LEFT BLANK)

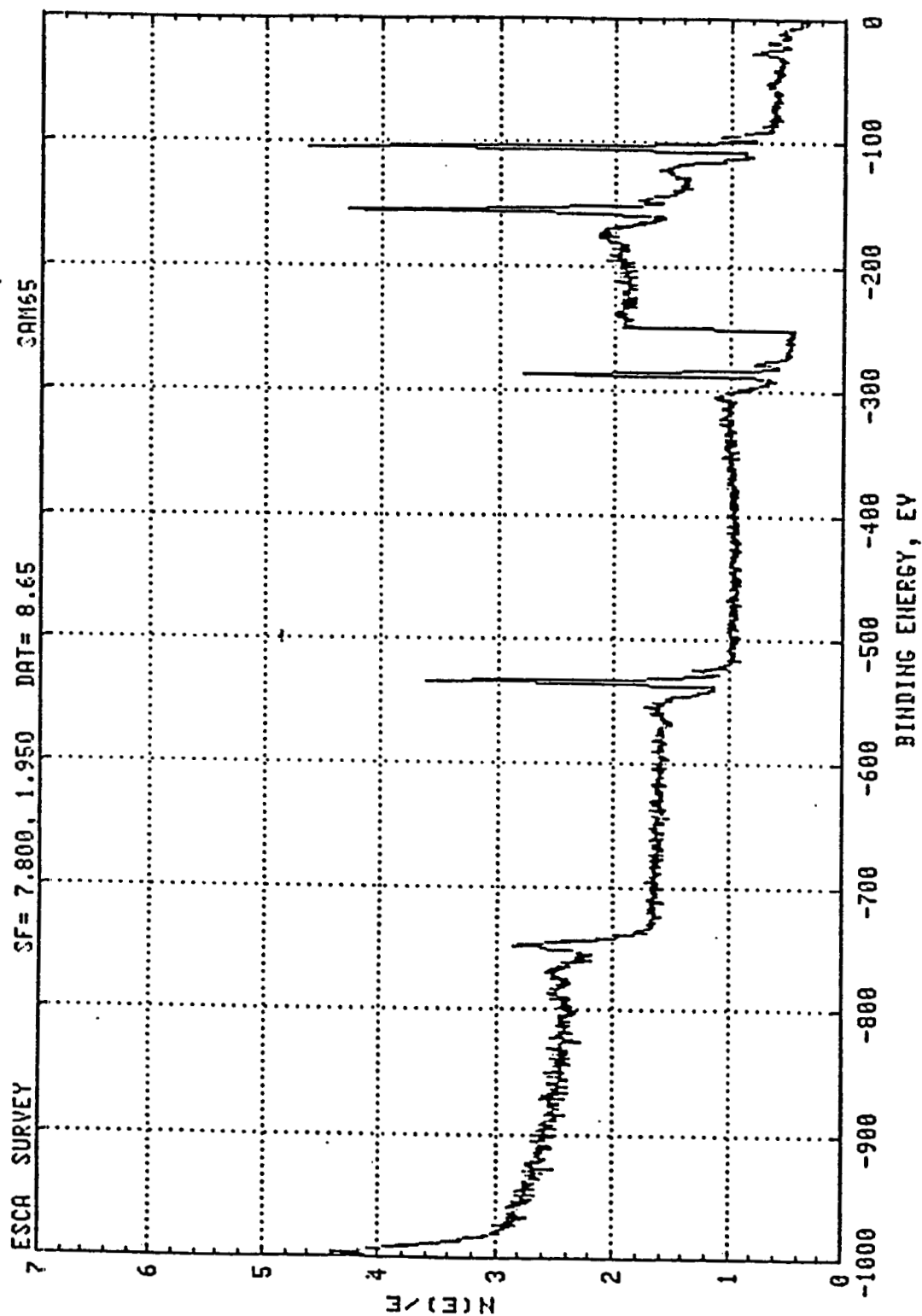


Figure 131: X-Ray Photoelectron Spectrum of CVI-1144-0 (Silicone) Coating on Kapton. The Sample was not Previously Exposed to Atomic Oxygen.

(THIS PAGE INTENTIONALLY LEFT BLANK)

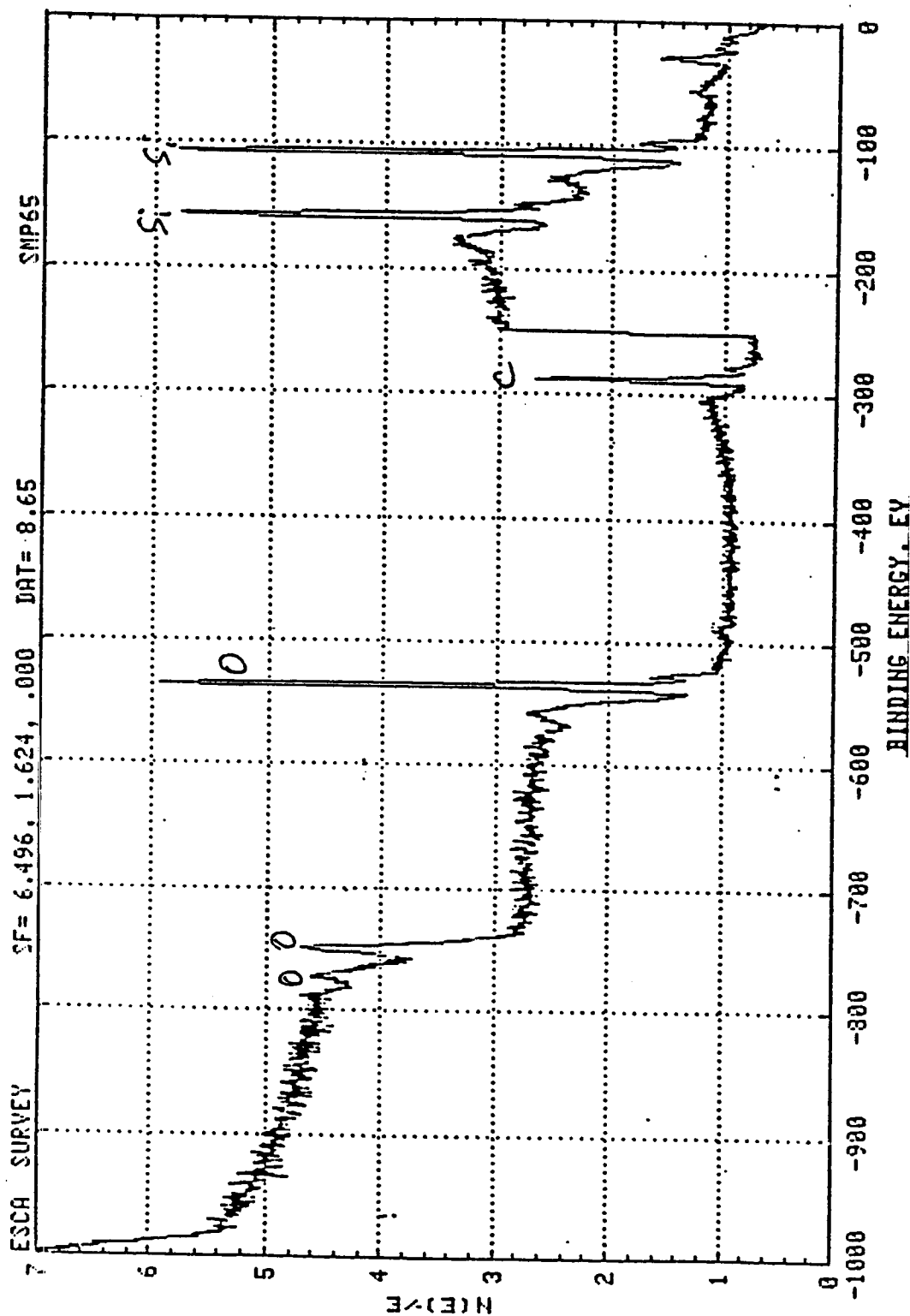


Figure 132: X-Ray Photoelectron Spectrum of CVI-1144-0 (Silicone) Coating on Kapton. The Sample was Previously Exposed to Atomic Oxygen for 48 Hours.

(THIS PAGE INTENTIONALLY LEFT BLANK)

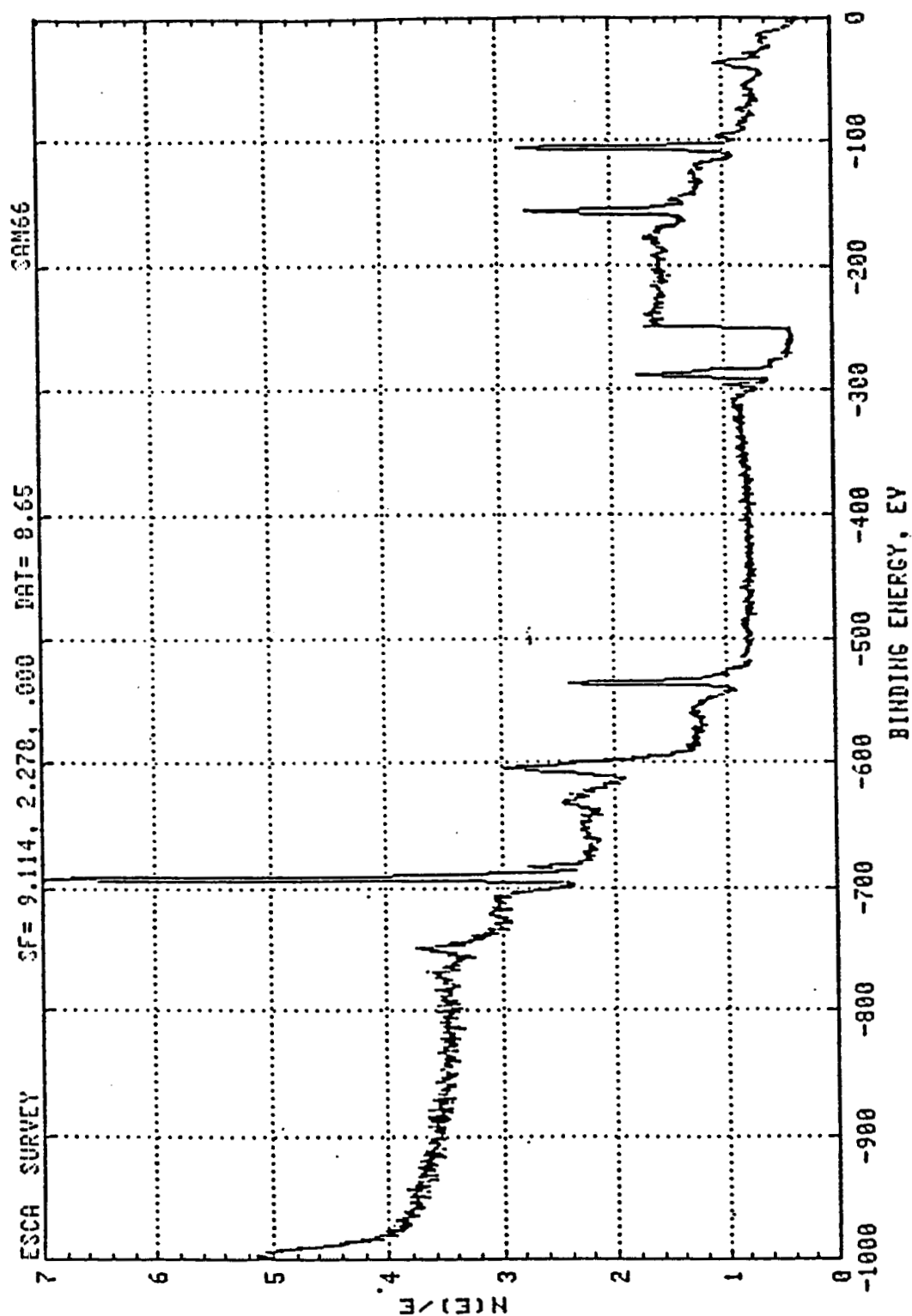


Figure 133: X-Ray Photoelectron Spectrum of CV-3530 (Fluorosilicone) Coating on Kapton. The Sample was not Previously Exposed to Atomic Oxygen.

(THIS PAGE INTENTIONALLY LEFT BLANK)

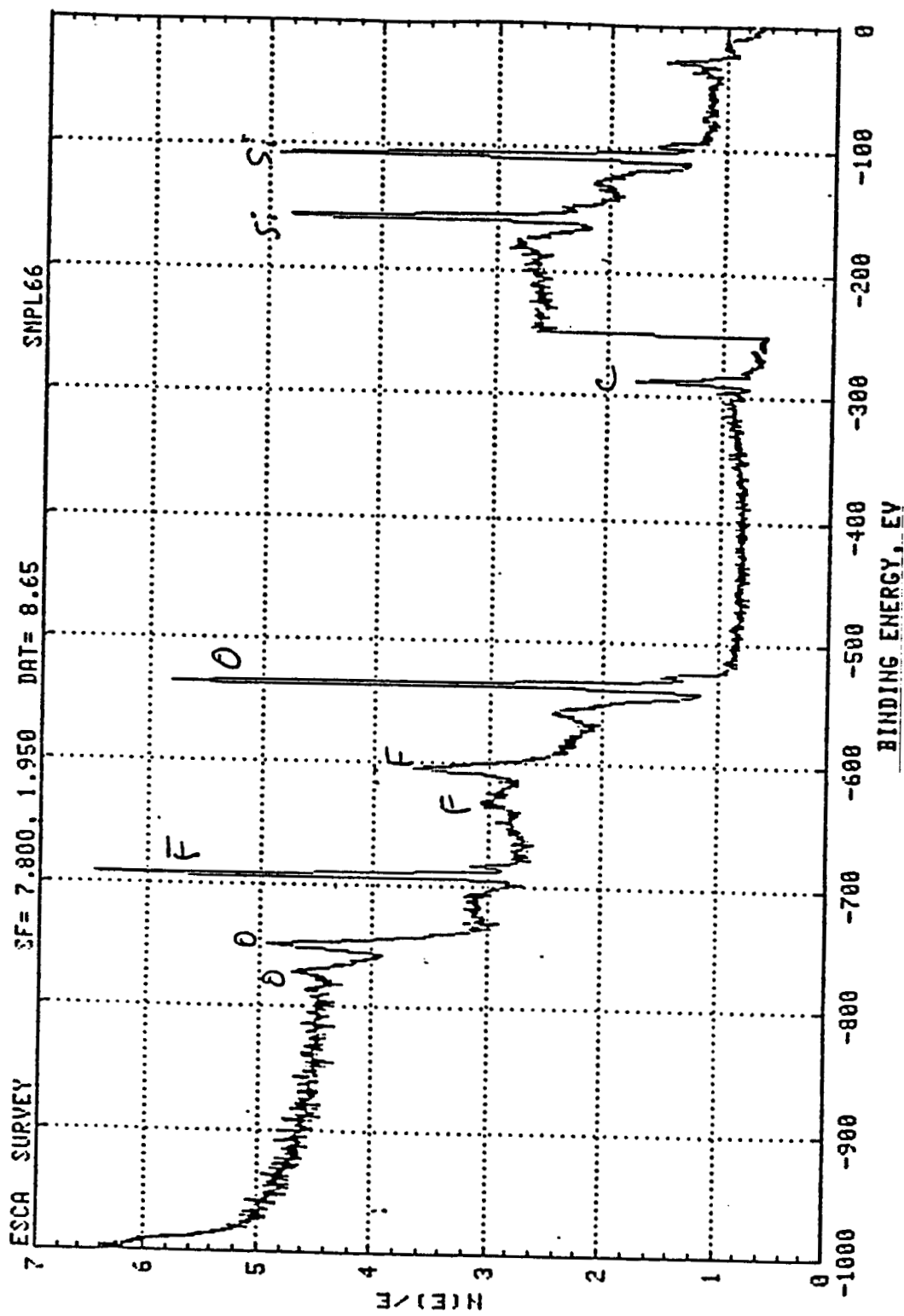


Figure 134: X-Ray Photoelectron Spectrum of CV-3530 (Fluorosilicone) Coating on Kapton. The Sample was Previously Exposed to Atomic Oxygen for 24 Hours.

(THIS PAGE INTENTIONALLY LEFT BLANK)

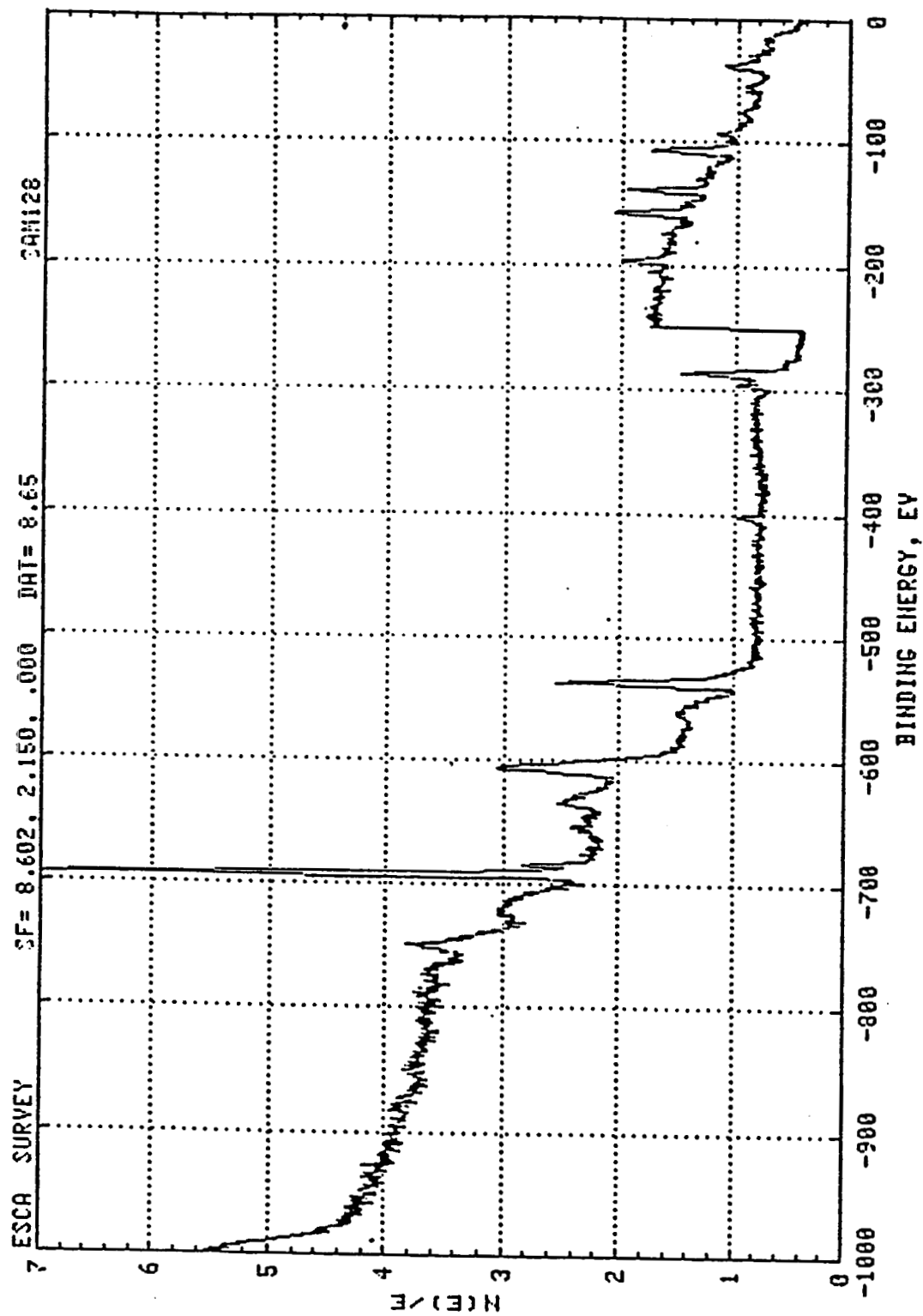


Figure 135: X-Ray Photoelectron Spectrum of X-128 (Phosphazene) Coating on Kapton. The Sample was not Previously Exposed to Atomic Oxygen.

(THIS PAGE INTENTIONALLY LEFT BLANK)

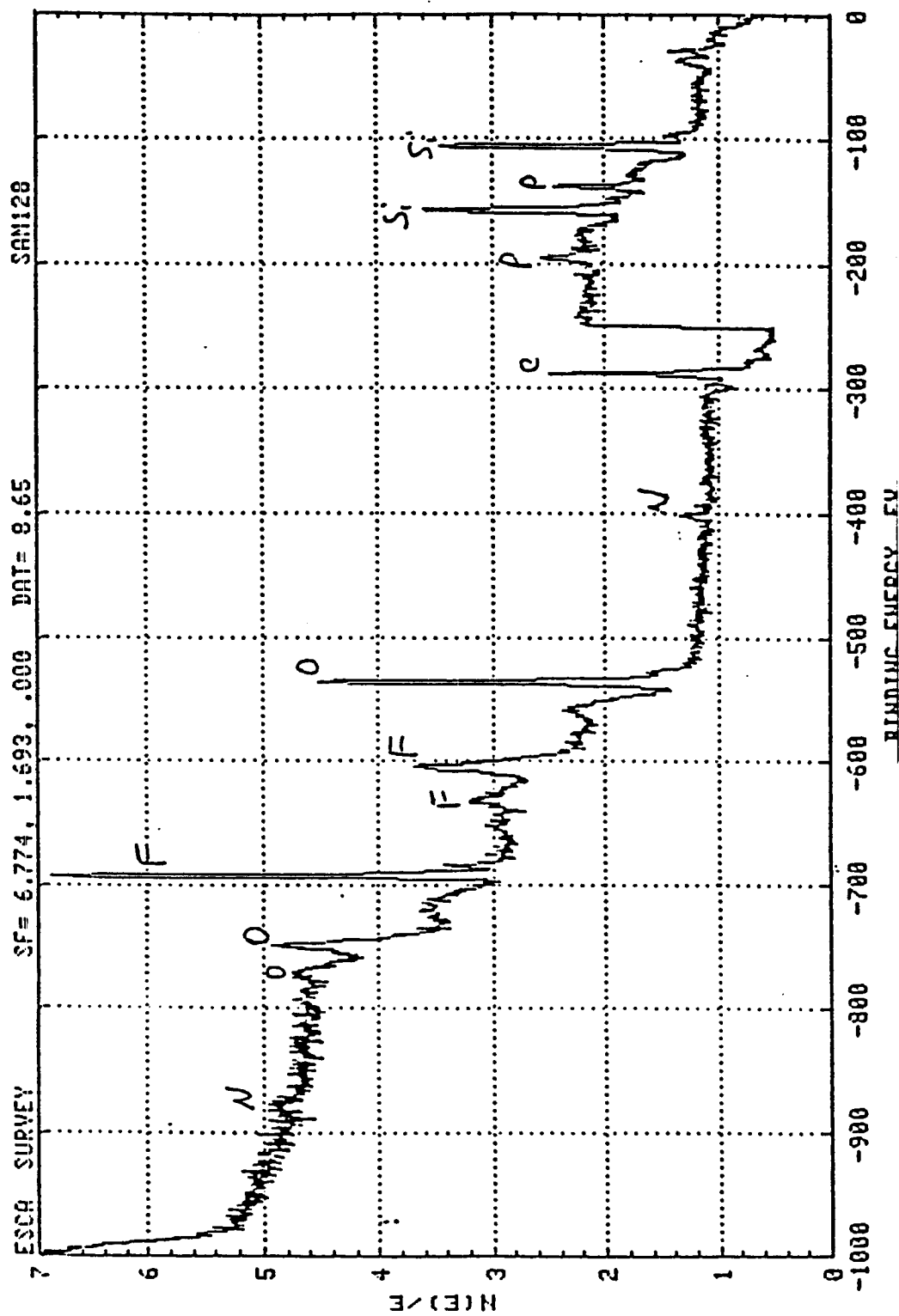


Figure 136: X-Ray Photoelectron Spectrum of X-128 (Phosphazene) Coating on Kapton. The Sample was Previously Exposed to Atomic Oxygen for 49 Hours.

(THIS PAGE INTENTIONALLY LEFT BLANK)

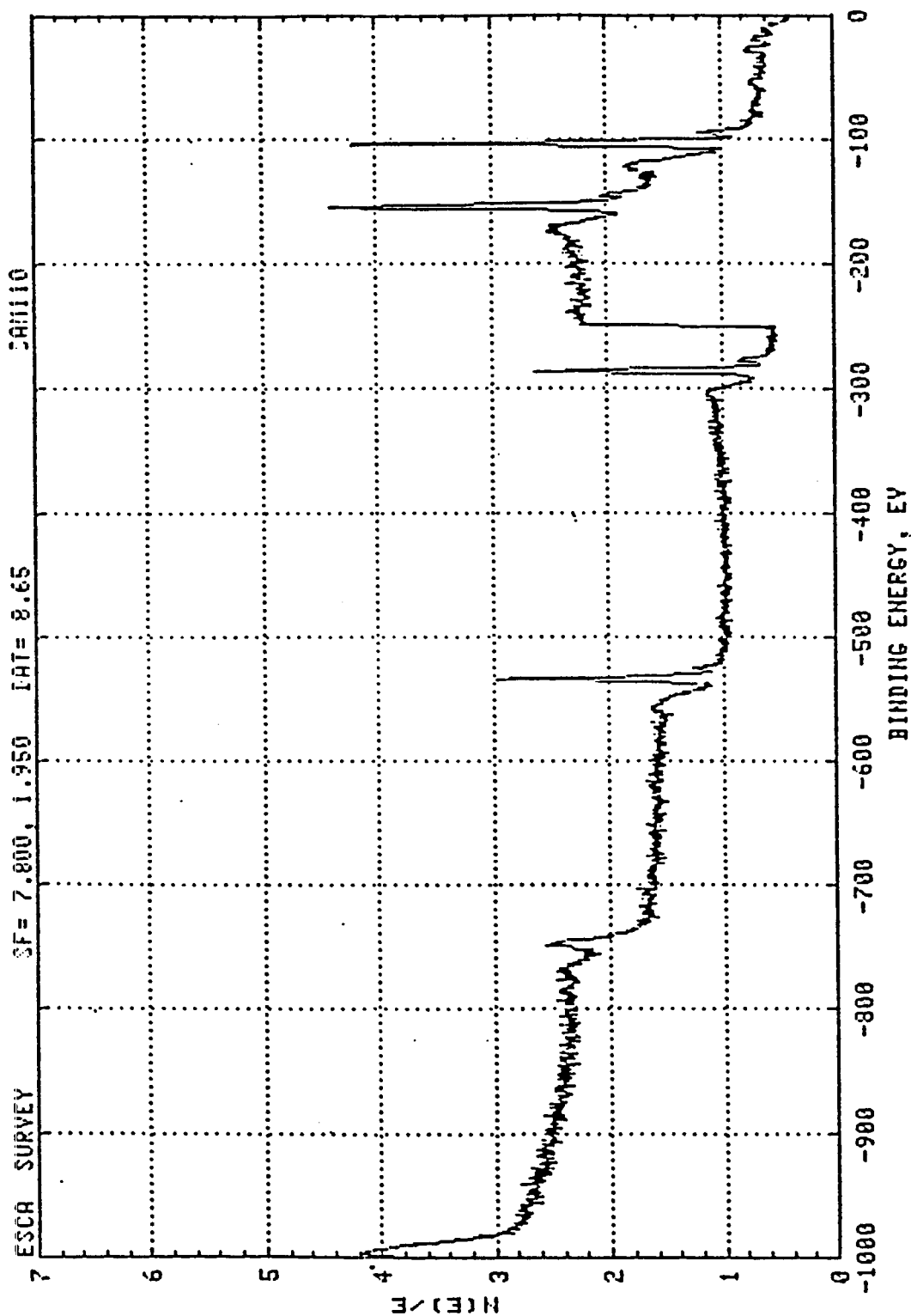


Figure 137: X-Ray Photoelectron Spectrum of Plasma Polymerized Hexamethyldisiloxane Coating on Kapton. The Sample was not Previously Exposed to Atomic Oxygen.

(THIS PAGE INTENTIONALLY LEFT BLANK)

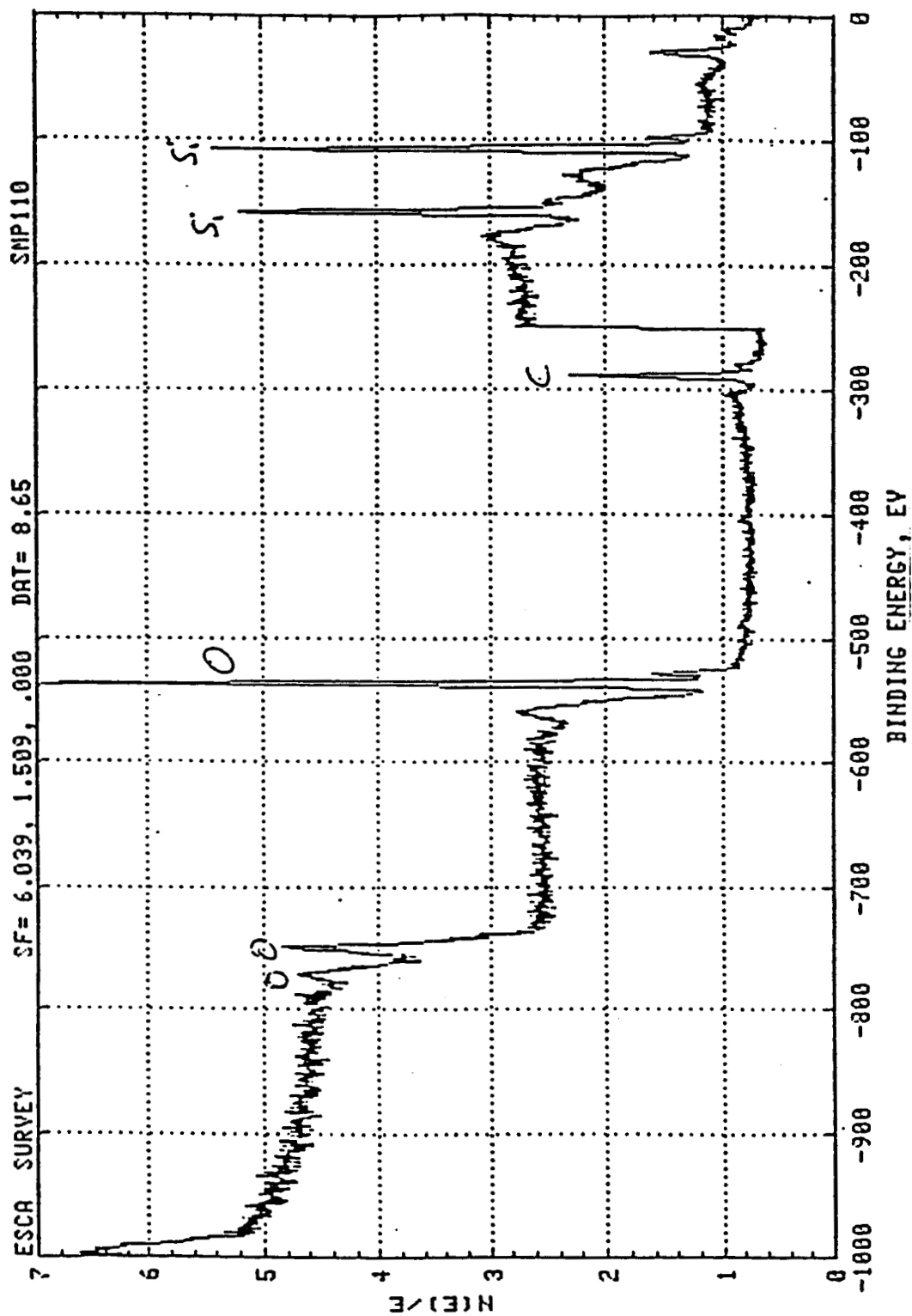


Figure 138: X-Ray Photoelectron Spectrum of Plasma Polymerized Hexamethyldisiloxane Coating on Kapton. The Sample was Previously Exposed to Atomic Oxygen for 48 Hours.

(THIS PAGE INTENTIONALLY LEFT BLANK)

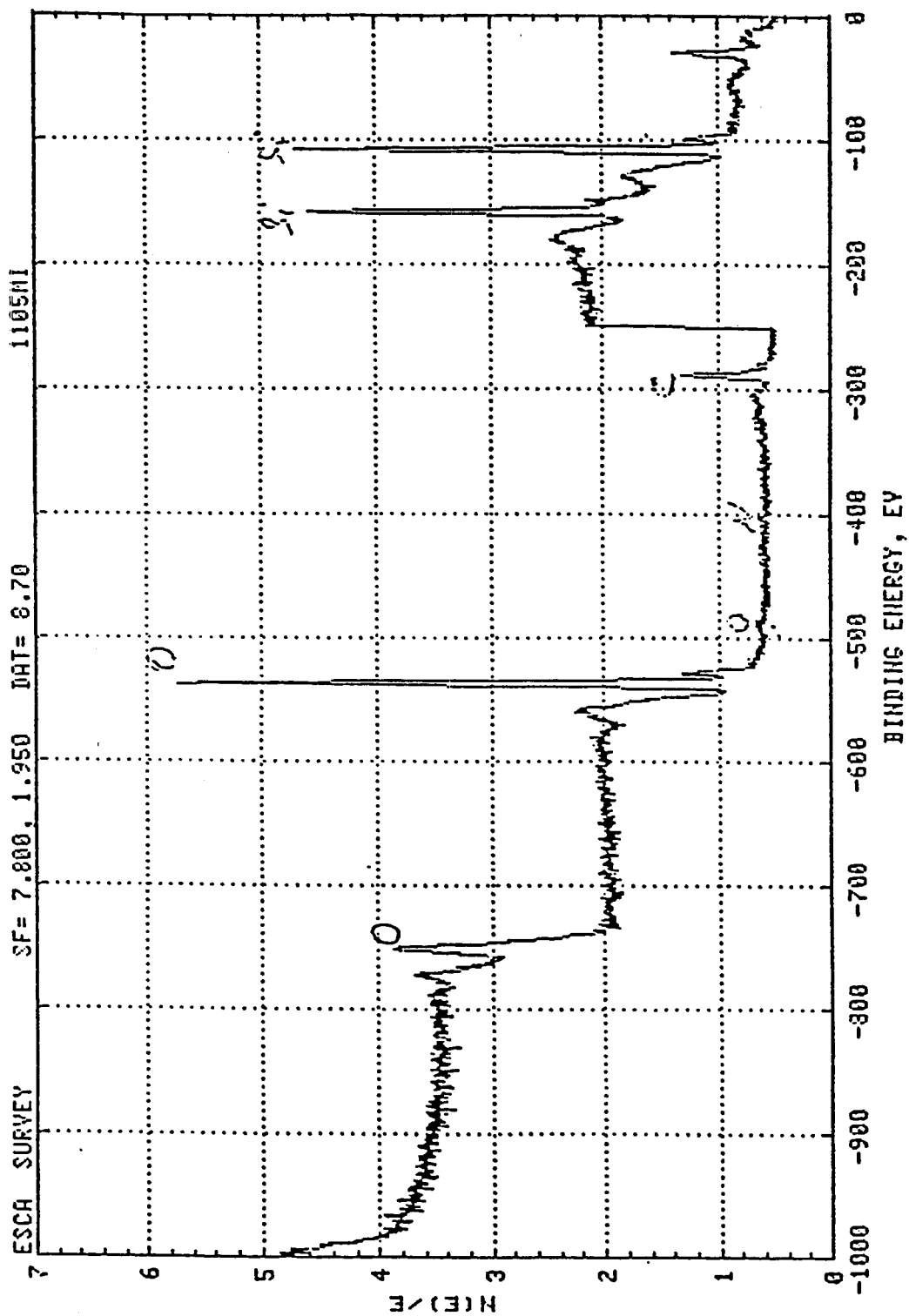


Figure 139: X-Ray Photoelectron Spectrum of Plasma Polymerized Hexamethyldisiloxane Coating on Kapton. The Sample was Previously Exposed to Atomic Oxygen for 25 Hours.

(THIS PAGE INTENTIONALLY LEFT BLANK)

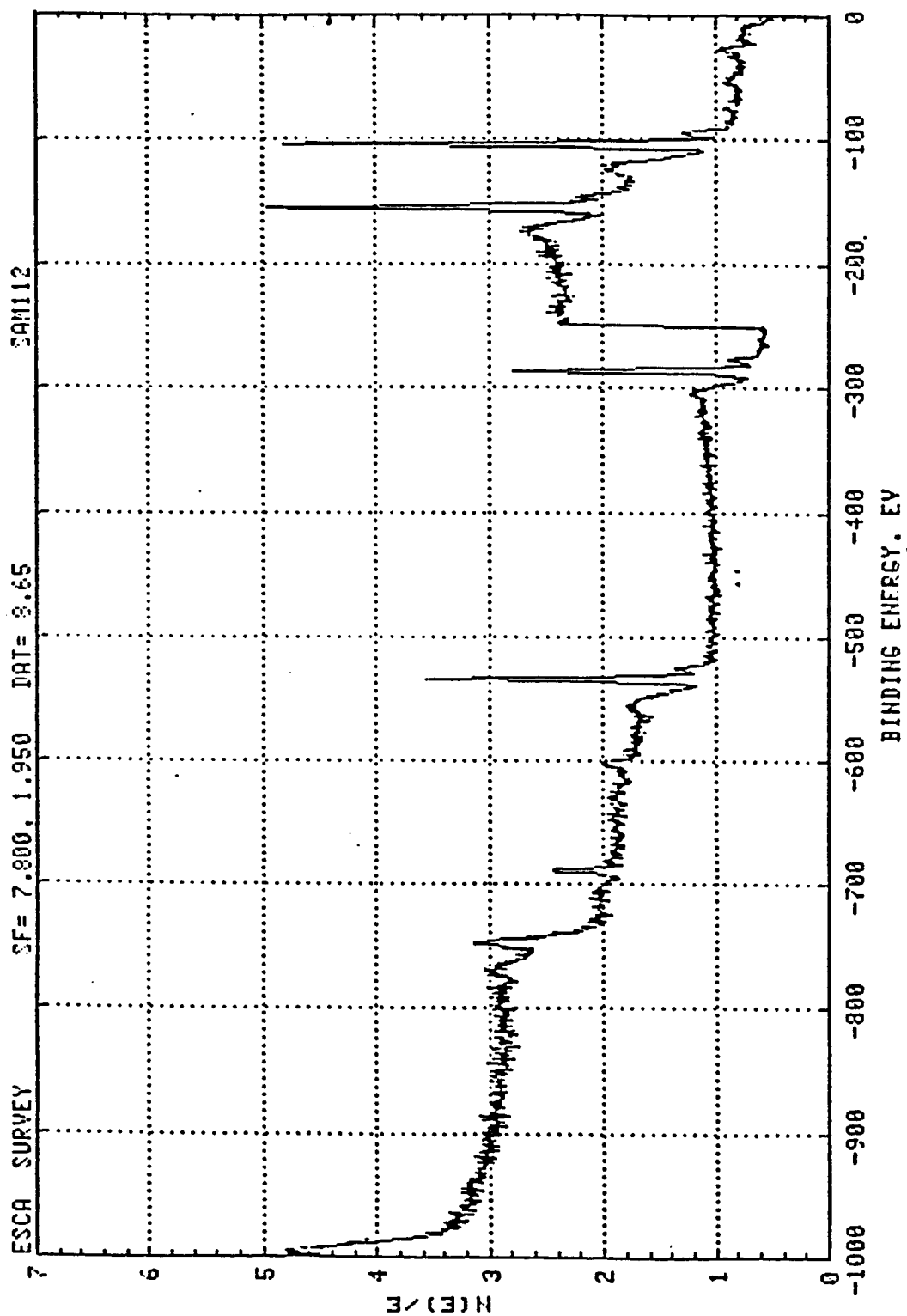


Figure 140: X-Ray Photoelectron Spectrum of Plasma Polymerized Hexamethyldisiloxane/Tetrafluoroethylene Coating on Kapton. The Sample was not Previously Exposed to Atomic Oxygen.

PRECEDING PAGE BLANK NOT FILMED

(THIS PAGE INTENTIONALLY LEFT BLANK)

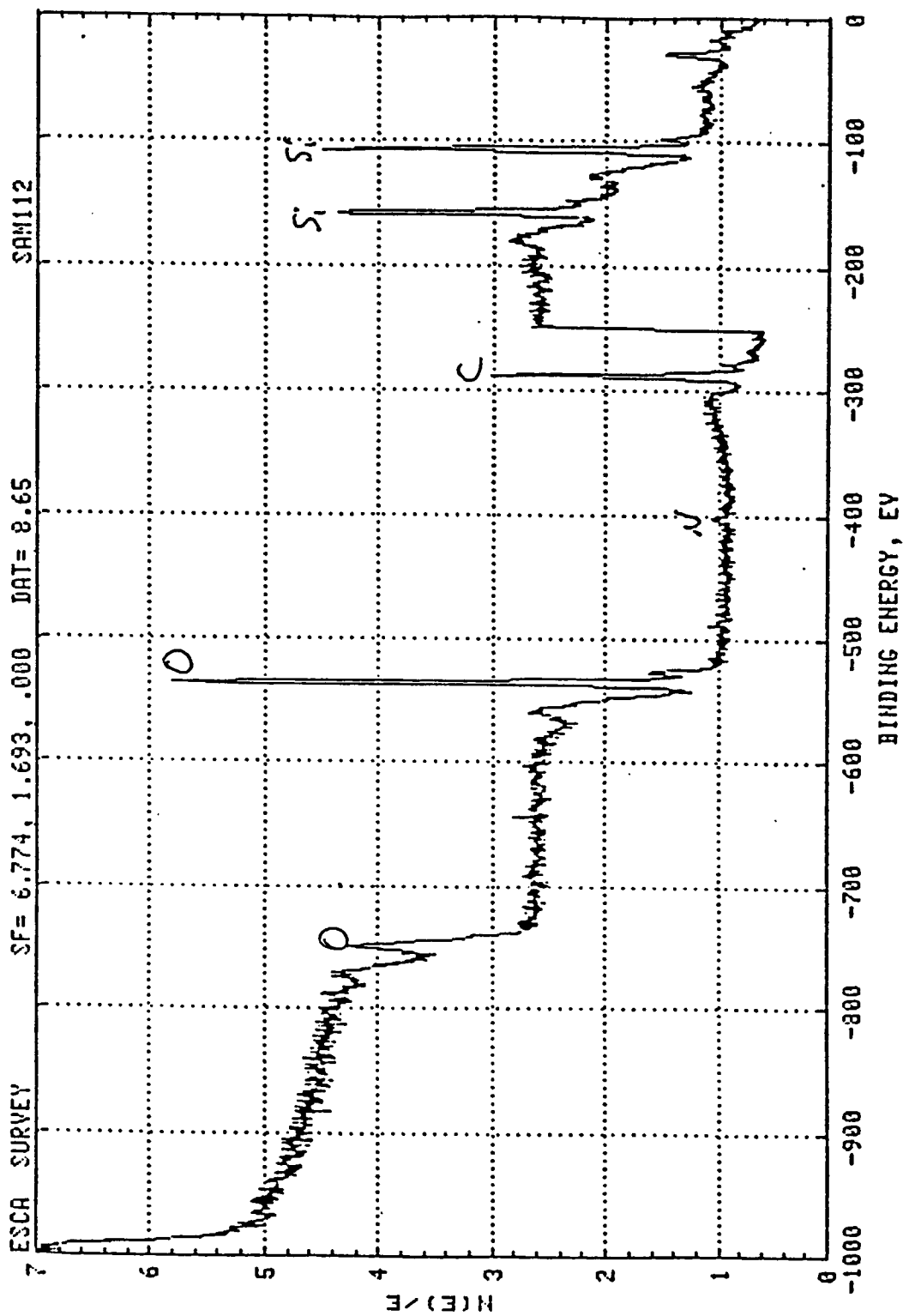


Figure 141: X-Ray Photoelectron Spectrum of Plasma Polymerized Hexamethyl-disiloxane/Tetrafluoroethylene Coating on Kapton. The Sample was Previously Exposed to Atomic Oxygen for 95.75 Hours.

PRECEDING PAGE BLANK NOT FILMED

(THIS PAGE INTENTIONALLY LEFT BLANK)

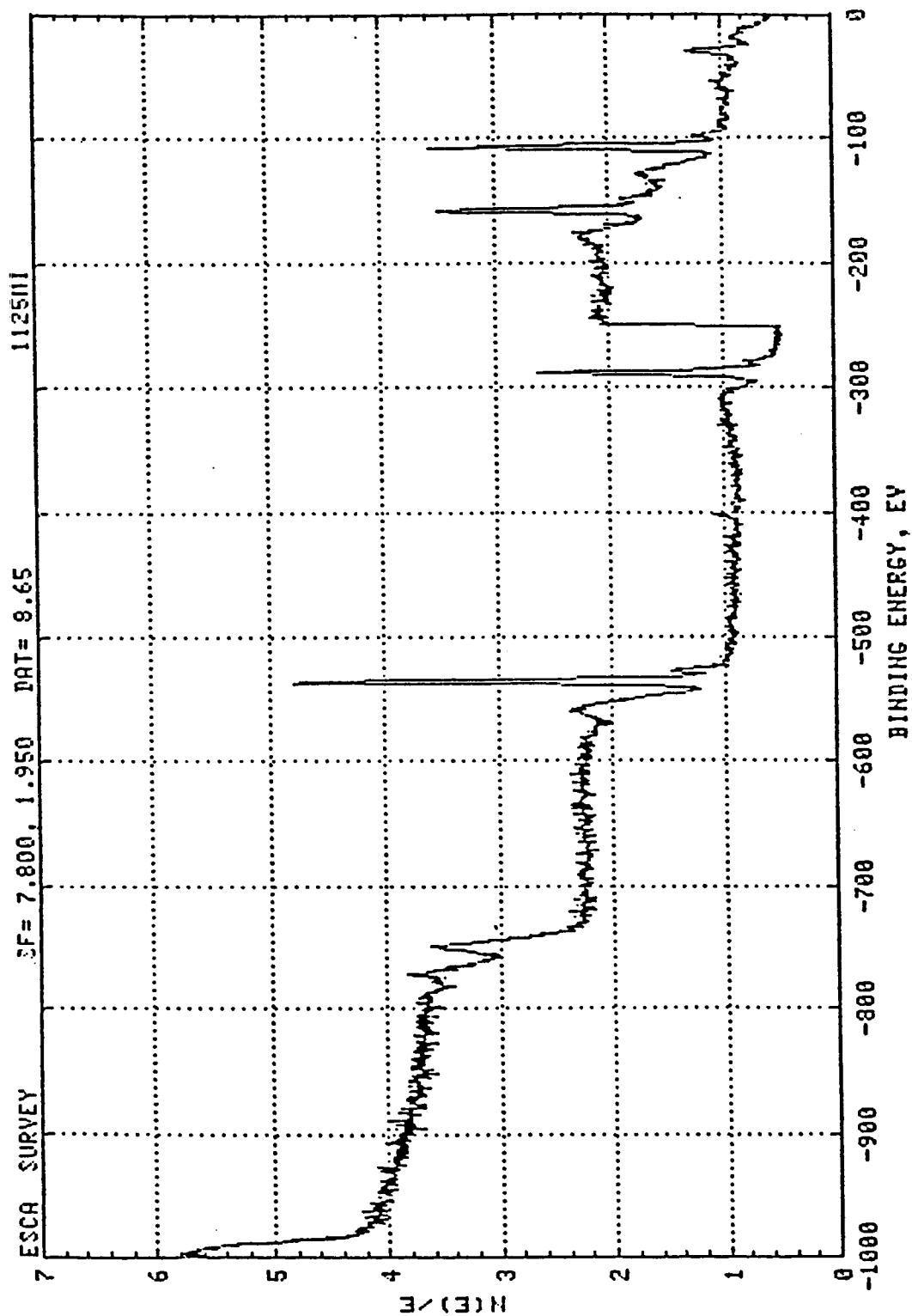


Figure 142: X-Ray Photoelectron Spectrum of Plasma Polymerized Hexamethyl-
disiloxane/Tetrafluorethylene Coating on Kapton. The Sample was
Previously Exposed to Atomic Oxygen for 95.75 Hours.

(THIS PAGE INTENTIONALLY LEFT BLANK)

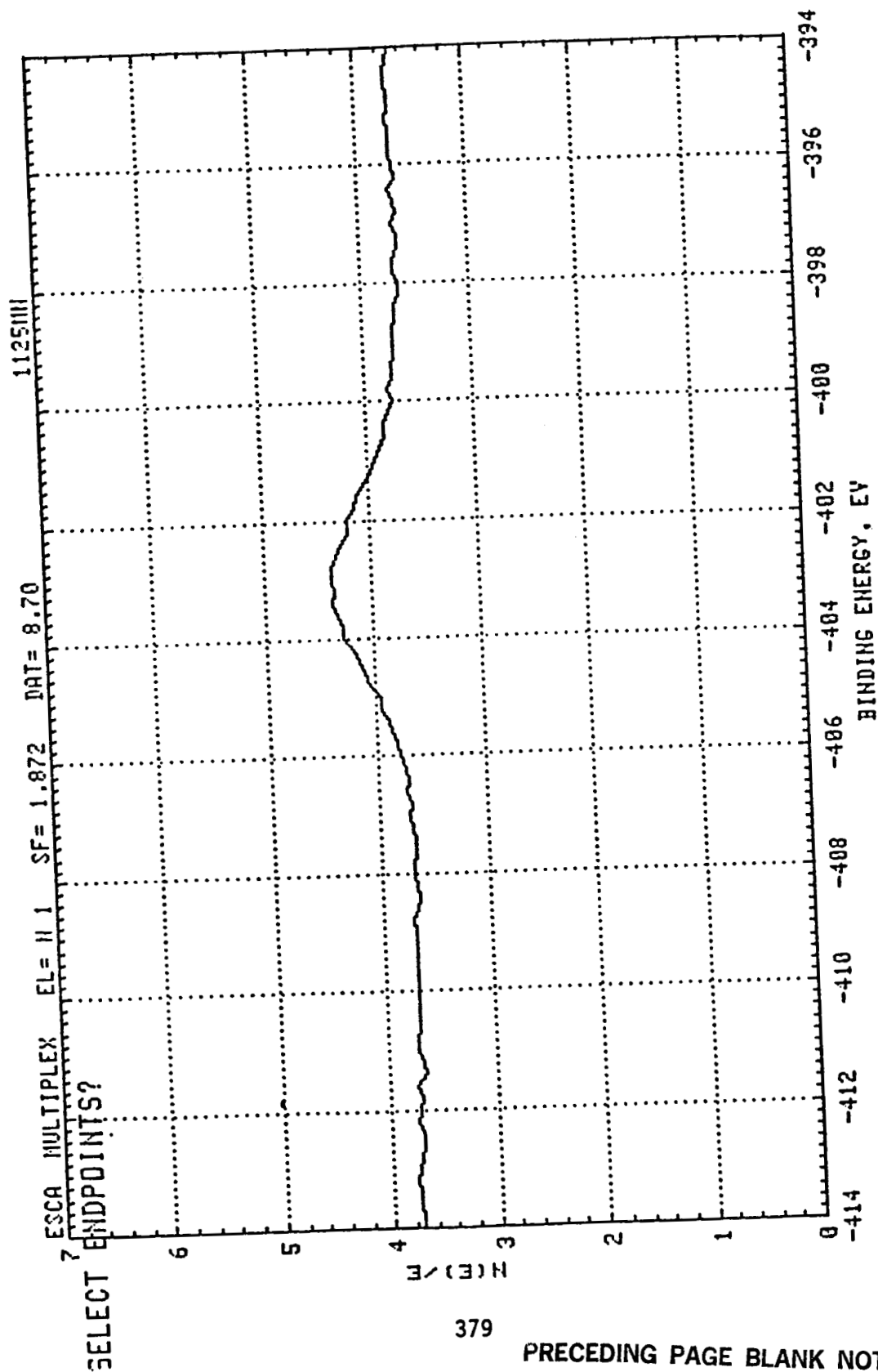


Figure 143: X-Ray Photoelectron Spectrum of Plasma Polymerized Hexamethyl-
disiloxane/Tetrafluoroethylene Coating on Kapton. This Spectrum
is an Expansion of the Region Around the Nitrogen Peak in the
Spectrum From Figure 142.

(THIS PAGE INTENTIONALLY LEFT BLANK)

<u>SPECIMEN</u>	<u>ATOMIC OXYGEN EXPOSURE (HOURS)</u>	<u>ELEMENT</u>	<u>MOLE PERCENT</u>	<u>RATIOS RELATIVE TO CARBON</u>
#65	48	O	28.6	0.73
		C	39.4	1.0
		Si	32.0	0.81
#128	49	O	15.9	0.23
		C	67.8	1.0
		Si	8.5	0.13
		F	0.9	0.1
		N	3.7	0.005
		P	3.1	0.05
#93	6	O	38.1	1.28
		C	29.8	1.0
		Si	32.0	1.07
#93	51	O	43.4	2.14
		C	20.3	1.0
		Si	36.3	1.79

Table 37: Results of X-Ray Photoelectron Spectroscopy
Surface Analysis on Selected Coating Specimens

PRECEDING PAGE BLANK NOT FILMED

(THIS PAGE INTENTIONALLY LEFT BLANK)

<u>SPECIMEN</u>	<u>ATOMIC OXYGEN EXPOSURE (HOURS)</u>	<u>ELEMENT</u>	<u>MOLE PERCENT</u>	<u>RATIOS RELATIVE TO CARBON</u>
#26	3	F	4.5	0.06
		O	13.1	0.17
		N	1.6	0.02
		C	75.4	1.0
		Si	5.5	0.07
#26	9	F	0.8	0.01
		O	21.0	0.30
		N	6.0	0.08
		C	70.6	1.0
		Si	1.6	0.02

Table 38: Results of X-Ray Photoelectron Spectroscopy
Surface Analysis on Ultrathin (20000 Å) Coatings
From Battelle

PRECEDING PAGE BLANK NOT FILMED

(THIS PAGE INTENTIONALLY LEFT BLANK)

<u>SPECIMEN</u>	<u>ATOMIC OXYGEN EXPOSURE (HOURS)</u>	<u>ELEMENT</u>	<u>MOLE PERCENT</u>	<u>RATIOS RELATIVE TO CARBON</u>
#66	1	O	39.9	1.98
		C	20.2	1.0
		Si	30.7	1.52
		F	9.2	0.46
#66	0	O	13.9	0.31
		C	44.9	1.0
		Si	15.1	0.34
		F	26.0	0.58
#66	24	O	33.5	1.32
		C	25.3	1.0
		Si	24.3	0.96
		F	17.0	0.67
Kapton	1	O	25.3	0.44
		C	57.5	1.0
		N	4.5	0.078
	4	O	23.6	0.38
		C	62.8	1.0
		N	5.4	0.086
	49	O	22.4	0.33
		C	67.2	1.0
		N	4.8	0.049
Polyimide	0	O	17.0	0.23
		C	76.0	1.0
		N	7.0	0.09

Table 39: Results of X-Ray Photoelectron Spectroscopy
Surface Analysis on Ultrathin (20000 Å) Coatings
From Battelle

PRECEDING PAGE BLANK NOT FILMED

A large number of materials were exposed to atomic oxygen plasma as the essential test of the preliminary screening of candidate coating materials. Silicone based materials appeared to perform relatively well in this test environment. The exposure conditions were so severe that most coatings failed within the 2 or 4 hour exposure times. This makes analysis of the mass loss measurement difficult because once a coating has cracked, an unknown fraction of the mass loss is due to reaction of exposed Kapton. All hydrocarbon materials were rapidly degraded. In addition to the silicone materials, several types of fluorinated species were selected for further investigation. This was to examine as broad a distribution of candidates as possible with available resources. There was variation in the results following bending of specimens over sharp radii. This is partially attributed to batch to batch processing variation. There was some indication that certain specimens were annealed during the combined vacuum thermal cycling/UV exposure.

Several of the top candidate coatings were tacky and blocked upon being pressed together. Attempts to minimize the tackiness by adding inorganic filler to CV-1144 and CV-3530 did not meet with success. These specimens were still tacky and tended to crack more than unfilled specimens of like material. Exposure to atomic oxygen decreased the tackiness of all materials tested.

CHAPTER 6

Large Scale Technology Demonstration

Two types of coating processes have been used to demonstrate the capability for coating large areas of Kapton. Battelle has carried out a series of experiments designed to show that the plasma polymerization process can be used to coat large areas. Sheldahl used a series of coating materials to demonstrate a roll to roll coating process on Kapton.

Battelle's initial attempts were with a roll coating process using 18" and 6" wide, 1 mil thick, Kapton sheets. These attempts represent the first plasma polymerized coatings produced using a roll coating process. Approximately 37 ft. of the 18" wide sheet and about 32 ft. of the 6" wide sheet were produced from this effort.

Several problems were encountered while producing these materials. The observations and suggested solutions are discussed in the following paragraphs. Table 40 is a schematic of the coating parameters used to make the test precise.

Tracking

The 18-inch-wide Kapton was slightly (approximately 1/8 inch) oversized which caused tracking problems when the material was translated across the system cathode. There were no tracking problems with the 6-inch-wide material. The problems with the 18-inch material can be solved by enlarging the fixturing and/or reducing the width of the material.

Powder Formation

There is powder on several areas of both the 18-inch and 6-inch-wide coated Kapton. Powder on the substrate is usually an indication of reactions in the gas phase, forming long chain polymers which precipitate out of the plasma and land on the substrate. This material is loosely adherent to the

(THIS PAGE INTENTIONALLY LEFT BLANK)

<u>Coating Material Partial Pressure</u>	<u>Power, W</u>	<u>Flow Rate, S cc/m</u>	<u>Average Coating Thickness, KAngstroms</u>
HMDS/36 , TFE/4	50	153	30-40

Table 40: Parameters For Battelle's Large Scale Demonstration

PRECEDING PAGE BLANK NOT FILMED

substrate and can usually be rubbed or blown off. However, it does prevent the formation of an adherent protective coating on the substrate. Powder formation can be prevented by adjusting any one of several process variables - gas pressure, gas flow and/or plasma power. However, at this time, we have no method of determining when powder formation is taking place. It seems to be a problem only at the end of very long depositions and only when the monomer gas is pure HMDS. We have seen no evidence of powder formation in any deposition where TFE monomer was added to the HMDS monomer.

Coating Stress

Stresses in the coating cause the substrate to curl, which can cause creases and cracks in the protective coating. Coating both sides of the material simultaneously should balance the stresses and eliminate the tendency to curl. The 6-inch-wide material was coated on both sides with each side coated in a separate run. The fact that both sides were not coated simultaneously may be the cause of this strip of material to curl.

Material Flaking

During the long deposition times required to coat strips of the lengths delivered to Boeing, material builds up on all the surfaces of the system fixturing. When thick enough, the stresses in these buildups will cause the material to delaminate and flake. This flaking is only a problem when it lands on the surface to be coated and prevents the deposition of the protective coating in the affected area.

All of these problem areas are amenable to solutions - primarily through modifications to the fixture design and slight adjustments to the coating process.

Polymer Ratio HMDS/TFE	Coated Length, feet	Coating Thickness Profile
8/5	4	<p>← 1.5' → ← 4' → ← 1.5' → 8kÅ</p>
1/0	8	<p>← 1.5' → ← 8' → ← 1.5' → 8kÅ</p>
20/1	25	<p>← 1.5' → ← 25' → ← 1.5' → 8kÅ</p>

Table 41: Plasma Polymerized Coatings Deposited Onto One Side
Of 18-Inch Wide Kapton

(THIS PAGE INTENTIONALLY LEFT BLANK)

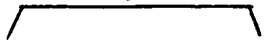
Polymer Ratio HMDS/TFE	Coated Length, feet	Coating Thickness Profile
1/0	8	←1.5'→ ← 5'→ ←1.5'→ 
20/1	8	Ditto
8/1	8	"
4/1	8	"

Table 42: Plasma Polymerized Coatings Deposited Onto Both Sides
Of 6-Inch-Wide Kapton

PRECEDING PAGE BLANK NOT FILMED

(THIS PAGE INTENTIONALLY LEFT BLANK)

18 x 18-Inch Samples

A set of 18 x 18-inch coated samples was produced by Battelle for this contract. The coating materials and the deposition conditions used are shown in table 43.

<u>Sample Number</u>	<u>Side</u>	<u>Coating Material Partial Pressure</u>	<u>Power, W</u>	<u>Flow Rate, S cc/m</u>	<u>Average Coating Thickness, KAngstroms</u>
41641-60-55	1	HMDS/18 , TFE 2	25	85	11.4
41641-60-55	2	HMDS/36 , TFE/4	50	153	17.9
41641-57-52	1	HMDS/40	75	139	22.7
41641-56-52	2	HMDS/40	75	139	15.6
41641-56-51	1	HMDS/40	50	139	16.0
41641-56-51	2	HMDS/40	50	139	14.9
41641-55-50	1	HMDS/40	25	139	5.1
41641-55-50	2	HMDS/40	25	139	8.1
41641-58-53	1	HMDS/36 , TFE/4	50	128	12.5
41641-58-53	2	HMDS/36 , TFE/4	50	128	12.5

Based on the results of tests performed on these samples, coating conditions and materials used with sample No. 41641-60-55-side 2 were selected to as produce the larger samples required.

Table 43: Coatings on 18 x 18-Inch Samples

PRECEDING PAGE BLANK NOT FILMED

18 x 72-Inch Samples

Two 18 x 72-inch samples were coated under the specified conditions using a large area electrode especially constructed for the application. The first sample was produced during an on-site process demonstration witnessed by personnel from Boeing, NASA Marshall, and NASA Lewis. The average thickness of this coating was 20 microns. Samples of the coated material were provided to those who attended the process demonstration. The second sample was coated subsequent to the process demonstration. The average thickness of this coating is 40 KA.

CHAPTER 7

Discussion

Atomic Oxygen Flux

There are two techniques for determining atomic oxygen flux; and light titration. For most measurements, a small differential calorimeter was used to determine the flux. A silver oxide surface, placed for ease of operation on a glass substrate, is catalytic for the recombination of oxygen. A reference probe of uncoated glass is placed near the coated probe. The glass surface does not promote recombination and simply measures the gas temperature. The coated probe is created by painting the end of a glass cylinder with a silver paint and exposing the surface to atomic oxygen. The organic binder is oxidized and volatilized, the silver is oxidized and forms the black surface of the detector.

The silver oxide coated calorimetric probe is heated by the recombination of oxygen atoms on its surface as well as the thermal energy of the flowing gas. This heat is dissipated predominantly by radiative processes. A reference probe, which is an uncoated glass surface, detects heat contribution only from the thermal energy of the gas. Both the calorimetric probe and the glass reference lose some heat due to convection and some by conduction down the thermocouple. These processes should cause virtually the same heat loss in both probes. Thus, the temperature difference between the two probes is due to the fact that the silver oxide surface is catalytic for oxygen atom recombination and the glass surface is not. Perhaps 1 in 10^4 atoms striking the glass surface recombine on this surface. To convert the temperature difference into a flux, one must equate the heat of reaction for recombination to the difference in emitted energy of the two probes, using the

Stefan-Boltzmann law, and taking into account the fact that the emissivities of the silver oxide and glass surfaces are different.

The Stefan-Boltzmann equation is

$$E = \epsilon \sigma T^4,$$

$$\text{where } \sigma = 5.67 \times 10^{-8} \frac{\text{kJ}}{\text{m}^2 \text{secK}^4},$$

K is the temperature in Kelvin, E is the rate of energy emitted from a source per unit area, and ϵ is the emissivity of the source.

For the earlier estimates of the atomic oxygen flux, it was assumed $\epsilon = 1$ for each surface; this was not sufficiently precise. An epsilon of 0.965 for the silver oxide coating and an epsilon of 0.80 for the glass surface were measured. The equation used to calculate the flux is:

$$(\#RXNS) (\text{Heat Per RXN}) = (\epsilon_{\text{Ag}_2\text{O}} T_{\text{Ag}_2\text{O}}^4 - \epsilon_{\text{Glass}} T_{\text{Glass}}^4).$$

The number of reactions determined by this equation must be multiplied by two to obtain the number of oxygen atoms.

The assumption is made that 5.0 eV are available per reaction. If a product molecular oxygen is in an excited vibrational state then less energy will be deposited in the surface by that particular reaction.

In addition, a fraction of the oxygen atoms which impinge upon the surface will scatter and not be available to recombine. Also, while the silver oxide surface is known to be highly catalytic for recombination, an independent measurement is needed to determine if the efficiency is 100% or whether it is somewhat lower.

Consideration of the uncertainties and assumptions made using this method of determining flux leads to the conclusion that the flux is underestimated by this measurement. To improve this situation, an independent method must be used; light titration.

Data Base

The data base contains information from experiments conducted at Boeing under this contract, data from the laboratories, data from space flights, basic material properties, and a survey of atomic oxygen sources. Figures 144 through 148 show the layout of the screens. The data is actually separated into four data bases using the Smart Data Manager Program on a Zenith 150 PC.

One section contains results of measurements of mass loss of materials upon exposure to atomic oxygen made at Boeing, one contains results of other tests carried out under this contract, one contains results of on-orbit measurements, and one contains descriptions of the laboratory test facilities for exposing materials to atomic oxygen.

Not all information is available for each record. The Smart Data Manager package of the SMART software system by innovative software is used to set up the structure of the data bases.

Atomic Oxygen Facility Data Base

Facility: Boeing M&P

Date Entered: 02-16-88

Source: RF Plasma discharge

	Current	Future (Date 09-15-88)
Flux	5.00	5.00
Energy	0.05	0.05
Beam Size		

Beam Composition: neutral oxygen atoms(5%) and molecules(95%)

Mass Loss Data (y/n): y

Optical Data (y/n): y

Contact Name: H.G. Pippin

Address: Boeing Aerospace

Tel. (206) 251-3040

P.O. Box 3999 M/S 2E-01

City: Seattle

State: Wa Zip: 98124

Remarks:

Figure 144: Atomic Oxygen Facility Data Base

Combined UV/Thermal Cycling Test Results

	Initial Value	Final Value	Loss
Weight (mg)			0.00
Emmissivity			
Absorbance			

Blocking and Peel Test Results

Sample Size:

Peel Load: psi

Remarks:

Figure 145: Combined UV/Thermal Cycling Test Results &
Blocking and Peel Test Results

Combined Effects Data Base

Material:

Sample No: 8

Test Date: 04-15-87

Combined Radiation Test

Electron Potential:	30 keV	Electron Flux:	
Proton Potential:	35 keV	Proton Flux:	
UV Fluence:	ESH	UV Flux Rate:	1.50

Results

Data Point	Absorbance	Time
1	0.360	0.0
2	0.394	200.0
3	0.441	500.0
4	0.489	1000.0
5		
6		
7		
8	4.000	
9		
10		

Combined UV/Thermal Cycling Test

UV Conditions	Thermal Cycling Conditions
UV Flux:	Temp. Range (C):
UV Fluence:	No. Cycles:
	Cycle Time: (minutes)

Interval	Exposure (UV or TC)	Time (hrs.)
1		
2		
3		
4		
5		
6		

Figure 146: Combined Effects Data Base

X-Ray Photoelectron Spectroscopy Data

Element	Mole Percent	Ratios Relative To Carbon
---------	--------------	---------------------------

Scanning Electron Microscopy Results

Figure 147: X-Ray Photoelectron Spectroscopy Data

Atomic Oxygen Data Base

Material: Kapton H

Description: 2 mil thick, reference standard, 24 ft by 42 in roll.

Vendor: Dupont

Test Parameters

Sample No. 2 Test Site: Boeing Aerospace Date: 02-17-87

Source RF plasma discharge

Area 2.850 sq.cm.

Thickness: 2.00000 mils

Density 1.420 g/cc.

Flux 1.450 Atoms/sq.cm.-sec x E16

Time 4.5 Hours

Fluence 2.3 Atoms/sq.cm. x E20

Temp. (C) 195

Specimen Preparation

1" diameter specimens were punched from the stock material. The specimens were heated in a thermal vacuum drying oven to 150F and held at that temperature for 1 hour. Upon colling the samples were weighed and immediately placed in the sample holder. The sample holder was positioned in the vacuum apparatus, which was then sealed and evacuated. Sample numbers are recorded by position within the sample holder. This holder may contain up to four samples.

Results

Property	Initial Value	Final Value	Loss
Weight (mg)	36.600	34.900	1.700
Emmissivity			
Absorbtivity			

Reaction Efficiency: 1.826 cc/Atom x E-24

Remarks

Figure 148: Atomic Oxygen Data Base - Results

Candidate Materials

Silicone based materials appear to be the best available candidate coatings for application to flexible Kapton^R substrates. Both linear chain polymeric siloxanes and highly crosslinked plasma polymerized siloxane based materials performed well relative to other materials tested. Fluorosilicones also survive relatively well.

The silicones have low mass loss rates under exposure to atomic oxygen although the surfaces of these materials show evidence of extensive oxidation under such exposure. Combined effects testing by exposure to simulated solar UV and thermal cycling changed the absorptance of all materials. Some micro-cracking occurred on these specimens. Combined effects testing by simultaneous exposure to simulated solar UV, protons and electrons caused some changes in the absorptance as measured in situ.

Tetrafluoroethylene (TFE) shows very little mass loss when exposed to only neutral atomic oxygen. However, when placed in a dilute plasma environment which contains excited state species, UV, and ions as well as atomic oxygen, the TFE mass loss rate is greater than for Kapton under identical conditions. This data is shown in figures 149 to 151; data on FEP is included for comparison. In each figure the curve showing greater mass loss is for a sample placed at the center of the plasmod. The lower curve in each figure is for a sample near one end of the plasmod.

There is some indication that materials previously exposed to the combined effects environments degrade at a slightly higher rate when exposed to atomic oxygen but measurements to date are not conclusive.

Fluorophosphazene had relatively low mass loss rates, however this materials showed sensitivity to the combined effects exposure (UV, H⁺, e⁻).

All hydrocarbon based materials oxidize at a rate that is essentially

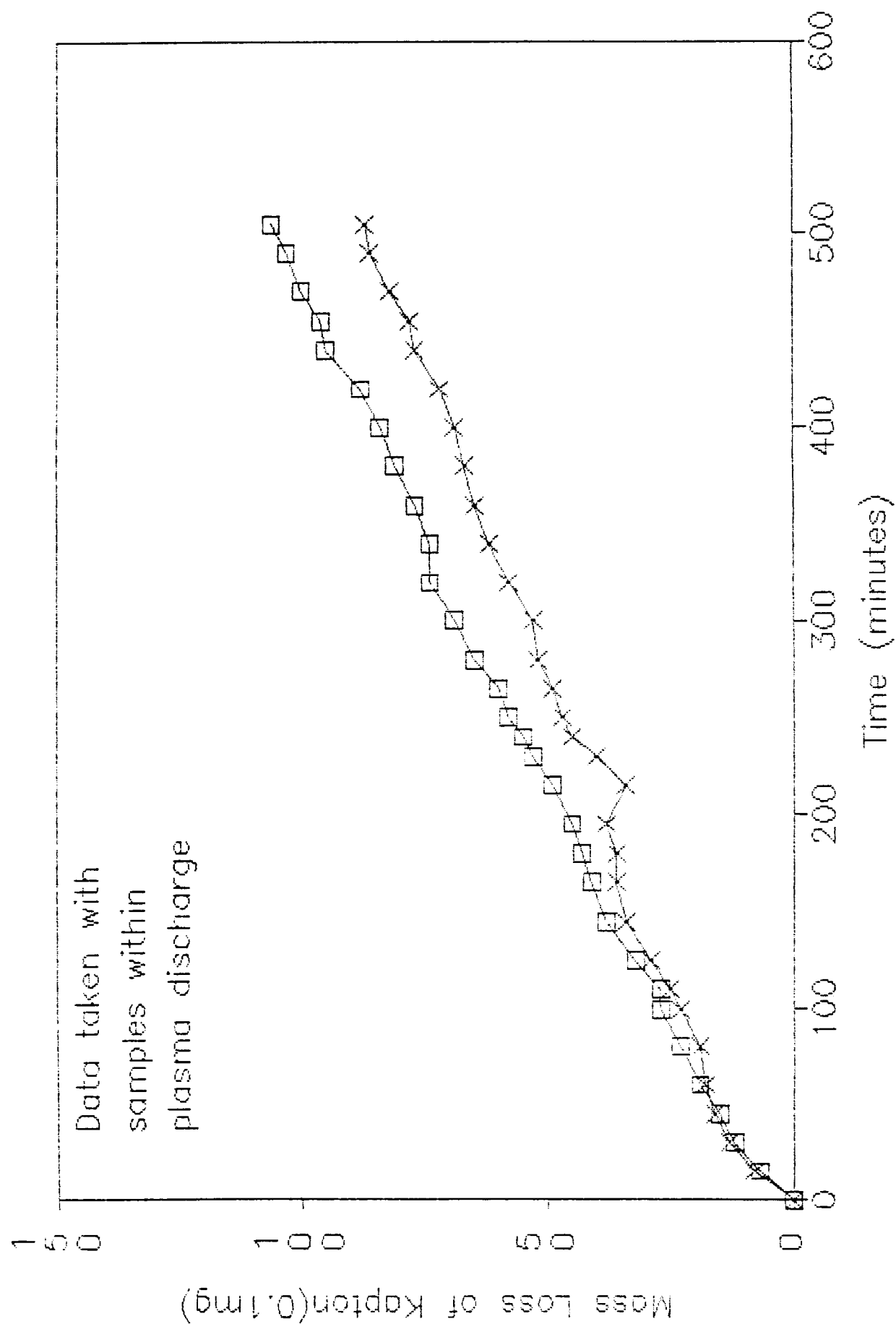


Figure 149: Mass Loss of Kapton Exposed to an Atomic Oxygen Plasma.
Specimens Were 1.5" in Diameter.

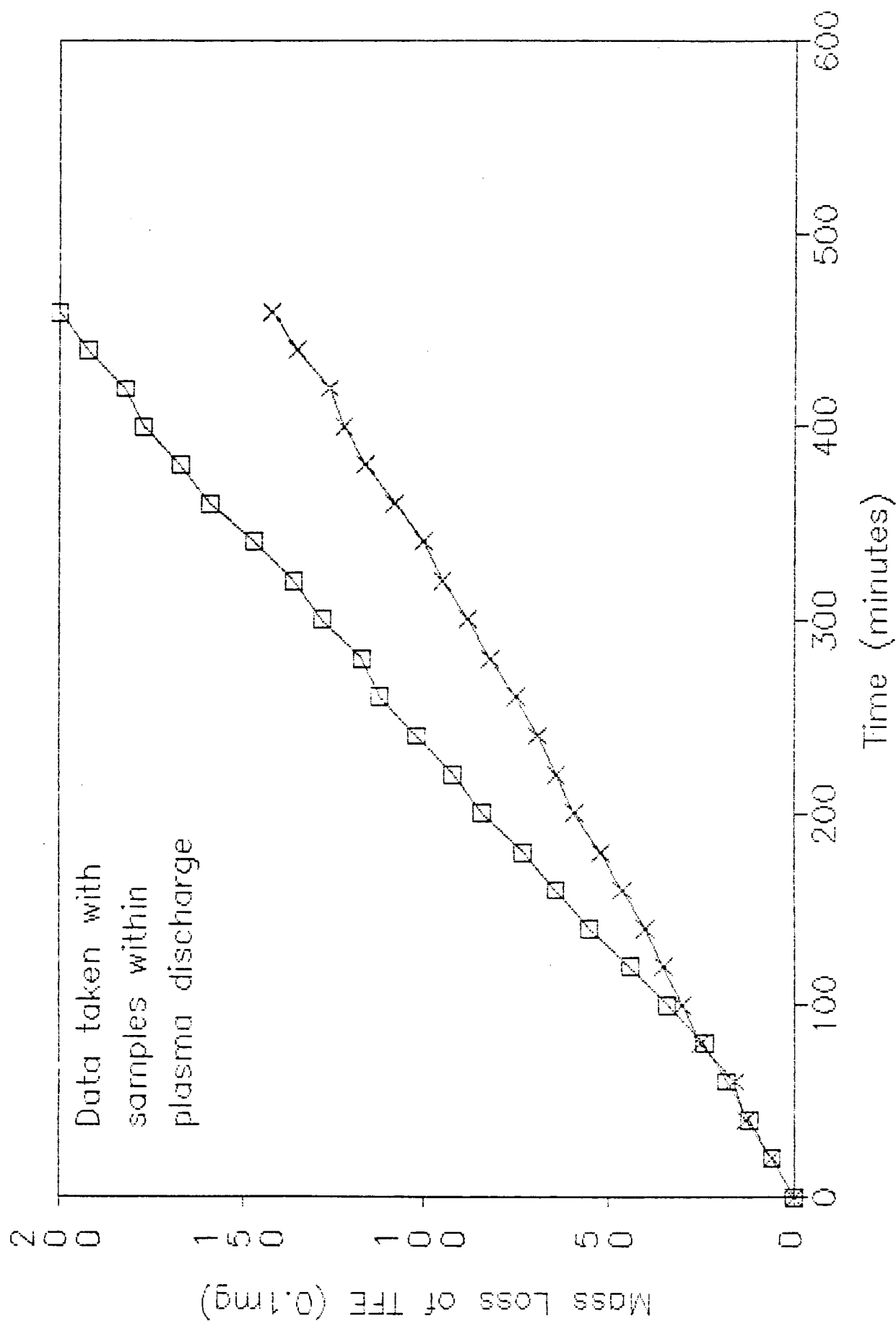


Figure 150: Mass Loss of TFE Exposed to an Atomic Oxygen Plasma. Specimens Were 1.5" in Diameter.

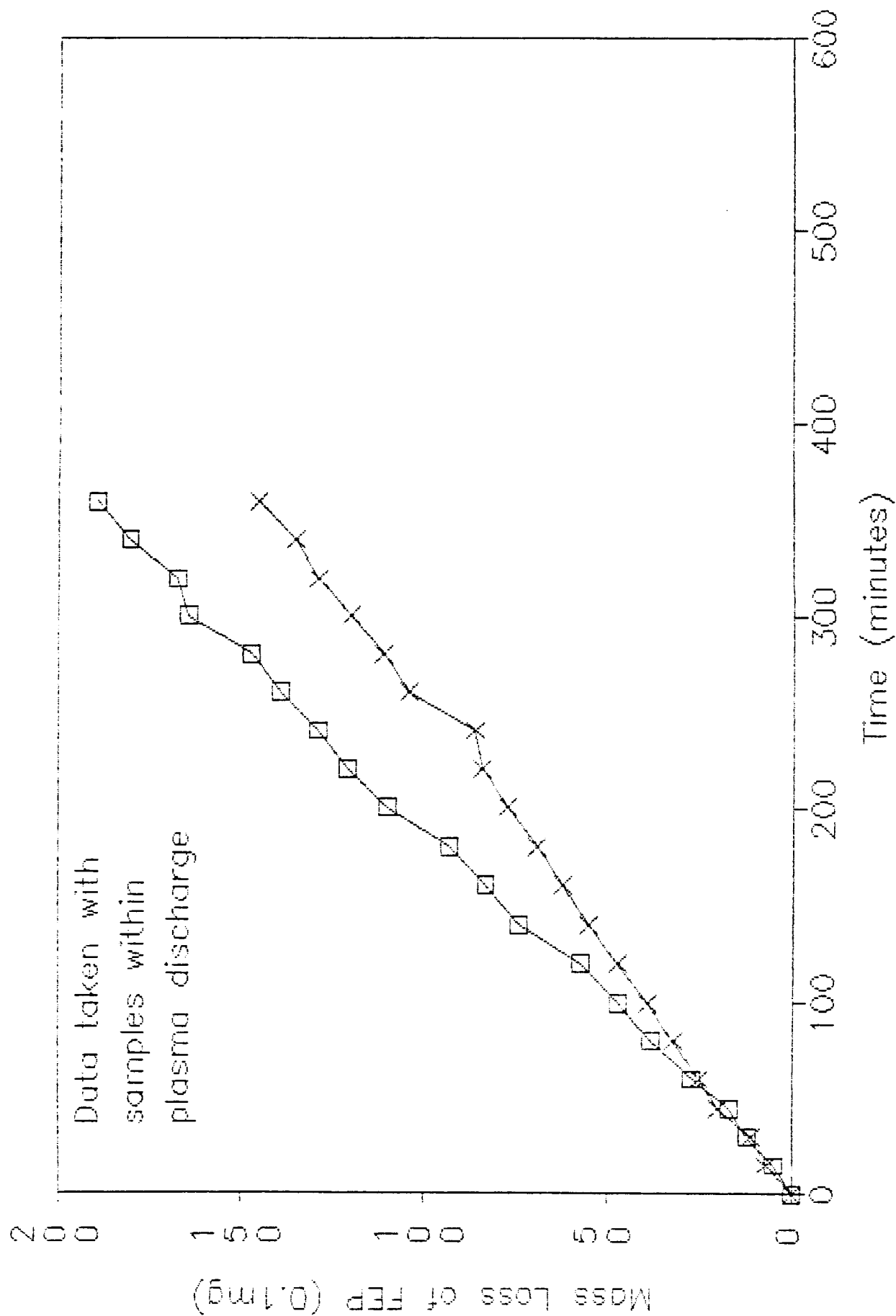


Figure 151: Mass Loss of FEP Exposed to an Atomic Oxygen Plasma. Specimens Were 1.5" in Diameter.

dependent on the rate of arrival of oxygen atoms to the surface of the material. While the detailed rate constant varies in each case the same conclusion holds-these materials will not survive the LEO space environment for extended periods of time.

Many of the candidate materials tended to block due to residual tackiness after cure. Exceptions included the Battelle coatings and the S13-G/L0. Attempts to overcome this problem included adding further inorganic filler to certain polymers; which met with limited success, and overcoating particular materials with thin plasma polymerized coatings.

The blocking tendencies of all specimens examined decreased upon exposure to atomic oxygen.

Two avenues of further development should be continued in this area. One, improved simulation capabilities should be achieved. The effects of simultaneous exposure to UV and atomic oxygen are unknown. A clear determination must be made of which effects need to be simulated and which are not as significant. Appropriate test lab facilities are important and necessary. Results from simulation chambers can guide the development of more resistant materials, confirm the performance of such materials, and establish which types of materials will not be resistant.

Two, intrinsically resistant polymeric materials should be produced. Such materials will have relatively strong bonds, particularly where the side group is attached to the main chain, side groups already oxidized, and bulky enough to physically impede the oxygen atoms from reaching the backbone bonds. Stable species will have a minimum of products thermodynamically more stable than the coating itself. For example, fluorination often improves the stability, other things being equal. Atomic oxygen will not abstract a fluorine atom, because the O-F bond is quite weak ($\sim 2.2\text{ev}$) relative to other

fluorine bonds.

The mass loss of selected materials on Kapton substrate has been compared with mass loss of uncoated Kapton reference samples after simultaneous exposure to atomic oxygen. Most tests were conducted at 85°C, and a few at 195°C. The mass loss ratios for two siloxanes, a fluorosilicone, FEP, several silicone-polyimide copolymers, a fluorophosphazene and several plasma polymerized siloxane copolymers, a fluorophosphazene and several plasma polymerized siloxane and siloxane-tetrafluoroethylene coatings vs. Kapton are reported in tables 44 through 48. These materials do relatively well compared to the Kapton. The mass loss ratios reported are upper bounds on the mass loss rate of the pure material. This is because the system is a coating plus substrate and if flaws or cracks exist in the coating then exposed Kapton may be degraded and contribute to the observed mass loss. Drastic changes in the ratio after relatively long times are an indication that the coating has failed. This may be seen in table 47. Samples of materials #111 and #112, side 1, which are HMDS/TFE plasma polymerized coatings, show clear evidence of failure at 47 hours, whereas #112, side 2 does not.

Table 44 shows results from two tests each of three materials. Material (#52) shows evidence of failure at 14 hour exposure. The RTV fluorosilicone specimen used in the longer test had an unusually large ratio after 6 hours exposure. However, the absolute mass losses being measured are very small and short term values are not very precise. Also, these tests were conducted with samples at 196°C and this sample may have had some initial volatility.

Measurements were made on two separate occasions to see if there was an effect on polyimides due to simultaneous exposure to UV and atomic oxygen.

Exposure Time (Hrs)	6	10	14
HMDS/TFE (#52)	0.13		
Mass Loss Ratio	0.13	0.14	0.41
Silicone-Polyimide (#93)			
Mass Loss Ratio	0.09		
	0.13	0.12	0.08
RTV Fluorosilicone (#101)			
Mass Loss Ratio	0.18		
	0.45	0.20	0.11

Table 44: Mass Loss of Selected Materials Relative to Kapton Mass Loss, Under Exposure to Atomic Oxygen. For Long Term Exposure RF Power was 200 Watts During First Six Hours of Exposure and 350 Watts for Remainder of Exposure. For Short Term Six Hour Exposure, RF Power was 250 Watts. Samples were Maintained at 195°C.

Exposure Time (Hrs)	6.5	10.5	15	
FEP/Kapton (#31)				
Mass Loss Ratio	0.2	0.5	0.5	
Exposure Time (Hrs.)	4	8	15	22
Silicone-Polyimide (#93)				
Mass Loss Ratio	0	0	0.03	0.02
Exposure Time (Hrs.)	6	14.10	20	
Silicone-Polyimide (#94)				
Mass Loss Ratio	0.9	1.1	0.8	
Silicone-Polyimide (#95)				
Mass Loss Ratio	0.8	1.0		
Apricall (#106)				
Mass Loss Ratio	1.0	1.1	1.3	

Table 45: Mass Loss Of Selected Materials Relative To Kapton Mass Loss Under Exposure To Atomic Oxygen. Samples Maintained at 85°C.

Exposure Time (Hrs)	6	10	15	20	25
CVI-1144 (#65)					
Mass Loss Ratio	0.08	0.07	0.05	0.06	0.05
Fluorophosphazene (#58)					
Mass Loss Ratio	0.15	0.13	0.10	0.18	0.15
RTV Diphenyl Dimethyl Silicone (#100)					
Mass Loss Ratio	0.0	0.20	0.15	0.32	0.27

Table 46: Mass Loss Ratio Of Selected Coatings Vs. Uncoated Kapton
Upon Exposure To Atomic Oxygen. Sample Temperature
Maintained At 85°C.

Exposure Time (Hrs>)

Mass Loss Ratio	24	47
#111	0.29	0.57
#112, Side 1	0.32	0.52
#112, Side 2	0.19	0.16

Table 47: Mass Loss Of Battelle HMDS/TFE Mixtures Relative To Kapton Mass Loss, Under Exposure To Atomic Oxygen. Samples Were Maintained at 85°C. Atomic Oxygen Flux Was $4 \times 10^{16}/\text{cm}^2\text{-Sec.}$

Exposure Time (Hrs)	24	48	72	96
Mass Loss Ratio	0.2, 0.15	0.30, 0.25	0.35, 0.35	0.4, 0.5
CV-3530 (#112)				

Exposure Time (Hrs)	12	18
HMDS/TFE (#112)	1.0, 0.6	0.6, 0.7
Mass Loss Ratio		

Table 48: Mass Loss Ratio Of CV-3530 (#66) And HMDS/TFE, 9:1 Ratio (#112) Coatings Relative To Kapton Vs. Exposure To Atomic Oxygen. Samples were maintained at 85°C.

Both tests showed a slight increase in mass loss with simultaneous exposure. However, due to uncertainty of the atomic oxygen flux and slight differences in sample location, the test is not well quantified. This possibility should be pursued for top potential coatings, actual results are shown in table 49.

The performance lifetime of a coating will depend on the thickness, location, engineering function, and material used to make the coating. Lifetime estimates suffer from the fact that very little long term data exists for materials at LEO conditions and extrapolations of currently available short term data assume only simple, linear revisions will occur.

Table 50 gives a list of time estimates, in hours, for particular materials to lose a mg per square centimeter of exposed area when placed in the materials screening test chamber at Boeing. The low earth orbit material lifetime estimates are based on the relative performance in the screening chamber, scaled by the on-orbit recession rate of uncoated Kapton (taken as 3×10^{-24} cm³/oxygen atom) the on-orbit-flux taken as 1×10^{15} /cm¹⁵/cm²-sec, and the relative densities of the coatings. The lifetimes are for nominal 1 mil thick coatings. The Battelle coatings do quite well on this basis; however, it should be understood that the actual plasma polymerized coatings are 1 to 3 microns in thickness and that producing a 1 mil coating of these materials might cause problems with the flexibility or other difficulties not expected.

There are many factors that are different between laboratory and orbital conditions. The densities of the coatings are not always well known. The actual densities of the coatings may be considerably less than the maximum theoretical density. The estimated density values used for lifetime estimates are also given in table 50. Notice that these are times required to remove

<u>Material</u>	<u>Exposure Time</u>	<u>Exposure Conditions</u>	<u>Mass Loss (mg)</u>
Kapton	5.5	A.O.	2.4
	5.5	A.O./UV	2.95
Kapton	3	AO	1.2
	3	AO	1.4
	3	AO/UV	1.7
	3	AO/UV	1.6
Apical	3	AO	1.2
	3	AO	0.7
	3	AO/UV	1.4
	3	AO/UV	1.8

Table 49: Mass Loss Of Kapton And Apical Under Exposure To Atomic Oxygen Or Simultaneous Exposure To Atomic Oxygen And UV Radiation.

<u>Material</u>	<u>Density</u> <u>(g/cm³)</u>	Time Per Unit* Weight Loss Per Unit Area (HR/mg/cm ²)	Material Lifetime** Estimates (Days) Solar Panel	
			Rear	Front
Kapton-H	1.42	40	150	75
Kapton-F	2.15	70	400	200
Fluorophosphazene (X-128)	1.8	280	1200	620
CVI-1144	1.01	830	2210	1105
HMDS/TFE				
#112, Side 1	1.66	120	525	260
#112, Side 2	1.66	200	880	400
Silicone-Polyimide	1.5	570	2260	1130

Table 50: Material Lifetime Estimates For Selected Candidate Materials.

* Based on a flux of 4.2×10^{16} atoms/cm²-Sec.

** Lifetimes based on Leo flux of 1×10^{14} atoms/cm²-sec and a scale factor from laboratory to orbit of 30 times greater mass loss per atom in orbit. Flux is averaged over 20 year life, based on a 1993 launch date.

100% of each material if a 1 mil thick coating was present initially. The actual performance lifetime of the material is expected to be even shorter.

In addition, the decomposition mechanisms of each material may be different. The estimate shown in the table assume each material undergoes a steady linear recession. Certain materials are known to have induction periods before any mass loss occurs; FEP is an example of such a material.

It should be remembered that these lifetime predictions are for ram facing surfaces. Also, the mass loss measurements are for coating--substrate systems. If the coatings have failed at defect sites, or due to microcracking and subsequent exposure of underlying Kapton, the mass loss rates will be overestimated.

BIBLIOGRAPHY

A High Flux Pulsed Source of Energetic Atomic Oxygen
R.H. Krech and G.E. Caledonia
18th International SAMPE Technical Conference, Oct 7-9, 1986,
Seattle, Wa

High Intensity 5 ev CW Laser Sustained O-Atom Exposure Facility
for Material Degradation Studies
J.B. Cross, L.H. Spangler, M.A. Hoffbauer, F.A. Archuleta
18th International SAMPE Technical Conference, Oct 7-9, 1986,
Seattle, Wa

The Vanderbilt University Neutral O-Beam Facility
N.H. Tolk, R.F. Haglund et al
18th International SAMPE Technical Conference, Oct 7-9, 1986,
Seattle, Wa

Production of a Beam of Ground State Oxygen Atoms
R.D. Rempt
18th International SAMPE Technical Conference, Oct 7-9, 1986,
Seattle, Wa

Production of Pulsed Atomic Oxygen Beams via Laser Vaporization
Methods
D.E. Brinza, D.R. Coulter, R.H. Liang, and A. Gupta
18th International SAMPE Technical Conference, Oct 7-9, 1986,
Seattle, Wa

Reaction of Atomic Oxygen with Polyimide Films
G.S. Arnold and D.R. Peplinski
AIAA Journal, Oct. 1985

STS Flight 5 LEO Effects Experiment--Background Description and
Thin film Results
L.J. Leger, I.K. Spiker, J.F. Kuminecz, T.J. Ballentine,
and J.T. Visentine
AIAA-83-2631-CP, AIAA Shuttle Environment and Operations Meeting,
Oct.31-Nov.2, 1983, Washington, D.C.

Orbital Atomic Oxygen Effects on Thermal Control and Optical
Materials STS-8 Results
A.F. Whitaker, S.A. Little, R.J. Harwell, D.B. Griner, R.F.
DeHaye, and A.T. Fromhold, Jr.
AIAA-85-0416, AIAA 23rd Aerospace Sciences Meeting,
Jan.14-17,1985, Reno, Nv.

Reaction of Atomic with Vitreous Carbon: Laboratory and STS-5 Data
Comparisons
G.S. Arnold and D.R. Peplinski
AIAA Journal

Reactions of High Velocity Atomic Oxygen with Carbon
G.S. Arnold and D.R. Peplinski
AIAA-84-0549, AIAA 22nd Aerospace
Sciences Meeting, Jan. 9-12, 1984, Reno, Nv.

A Facility for Investigating Interactions of Energetic Atomic
Oxygen with Solids
G.S. Arnold and D.R. Peplinski
NASA Conference Publication 2340, 13th Space Simulation
Conference, Oct 8-11, 1984, Orlando, Fl.

Low Earth Orbit Atomic Oxygen Effects on Surfaces
L.J. Leger, J.T. Visentine, and J.F. Kuminecz
AIAA-84-0548, AIAA 22nd Aerospace Sciences Meeting, Jan. 9-12,
1984, Reno, Nv.

Oxygen Atom Reaction with Shuttle Materials at Orbital Altitudes
L.J. Leger
NASA Technical Memorandum 58246, May, 1982

Laboratory Degradation of Kapton in a Low Energy Oxygen Ion Beam
D.C. Ferguson
AIAA

Effects on Optical Systems from Interactions with Oxygen Atoms
in Low Earth Orbits
P.N. Peters, J.C. Gregory, and J.T. Swann
Applied Optics, Vol. 25, No. 8, April 15, 1986, Pp. 1290-1298

Kinetics of Oxygen Interaction with Materials
G.S. Arnold and D.R. Peplinski
AIAA-85-0472, AIAA 23rd Aerospace Sciences Meeting, Jan. 14-17,
1985, Reno, Nv.

The Energy Dependence and Surface Morphology of Kapton
Degradation Under Atomic Oxygen Bombardment
D.C. Ferguson

A Preliminary Spectroscopic Assessment of the Spacelab 1/Shuttle
Optical Environment
M.R. Torr and D.G. Torr
J. of Geophysical Research, Vol. 90, No. A2, Feb. 1, 1985, Pp.
1683-1690.

Effects of Atomic Oxygen on Graphite Ablation
C. Park
AIAA Journal, Vol 14, No. 11, Nov. 1976, Pp 1640-1642

Coatings in Space Environments
J.J. Triolo, J.B. Heaney, and G. Hass
SPIE, Vol. 121, Optics in Adverse Environments, 1977, Pp. 46-66.

Interaction of Atomic Oxygen with Various Surfaces

J.A. Riley and C.F. Giese

J. of Chemical Physics, Vol. 53, No. 1, July 1, 1970, Pp. 146-150

An Atomic Oxygen Facility for Studying Polymer Materials for
Spacecraft Applications

R.C. Tennyson, J.B. French, et al

NASA 13th Space Simulation Conference: The Payload-Testing for
Success, Oct. 8-11, 1984

Supersonic Nozzle Beam Source of Atomic Oxygen Produced by
Electrical Discharge Heating

J.A. Silver, A. Freedman, et al

Review of Scientific Instruments, Vol. 53, No. 11, Nov. 1982,
Pp. 1714-1718.

Investigation of Atomic Oxygen in Mass Spectrometer Ion Sources

L.R. Lake and K. Mauersberger

International Journal of Mass Spectrometry and Ion Physics, Vol.
13, 1974, Pp. 425-436.

Survey of Chemi-ionization Reactions in Accelerated Atom-O₂
Crossed Molecular Beams

C.E. Young R.B. Cohen, et al

J. of Chemical Physics, Vol. 65, No. 7, Oct. 1, 1976, Pp.
2562-2567.

Effective Cross Sections for Excitation of Atomic Oxygen by
Electron Impact

A.A. Haasz

Journal of Chemical Physics, Vol. 65, No. 5, Sept 1, 1976,
Pp. 1642-1649.

The Mode of Attack of Oxygen Atoms on the Basal Plane of Graphite

C. Wong, R.T. Yang, and B.L. Halpern

J. of Chemical Physics, Vol. 78, No. 6, Part 1, March 15, 1983,
Pp. 3325-3328

Some Reactions of Oxygen Atoms. III. Cyclopropane, Cyclobutane,
Cyclopentane, and Cyclohexane

W.K. Stuckey, and J. Heicklen

J. of Chemical Physics, Vol. 46, No. 12, June 15, 1967, Pp.
4843-4846

Hydroxylation of Polymethylsiloxane Surfaces by Oxidizing Plasmas

J.R. Hollahan and G.L. Carlson

Journal of Applied Polymer Science, Vol. 14, 1970, Pp. 2499-2508

Effect of Atomic Oxygen on Polymers

R.H. Hansen, J.V. Pascale, et al

J. of Polymer Science: Part A, Vol. 3, 1965, Pp. 2205-2214

ML-101 Thermal Control Coatings: Five Year Space Exposure

R.A. Winn

AFML Technical Report AFML-TR-78-99, July 1978

Composite Space Antenna Structures: Properties and Environmental Effects

C.A. Ginty and N.M. Endres

18th International SAMPE Technical Conference, Oct. 7-9, 1986, Seattle, Wa.

A Space Debris Simulation Facility for Spacecraft Materials Evaluation

R.A. Taylor

18th International SAMPE Technical Conference, Oct. 7-9, 1986, Seattle, Wa.

Standardized Spacecraft Materials Outgassing and Surface Effects Measurements Tests

P.M. Falco, Jr.

18th International SAMPE Technical Conference, Oct. 7-9, 1986, Seattle, Wa.

Structure-Property Relationships in Polymer Resistance to Atomic Oxygen

L.P. Torre and H.G. Pippin

18th International SAMPE Technical Conference, Oct. 7-9, 1986, Seattle, Wa.

Microcrack Resistant Structural Composite Tubes for Space Applications

H.W. Babel, T.M. Shumate, and D.F. Thompson

18th International SAMPE Technical Conference, Oct. 7-9, 1986, Seattle, Wa.

Selected Materials Issues Associated with Space Station

L.J. Leger and B. Santos-Mason

18th International SAMPE Technical Conference, Oct. 7-9, 1986, Seattle, Wa.

Degradation and Aging Effects of Teflon Exposed to an Oxidizing Plasma Environment

H.B. Gjerde, T.R. Chun, and S.J. Low

18th International SAMPE Technical Conference, Oct. 7-9, 1986, Seattle, Wa.

Effects on Optical and Metallic Surfaces: Results of the Evaluation of Aerospace Trays A51 and A53 on the Oxygen Interaction with Materials

W.K. Stuckey, E.N. Borson et al

AIAA Shuttle Environment and Operations Meeting, Oct. 31-Nov. 2, 1983 Washington, D.C.

Reaction of Excited Oxygen Species with Polymer Films
J.R. MacCallum and C.T. Rankin
Die Makromolekulare Chemie, Vol. 175, 1974, Pp. 2477-2482

Atomic Oxygen Surface Interactions-Mechanistic Study Using
Ground-Based Facilities
J.B. Cross and D.A. Cremers
AIAA-85-0473, AIAA 23rd Aerospace Sciences Meeting, Jan. 14-17,
1985 Reno, Nv.

Laboratory Simulation of Low Earth Orbital Atomic Oxygen
Interaction with Spacecraft Surfaces
B. Singh, L.J. Amore, et al
AIAA-85-0477, AIAA 23rd Aerospace Sciences Meeting, Jan. 14-17,
1985 Reno, Nv.

A Consideration of Atomic Oxygen Interactions with Space Station
L.J. Leger, J.T. Visentine, and J.A. Schliesing
AIAA-85-0476, AIAA 23rd Aerospace Sciences Meeting, Jan. 14-17,
1985 Reno, Nv.

Sputtered Coatings for Protection of Spacecraft Polymers
B.A. Banks, M.J. Mirtich, S.K. Rutledge, and D.M. Swec
NASA Technical Memorandum 83706

Ion Beam Sputter-Deposited Thin Film Coatings for Protection of
Spacecraft Polymers in Low Earth Orbit
B.A. Banks, M.J. Mirtich, S.K. Rutledge, D.M. Swec, and H.K. Nahra
NASA Technical Memorandum 87051

High-Flux Atomic Oxygen Source
A. Cutjian and O. Orient
NASA Tech Briefs, March/April 1986, p. 66

Atomic Oxygen-Metal Surface Studies as Applied to Mass
Spectrometer Measurements of Upper Planetary Atmospheres
G.W. Sjolander
J. of Geophysical Research, Vol. 81, No. 22, Aug 1, 1976, Pp.
3767-3770

Measurement of Atomic Concentrations in Discharged Nitrogen,
Oxygen, and Hydrogen
L. Elias
J. of Chemical Physics, Vol. 44, No. 10, May 15, 1966, Pp.
3810-3818

Dissociation of Oxygen in a Radiofrequency Electrical Discharge
A.T. Bell and K. Kwong
AIChE Journal, Vol. 18, No. 51, Sept, 1972, Pp 990-998

Infrared Emission Associated with Chemical Reactions on Shuttle and SIRTf Surfaces

D.J. Hollenbach and A.G.G.M. Tielens

NASA Technical Memorandum 85875

The Effect of Plasma on Solar Cell Array Arc Characteristics

D.B. Snyder and E. Tyree

AIAA-85-0384, AIAA 23rd Aerospace Sciences Meeting, Jan. 14-17, 1985, Reno, Nv.

Reactions of Atomic Oxygen with Polyimide Films

G.S. Arnold and D.R. Peplinski

AIAA Journal, October, 1985

A Facility for Investigating Interactions of Energetic Atomic Oxygen with Solids

G.S. Arnold and D.R. Peplinski

NASA Conference Publication 2340, 13th Space Simulation

Conference, Oct. 8-11, 1984, Orlando, Fl.

Laboratory Experiments to Study Surface Contamination and Optical Coatings and Materials in Simulated Space Environments

G. Hass and W.R. Hunter

Applied Optics, Vol. 9, 1970, P. 2101

Space Environment Effects on Spacecraft Surface Materials

H.K.A. Kan

SPIE, Radiation Effects in Optical Materials, Vol. 541, 1985, Pp. 164-179

Solar Absorptance Changes of Thermal Control Coatings During Flight

H.A. Papazian

AIAA-84-0059, AIAA 22nd Aerospace Sciences Meeting, Jan. 9-12, 1984, Reno, Nv.

Suitability of Metallized FEP Teflon as a Spacecraft Thermal Control Surface

J.B. Heaney

ASME 71-Av-35, ASME/SAE/AIAA Life Support and Environmental Control Conference, July 12-14, 1971, San Francisco, Ca.

Silver-Teflon Contamination UV Radiation Study

J.A. Muscari

NASA-JSC Contract NAS9-15436 Final Report, MCR-78-567, June 9, 1978

Skylab D024 Thermal Control Coatings and Polymeric Films Experiment

W.L. Lehn and C.J. Hurley

AIAA-74-1228, AIAA/AGU Conference on Scientific Experiments of Skylab, Oct. 30-Nov. 1, 1974, Huntsville, Al.

Effects of Charged Particle and UV Radiation on the Stability
of Silverized and Aluminized FEP Teflon Second Surface

W.A. Wappus

NASA Technical Memorandum 65559, May 1971

Long-Duration Exposure of Spacecraft Thermal Coatings to Simulated
Near-Earth Orbital Conditions

K.E. Steube and R.M.F. Linford

AIAA-71-454, AIAA 6th Thermophysics Conference, April 26-28, 1971,
Tulahoma, Tn.

Development of Space Stable Thermal Control Coatings for use on
Large Space Vehicles

J.E. Gilligan and Y. Harada

NASA-MSFC Contract No. NAS8-26791, Report No. IITRI-C6233-40,
August, 1974

Ultraviolet Radiation Effects on the Infrared Damage Rate of a
Thermal Control Coating

J.A. Bass

NASA Technical Memorandum 65704

An Analysis of Return Flux from the Space Shuttle Orbiter RCS
Engines

H.K.F. Ehlers

AIAA-84-0551, AIAA 22nd Aerospace Sciences Meeting, Jan. 9-12,
1984, Reno, Nv.

The Shuttle Environment

B.D. Green and G.E. Caledonia

AIAA-84-0546, AIAA 22nd Aerospace Sciences Meeting, Jan. 9-12,
1984, Reno, Nv.

Study of Thermal Control Surfaces Returned from Surveyor III

P.M. Blair, Jr., W.F. Carroll, S. Jacobs, L.J. Leger

AIAA-71-479, AIAA 6th Thermophysics Conference, April 28-29, 1971,
Tulahoma, Tn.

Apollo 9 Thermal Control Coating Degradation

J.A. Smith

NASA Technical Note D-6863, June, 1972

Ultraviolet and Electron Irradiation of DC-704 Siloxane Oil on
Zinc Orthotitanate Paint

D.L. Mossman, M.K. Barsh, and S.A. Greenberg

AIAA-82-0865, AIAA/ASME Joint Thermophysics, Fluids, Plasma and
Heat Transfer Conference, June 7-11, 1982, St. Louis, Mo.

Formulation Procedures, Rationale, and Preliminary IMP-H Flight
Data for Silicone Paints with Improved Stability

J.B. Schutt and C.M. Shai

NASA TM 70560, Dec. 1973

Degradation of Thermal Control Coatings by Ultraviolet and Particle Irradiation

A. Paillous

European Space Agency Technical Translation ESA TT-388

Active Cleaning Technique for Removing Contamination from Optical Surfaces in Space: Final Report

R. Shannon, R. Gillette, and G. Cruz

NASA-MSFC, Contract NAS8-26385, Final Report, August, 1973

Results of Apparent Atomic Oxygen Reaction on Ag, C and Os Exposed During the Shuttle STS-4 Orbits

P.N. Peters, R.C. Linton and E.R. Miller

J. of Geophysical Research, Vol. 10, July, 1983, Pp. 569-571

Effects of Low Earth Orbits on Indium-Tin Oxide Coated Kapton

E.N. Borson, M.S. Leung, W.K. Stuke, and L.J. Amory

AIAA Paper 83-0072, Jan., 1983

Mechanistic Studies of Kapton Degradation in Shuttle Environments

R. Liang and A. Gupta

AIAA Paper 83-2656, AIAA Shuttle Environment and Operations

Meeting, Washington, D.C., Oct-Nov, 1983

Effects on Optical Surfaces at Shuttle Altitudes

T.R. Gull, et al

AIAA Paper 85-0418, AIAA 23rd Aerospace Sciences Meeting, Jan. 14-17, 1985, Reno, Nv.

Measurement of Reaction Rates and Activation Energies of 5ev Oxygen Atoms with Graphite and Other Solid Surfaces

J.C. Gregory and P.N. Peters

AIAA Paper 85-0417, AIAA 23rd Aerospace Sciences Meeting, Jan. 14-17, 1985, Reno, Nv.

Materials Interaction with the Low Earth Orbital Environment:

Accurate Reaction Rate Measurements

J. T. Visentine and L.J. Leger

AIAA Paper 85-7019, AIAA Shuttle Environment and Operations II Conference, Nov., 1985, Houston, Tx.

Metal Clad Tubular Structures for Atomic Oxygen Environments

D.M. Mazenko, B.C. Petrie, and R.M. Bluck

SAMPE Quarterly, Vol. 17, No. 3, April, 1986

Atmospheric Effects in Low Earth Orbit and the DMSP ESA Offset Anomaly

G.S. Arnold, R.R. Herm, and D.R. Peplinski

NTIS Technical Report SD-TR-82-81, Sept., 1982

Prediction of Thermal Control Surface Degradation Due to Atomic Oxygen Interaction

A.L. Leeland and G.D. Rhoads

AIAA Paper 85-1065, AIAA 20th Thermophysics Conference, June 19-21, 1985, Williamsburg, Va.

Ion Beam Sputter Deposited Diamondlike Films

B.A. Banks and S.K. Rutledge

NASA TM-82873, 1982

The Production of Glow Precursors by Oxidative Erosion of Spacecraft Surfaces

J.C. Gregory and P.N. Peters

NASA CP-2391, Second Workshop on Spacecraft Glow, 1985, Pp. 174-179

Interaction of Atomic Oxygen with Solid Surfaces at Orbital Altitudes

J.C. Gregory and P.N. Peters

Proceedings of the First LDEF Mission Working Group Meeting, NASA Langley Research Center, 1981, P. 48.

The Simulation of Ultraviolet Irradiation Effects on Candidate Spacelab Thermal Control Coatings

S.J. Bosma and F. Levadou

AIAA Paper 78-1621, AIAA 10th Space Simulation Conference, 1978

Correlation of Laboratory and Flight Data for the Effects of Atomic Oxygen on Polymeric Materials

M. McCargo, R.J. Martin, R.E. Dammann, and P.W. Knopf

AIAA Paper 85-1066, June, 1985

Satellite Exposure to Atomic Oxygen in Low Earth Orbit

D.R. Peplinski, G.S. Arnold, and E.N. Borson

Proceedings, 13th NASA/AIAA/ASTM Space Simulation Conference, Oct. 1984 Orlando, Fl., NASA Conf. Publication 2340

Atomic Oxygen Fluence Monitor

C.R. Maag

NASA New Technology Report, Dec. 1984

Evaluation of Surface Modification Procedures Leading to Atom Resistant Thermal Control Coating

R.M. Liang

JPL Quarterly Report, UPN 482-53-25-28-00, Feb 1985

Proceedings of the SMRM Degradation Study Workshop, NASA-Goddard Space Flight Center, May 9-10, 1985

Atomic Oxygen Effects Measurements for Shuttle Missions STS-8 and 41G

J.T. Visentine

NASA Technical Memorandum, Vols. 1-3, 1988

Development of Low-energy Oxygen Ion Beams for Surface Studies
S.R. Walther, K.N. Leung, and W.B. Kunkel
J. App. Physics, 60, P. 3015, 1986

ESCA Study of Kapton Exposed to Atomic Oxygen in Low Earth Orbit
Downstream from a Radio-frequency Oxygen Plasma
M.A. Golub and T. Wydeven
Polymer Communications, Vol 29, October 1988

Reactions of Atomic Oxygen(O triplet P) with Various Polymer Films
M.A. Golub and T. Wydeven
Polymer Degradation and Stability, Vol 22, 1988, Pp. 325-338

J.W. Linnett and D.G.H. Marsden
Proc. Roy. Soc. A Vol 234, P489, P504

Measurement of Concentration and Study of Recombination of Atomic
Hydrogen by Wrede-Hartek Method
V. Kumar and E. Krishnakumar
Rev. Sci. Instruments, Vol 50, No. 6, June 1979

Effect of Hard Particle Impacts on the Atomic Oxygen Survivability
of Reflector Surfaces with Transparent Protective Overcoats
D.A. Gulino, NASA-LeRC

Solar Absorptance and Thermal Emittance of Some Common Spacecraft
Thermal-Control Coatings
J.H. Henninger
NASA Reference Publication 1121, 1984

Mechanism of Oxygen Plasma Etching of Polydimethyl Siloxane Films
N.J. Chou, C.H. Tang, J. Paraszczak, and E. Babich
Appl. Phys. Lett. Vol. 46, No. 1, January 1, 1985

Oxygen Reactive Ion Etching of Organosilicon Polymers
F. Watanabe and Y. Ohnishi
J. Vac. Sci. Technol. B, Vol 4, No. 1, Jan/Feb 1986

G.N. Taylor and T.M. Wolf
Polym. Eng. Sci., Vol. 20, 1980, P. 1087